

**Transcription factor networks directing pancreas
development in *Xenopus laevis***

Dissertation zur Erlangung des Doktorgrades
der Mathematisch-Naturwissenschaftlichen Fakultäten
der Georg-August Universität zu Göttingen

vorgelegt von

Christine Jäckh
aus Heidelberg

Göttingen 2008

D7

Referent: Prof. Dr. Tomas Pieler

Korreferent: Prof. Dr. Ernst Wimmer

Tag der mündlichen Prüfung: 29. 10. 2008

dedicado a Ingo- Felix

Table of Contents

Table of Contents

List of Figures

List of Tables

Abstract

1	Introduction	1
1.1	From endoderm specification to pancreas organogenesis in <i>Xenopus laevis</i>	2
1.1.1	Endoderm specification	2
1.1.2	Gut tube formation and patterning	3
1.1.3	Pancreas organogenesis	4
1.2	Molecular mechanism regulating pancreas development	7
1.2.1	Signalling pathways involved in pancreas development	7
	1.2.1.1 Signalling pathways involved in endocrine cell differentiation	8
	1.2.1.2 Retinoic acid signalling	9
1.2.2	Transcription factors involved in pancreas development	11
	1.2.2.1 The homeobox transcription factor Pdx1/ XIHbox8	11
	1.2.2.2 The role of HNF1 β in pancreas development	13
	1.2.2.3 The role of HNF6 in pancreas development	16
1.3	Screening for novel pancreas specific marker genes in <i>Xenopus laevis</i>	17
1.4	<i>Xenopus laevis</i> as experimental model system	17
1.5	Aims of this study	18
2	Materials and Methods	19
2.1	Materials	19
2.1.1	Chemicals	19
2.1.2	Buffers and solutions	19
2.1.3	Enzymes	19
2.1.4	Reaction and purification kits	19

2.1.5	Antibodies	20
2.1.6	Antibiotics	20
2.1.7	Oligonucleotides	20
2.1.7.1	Morpholinos	20
2.1.7.2	DNA oligonucleotides	21
2.1.8	Vector systems	22
2.1.8.1	pGEM [®] -T and pGEM [®] -T Easy vector system (Promega)	22
2.1.8.2	pCS2+ vector and derivatives	22
2.1.8.3	pETZ2-9d	23
2.1.9	Constructs	23
2.1.10	Experimental organisms	26
2.1.11	Technical equipment	26
2.1.12	Hard- and Software	27
2.2	Methods	28
2.2.1	Working with <i>Xenopus laevis</i>	28
2.2.1.1	Culturing <i>Xenopus laevis</i> embryos	28
2.2.1.2	Microinjection	29
2.2.1.3	Embryo fixation	29
2.2.1.4	β- galactosidase staining	30
2.2.1.5	Embryonic explant preparation	30
2.2.1.6	Chemical treatments of embryos and explants	31
2.2.2	Bacterial work	31
2.2.2.1	Generation of chemical competent cells	31
2.2.2.2	Chemical transformation of competent cells	32
2.2.2.3	Glycerol stocks	32
2.2.3	DNA work	32
2.2.3.1	Native agarose gel electrophoresis	32
2.2.3.2	DNA purification	33
2.2.3.3	Measurement of nucleic acid concentration	34
2.2.3.4	Polymerase chain reaction (PCR)	34
2.2.3.5	DNA sequencing	35
2.2.3.6	Plasmid linearisation	36
2.2.3.7	Double restriction digest	36
2.2.3.8	Ligation of DNA fragments	37
2.2.4	RNA work	37
2.2.4.1	Total RNA extraction from embryos, adult tissues and explants	37
2.2.4.2	RNA purification from enzymatic reactions	38

2.2.4.3	Reverse transcriptase polymerase chain reaction (RT- PCR)	39
2.2.4.4	5'-/ 3'- Rapid amplification of cDNA ends (RACE- PCR)	40
2.2.4.5	<i>In vitro</i> RNA transcription	41
2.2.4.6	Whole mount <i>in situ</i> hybridisation (WMISH)	43
2.2.5	Vibratome sections	46
2.2.6	Protein work	47
2.2.6.1	Protein extraction from <i>Xenopus laevis</i> embryos	47
2.2.6.2	SDS- Polyacrylamide gel electrophoresis (PAGE)	48
2.2.6.3	Coomassie staining	49
2.2.6.4	Western blotting	49
2.2.6.5	Bradford assay	50
2.2.6.6	<i>In vitro</i> transcription and translation assay (TnT [®])	50
2.2.7	Generation of malectin specific antibody	51
2.2.7.1	Cloning of malectin core domains	51
2.2.7.2	Overexpression and purification of antigen	52
2.2.7.3	Purification of rabbit polyclonal antibody	53
2.2.8	Eukaryotic cell culture	55
2.2.8.1	Culturing, media and solutions	55
2.2.8.2	Transient cell transfection	56
2.2.9	Immunofluorescent (IF) protein detection	57
2.2.9.1	IF in eukaryotic cells	57
2.2.9.2	IF in animal caps	57
3	Results	59
3.1	Characterisation of HNF1 β during pancreas development	59
3.1.1	Expression profile of HNF1 β during embryogenesis	59
3.1.2	Functional characterisation of HNF1 β during pancreas development	62
3.1.2.1	Knockdown of HNF1 β leads to pancreatic hypoplasia	63
3.1.2.2	Induction of HNF1 β expands expression of pancreatic marker genes	70
3.1.3	Requirement of RA- signalling for endodermal HNF1 β expression	80
3.1.3.1	HNF1 β expression is responsive to RA- signalling	80
3.1.3.2	HNF1 β responds to RA- signalling in the endoderm	83
3.1.3.3	HNF1 β expression responds to RA-signalling in the dorsal and ventral endoderm	85
3.2	Isolation and characterisation of HNF6/ oncut-1 of <i>Xenopus laevis</i>	87
3.2.1	Isolation of an oncut transcription factor	87

3.2.2	The <i>Xenopus laevis</i> onecut protein corresponds to HNF6/ onecut-1	88
3.2.3	Comparative expression analysis of XHNF6 within the endoderm	90
3.2.3.1	XHNF6 expression precedes the onset of pancreatic marker genes	90
3.2.3.2	XHNF6 is expressed in the neural tissue and anterior endoderm	92
3.2.3.3	XHNF6 is expressed in the ventral and dorsal pancreas	95
3.2.3.4	XHNF6 and HNF1 β are expressed in the dorsal endoderm	96
3.2.3.5	Tissue distribution of XHNF6 in adult <i>Xenopus laevis</i>	98
3.2.4	Functional characterisation of XHNF6 during pancreas development	99
3.3	Malectin, a novel ER- resident protein in <i>Xenopus laevis</i>	101
3.3.1	Malectin is an ubiquitously expressed protein	103
3.3.2	Malectin resides in the endoplasmic reticulum (ER)	106
3.3.3	Functional analysis of malectin in <i>Xenopus laevis</i> organogenesis	110
4	Discussion	115
4.1	The requirement of HNF1 β for pancreas development	116
4.1.1	HNF1 β is necessary for pancreas specification	117
4.1.2	HNF1 β is not sufficient for pancreas formation	119
4.2	The requirement of HNF1 β for endocrine cell differentiation	122
4.3	HNF1 β is a mediator for RA- signalling in the endoderm	125
4.4	Ectopic activation of XHNF6 promotes pancreas development	128
4.5	Malectin, a novel ER resident protein in <i>Xenopus laevis</i>	129
5	Abbreviations	133
6	Bibliography	135
7	Appendix	155
7.1	Effect on XlHbox8 expression upon ectopic activation of HNF1 β	155
7.2	Phenotypes induced upon misexpression of HNF1 β	156
7.3	Statistical values of affected insulin expression upon HNF1 β misexpression	157
7.4	Sequence alignment of XHNF6 and eukaryotic onecut proteins	158

List of publications

Acknowledgements

Curriculum Vitae

List of Figures

Figure 1.1	Endoderm formation and gut tube patterning	3
Figure 1.2	Pancreas development in <i>Xenopus laevis</i>	5
Figure 1.3	Metabolic pathway and mechanism of retinoic acid (RA)- signalling	9
Figure 1.4	Expression of RALDH2 and CYP26 at gastrula stage of <i>Xenopus laevis</i>	10
Figure 1.5	Regulatory factors directing pancreatic lineage specification in <i>Xenopus laevis</i>	14
Figure 2	Schematic drawing of a semi- dry western blot sandwich	49
Figure 3.1.1	Expression pattern of HNF1 β during <i>Xenopus laevis</i> development	60
Figure 3.1.2	Position and sequences of HNF1 β - specific morpholinos	63
Figure 3.1.3	Determination of knockdown efficiency of HNF1 β - specific morpholinos	64
Figure 3.1.4	Knockdown of HNF1 β reduces expression of pancreatic marker genes	66
Figure 3.1.5	Knockdown of HNF1 β leads to reduced insulin expression	69
Figure 3.1.6	Phenotypes induced upon ectopic expression of HNF1 β in the endoderm	71
Figure 3.1.7	HNF1 β constructs used for gain- and loss of function approaches	73
Figure 3.1.8	Changes in pancreatic marker gene expression upon ectopic activation of HNF1 β	75
Figure 3.1.9	Ectopic activation of HNF1 β leads to induced insulin expression	77
Figure 3.1.10	HNF1 β positively regulates XIHbox8 expression	79
Figure 3.1.11	HNF1 β expression is responsive to RA- signaling	81
Figure 3.1.12	HNF1 β expression in the endoderm is responsive to RA- signalling	84
Figure 3.1.13	HNF1 β expression in the dorsal and ventral endoderm is responsive to RA- signalling	86
Figure 3.2.1	Isolation of an onecut transcription factor from <i>Xenopus laevis</i>	88
Figure 3.2.2	Nucleotide and amino acid sequence of the isolated <i>Xenopus laevis</i> onecut protein	89
Figure 3.2.3	XHNF6 preceds expression of pancreatic marker genes	92
Figure 3.2.4	Expression pattern of XHNF6 during <i>Xenopus laevis</i> development	93
Figure 3.2.5	XHNF6 is expressed in the ventral pancreas	97
Figure 3.2.6	XHNF6 is expressed in the dorsal and ventral endoderm by the onset of pancreatic budding	98
Figure 3.2.7	XHNF6 is expressed in liver, pancreas and brain of the adult <i>Xenopus laevis</i>	99
Figure 3.2.8	Ectopic expression of XHNF6 promotes pancreas development	100
Figure 3.3.1	Sequence comparison of <i>Xenopus laevis</i> malectin with eukaryotic homologues	103
Figure 3.3.2	Spatial and temporal expression profile of malectin in <i>Xenopus laevis</i> embryos and adult	105
Figure 3.3.3	Malectin constructs generated for protein overexpression	107
Figure 3.3.4	Malectin resides in the endoplasmic reticulum	109
Figure 3.3.5	Position and sequences of malectin- specific morpholinos	111
Figure 3.3.6	Determination of knockdown efficiency of malectin- specific morpholinos	112
Figure 3.3.7	Misexpression of malectin affects endoderm development	114
Figure 7.1	Effect on XIHbox8 expression upon ectopic activation of HNF1 β	155
Figure 7.2	Phenotypes induced upon misexpression of HNF1 β	156
Figure 7.3	Sequence anlgiment of XHNF6 and eukaryotic onecut proteins	158

List of Tables

Table 1	Genetic mutations that are linked to MODY-type of diabetes	1
Table 2	Duration of proteinase K treatment during WMISH for different developmental stages	44
Table 3.1	Phenotypes induced upon ectopic expression of HNF1 β in the endoderm	72
Table 3.2	Sequence homology between isolated XHNF6 and onecut proteins	91
Table 3.3	Sequence comparison of malectin with eukaryotic homologues	102
Table 4	Comparison of RA and HNF1 β induced effects on pancreas development	126
Table 5	Statistical values of affected insulin expression upon HNF1 β misexpression	157

Abstract

On the background of severe clinical conditions as diabetes type I, it is essential to understand pancreas development, in particular endocrine cell differentiation. Pancreas development is under control of signalling pathways and a complex transcription factor network. It was previously reported that in *Xenopus laevis* retinoic acid (RA)- signalling was required for dorsal pancreas development and endocrine cell differentiation as early as during gastrulation. It was also shown, that a combined expression of the two transcription factors Pdx1/ XlHbox8 and Ptf1a/Xp48 in the endoderm is sufficient to induce pancreatic cell fate. However, it remained unknown how these early RA induced pre patterning events contribute to later organ formation that is marked by the onset of Pdx1/XlHbox8 and Ptf1a/p48 expression in the gut epithelium.

This study focused on the identification of regulatory factors that link early RA- signalling with the onset of pancreas formation in *Xenopus laevis*. In this context, the two transcription factors HNF1 β /TCF2 and HNF6/ onecut-1 were identified as positive upstream regulators for Pdx1/XlHbox8 and Ptf1a/Xp48. HNF1 β was shown to be necessary but not sufficient for pancreas specification and outgrowth. Whereby, in contrast to HNF1 β deficient mice, knockdown of HNF1 β in *Xenopus laevis* did not lead to complete pancreas agenesis. HNF1 β was also shown to be responsive to RA- signalling within the early endoderm, and that it was able to promote endocrine cell differentiation. HNF6 was newly isolated, its spatial and temporal expression was confined to the anterior endoderm, and gain of function studies revealed a pancreas promoting activity.

A second aspect in this study concerned the identification of new pancreas specific marker genes that could serve as useful tools for the descriptive analysis of organogenesis. The putative pancreatic marker gene malectin revealed an ubiquitous expression in *Xenopus laevis* and an intracellular ER residence. In collaboration, it was shown that malectin was a carbohydrate binding protein playing a putative role in the N- glycosylation pathway, implying a general function in *Xenopus laevis* development.

1 Introduction

The importance of the pancreas is evident from the number of clinical conditions resulting from the malfunction of this organ, notably *diabetes mellitus*. Diabetes is characterised by abnormal high blood glucose levels that are caused by absence of pancreatic β -cells, their impaired insulin secretion or reduced insulin responsiveness of the metabolic system. According to the time point of clinical manifestation and insulin requirement, diabetes is classified into two major forms: an early insulin- dependent diabetes type I and a later non-insulin dependent diabetes type II. The most frequent form of diabetes type I is an autoimmune disease leading to neonatal self-destruction of β -cells. A second variant of β -cell disorder is the maturity onset diabetes of the young (MODY). This milder form of diabetes is based on genetic mutations that lead to disrupted β -cell formation or impaired insulin production (summarized in table 1, reviewed in Fajans et al., 2001).

Over several years, basic research has gathered information on factors, which are crucial to activate the genetic program for β -cell generation during normal pancreas development.

Type	affected gene	function	reference
MODY1	HNF4 α (TCF14)	TF regulating HNF1 α and HNF1 β as well as gene expression for glucose metabolism	Frayling et al., 2001; Yagamata et al., 1996
MODY2	Glucokinase	blood glucose sensor	Hattersley et al., 1992
MODY3	HNF1 α (TCF1)	TF regulating insulin expression	Frayling et al., 2001
MODY4	Ipf1 (Pdx1, XIHbox8)	TF regulating pancreas development and gene expression of glucose metabolism	Stoffers et al., 1997
MODY5	HNF1 β (TCF2, LFB3)	TF regulating pancreas development and gene expression for glucose metabolism	Horikawa et al., 1997; Haumatire et al., 2005
MODY6	Neurogenic differentiation 1 (NeuroD1)	TF promoting exocrine versus endocrine cell differentiation	Copeman et al., 1995
MODY7	Krüppel-like factor 11 (KLF-11)	TF promoting endocrine gene expression versus exocrine differentiation	Neve et al., 2005
MODY8	Bile salt dependent lipase (CEL)	enzyme involved in lipid metabolism and linked by observational studies to diabetes	Raeder et al., 2006

Table 1: Genetic mutations that are linked to MODY-type of diabetes. The table lists all types of diabetic disorders known for human maturity onset diabetes of the young (MODY). Genes related to the disorder and their function are stated as well as their literature reference. TF= transcription factor; names in brackets state synonyms.

Due to the identification of essential regulating factors, as transcriptional regulators and signalling molecules, human embryonic stem cells could be fated under optimized conditions towards a mature insulin producing β -cell *in vitro* (D'Amour et al., 2006). Recently a breakthrough in diabetes research was achieved by *in vitro* generation of pancreatic endoderm that was transplanted into mice and that subsequently generated endocrine cells that were responsive to high blood glucose levels *in vivo* (Kroon et al., 2008).

Many of these factors, that direct endocrine cell fate are not only essential to determine and maintain identity of a mature pancreatic cell, but they also play decisive roles during the three key events of pancreas development, namely endoderm specification, gut tube formation and patterning as well as pancreas organogenesis (reviewed in Oliver-Krasinski and Stoffers, 2008).

Most studies that focus on revealing the developmental aspects during pancreas organogenesis made use of vertebrate model systems as mouse (*Mus musculus*) and zebrafish (*Danio rerio*). In this study, the amphibian model system *Xenopus laevis* was used to reveal in detail the regulatory mechanisms that direct pancreas development.

1.1 From endoderm specification to pancreas organogenesis in *Xenopus laevis*

1.1.1 Endoderm specification

The early *Xenopus laevis* embryo is divided into three regions: the animal pole, the marginal zone and the vegetal pole (figure 1.1). Upon dynamic cell movements during gastrulation, these distinguished regions give rise to the three germ layers, namely the ecto-, meso- and endoderm respectively. The ectoderm differentiates into the epidermis and the nervous system, the mesoderm develops into muscle, vascular system, kidney and connective tissue, while the endoderm forms the digestive tract, including liver and pancreas, as well as the respiratory organ.

Establishment of the endodermal fate depends on maternal factors in the vegetal hemisphere as the T-box transcription factor VegT (Zhang et al., 1998; Yasuo and Lemaire, 1999). Veg-T induces zygotic expression of downstream targets as the nodal-related genes (Xnr; Jones et al., 1995), the homeobox factor Mixer and mix-like protein (Henry and Melton, 1998), which in turn induce expression of pro-endodermal transcription factors as Xsox17, FoxA1 and 2 (HNF3 α , HNF3 β) and GATA 4- 6 as well as synthesis of vegetal mesoderm antagonists like Cerberus (Xanthos et al., 2001). Maintenance of Gata 4-6 and Xsox17 expression is mediated by TGF β (nodal) signalling. Their persistent expression is required to activate expression of genes that promote general endoderm and genes that coordinate axis

specification (Afouda et al., 2005). Dorso-ventral axis specification is already established after fertilisation by stabilisation of the transcriptional regulator β -catenin in the prospective dorsal half of the embryo, where it overlaps the VegT containing region, specifying the Nieuwkoop center. Studies using the animal cap system in *Xenopus laevis* demonstrated that combined overexpression of VegT and β -catenin changed the prospective ectodermal fate of isolated animal pole cells into dorso- endodermal fate. The dorsal endoderm inducing activity of VegT/ β -catenin was shown by their capacity to induce gene expression of pancreas specific genes as Pdx1/XlHbox8, insulin and XPDip (Chen et al., 2004). Specification of dorsal-ventral and anterior-posterior axis is crucial for subsequent gut tube formation and patterning.

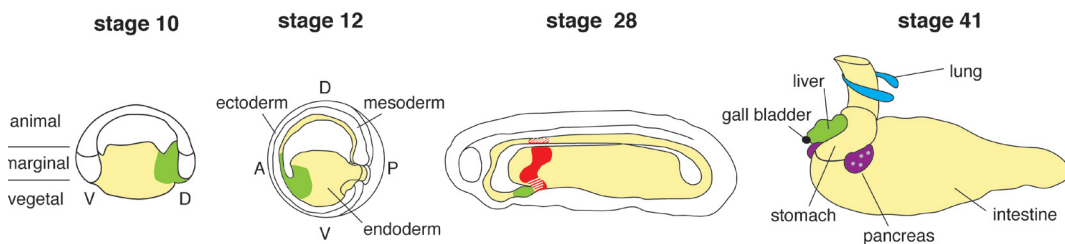


Figure 1.1 Endoderm formation and gut tube patterning. Before stage 10, the embryo is subdivided into three regions: animal pole, marginal zone and vegetal pole, the later endodermal germ layer (yellow). At the onset of gastrulation the dorsal blastopore lip specifies dorso-ventral axis (D, V) evident in asymmetric gene expression, e.g. Hex (green). At stage 12 the three germ layers ecto- meso- and endoderm are separated and the anterior-posterior axis (A, P) is determined. The endoderm forms the primitive gut tube that activates organ specific gene expression (stage 28) in distinct regions like Pdx1/ XlHbox8 (red) and Ptf1a/ Xp48 (black lines), both marking the prospective pancreatic epithelium. During subsequent development the primitive gut tube gives rise to the lung and the gastrointestinal tract at stage 41 (modified after Zorn: <http://www.cincinnatichildrens.org/research/div/dev-biology/fac-labs/zorn-lab/liver-dev.htm>)

1.1.2 Gut tube formation and patterning

Anterior-posterior axis specification in respect to the gut tube occurs between stage 12 and 20. Transplantation experiments revealed that dorsal vegetal cells give rise to the anterior gut endoderm and the ventral vegetal cells to the posterior gut endoderm (Gamer and Wright, 1995; Henry et al., 1996). Establishment of the A-P axis is also reflected by the asymmetric gene expression within the dorsal involuting endoderm of the hematopoietically expressed homeobox transcription factor (Hex), the secreted factor Cerberus (Bouwmeester et al., 1996) and the pancreatic progenitor gene XlHbox8 (Wright et al., 1989). Fate mapping determined that Hex, Cerberus and XlHbox8 expressing cells translocate to the anterior region of the embryo and will give rise to the organs of the anterior foregut,

including liver and pancreas, **whereas ventral involuting endoderm was fated to become posterior gut tissue** (Chalmers and Slack, 2000). Apart from Wnt-signalling it was shown that BMP signalling was repressed in order to determine dorsal endoderm tissue (Sasai et al., 1996).

The primitive gut tube is patterned along the anterior- posterior (A- P) and dorsal- ventral (D- V) axis into subregions that form different organs. Tissue identity within the **gut tube** relies on mesoderm- endoderm interactions that promote **region restricted expression** of genes via intrinsic and extrinsic factors. **Region specific gene expression establishes organ boundaries** that are required to **coordinate anterior-posterior, dorsal-ventral and left-right** position of the organ in the primitive gut (Horb and Slack, 2001). **In context of pancreas organogenesis**, research focused predominately on the gene expression profile of the anterior gut epithelium.

1.1.3 Pancreas organogenesis

In *Xenopus laevis*, the pancreas develops from the anterior foregut epithelium as one dorsal anlage and two ventral anlagen at stage 35 and 37, respectively. The pancreatic buds, positioned posterior to the liver diverticulum, grow and branch from the foregut into the mesenchyme. At stage 40, the pancreatic lobes fuse to one discrete organ that is positioned to the right side of the embryos due to gut rotation movements, behind the stomach and duodenum (Figure 1.2; Pieler and Chen, 2006).

Based on studies in mouse, many transcription factors have been identified that are required for the specification of pancreatic cell fate in the primitive gut, among them the pancreatic and duodenum transcription factor 1 (Pdx1; also called XlHbox8 in *Xenopus laevis*; Jonsson et al., 1994) and pancreatic transcription factor 1a (Ptf1a; also called Xp48; Kawaguchi et al., 2002). **These two transcription factors mark a subset of multipotent progenitor cells that give rise to all cell lineages of the mature organ** (Gu et al., 2002).

Also in *Xenopus laevis*, XlHbox8 (Wright et al., 1989) and Xp48 (Afelik et al., 2006) are the first genes that **exclusively mark multipotent pancreatic progenitor cells in the anterior foregut, the pre-pancreatic endoderm**, and it was reported that they play crucial roles for pancreas specification and differentiation of cell lineages of the mature organ (Afelik et al., 2006; Jarikji et al., 2007).

The mature pancreas contains two functional units: the exocrine and the endocrine compartment. The exocrine pancreas represents the majority of the tissue and comprises acinar and duct cells. During food uptake, acinar cells secrete digestive enzymes that are collected in the pancreatic duct system and that are further educed into the intestine. To prevent self-

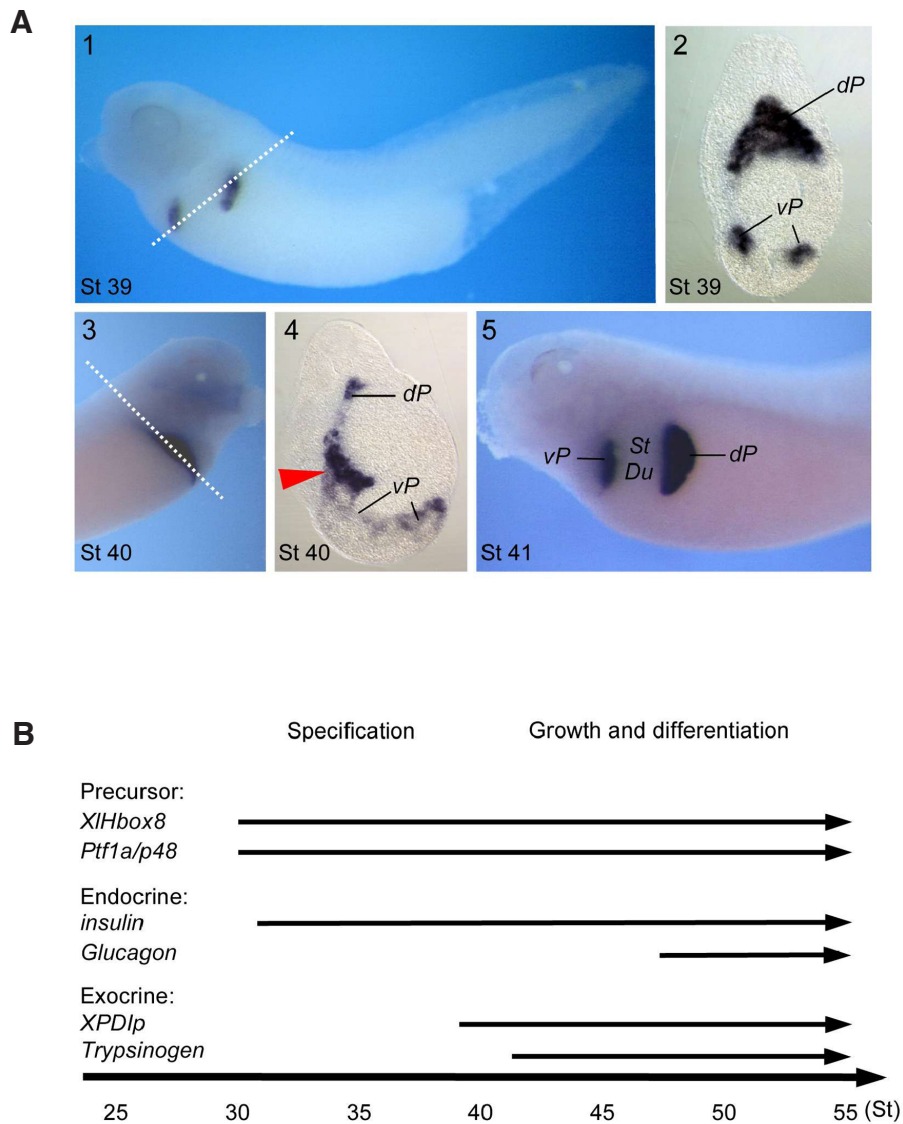


Figure 1.2 Pancreas development in *Xenopus laevis*. (A) At stage 39 two ventral and one dorsal pancreatic anlagen are marked by exocrine XPDip, also seen in the transversal section (1). At stage 40 (3) the ventral pancreatic anlage come in close proximity to the dorsal bud due to gut rotation movements and fuse to one organ (4, red arrow indicates the fusing region). After fusion, the pancreas is positioned to the left side of the embryo underneath the stomach and duodenum region. Developmental stages are indicated to the left. White lines represent the position of transversal sections. (B) Temporal expression profile of pancreatic genes in *Xenopus* embryos. Pdx1/*XIHbox8* and *Ptf1a/p48* are expressed early (stage 29/30), and this early expression can serve in the identification of the pancreatic precursor cells (Afelik et al., 2006). During late development, Pdx1/*XIHbox8* expression is restricted to β -cells, whereas *Ptf1a/p48* expression is confined to exocrine cells. Insulin is expressed slightly later at stage 32 and is initially observed only in the dorsal pancreatic bud. In contrast glucagon expression in the pancreas is quite late (stage 46/47; Kelly and Melton, 2000; Horb and Slack, 2002; Afelik et al., 2004). As for exocrine markers, XPDip is expressed earlier (stage 39) than trypsinogen (stage 41/42; Afelik et al., 2004). Abbreviations: vp: ventral pancreas, dp: dorsal pancreas, st: stomach, du: duodenum. (Pieler and Chen, 2006)

digestion of the organ, duct cells secrete bicarbonate, sodium chloride and water to buffer the pancreatic fluid. The earliest exocrine differentiation marker in *Xenopus* is the pancreas specific protein disulfide isomerase (XPDip). It is expressed from stage 39 onwards in the

dorsal and ventral pancreatic anlage whereas digestive enzymes as amylase, trypsinogen and elastase are initiated after bud fusion at stage 41- 42 and carboxypeptidase at stage 44 (Figure 1.2; Pieler and Chen, 2006; Horb and Slack, 2002).

The endocrine compartment is composed of five cell types that are clustered as islets of Langerhans within the exocrine tissue. Specific peptide hormones involved in glucose homeostasis and metabolism are produced in these cell types, namely glucagon by α -cells, insulin and amylin by β -cells, somatostatin by δ -cells, pancreatic polypeptide by PP-cells and the appetite stimulating hormone ghrelin by ϵ - cells (reviewed in Blitz et al., 2006; Murtaugh, 2007).

As observed in mouse, differentiation of endocrine cells occurs in two distinct waves, referred as primary and secondary transition. During primary transition between E9.5 and E13.0 early endocrine cells expressing glucagon and insulin appear in the Pdx1- positive epithelium. Lineage tracing experiments revealed that these early endocrine cells do not originate from Pdx1- positive progenitor cells and that they do not contribute to the endocrine cell mass of the mature islet (Burlison et al., 2008).

Endocrine cells of the mature islets rather differentiate from a common progenitor pool of the branching Pdx1- positive epithelium at E13.5 and E16 during secondary transition. Appearance of Ngn3 that is expressed in all endocrine progenitor cells marks the onset of the secondary transition which is characterised by a vast increase in cell proliferation and subsequent differentiation of all endocrine as well as exocrine cell types (Gradwohl et al., 2000).

In *Xenopus laevis*, the first endocrine gene insulin is expressed from stage 32 onwards exclusively in the dorsal gut epithelium. These insulin positive cells move anteriorly along with the XlHbox8 positive pancreatic anlage and accumulate in the forming dorsal pancreas (Kelly and Melton, 2000). **Studies showed that these insulin positive cells appear to differentiate within the dorsal pancreatic region independently from the XlHbox8- p48 positive progenitor cell pool and it was suggested that they correspond to cells of the primary transition in mouse (Afelik et al., 2006). A later endocrine differentiation phase is initiated at stage 46 when glucagon, somatostatin and PP positive cells appear scattered in the exocrine tissue. During subsequent development, all endocrine cells cluster to form islet- like structures at stage 50 (Afelik et al., 2004; Kelly and Melton, 2000). However, in contrast to the mouse system, it remains unclear when and how this later phase of endocrine differentiation is initiated in *Xenopus laevis*. So far, there is no gene known in this system that specifies a common endocrine progenitor pool, thereby rising the interest to investigate transcriptional regulation in context of endocrine cell differentiation in *Xenopus laevis*.**

The pancreas arises as ventral and dorsal anlagen that fuse during development to one mature organ. The ventral gut epithelium gives not only rise to the pancreatic rudiment but also to the adjacent liver. It was shown that both organs derive from a common bipotential progenitor pool (Deutsch et al., 2001). On one side, the genetic program must be similar in both pancreatic anlagen to generate a common tissue, but at the same time it must differ to specify the two organ anlagen from its neighbouring tissue, that differs between the ventral and dorsal gut epithelium. Specification of ventral and dorsal pancreas from a different location and varying surrounding tissues requires a divergent set of genetic regulators in the ventral versus dorsal gut epithelium (reviewed in Zaret, 2008).

1.2 Molecular mechanism regulating pancreas development

1.2.1 Signalling pathways involved in pancreas development

Various extrinsic signals from the surrounding mesoderm are required for region-specific gene expression in the epithelium that coordinates organogenesis along the anteroposterior and dorsoventral axis of the gastro-intestinal tract, emphasizing the importance of mesenchymal-endodermal cross-talk for gut tube patterning (Oliver-Krasinski and Stoffers 2008; Pieler and Chen, 2006). Extrinsic signals include members of the secreted factors of the Wnt-, TGF β -, hedgehog (HH)-, Notch-, FGF- and retinoic acid (RA)- signalling pathways. These signalling pathways maintain either a negative or a positive regulatory function on pancreas specification and determination of cell lineage. In this context, it was shown that canonical Wnt- signalling was required for exocrine cell differentiation in the mouse (Murtaugh et al., 2005). A recent study demonstrated that early endodermal Wnt- signalling must be inhibited during gastrulation, to maintain foregut identity and to promote liver and pancreas development in *Xenopus laevis* (McLin et al., 2007). These findings define a strict time window of signalling action for endoderm patterning.

The segregation of neighbouring tissues as liver and ventral pancreas, shown to derived from a common progenitor pool, requires distinct molecular mechanism to determine either hepatic or pancreatic cell fate in the ventroanterior gut tube. Ventroanterior endodermal progenitor cells would normally adopt pancreatic fate. The exposure of these ventroanterior cells to secreted molecules of the TGF β superfamily, namely BMP and FGF, they adopt hepatic cell fate. BMP and FGF are secreted from the adjacent cardiac mesoderm and septum transversum (Deutsch et al., 2001). Apart from Wnt- signalling, hedgehog signalling is also repressed in restricted territories in order to render the epithelium competent for pancreatic cell fate acquisition. From studies in chicken, it was postulated that FGF2, secreted from the notochord, represses sonic hedgehog (SHH) the gut epithelium

and consequently activates Pdx1 expression and permits pancreas organogenesis (Hebrok et al., 1998). Expansion of SHH can be induced in the pancreatic region upon inhibition of the RA-signalling pathway which is associated with a reduced Pdx1/ XlHbox8 and insulin expression (Chen et al., 2004).

1.2.1.1 Signalling pathways involved in endocrine cell differentiation

Specification of the endocrine cell lineage depends on permissive signals from the surrounding tissues as the vascular epithelium (Lammert et al., 2001; Nicolova et al., 2006) or the neural crest cells (Nekrep et al., 2008). However, the best analysed molecular mechanism regulating the segregation of the exocrine and the endocrine cell lineage is the Notch- signalling pathway.

This cell-cell signalling pathway is activated by binding of Notch- ligands, the transmembrane proteins delta and serrate, to the Notch receptor of the neighbouring cell. Upon ligand binding, the intracellular domain of the Notch receptor, Notch- ICD, translocates into the nucleus, where it recruits the DNA-binding protein RBP-J κ (recombining binding protein suppressor of hairless) and activates gene expression of the Hairy and Enhancer of Split (HES) gene family. Hes1 has been shown to repress expression of the pro- endocrine gene Ngn3 in the same cell, thereby promoting its exocrine fate (Jensen et al., 2000). This negative regulation of gene expression between neighbouring cells is therefore called lateral inhibition. Lack of Ngn3 resulted in absence of all endocrine cell types within the pancreatic islets (Gradwohl et al., 2000).

Overactivation of Notch- signalling maintained pancreatic progenitor cells in a proliferating state, resulting in delayed cell differentiation. Consequently, impaired maturation of endocrine and exocrine tissue was evident in a hypoplastic pancreas (Murtaugh et al., 2003). In contrast, inhibition of Notch- signalling or overexpression of Ngn3 leads to premature differentiation of endocrine cells and to defects in pancreatic outgrowth (Apelqvist et al., 1999; Kim et al., 1997; Schwitzgebel, 2000). Hes1 also was reported to directly repress Ptf1/p48 expression and therefore inhibiting exocrine differentiation in mouse (Ghosh and Leach, 2006). Together these data underline the bifunctional role of Notch- signalling during early proliferation and on later differentiation of the pancreas. Another signalling factor that has been associated with pancreatic cell lineage commitment of the endocrine compartment is retinoic acid (RA).

1.2.1.2 Retinoic acid signalling

Retinoic acid (RA) is a small lipophilic molecule that derives from vitamin A (retinol) that is uptaken by dietary and maintained in the blood system bound to retinoic binding proteins (Noy, 2000). After passive diffusion into the cell, retinol binds to the retinal binding protein (CRBP) and is oxidised to retinal by retinal dehydrogenases (RDH). Retinal is subsequently metabolised by the enzyme Raldh2 in a rate limiting step to RA (figure 1.3). Binding to CRAB promotes translocation of RA into the nucleus where it is transferred to its nuclear receptor RAR and the retinoic X receptors RXR that are both members of the

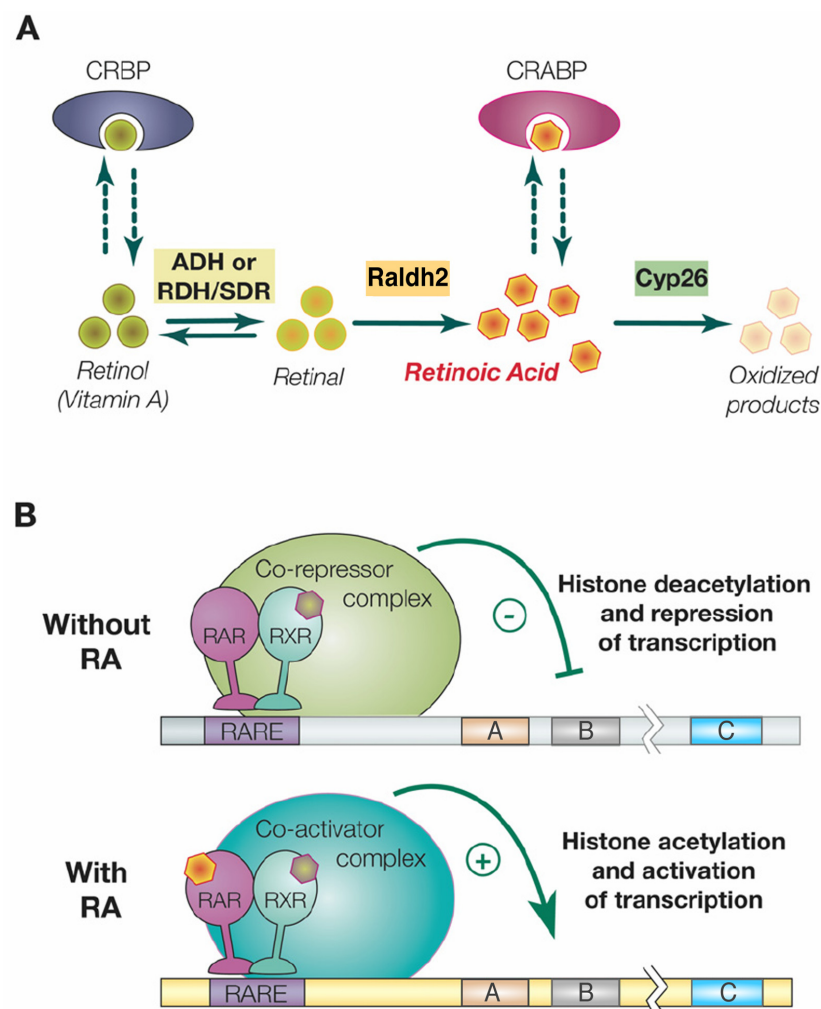


Figure 1.3 Metabolic pathway and mechanism of retinoic acid (RA)- signalling. (A) Cellular retinol binding protein (CRBP) binds retinol, which is oxidised to retinal by retinaldehyde dehydrogenase (ADH) or short-chain dehydrogenase/reductase (RDH/SDR). Retinal is oxidised to retinoic acid by retinaldehyde dehydrogenase 2 (Raldh2), which is bound by cellular retinoic acid binding protein (CRABP). Retinoic acid is degraded by the enzyme CYP26. **(B)** In the absence of RA, the retinoic receptors RAR and RXR are bound as heterodimer to their DNA target sequence and recruits a corepressor complex that inhibits transcription of target genes (A, B, C) through histone deacetylation and repression of transcription. Binding of ligand (RA) induces conformational changes and binding of co-activator leading to histone acetylation and activation of transcription (modified after Marlétaz et al., 2006).

Cx- type zinc finger family. RAR and RXR are composed of α , β and γ isoforms, which homo- or heterodimerise to form DNA binding complexes (reviewed in Maden, 2001). DNA binding is restricted to conserved sequences referred to as retinoic acid responsive elements (RAREs). Further cofactors are recruited to the RA- receptor complex to achieve transcriptional induction or repression. After activating its nuclear receptors, RA returns to the cytoplasm binds to the retinol binding protein 1 (RBP1) that targets RA for its metabolizing enzyme CYP26. This P450- class enzyme oxidises RA to inactive metabolites. In *Xenopus laevis*, RA is synthesised at the beginning of gastrulation by the retinol dehydrogenase 2 (RALDH2). RALDH2 expression is initiated in the deep mesodermal layer adjacent to the involuting endoderm region (figure 1.4; Chen et al., 2001). According to

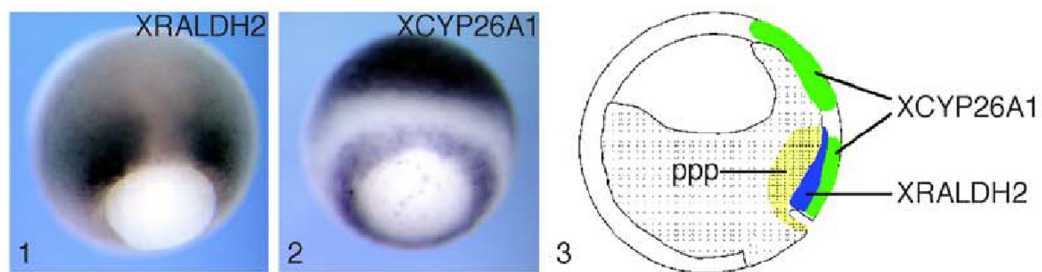


Figure 1.4 Expression of RALDH2 and CYP26 at gastrula stage of *Xenopus laevis*. The RA synthesising enzyme RALDH2 (1; 3 blue) is expressed as two lateral stripes in the involuting mesoderm adjacent to the prospective pancreatic progenitor cells in the endoderm (yellow, PPP). The RA degrading enzyme CYP26A1 (2) is expressed in the epithelial layer of the dorsal animal hemisphere, the neuro ectoderm, and the circumporal marginal zone (Chen et al., 2004).

lineage tracing experiments this region, expressing anterior endodermal marker genes like XHex and XIHbox8 (Zorn et al., 1999), will give rise to pancreatic and hepatic progenitor cells (Kelly and Melton, 2000; Chalmers and Slack, 2000) and thereby supporting the idea that RA is involved in pre patterning the prospective anterior gut endoderm. Cyp26 is expressed in the gastrula ectoderm adjacent to the involuting endoderm (figure 1.4; Hollemann et al., 1998).

Inhibition of RA signalling by the synthetic RA antagonist BMS453, directed against retinoic acid receptor α and γ (Matt et al., 2003), leads to reduced exocrine and endocrine tissue in the dorsal pancreas and to a slightly reduced ventral pancreas (Chen et al., 2004). Conversely, RA treatment of gastrula stage embryos causes an increase of endocrine at the expense of exocrine tissue in the dorsal pancreas whereas the ventral exocrine pancreas was expanded.

Since later RA application did not result in a pancreatic phenotype (Zeynali and Dixon, 1998), these data suggest an early role for RA in patterning the endoderm and in *Xenopus*

pancreas organogenesis, in particular for the dorsal anlage (Chen et al., 2004). The requirement of the vitamin A derivative for pancreas development was further observed in *Xenopus laevis* using the animal cap assay. Coinjection of VegT and β -catenin activates a dorsal endodermal fate in pluripotent animal cap cells. Exocrine and endocrine gene expression was only initiated upon RA treatment (Chen et al., 2004). As VegT is also inducing mesodermal tissue, the question of indirect or direct signalling of RA on the endoderm was subsequently studied by analyzing changes in gene expression within dissected endodermal explants that were exogenously treated with RA or BMS453 (Pan et al., 2007).

Until now it remains obscure how pancreas development proceeds between these RA induced pre-patterning steps and the actual induction of pancreas formation that is marked by the onset of the expression of two transcription factors Pdx1/XIHXbox8 and Ptf1a/p48 in the foregut. The two transcription factors Pdx1/XIHXbox8 and Ptf1a are not the only modulators that direct pancreas development in the gut endoderm promoting endocrine cell differentiation. Indeed, it is a whole set of transcription factors that form a complex regulatory network (reviewed in Zaret, 2008).

1.2.2 Transcription factors involved in pancreas development

Specification of the different pancreatic cell types from pancreatic progenitors in the gut epithelium is driven by a variety of transcription factors. Previously these transcription factors were supposed to regulate their downstream targets in a linear cascade. But the constant growing number of genetic regulators and analysis of their interactive relations implies a complex regulatory network rather than a simple hierarchical model (Zaret, 2008; Oliver-Krasinski and Stoffers, 2008).

Focusing on the factors analysed in the context of this study, the key regulators in pancreas development are the two transcription factors Pdx1/ XIHXbox8 and Ptf1a/ p48. Pdx1- Ptf1a positive cells give rise to all pancreatic cell types of the mature organ (figure 1.5; Kawaguchi et al., 2002; Burlison et al., 2008).

1.2.2.1 The homeobox transcription factor Pdx1/ XIHXbox8

In mice, the homeobox domain protein Pdx1 is expressed in the foregut from E8.5 onwards including the stomach, duodenal and pancreatic region (Ohlson et al., 1993; Jonsson et al., 1994). At E11.5 the expression extends towards the cystic duct, the antral stomach and the common bile duct. Analysis of Pdx1^{-/-} mice revealed that ventral and dorsal pancreatic budding from the posterior foregut still occurred. However, further outgrowth and differentiation of the rudiment was impaired. Inhibited pancreatic development upon Pdx1

depletion also became obvious by the lack of endocrine islet cells in the adult organ. Here, Pdx1 was essential for β -cells maintenance as it was evident by the linkage to MODY4 (table 1; Gannon et al., 2008; Holland et al., 2005).

In contrast, activation of early glucagon and insulin expressing cells deriving from the primary transition within the Pdx1+ epithelium were still detectable in the Pdx1-homozygous mutants demonstrating that these early endocrine cells are Pdx1 independent (Offield et al., 1996; Burlison et al., 2008). In the dorsal pancreas Pdx1 is regulated by transcription factors Hb9 or by Isl1, a lim1 homeobox protein which is expressed in the surrounding mesoderm (reviewed in Edlund, 2002). In the ventral pancreas Pdx1 expression is regulated by HNF1 β and HNF6 (Haumaitre et al., 2005; Jaquemin et al., 2003a). Although Pdx1 owns a high pancreas promoting capacity, it was otherwise shown that Pdx1 alone is not sufficient to induce pancreatic tissue (Horb et al., 2003; Grapin-Botton et al., 2001).

The second key regulator that is subscribed to pancreatic development is the basic helix loop helix (bHLH) protein Ptf1a/ p48 (pancreatic transcription factor 1a). Ptf1a is part of a trimeric DNA binding complex Ptf1. This complex was originally identified as protein complex, activating expression of exocrine genes in the adult pancreas in mice (Krapp et al., 1998). In addition to the bHLH protein p48, the trimeric complex consists of the two transcription factor subunits ribosomal binding protein -J (RBP-J) and an E-box binding bHLH protein (E-box protein). p48 dimerises with the E-box protein and binds to a specific PTF1a-binding site on the DNA. Gene activation requires recruitment of RBP-J. Recent studies in knockout mice showed that lack of p48 disrupts proper outgrowth of the dorsal pancreas and the specification of the ventral pancreas. Instead, the p48^{-/-} foregut epithelium acquires duodenal fate (Kawaguchi et al., 2002). In humans, p48 mutations manifest pancreatic and cerebellar agenesis (Sellick et al., 2004). In context of endocrine cell differentiation, it was shown that upon p48 depletion, few endocrine cells can be found in the adjacent intestine (Kawaguchi et al., 2002).

P48 not only plays a role in establishing a pancreatic progenitor pool, but it was also described as driving factor for differentiation of the exocrine compartment as it was shown to promote outgrowth of the proliferating tips of the branching epithelium. During subsequent morphogenesis, these tip structures differentiate into acinar cells (Stanger et al., 2007). The Ptf1 complex is differentially active within these tips, as it replaces RBPJl against RBPJk after which precursor cell proliferation is blocked and exocrine cell differentiation is initiated (Masui et al., 2007). Similar to Pdx1, dorsal and ventral p48 expression depends on permissive signals from the surrounding tissue as the endothelial cells (Yoshitomi and Zaret, 2004) and FGF10 (Jaquemin et al., 2006).

In *Xenopus laevis*, it was reported that a combined expression of XIHbox8 and Xp48 was sufficient to induce pancreatic fate in the gut epithelium (Afelik et al., 2006). Downregulation of Xp48 and XIHbox8 function resulted in loss of exocrine and late endocrine pancreatic tissue, whereas early insulin expressing cells remained unaffected.

Similar observations were reported upon overactivation of p48 within the pancreatic endoderm in Hes1- knockout mice. Here, pancreatic enlargement only occurred where p48 expression overlapped with endogenous Pdx1 expression within the stomach, bile duct and duodenum, thereby causing cell fate conversion into pancreas of the Pdx1- p48 positive domain (Fukuda et al., 2006).

Data obtained from *in vivo* experiments using transgenic mice indicated that Pdx1 and p48 regulate each other and auto-regulate themselves (Hale et al., 2005; Wiebe et al., 2007). However, it remained unclear how initial gene activation of Pdx1 and p48 is activated in the restricted boundary of the gut epithelium. Direct gene activation requires earlier expression of the upstream regulator in the same cell, which is supposed to induce target gene expression. In this regard, the two transcription factors HNF1 β and HNF6, that are both expressed prior the onset of Pdx1 and p48 in an overlapping but broader regions of the foregut epithelium, represented potential upstream regulators.

1.2.2.2 The role of HNF1 β in pancreas development

The transcription factor HNF1 β [variant hepatocyte factor one (vHNF1), transcription cell factor two (TCF2) or homologue liver specific factor B (LFB3) (DeSimone et al., 1991; Dermatis et al., 1994)], belongs to the group of liver enriched transcription factors known as hepatocyte nuclear factors (HNFs). HNF-group members belong to different transcription factor families, like the homeobox proteins HNF1 β and its close relative HNF1 α , nuclear receptor HNF4 α , forkhead box proteins HNF3 α , β and γ (FoxA1-3) and the onecut family member HNF6 (oncut-1: Cereghini, 1996). All group members were reported to play essential roles during liver specification, as it was also recently demonstrated for HNF1 β (Lokmane et al., 2008). As previously described, dominant negative mutations in the HNF1 β gene are also linked to diabetic disorder MODY5 that is characterised by impaired glucose- stimulated insulin secretion and is associated with a severe glomerulocystic kidney disease (GCKD; Fajans et al., 2001).

HNF1 β was first isolated as albumin promotor binding protein from a rat hepatoma cell line (Cereghini et al., 1988) and demonstrated to be a strong transcriptional activator (DeSimone et al., 1991). The HNF1 β protein contains an N-terminal DNA-binding region that is composed of a dimerisation domain, a POU-like DNA binding motif and a downstream HOMEBOX motif (Nicosia et al., 1990). Structural analysis of the human homologue

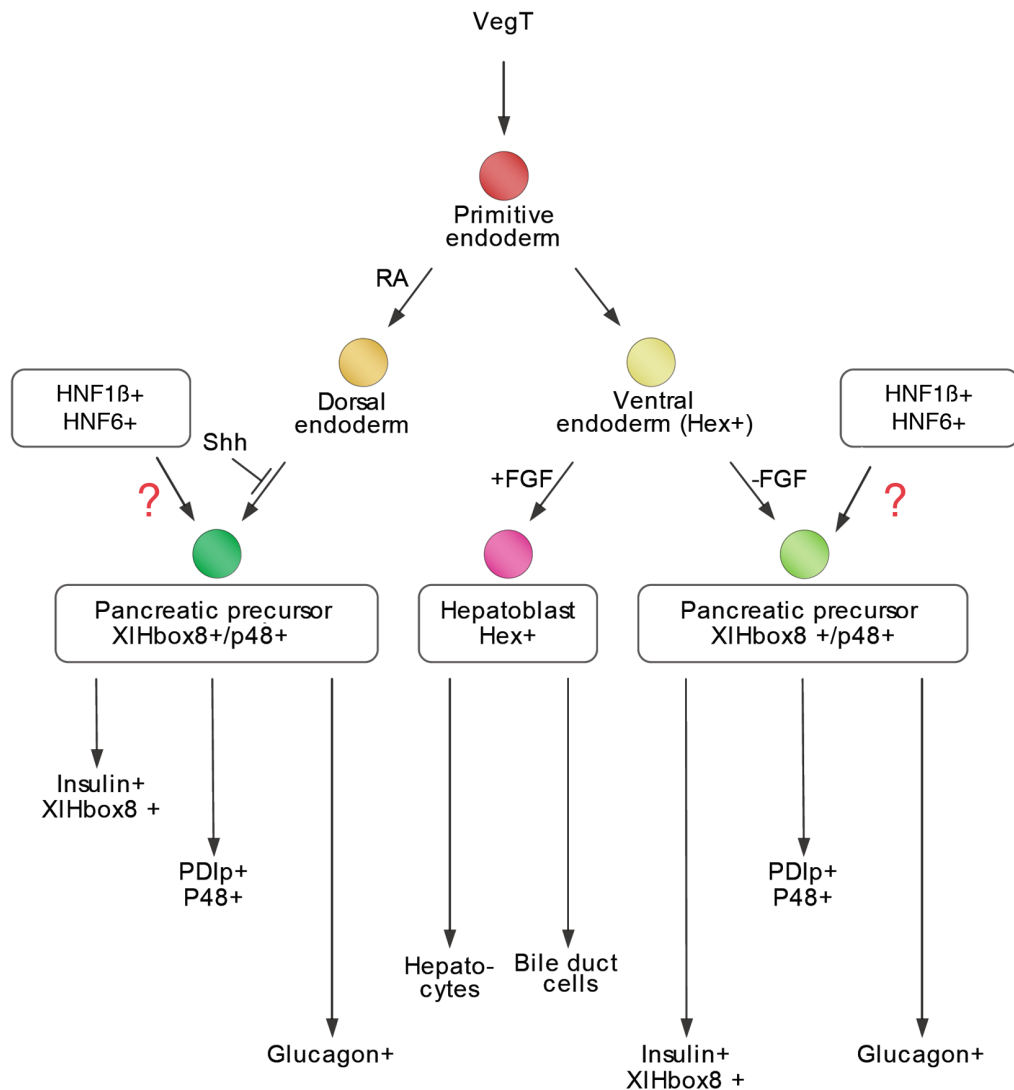


Figure 1.5 Regulatory factors directing pancreatic lineage specification in *Xenopus laevis*. A simplified model for the role of the major transcription factors and signalling pathways involved in pancreatic lineage determination. Circles indicate cell subtypes. Boxes state transcription factors that are required for cell fate determination. Arrows indicate directions of cell lineages that are specified according to the expressed marker gene (s). Different arrow lengths indicate the relative time point of final differentiation modulus after precursor cell determination. Blunt lines indicate inhibition of particular cell lineages. Question marks indicate instances where gene (s) in particular lineage determination is not known in *Xenopus laevis* (modified after Pieler and Chen, 2006).

revealed that the homeobox contains a helix- turn- helix motif (HTH), but which differs from other homeobox proteins by an extension of 21 amino acids between the second and third helix (Bach et al., 1991) and which was suggested to stabilize DNA- binding (Finney et al., 1990). The POU- like DNA binding motif is formed by five helices, similar to the POU DNA binding domain, and is therefore also referred as pseudo- POU structure (Kissinger et al., 1990). Apart from this human HNF1β-A form, two additional human iso-

forms were identified, namely HNF1 β - B and HNF1 β - C (Tronche and Yaniv, 1992). In this respect, HNF1 β - C that lacks the C- terminal transactivation domain might function as an endogenous dominant negative variant of the transcription factor (Bach and Yaniv, 1993). HNF1 β and the closely related HNF1 α bind to identical DNA binding sites as homo- or heterodimers (g/aGTTAATNATTAACc/a; Rey-Campos et al., 1991) but it is unclear which protein region is preferred for either interaction. The dimerisation process is promoted by the dimerisation cofactor DCoH. DCoH does not bind to the DNA but stabilizes the structure of the HNF1 dimer, thereby enhancing interaction with nucleic acids (Cerenghini, 1996). Subsequent studies in mice specified its expression profile during development to the extraembryonic visceral endoderm and later to the definitive endoderm where it is expressed in cells of the neural tube and of the foregut epithelium, including the hepatic and pancreatic primordia. Along the gut tube, differential HNF1 β expression was detectable in the gallbladder, duodenum and both pancreatic anlagen at stage E8.5. Here, HNF1 β expression was detectable in the Pdx1-positive epithelium of the budding pancreatic rudiments, where it became restricted to the developing duct cells, excluded from acinar or endocrine cells, in the branching pancreatic epithelium (E12.5). In adult mice, HNF1 β was transcribed in the epithelial cells of liver, genital tract, kidney, pancreas and lung (Barbacci et al., 1999; Reber et al., 2001).

HNF1 β -deficient mice died before gastrulation due to defective formation of the visceral endoderm. This lethality was prevented by generation of HNF1 β -null embryos with a wildtype (WT) extraembryonic endoderm using tetraploid embryo complementation (Barbacci et al., 1999). These tetraploid HNF1 β deficient mice were completely devoid of ventral pancreatic structures and demonstrated a severe hypoplasia of dorsal pancreas (Haumaitre et al., 2005). Interestingly, inhibited pancreatic development upon HNF1 β depletion phenocopied effects caused by impaired expression of the pancreatic progenitor marker Pdx1 (Offield et al., 1996) and Ptf1a/p48 (Kawaguchi et al., 2002). Therefore, data obtained from studies in knockout mice support the idea that the transcription factor HNF1 β functions as an upstream regulator of Pdx1 and p48. HNF1 β -hypomorphic zebrafish mutants showed a similar phenotype regarding pancreatic agenesis, suggesting that HNF1 β function during vertebrate development is conserved (Sun and Hopkins, 2001).

In 1994, the *Xenopus laevis* HNF1 β homologue was isolated and its expression traced during different stages of embryogenesis (Demartis et al., 1994). HNF1 β expression was activated after mid blastula transition (MBT) in ecto- and endoderm as well as later in the mesoderm. In early tadpole stages, HNF1 β transcripts were found in the foregut marking the prospective hepatic and pancreatic domain. In adult tissues, HNF1 β transcripts were detected abundantly in liver, kidney, digestive tract and lung, but also in the pancreas (Demartis et al., 1994; Vignali et al., 2000).

HNF1 β regulates a gene expression cascade essential for differentiation of epithelial cells lining the ducts. In 2002, Clotman et al. revealed that one of the upstream regulators of HNF1 β in biliary duct differentiation is the onecut 1 transcription factor HNF6 (Clotman et al., 2002; Coffinier et al., 2002). An additional link between HNF1 β and HNF6 was discovered regarding endocrine cell differentiation as both **were reported as Ngn3 upstream regulators associated with the diabetic disorder MODY6** (Maestro et al., 2003; Horikawa et al., 1997).

Conversely, it was revealed that the mouse HNF6 gene contained an **intronic HNF1 β binding site with high potency to activate transcription of a reporter construct *in vitro***. These data located HNF1 β upstream of HNF6 in the regulation hierarchy (Poll et al., 2006).

1.2.2.3 The role of HNF6 in pancreas development

The hepatic nuclear factor 6 (HNF6) belongs to the class of the cut- homeobox domain transcription factors. The name of the cut- transcription factor family is based on the previously identified CUT protein from *Drosophila melanogaster* (Blochlinger et al., 1988). All onecut family members contain a characteristic C-terminal DNA binding domain, composed of one CUT motif and one downstream HOMEBOX motif. The N-terminus differs between onecut family members classifying them into three subgroups: onecut-1, 2 and 3 (OC-1, 2 and 3).

HNF6 contains one CUT DNA binding motif, therefore also called onecut-1 (OC-1), that functions together or independent with the downstreamHOMEBOX. Beside onecut-1, there are two paralogues known in mice and humans, namely onecut-2 (OC-2) and onecut-3 (OC-3) that share common expression domains with OC-1, but play different or partially redundant roles in organogenesis (Jaquemin et al., 1999; Vanhorenbeeck et al., 2007).

HNF6/ OC-1 was originally identified in rat as liver enriched transcription factor binding to a gene involved in glucose metabolism (Lemaigre et al., 1996). Studies on its temporal and spatial expression profile in mouse embryogenesis reported an early onset of expression in the developing nervous system and in endoderm derivatives like liver and pancreas at E8.0 (Landry et al., 1997). **In the pancreas, HNF6 transcripts were detectable next to HNF1 β in the Pdx1 positive epithelium of the developing foregut.** Therefore HNF6 expression in the anterior endoderm was present in all pancreatic progenitor cells prior to pancreatic bud formation. Later, HNF6 RNA became restricted to the pancreatic acinar and duct cells (Pierreux et al., 2006). In the adult organism HNF6 expression was evident in the liver, brain, testis, spleen and pancreas (Lemaigre et al., 1996; Hong et al., 2002).

In accordance with its early endodermal expression, gene knockout studies in mice demonstrated that HNF6 plays an important role in liver and biliary duct specification (Clotman et al., 2005), as well as in pancreas organogenesis (Poll et al., 2006). Studies in knockout mice reported that lack of HNF6 caused a delay in Pdx1 induction at E9 resulting in pancreatic hypoplasia. Promotor studies confirmed that the Pdx1 promotor contained HNF6 site (Jacquemin et al., 2003a). In addition to its role during early pancreas organogenesis it was also shown that HNF6 stimulated the promotor of the endocrine precursor marker Ngn3 and maintained its activity for proper endocrine cell differentiation and islet formation (Jacquemin et al., 2000; Maestro et al., 2003).

As the *Xenopus laevis* homologue was not yet identified, it would be of further interest to identify the homologue and to elucidate its function during *Xenopus laevis* organogenesis.

1.3 Screening for novel pancreas specific marker genes in *Xenopus laevis*

In an attempt to identify new molecular markers for pancreas development, a cDNA library screen was performed of an adult pancreas cDNA library from *Xenopus laevis* (Afelik et al., 2004). The subtractive filter hybridization screen excluded all clones corresponding to digestive enzymes. Clones that were negative in the filter hybridisation screen were randomly picked and used for expression analysis in *Xenopus laevis* embryos. One of them was clone number 150 ("pancreas clone 150"/ p150), that showed pancreas expression at tadpole stage 41. Hence, p150 became interesting for subsequent analysis of pancreas organogenesis.

1.4 *Xenopus laevis* as experimental model system

In this study, the African clawed frog *Xenopus laevis* is used as model system to study organogenesis. The possibility of easy *in vitro* fertilization, high number of progeny and fast external development allows rapid and effective manipulation by microinjection and chemical treatment. Existing cell fate maps allow to target microinjected substances to a predicted region of interest at later developmental stages. In addition, the generation of embryonic tissue explants and transplantation assays can serve as important tools to analyze the influence of extrinsic factors on cell fate determination (Vize et al., 1991).

1.5 Aims of this study

Pancreas formation from the gut epithelium requires the activation of a genetic program to specify organ precursor cells. It was shown that early RA- signalling is essential for pancreas specification and early endocrine cell fate determination. Pancreas formation is initiated with the onset of the expression of the transcription factors Pdx1/XIHbox8 and Ptf1a/p48. The two transcription factors HNF1 β and HNF6 were described as putative upstream regulators of Pdx1/XIHbox8 and Ptf1/P48 in mouse. However in *Xenopus laevis* Pdx1/XIHbox8 and Ptf1/P48 regulation remains obscure.

This study focused on the identification of regulatory mechanism, that link early RA- signalling to later expression of Pdx1/ XIHbox8 and Ptf1a/ p48 during organogenesis. Therefore, we analysed the two transcription factors HNF1 β and HNF6. This included the isolation of the *Xenopus laevis* HNF6 homologue, the generation of its temporal and spatial expression profile and primary functional analysis by ectopic expression within the endoderm. The HNF1 β expression profile was refined and its role during pancreas development characterised by loss- and gain of function approaches. As HNF1 β was known to be a RA downstream target in the nervous system (Hernandez et al., 2004), it was of further interest how RA influenced HNF1 β expression within the endoderm. Therefore, RA- signalling was activated and inhibited in whole embryos and in endodermal explants. Furthermore, the novel putative pancreas specific marker gene p150 was analysed regarding its expression and its functional analysis was approached by loss- and gain of function studies. In addition, protein structure and biochemical interactions of this undescribed protein were analysed in collaboration with the group of Muhle-Goll (EMBL, Heidelberg).

2 Materials and Methods

2.1 Materials

2.1.1 Chemicals:

Basic chemicals used in this study were obtained from companies Fluka, Baker, Sigma-Aldrich, Roth and Merck in high purity grade (p.A.). Special chemicals were obtained from Roche Diagnostics, Fluka, Sigma-Aldrich and Serva.

2.1.2 Buffers and solutions

All media and buffer solutions were made as described in (Sambrook et al., 1989). If not stated differently solutions were made in dH₂O and autoclaved for 20 min at 120°C. Heat sensitive chemicals were filtersterilized (0.2µm, Sartorius).

2.1.3 Enzymes

DNaseI (10 U/µl)	Biozyme, Cardiff (UK)
RNase Out (40U/µl)	Invitrogen, Karlsruhe
RNaseT1 (R-8251) (2000 U/µl)	Sigma-Aldrich, Deisenhofen
RNaseA (R-5000) (10 mg/ml)	Sigma-Aldrich, Deisenhofen
Restriction enzymes (10 U/µl)	MBI-Fermentas, St. Leon-Rot
Pyrophosphatase (0.1 U/µl)	MBI-Fermentas, St. Leon-Rot
T4 DNA- ligase (3 U/µl)	Promega Germany, Mannheim
Sp6 RNA- polymerase (50 U/µl)	Stratagene GmBH, Heidelberg
T3 RNA- polymerase (50 U/µl)	Stratagene GmBH, Heidelberg
T7 RNA- polymerase (50 U/µl)	Stratagene GmBH, Heidelberg
GoTaq Flexi DNA-Polymerase (50 U/µl)	Promega Germany, Mannheim
High Fidelity Polymerase Mix	MBI-Fermentas, St. Leon-Rot
PowerScript ReverseTranscriptase (50 U/µl)	BD Bioscience Clontech, Heidelberg
Lysozyme (10 mg/ml)	Invitrogen, Karlsruhe
Proteinase K (20 mg/ml)	Merck KGaA, Darmstadt
AcTEV protease (10U/µl)	Invitrogen, Karlsruhe

2.1.4 Reaction and purification kits

mMESSAGE mMACHINE™ SP6, T7, T3	Ambion Ltd., Huntingdon (UK)
ECL+ plus Western Blotting Detection Kit	Applied Bioscience GmbH, Weiterstadt
SMART™ RACE cDNA Amplification Kit	BD Bioscience Clontech, Heidelberg
TNT®-coupled Reticulocyte Lysate System	Promega Germany, Mannheim

Illustra™ plasmid spin Mini Kit	GE healthcare, Buckinghamshire (UK)
Illustra™ GFX PCR DNA and Gel Band purification Kit	GE healthcare, Buckinghamshire (UK)
Illustra™ RNAspin Mini Kit	GE healthcare, Buckinghamshire (UK)
Plasmid Midi purification Kit	Quiagen GmbH, Hilden
pGEM®-T and pGEM®-T Easy Vector Systems	Promega Germany, Mannheim
AminoLink® Plus Immobilisation Kit	PIERCE, Rockford (US)
High fidelity polymerase Kit	MBI-Fermentas
Big Dye Terminator v.1.1 Cycle Sequenceing Kit	Applied Biosystems, Weiterstadt

2.1.5 Antibodies

Sheep- anti- Digoxigenin- AP (11093274910)	Roche Diagnostics, Mannheim
Sheep- anti- Fluoreszein- AP (11426338910)	Roche Diagnostics, Mannheim
Mouse- anti- FlagM2- FITC (F4049)	Sigma, Deisenhofen
Mouse- anti- human Hsp47 (SR-B470)	MoBiTec, Göttingen
Goat- anti- mouse- Alexa 594 (A-11005)	Invitrogen, Karlsruhe
Goat- anti- rabbit- HRP (111-035-003)	Dianova, Hamburg
Mouse- anti- FlagM2 (F 3195)	Sigma, Deisenhofen
Goat-anti-mouse-HRP (sc-2005)	SantaCruz
Goat-anti-rabbit-FITC	Sigma, Deisenhofen
Rabbit-anti-malectin	Biosystems, Göttingen

2.1.6 Antibiotics

Ampicillin	100 mg/ml in dH ₂ O (use 50 µg/ml)
Kanamycin	10 mg/ml in dH ₂ O (use 50 µg/ml)
Penicillin/ Streptomycin	10 000 U/ml penicillin, 10 mg/ml streptomycin in 0.9% (w/v) NaCl (use 10 U/ 10 µg/ml)

2.1.7 Oligonucleotides

2.1.7.1 Morpholinos

Morpholino antisense oligonucleotides were purchased from Gene Tools (Philomath, USA). Translation initiation site is marked in brackets.

name	sequence 5'→ 3'
XHNF1β- Mo1	GCAAAGGCGATAGCTTGGACAC(CAT)
XHNF1β- Mo2	C(CAT)TTTCAAGGGGAAAAAGAAGG
p150/malectin- Mo1	GCCCTAGTACTGTCCGGATGCTGAG-3'-(CAT)
p150/malectin- Mo2	TCCGGATGCTGAG(CAT)CTCCTCCAG
standard control (CoMo)	CCTCTTACCTCAGTTACAATTTATA

2.1.7.2 DNA oligonucleotides

Oligonucleotides used for DNA sequencing, RT-PCR and general cloning were obtained from Sigma-Genosys (Steinheim).

Oligonucleotides used for sequencing

name	sequence 5'→ 3'	aT
SP6	TTAGGTGACACTATAGAATAC	50°C
T3 (pCS2+)	ATTAACCCTCACTAAAGGGA	56°C
T7 (pCS2+)	TCTACGTAATACGACTCACTATAG	56°C
T7 (pGEM-T)	TAATACGACTCACTATAGGGCGA	56°C
CMV-for	CGCGCCTGCAGGTCGACACTA	58°C
CMV-rev	GCAAGGCGATTAAGTTGGGTA	58°C
P150/malectin-F2	GCTAAGCATCATACAGCC	56°C
P150/malectin-R1	GTGAGCCTGTACAGAGGTG	56°C

Oligonucleotides used for RT-PCR

name	sequence 5'→ 3'	aT, cycles
Histone H4- for	CGGGATAACATTCAGGGTATCACT	56°C, 26×
Histone H4- rev	ATCCATGGCGGTAAGTGTCTTCCT	
Insulin- for	GCCTCAGCGACCCAATAGAA	56°C, 32×
Insulin- rev	ATGGCTCTATGGATGCAGTG	
XPDIp- for	GGAGGAAAGAGGGACCAA	60°C, 30×
XPDIp- rev	GCGCCAGGGCAAAAGTG	
XIHbox8- for	AATCCACCAAATCCCACACCT	60°C, 32×
XIHbox8- rev	GCCTCAGCGACCCAATAGAA	
Xp48 RT-R	CATCAGTCCATGAGAGAG	60°C, 30×
Xp48 RT-F	GAGAAGCGACTGTCCAAG	
p150/malectin RT-5'	ACGACAACCCCAAAGTATG	60°C, 30×
p150/malectin RT-3'	CCGAAGGCCACCAGGAT	
HNF1β-RT F	TGTACAGTTTTCACAGCA	56°C, 30×
HNF1β-RT R	ATTATTCCTGTCAGCAGC	
HNF1β-Δ26 for	GAGGATCCATGGAGGGCTGC	56°C, 30×
HNF1β-Δ26 rev	GGCAGGCTCTGAGCAGGAAT	
CX397211_for	CATGAACGCTCAGCTGACTAT	56°C, 32×
CX397211_rev	GCACTGGGATGGGCATAGTG	
Xbra-for	GGATCGTTATCACCTCTG	56°C, 30×
Xbra-rev	GTGTAGTCTGTAGCAGCA	
N-tubulin F	ACACGGCATTGATCCTACAG	56°C, 32×
N-tubulin R	AGCTCCTTCGGTGTAAATGAC	
Cerberus F	TGCCCATGGAAACAAAAGTGC	56°C; 28×
Cerberus R	AGCGTCAGGTGGTTCAGGGTAA	
XHNF6 3' race	GTAGTTCGTGAACATGGTTTCGACT	56°C, 30×

Oligonucleotides used for cloning

name	sequence 5'→ 3'	aT
xHNF1 β _5'ClaI	ccATCGATATGGTGTCCAAGCTATCGCC	60°C, 30×
xHNF1 β _3'XhoI	ccgCTCGAGCCATGCTTGCAAAGGACACTG	
xHNF1 β -5'UTR ClaI	ccATCGATGGAGGAGTTCCTG	60°C, 30×
xHNF1 β -5'UTR BamHI-2	TGGGACAAGGGGATCCAGAT	
XI_HNF6-5'ClaI	ccATCGATATGAACGCTCAGCTGACTAT	60°C, 30×
XI_HNF6-3'XhoI	ccCTCGAGTCATGCTTTGGTACAAGTGCTT	
HNF6-Mo1 5'BamHI	cgGGATCCACGTTCCACCATGAACGCTC	60°C, 30×
HNF6 Mo1 3'ClaI	ccATCGATGATGCTCATGGCTCACCCCG	
Xp150-5'-ClaI	gcgATCGATATGCTCAGCATCCGGACAGTACTAG	60°C, 30×
Xp150-3'-XhoI	cgcCTCGAGTAATAGCCGACACAGACAGAAGAG	
N-flag-p150-5'BamHI	cgGGATCCATGCTCAGCATCCCGGAC	60°C, 30×
N-flag-p150-3'ClaI	ccATCGATCGCTAGACCAGATCCATGC	
P150-Mo2 BamHI	cgGGATCCCTGGAGGAGATGCTCAGCATC	60°C, 30×
Np150-GFP-ClaI	ccATCGATTTCGCTAGACCAGATCCATGCG	
dN-flag p150 5'XhoI	ccCTCGAGGATAAAGTGATGTGGGCAGTG	60°C, 30×
dN-flagp150 5XhoI	ccTCTAGATTATAGCCGACACAGACAGAAG	
N-flag-p150-5'BamHI	cgGGATCCATGCTCAGCATCCCGGAC	60°C, 30×
N-flag-p150-3'ClaI	ccATCGATCGCTAGACCAGATCCATGC	

2.1.8 Vector systems

2.1.8.1 pGEM[®]-T and pGEM[®]-T Easy vector system (Promega)

The pGEM[®]-T vector is a bacterial expression vector that allows non side directed cloning of PCR fragments. After PCR reaction the Taq-DNA polymerase adds a poly-Adenine (A) stretch to the 5'-end during a final elongation step (10 min, 72°C). This poly-A stretch can pair to an overhanging Thymidine (T) residue at the 3'end of the vector thereby improving insertion efficiency. An additional advantage of the system is the possibility of IPTG enhanced blue-white screening of positive clones. The insertion of a DNA fragment leads to destruction of an LacZ cassette resulting in white colonies on the LB^{Amp} agar.

2.1.8.2 pCS2+ vector and derivatives

The pCS2+ expression vector (Rupp et al., 1994; Turner und Weintraub, 1994), a derivative of the pBluescript II KS+ vector, was used for site directed cloning of open reading frames (ORF) for overexpression analysis. 5' and 3' untranslated regions (UTR) were excluded to prevent translational regulation in the embryo. pCS2+ derivatives like the inducible variants containing a glucocorticoid receptor binding site (GR) pCS2+-GR, pCS2+-EngGR, pCS2+VP16GR (Yonglong Chen, unpublished) as well as pCS2+- Flag, pCS2+myc-GFP were used.

2.1.8.3 pETZ2-9d

This prokaryotic expression vector contains a negative charged 6× His-tag that allows affinity purification of fusion proteins over a Ni²⁺ matrix. In addition the vector encodes a SET 2 (soluble enhancement tag, “Z 2”) carrier, a short amino acid sequence that improves solubility of a fusion protein. To remove the tag after purification, a TEV protease cleavage site (aa DNLYFQ) is located between the 6× His-tag/ Z2-carrier and the protein of interest. Expression is controlled by the IPTG inducible LacO-operon. As expression efficiency varies between constructs optimal IPTG concentration and protein expression is optimized in a time course experiment. (Günther Stier, EMBL Heidelberg; http://www.embl-heidelberg.de/ExternalInfo/geerlof/draft_frames/index.html)

2.1.9 Constructs

- HNF1β- WT: The ORF of HNF1β (1686 bp) was isolated by RT- PCR from stage 39 total RNA extracts using primers xHNF1β_5'ClaI: ccATCGATATGGTGTC-CAAGCTATCGCC and xHNF1β_3'XhoI: ccgCTCGAGCCATGCTTGCAAAG-GACACTG and fused into ClaI and XhoI restriction sites of the pCS2+ vector. This construct was used for overexpression analysis in embryos. The plasmid was linearized with NotI and capRNA transcribed with Sp6 polymerase.

- HNF1β- GR: The ORF of HNF1β was PCR amplified from the HNF1β-WT construct using the primers xHNF1β_5'ClaI and HNF1β_3'XhoI and fused to the 5'end of the ligand binding domain of the glucocorticoid receptor (GR). Therefore pCS2±GR vector was restricted using ClaI and XhoI and the ORF fused inframe to the GR domain (810 bp). This dexamethason inducible construct was used to analyse time point specific function of HNF1β in embryos. The plasmid was linearized with NotI and capRNA transcribed with Sp6 polymerase.

- HNF1β- EngGR: The ORF of HNF1β was PCR amplified from the HNF1β-WT construct using the primers xHNF1β_5'ClaI and HNF1β_3'Xho and fused to the 5'end of the Engrailed repressor domain. Therefore pCS2±EngGR vector was restricted using ClaI and XhoI and the ORF fused inframe to the EngGR domain (ca.1.6kb). This dexamethason inducible construct was used to analyse time point specific function of HNF1β in embryos. The plasmid was linearized with NotI and capRNA transcribed with Sp6 polymerase.

- **HNF1 β -VP16GR:** The ORF of HNF1 β was PCR amplified from the HNF1 β -WT construct using the primers xHNF1 β _5'ClaI and HNF1 β _3'XhoI and fused to the 5'end of the VP16 activation domain. Therefore pCS2 \pm VP16GR vector was restricted using ClaI and XhoI and the ORF fused inframe to the GR domain (ca. 1210 bp). This dexamethason inducible construct was used to analyse time point specific function of HNF1 β in embryos. The plasmid was linearized with NotI and capRNA transcribed with Sp6 polymerase.

- **HNF1 β - 5'UTR- GFP:** A fragment of from the HNF1 β 5'end containing the corresponding sequence of HNF1 β - Mo1 and HNF1 β - Mo2 was amplified using the HNF1 β -5'UTR-BamHI and HNF1 β -5'UTR-ClaI. The vector pCS2-myc-GFP was restricted with BamHI and ClaI and the fragment, including 60 bp of HNF1 β 5'UTR and 42 bp of HNF1 β ORF, fused inframe to the 5'end of myc-GFP coding sequence. This construct was used to test *in vivo* efficiency of translational inhibition by morpholino binding. The plasmid was linearized with NotI and capRNA transcribed with Sp6 polymerase.

- **XHNF6- pGEMT- E:** *Xenopus laevis* XHNF6 was isolated by RT-PCR from stage 37 OligodT amplified cDNA using the primers CX397211 for: CATGAACGCTCAGCTGACTAT and XHNF6 3'end-2: CGGAGTTTAAGTTTCTGGGGTTT (58°C, 40 \times) and cloned into pGEMT- E. This construct, containing the complete ORF (1482 bp) and 34 bp of the 3'UTR. This construct was used for asRNA transcription. The plasmid was linearised with AatII and asRNA transcribed with SP6 polymerase.

- **XHNF6- WT:** The XHNF6 ORF was PCR amplified out of the XHNF6/pGEMT-E construct using the primers XI_XHNF6 5'ClaI: ccATCGATATGAACGCTCAGCTGACTAT and XI_XHNF6 3'XhoI: ccCTCGAGTCATGCTTTGGTACAAGTGCTT and cloned into the ClaI and XhoI restriction sites of the pCS2+ vector. This construct was used for overexpression analysis of XHNF6 in embryos. The plasmid was linearized with XbaI and capRNA transcribed with Sp6 polymerase.

- **XHNF6- Mo1- GFP:** A fragment of 73 bp of XHNF6 5'end flanking the ATG codon, was PCR amplified using the primers XHNF6-Mo1 5'BamHI: cgGGATCCACGTTCCACCATGAACGCTCAGCTGAC and XHNF6-Mo1 3'ClaI: ccATCGATGATGCTCATGGCTCAC CCGTG. The vector pCS2 \pm myc-GFP was restricted with BamHI and ClaI and the fragment fused inframe to the 5'end of myc-GFP coding sequence. This construct was used to test *in vivo* efficiency of translational inhibition by morpholino binding. Plasmid was linearized with NotI and capRNA transcribed with Sp6 polymerase.

- **malectin:** The ORF of p150/ malectin (831 bp) was PCR amplified out of the original cDNA library clone pBK-CMV-p150 using the oligonucleotides Xp150-5'ClaI: gcgATC-GATATGCTCAGCATCCGGACAGTACTAG and Xp150-3'XhoI: cgCCTCGAGTAAT-AGCCGACACAGACAGAAGAG and cloned into ClaI and XhoI restriction sides of the pCS2+ vector. This construct was used for overexpression experiments in embryos.

- **ΔN- flag- malectin:** A fragment lacking the N-terminal signal peptide (aa 1-30 = dN-p150) was PCR amplified out of the p150- ORF construct using the primers chd-flag-5'-xhoI: cc-CTCGAGGATAAAGTGATGTGGGCAGTG and chd-flag-3'-XbaI: ccTCTAGATTATA-GCCGACACAGACAGAAG cloned into XhoI and XbaI restriction sides of the pCS2+/flag vector. This construct was used for analysis of the intracellular localisation of malectin.

- **N-flag-malectin:** The N-terminal signal peptide N-p150 (aa 1-30) was PCR amplified from the p150-ORF construct using the primers N-flag-p150-5'BamHI: cgGGATCCATGCTCAGCATCCCGGAC and N-flag-p150-3'ClaI: ccATCGATCGCTAGACCAGATC-CATGC and fused inframe into BamHI and ClaI restriction sides of the dN-flag-p150 construct. This construct was used for intracellular localisation of malectin.

- **malectin-Mo1-GFP:** The N-terminal signal peptide was PCR amplified from the N-flag-p150 construct using primers N-flag-p150-5'BamHI: cgGGATCCATGCTCAGCATCC-CGGAC and Np150-GFP-ClaI: ccATCGATTCGCTAGACCAGATCCATGCG. The fragment was restricted with BamHI and ClaI and fused inframe into the restriction sides of mycGFP-pCS2+. This construct was used to test *in vivo* efficiency of translational inhibition by morpholino binding. The plasmid was linearized with NotI and capRNA was transcribed with Sp6 polymerase.

- **malectin-Mo2-GFP:** The 5'UTR sequence (102 bp) of p150 was PCR amplified out of the original pBK-CMV-p150 using the primers P150-Mo2 BamHI cgGGATCCTGGAGGA-GATGCTCAGCATC and Np150-GFP-ClaI. An EST- alignment showed in 50% of compared sequences 3 mismatches for the Mo2 sequence. The fragment was fused inframe into the restriction side of mycGFP-pCS2+. This construct was used to test *in vivo* and *in vitro* inhibitory efficiency of p150-Mo2. The plasmid was linearised with and capRNA was transcribed with Sp6 polymerase.

- **HNF1β-full- pGEMT- 7Z:** This construct, obtained from Robert Vignali (Demartis et al., 1994), contains the full-length cDNA sequence of HNF1β (LFB3; NCBI: X76052) including 3'and 5'UTR. This construct was only used for asRNA synthesis, since it includes a point mutation in the ORF at nt 1414 (T- insertion).

Constructs used for antisense and sense „capRNA“ transcription

construct	restriction	polymerase	reference
XIHbox8- pGEM-T	NotI	T7	Afelik et al., 2006
Xp48- pGEM-T	NotI	T7	Chen et al., 2003
XPDIp- pBK-CMV	BamHI	T7	Afelik et al., 2004
Insulin- pGEM-T	NotI	T7	Chen et al., 2004
p150/ malectin- pBK-CMV	BamHI	T7	Schallus et al., 2008
HNF1 β - pGEMT- 7Z (pXLFB3)	KpnI	T7	Vignali et al., 2000
XHNF6- pGEM-T Easy	AatII	Sp6	Jäckh, unpublished
Trypsin- pCS2+	BamHI	T7	Afelik et al., 2004
eGFP-pCS2+ (capRNA)	NotI	Sp6	Klymkowsky, unpublished
β -galactosidase-pCS2+ (capRNA)	NotI	Sp6	Bier et al., 1989

2.1.10 Experimental organisms

<i>Xenopus laevis</i> :	Albino or pigmented African clawed frogs (family <i>Pipidae</i> , subfamily <i>Xenopinae</i>) were purchased from NASCO (Ft. Atkinson, Wisconsin, USA). Embryos were staged according to Nieuwkoop and Faber (1967).
<i>Escherichia coli</i> :	XL1-Blue I : recA1, endA1, gyrA96, thi-1, hsdR17, supE44, relA1, lac [F' proAB, lacI ^q Z Δ M15, Tn10(Tet ^r)] ^c (Bullock et al., 1987). Stratagene GmbH, Heidelberg BL21(DE3) : F' dcm ompT hsdS(r _B m _B) gal λ (DE3)
NIH 3T3: swiss embryonic mouse fibroblasts	obtained from DSMZ (Deutsche Sammlung von Mikroorganismen und Zellkulturen GmbH); stock stored in liquid N ₂ ; adherent growth , cultured in DMEM with 10% FCS

2.1.11 Technical equipment

Regular laboratory material was obtained from Eppendorf AG (Hamburg), BD Falcon (Heidelberg), Greiner Bio-One GmbH (Frickenhausen), Schütt Labortechnik (Göttingen), Schott (Mainz), Biometra GmbH (Göttingen), Corning GmbH-Corning International (Wiesbaden).

Cell culture

Cell Casy Counter	Schärfe System Reutlingen
CO ₂ Incubator Heraeus BBD 6220	Kendro, Langenselbold
Liquid nitrogen container Arpege 140	Air Liquide, Düsseldorf

Histology

Vibratom Leica VT1000 S	Leica Mikrosystems, Bensheim
Mikrotom Leica RM2065	Leica Mikrosystems, Bensheim
Gastromaster mikrodissector	XENOTEK Engineering, Belleville (USA)

Micromanipulation

Gastromaster	Xenotec Ltd., Corona del Mar, Ca, USA
Microinjector PV820	Harry Fein World Precision Instruments, Berlin
Needlepuller PN-30	Narishige, Japan
Glass kapillaries	GC100F-10, Harvard apparatus (Electromedical Instruments, Pangbourne Reading, Clark, England)

PCR

T3 Thermocycler	Biometra, Göttingen
-----------------	---------------------

Microscopes

Fluorescence Mikroskop Axioplan 2	Carl Zeiss AG, Oberkochen
Mikroskop Axioskop	Carl Zeiss AG, Oberkochen
Confocal Mikroskop Zeiss LSM 510 META	Carl Zeiss AG, Oberkochen
Confocal microscope Leica DRM IRE2 TCS SP2	Leica, Bensheim
Stereomikroskop SZX12	Olympus Microscopy, Hamburg
Stereomikroskop Stemi 2000	Carl Zeiss AG, Oberkochen
Camera MC 80	Carl Zeiss AG, Oberkochen
DXC-950P Colour Video Camera	Carl Zeiss AG, Oberkochen
Inverse Microscopee Axiovert 25	Carl Zeiss AG, Oberkochen

2.1.12 Hard- and Software

Microsoft Office (Word, Exel, Powerpoint)
 Adobe Creative Suite CS (Photoshop, Illustrator, Indesign)
 MacMolly Tetra, ImageJ, CLC free Workbench
 Apple- Power Book G4

***In vivo* staining of albino embryos**

To visualize cleavage stages of albino embryos, they were stained for 3 min with the vital colour dye Nile Blue after cysteination.

Nile Blue: 0.01% (w/v) Nile Blue chloride, 50 mM Na₂HPO₄*2H₂O, 50 mM NaH₂PO₄* H₂O, pH 7.8 in H₂O; mix oN and filter

2.2.1.2 Microinjection

Gene function analysis was performed by injection of morpholino antisense oligonucleotides or capped messenger RNA (capRNA) into *Xenopus laevis* embryos. Injection needles were prepared from glass capillaries using a needle puller. The sample to be injected was filled into a needle with microloading tips (Eppendorf) prior to be clamped to an air pressure regulated microinjector. **By cutting the needle tip carefully with forceps, the drop size was scaled to 2 nl using a scale (d= 0.2 mm ≈ 4.2 nl; d= 0.25 mm ≈ 8.2 nl) . Just before injection embryos were transferred to injection buffer containing 1% Ficoll. Its higher density prevents diffusion of injected material out of the embryo. Injection was performed under high pressure (2000 hPa) and short injection time (0.1- 0.3 s) on a glass slide with 1.6× objective enlargement. Embryos were kept in injection buffer for 1 hr retransferred to 0.1× MBS and cultured at 12- 18°C till desired developmental stage. To prevent embryo pigmentation 5% PTU was added to 0.1× MBS (40 µl/ 50 ml).**

10% (w/v) Ficoll-400: in dH₂O, filter sterilize, store at -20°C; Sigma
 Injection buffer: 1× MBS, 1% (v/v) Ficoll; Sigma
 N-phenylthiourea 5% PTU in DMSO; Sigma

2.2.1.3 Embryo fixation

When embryos reached the desired developmental stage, they were collected in 5 ml screw-cup tubes, fixed with 1× MEMFA for 1 hr on a shaker, dehydrated using 100% EtOH and stored until usage at -20°C.

10× MEM: 1M MOPS, 20 mM EGTA, 10 mM MgSO₄, pH 7.4; filter sterilize, keep dark
 1× MEMFA: 1× MEM, 4% (v/v) formaldehyde, prepare fresh!

2.2.1.4 β -galactosidase staining

Coinjection of β -galactosidase capRNA was used as cell lineage tracer. For detection embryos were fixed in 1× MEMFA for 20 min and incubated with the staining solution including β -galactosidase substrate X-Gal. When embryos showed light blue staining, colouring was stopped, embryos fixed and stored in 100% EtOH for WMISH.

step	buffer	time	repeat
1	1× MEMFA	20 min	1×
2	1× PBS	10 min	3×
3	colour solution	3 hr or oN at 4°C	1×
4	1× PBS	10 min	3×
5	1× MEMFA	40 min	1×

X-Gal:	40 mg/ml in DMSO or formamid, aliquot and store -20°C
colour solution:	1 mg/ml X-Gal, 2 mM MgCl ₂ , 5 mM K ₄ Fe(CN) ₆ , 5 mM K ₃ Fe (CN) ₆ in 1× PBS
K ₄ Fe(CN) ₆ :	0.5 M in dH ₂ O, keep dark at RT, toxic
K ₃ Fe(CN) ₆ :	0.5 M in dH ₂ O, keep dark at RT, toxic

2.2.1.5 Embryonic explant preparation

Animal cap explants

Embryos were injected at 2 to 4-cell stage into the animal pole of all blastomeres. At blastula stage 7-8 the vitellin membrane was removed with forceps and the blastocoel roof dissected using a gastromaster apparatus, equipped with a microsurgery tip (400-500 μ m width). Animal cap explants were transferred onto an agarose-coated petri dish and cultured in 0.8× MBS/ 0.1× Pen-Strep at 16°C till control siblings reached the desired developmental stage. Chemical treatments were performed as described in 2.2.1.7.

Agarose dish	0.7% agarose in 0.8× MBS (Ø 90 mm)
--------------	------------------------------------

Endoderm explants

Whole endoderm explants were isolated from stage 10.5 by removing the surrounding ecto- and mesodermal tissue using forceps and transferring the endodermal cone to an 0.7% agarose dish. Dorsal (DE) and ventral (VE) endoderm were distinguished according to the position of the blastopore lip. Explants were cultured in 1× MBS till control siblings reached the desired developmental stage.

2.2.1.6 Chemical treatments of embryos and explants

Retinoic acid (RA)

Whole embryos stage 8-9, endodermal explants or animal caps were incubated in 5 μ M RA (all-*trans*-RA) in corresponding buffer for 1 hr. After treatment, embryos and explants were cultured in their buffer till control siblings reached the desired developmental stage. Control treatment was done with corresponding amount of EtOH (Chen et al., 2004).

RA: 10 mM stock in 100% EtOH, store at -20°C, light sensitive; Sigma

BMS453

Whole embryos stage 8-9, endodermal explants or animal caps were incubated in 1 μ M BMS453 for 1 hr. After treatment, embryos and explants were cultured in 0.8 \times MBS till control siblings reached the desired developmental stage. Control treatment was done corresponding amount of DMSO (Chen et al., 2004).

BMS 453: 10 mM stock in DMSO, store at -20°C, light sensitive;
gift from Bristol Myers Squibb

Dexamethason (Dex)

Proteins fused to the glucocorticoid receptor (GR) binding domain are immobilised in the cytoplasm by heat shock proteins. Dexamethason, a steroid hormone, competitively binds to the GR domain releasing the protein from its heat shock inhibitors.

Dex (1000 \times): 8 mg/ml in 100% EtOH, store at -20°C, dilute 1:1000;

2.2.2 Bacterial work

2.2.2.1 Generation of chemical competent cells

To obtain chemical competent cells (Hanahan et al., 1991), a 5 ml oN culture was inoculated and diluted into 300 ml prewarmed LB-medium in a 2 l Erlenmeyer flask, shaking at 220 rpm. When the culture reached $OD_{600} = 0.3$, cells were grown at 18°C until $OD_{600} = 0.4-0.5$ (exponential growth phase). The culture was split in 50 ml falcon tubes and centrifuged at 4°C and 6000 \times g for 10 min. Working on ice, the supernatant was decanted, the pellet resuspended in 15 ml prechilled transformation buffer and incubated on ice for 15 min. The suspension of three tubes was pooled and re-centrifuged for 5 min at 4°C, 6000 \times g. The pellet was resolved in 15 ml transformation buffer and supplied with 525 μ l DMSO, incubated on ice for 5 min and supplied again with 525 μ l DMSO. After an incubation of 5 min 200 μ l aliquots were shock-frozen in liquid nitrogen and stored at -80°C.

LB- Medium:	1% (w/v) Bacto-Trypton (Difco), 0.5% (w/v) Yeast extract (Difco), 1% (w/v) NaCl, pH 7.5.
Transformation buffer:	10 mM PIPES (pH 6.7 with KOH), 15 mM CaCl ₂ , 250 mM KCl, addition of +55 mM MnCl ₂ prior to usage

2.2.2.2 Chemical transformation of competent cells

An 200 µl cell aliquot was unfrozen on ice. 5-10 ng of plasmid- DNA or 1 µl ligation mixture were added and cells incubated for 30 min on ice. DNA uptake was induced upon heat shock at 42°C for 50 s followed by immediate incubation on ice for 3 min. Bacteria were directly spread onto prewarmed LB-agarose plates using small glass beads and incubated oN at 37°C in an incubator. LB-plates contained antibiotics for selection (see 2.1.6) and, in need of blue-white screening, they were preincubated at 37°C with 40 µl X-Gal and 100µl IPTG.

LB- Agar:	1.5% (w/v) Agar (Difco) in LB-media
X-Gal:	20 mg/ml X-Gal in Dimethylformamid, store -20°C; Sigma
IPTG:	100 mM IPTG in dH ₂ O, store -20°C; Roth

2.2.2.3 Glycerol stocks

A glycerol stock was made for long time storage of bacterial culture. 1 ml of oN culture was spin down for 2 min in a table centrifuge. The pellet was resuspended in 500 µl fresh LB-media. 250 µl of 100% glycerol was added and the solution mixed on a rotor for 10 min. The glycerol stock was stored at -80°C.

2.2.3 DNA work (according to Sambrook et al., 1989)

2.2.3.1 Native agarose gel electrophoresis

1%– 2% (w/v) agarose gels were prepared in 1× TAE and supplied with 0.5 µg/ml EtBr. Analytic samples were mixed on parafilm with a drop of DNA loading dye prior to loading the sample to the gel pocket. Gels were run in 1× TAE (8 min, 100 mA) in a home made horizontal electrophorese chamber. The negative charged DNA fragments migrate in an electric field from anode to the kathode thereby separating according to their size. Fragment sizes were estimated in comparison to a molecular standard marker (Low-, Middle-, High range ladder, MBI- Fermentas). Images were taken with a video documentation system (Chemidoc, Biorad).

Glycerol loading buffer:	10 mM Tris-HCl pH 7.5, 10 mM EDTA pH 8, 0.025% (w/v) Bromphenol blue, 0.025% (w/v) Xylencyanol, 30% (v/v) Glycerol 99%
50× TAE buffer:	2 M TrisHCl, 1M acetat, 0.1 M EDTA
0.5 M EDTA	0.5 M Na ₂ EDTA*2H ₂ O, pH 8

2.2.3.2 DNA purification

Mini plasmid purification

Small amounts of plasmid were isolated using the *Illustra™ plasmid spin Mini Kit* according to the manufacturers protocol. 5 ml bacterial culture was spin down, resuspended and lysed in an alkaline buffer including RNase A. After 5 min incubation at RT the reaction was stoped by addition of a neutralisation buffer. Precipitate including lipids and denatured proteins, was spin down for 10 min. The supernatant was applied to the column and spin down whereby DNA bound to the column matrix. Salts were washed away using a EtOH containing buffer. Finally the DNA was eluted from the column in 50 µl elution buffer (1M TrisHCL, pH 8) or dH₂O. Plasmids were confirmed by sequencing and stored at -20°C.

Midi plasmid purification

To obtain high plasmid amounts, large scale plasmid preparation was done using *Plasmid Midi purification Kit* (Quiagen). 50 ml bacterial culture were spin down at 6000 × g (Heraeus megafuge 1.0 R) for 15 min. The pellet was resuspended in an alkaline lysis buffer and incubated for 5 min. To eliminate cell debries and proteins after addition of 5 ml neutralisation buffer, the solution was filtered before column application (Sartorius, grade 3 Hw). The column was emptied by gravity and washed twice with 10 ml highsalt/ EtOH washing buffer. DNA was eluted by 5 ml elution buffer, precipitated by addition of 3.5 ml Isopropanol and pelleted for 30 min. at 15000 × g at 4°C (Heraeus megafuge 1.0 R). The supernatant was discarded, the pellet was carefully transferred into a 1.5 ml eppendorf tube, washed with 70% EtOH, recentrifuged for 10 min and the pellet finally airdried (37°C). After re-suspension in 50 µl elution buffer, the concentration was measured, adjusted to 1 µg/µl and the sample stored at -20°C.

DNA purification from enzymatic reaction

DNA fragments from enzymatic reactions were purified using the *Illustra™ GFX PCR DNA and Gel Band purification Kit* according to the manufacturers protocol. Samples were mixed with acetate containing buffer, applied to a glass fiber matrix column and spin down.

DNA bound to the matrix while proteins and salts were eliminated by EtOH containing wash buffer (10mM TrisHCl, pH 8.0, 1mM EDTA). DNA was eluted in 50 µl dH₂O and 1µl analysed on a agarosegel. Concentration was measured and samples stored at -20°C.

Agarosegelpurification of DNA fragments

DNA fragments from restriction digests or PCR amplification were isolated by gelextraction using the *Illustra™ GFX PCR DNA and Gel Band purification Kit* according to the manufacturers protocol. DNA was eluted in 50 µl dH₂O. 1 µl of the sample was analysed on an agarosegel and the rest stored at -20°C until usage.

2.2.3.3 Measurement of nucleic acid concentration

The nucleic acid content of a solution was measured using a quarküvette and UV-spectrophotometer. The RNA/ DNA sample was diluted 1:50 in H₂O and measured at a wavelength of 260 nm.

$$O\Delta_{260} = 1: 50 \mu\text{g dsDNA}$$

$$O\Delta_{260} = 1: 40 \mu\text{g RNA}$$

Additionally the protein content of the sample was measured at OD₂₈₀ to estimate the purity of the sample. Protein contamination was excluded if the ratio of O Δ_{260} / OD₂₈₀ was 1.8 for DNA and 2.0 for RNA samples.

2.2.3.4 Polymerase chain reaction (PCR)

DNA fragments were specifically amplified using PCR (Mullis et al., 1987; Saiki et al., 1988). The *Taq*- DNA polymerase was used for general purpose. The *High fidelity polymerase Kit* was used for amplification of ORFs. The enzyme maintains a 3'→ 5' exonuclease “proof-reading” activity that reduces chances for point mutations during the amplification process. In addition, PCR was used to identify insert-positive bacterial clones (colony- PCR) after transformation. Single colonies were picked from the LB-plate, transferred to 100 µl LB-media (incl. antibiotic) in a 96-well plate and grown for 2.5 hr. Therefore 0.5 µl bacterial culture were used for a 25 µl PCR reaction.

reaction mix:	10 µl	5× reaction buffer incl. MgCl ₂
	1 µl	primer-mix (each 10µM)
	0.5 µl	25mM dNTPs
	1 µl	GoTag polymerase
	1 µl	template
	ad 50 µl	dH ₂ O

thermocycler program:	95 °C	2 min	(denaturation)
	95°C	45 s	(denaturation)
	*56°C	45 s	(annealing)
	**72°C	1-3 min	(synthesis)
	72°C	10 min	(final elongation)
	4°C	∞	(cooling)

*primer specific annealing temperature; **insert specific synthesis time (1 kb/min)

PCR products were analysed on a 1.5% agarose gel. In case of a colony- PCR, positive transformants were selected from the 96-well plate and grown for small or large scale plasmid purification.

25mM dNTPs: MBI Fermentas; 100 mM stock of dATP, dTTP, dGTP and dCTP were mixed in equal volumes, aliquoted and stored -20°C.

2.2.3.5 DNA sequencing

Correct DNA sequences were confirmed by sequencing (Sanger et al., 1977). The sequencing reaction was done according to the manufacturer's protocol *Big Dye Terminator Kit*.

Sequencing reaction:	300 ng	plasmid template
	0.8 µl	sequencing primer (10 µM)
	1.5 µl	"Seq- Mix"
	1.5 µl	"Seq- buffer"
	ad 10 µl	dH ₂ O

thermocycler program:	95°C	2 min	
	95°C	30 sec	× 25
	50°C	20 sec	
	60°C	4 min	
	4°C	∞	

DNA products were precipitated by addition of 1 µl 125 mM EDTA, 1 µl 3 M NaAc and 50 µl 100% EtOH. The sample was mixed, incubated for 5 min at RT and centrifuged for 15 min at max. speed in a table centrifuge. The supernatant was discarded, the pellet washed with 70% EtOH and centrifuged for 5 min at max. speed. The supernatant was removed entirely and the pellet air-dried at 37°C. The DNA pellet was resolved in 15 µl „HiDi“ formamid. Sequencing and documentation were performed at the internal service unit by Andreas Nolte using Abi Prism 3100 genetic analyzer (Applied Biosystems). Analysis

of the sequence read out was done using free available software: 4 Peaks, MacMolly Tetra Version 1.2 (Soft Gene GmbH, Berlin), CLC Free Workbench 4 as well as the NCBI BLAST (Altschul et al., 1997).

2.2.3.6 Plasmid linearization

Plasmids were linearized for *in vitro* sense and antisense RNA transcription (Sambrook et al., 1989).

reaction mix:	5-10 µg	plasmid
	5 µl	10× restriction buffer
	10 U	restriction enzyme
	ad 50 µl	dH ₂ O

The reaction was incubated oN at 37°C. Complete linearisation was confirmed by testing 1 µl on a 1% agarose gel. Linearized fragments were purified using *Illustra™ GFX PCR DNA and Gel Band purification Kit*. Elution was done in 50 µl dH₂O and samples used for *in vitro* RNA transcription.

2.2.3.7 Double restriction digest

For cloning purposes, DNA fragments and vectors were restricted with two differing enzymes resulting in overhanging „sticky“ ends.

reaction mix:	0.5-1 ng	DNA
	1 µl	restriction enzyme (10 U/µl)
	1 µl	restriction enzyme II (10 U/µl)
	5 µl	10 × restriction enzyme buffer
	ad 50 µl	dH ₂ O

The reaction mix was incubated oN at 37 °C, tested on a 1% agarose gel and the band of interest was purified with the gel- purification Kit. Double digest using two different enzymes at once could be performed using adequate enzyme amount and corresponding buffer condition (MBI-Fermentas online).

2.2.3.8 Ligation of DNA fragments

Nondirected ligation using the pGEM-T Easy vector

The reaction was setup according to the manufacturer protocol.

reaction mix:	10 ng	DNA insert
	0.5 μ l	vector
	0.5 μ l	ligase enzyme mix
	1 μ l	10 \times ligation buffer
	ad 10 μ l	dH ₂ O

Reaction was incubated for 2 hr at RT or 16°C oN prior to chemical transformation into *E.coli*.

Site directed ligation into pCS2+ and derivatives

Introduction of restricted DNA inserts into pCS2+ for cloning purposes was done using an T4 ligation reaction.

reaction mix:	10- 100 ng	DNA insert (restricted)
	10- 100 ng	pCS2+ vector (restricted)
	1 μ l	T4 ligase (3 U/ μ l)
	1 μ l	10 \times T4 ligase buffer
	ad 10 μ l	dH ₂ O

Reaction was incubated oN at 16°C prior to chemical transformation into *E.coli*.

2.2.4 RNA work

RNase free environment was assured by working on ice, using gloves, filter tips, autoclaved glas ware and solutions as well as DEPC- H₂O.

DEPC- H₂O: 0.1% (v/v) Diethylpyrocarbon in dH₂O, stirred oN at RT; autoclave

2.2.4.1 Total RNA extraction from embryos, adult tissues and explants

Total RNA was isolated from whole embryos, adult tissues and explants for semiquantitative RT-PCR analysis using the TRIzol Reagent (Invitrogen, Chomczynski, P. & Sacchi, N, 1987). RNA quality was analysed using Agilent 2100 Bioanalyzer (Agilent Technologies, Germany) prior to RT-PCR analysis.

RNA extraction from whole embryos

To analyse temporal gene expression patterns, total RNA was extracted and used in a semi-quantitative RT-PCR analysis (see 2.2.4.3). Five embryos were shock frozen in liquid nitrogen, homogenized in 400 µl TRIzol reagent (Invitrogen) using a syringe (Ø. 0.4 mm) and vortexed well. After a 5 min incubation at RT cell debris were spin down for 10 min (4 °C) and RNA containing supernatant was transferred into a clean eppendorf tube. 0.2 Vol chloroform were added, the mixture vortexed for 1 min, incubated at RT for 5 min and centrifuged for 10 min at 4 °C. The upper phase including soluble nucleic acids was transferred carefully to a clean tube and supplied again with 1 Vol chloroform, vortexed and centrifuged for 10 min at 4 °C. The lower organic phase including lipids and denatured proteins was discarded to phenol waste (fume hood). After the 2nd centrifugation, the aquatic phase was transferred into a new eppendorf tube to precipitate nucleic acids with Isopropanol for 2 hr at -20°C. Precipitate was pelleted for 30 min at 13.000 rpm at 4°C, washed with 75% EtOH, centrifuged for 10 min at 4°C and the pellet airdried before resolving it in 30 µl DEPC-H₂O. To obtain DNA- free samples an DNaseI digest was performed for 1h at 37°C by addition of 1/10 vol 10× DNase buffer and 1 µl DNaseI. The endonuclease, cutting single and double stranded DNA strands, was afterwards inactivated at 75°C for 15 min. The samples were stored at -20°C.

RNA extraction from adult tissues

Adult organs were dissected in the process of *Xenopus laevis* testis preparation. Organs were quickly washed in 1× MBS and shock frozen in liquid nitrogen and stored at -80°C. The tissue was grinded in liquid nitrogen in a grinder that was prewashed with 1M NaOH, 100% EtOH and DEPC-H₂O. The powder was filled into a clean 1.5 eppendorf tube. RNA extraction was done after addition of 1 ml TRIzol/ 100 mg tissue as previously described.

RNA extraction from explants

Total RNA extraction from 20 animal caps, 20 whole endoderm or 30 dissected endodermal explants was done after addition of 400 µl TRIzol as previously described.

2.2.4.2 RNA purification from enzymatic reactions

In vitro synthesised RNA was purified using the *Illustra™ RNAspin Mini Kit* according to the manufacturers protocol. The method is based on affinity chromatography by binding RNA to the column matrix. Samples were mixed with coupling buffer and 100% EtOH and the solution applied to the column. After washing away enzymes, salts and free ribonucleotides with a supplied washing buffer, RNA was eluted with 50 µl RNase free H₂O (2 min at 70°C), concentration was measured and samples were stored at -20°C.

2.2.4.3 Reverse transcriptase polymerase chain reaction (RT-PCR)

RT-PCR analysis was used to study temporal gene expression profiles or alterations of gene expression upon chemical treatment or microinjection. Total- RNA (equalized to 100 ng/ μ l for „semiquantitative RT-PCR analysis“) was reverse transcribed into cDNA that was used as template for the following PCR reaction. The general RT reaction was done using an unspecific “random XHexamer primer” (RH, Invitrogen) binding randomly to RNA strands. This short double stranded fragment serves as initiation side for the viral reverse transcriptase. An „Oligo-dT primer“ (dT, Invitrogen) for predominant reverse transcription, of mRNA was used in case of XHNF6 gene isolation. A primer containing RT- premix was prepared and stored at -20°C till usage. cDNA was stored at -20°C or used directly for gene expression analysis in a PCR reaction.

RT Premix:	100 μ l	25 mM MgCl ₂	
	400 μ l	5× Flexi GoTaq buffer (wo MgCl ₂)	
	50 μ l	RH/ Oligo- dT(100 ng/ μ l)	
	100 μ l	dNTP mix (each 10 mM)	
	300 μ l	DEPC-H ₂ O	
RT reaction mix:	7.5 μ l	RT premix	
	0.1 μ l	MuLV RT enzyme (50 U/ μ l)	
	0.2 μ l	RNase Out (40 U/ μ l)	
	1.5 μ l	Total RNA (100 ng/ μ l)	
	ad 10 μ l	DEPC-H ₂ O	
thermocycler program:	22°C	20 min	(primer annealing)
	42°C	60 min	(reverse transcription)
	99°C	5 min	(denaturation)
	4°C	∞	(cooling)
PCR reaction mix:	5 μ l	cDNA	
	1 μ l	25 mM MgCl ₂	
	4 μ l	5× Flexi GoTaq buffer	
	1.25 μ l	gene specific primer mix (each 10 μ M)	
	0.25 μ l	GoTaq polymerase	
	ad 25 μ l	dH ₂ O	

thermocycler program:	95°C	2 min	} × Y
	95°C	45 s	
	X °C	45 s	
	72°C	45 s	
	72°C	5 min	
	4°C	∞	

X= primer specific annealing temperature; Y= cycle number depends on the mRNA abundance of the gene of interest. Variables have to be optimized for each primer pair.

After PCR reaction, 20 µl of the PCR product were analysed on a 2% agarose gel. For cloning purposes the band of interest was cut out, purified and cloned into pGEM-T.

2.2.4.4 5' -/ 3' - Rapid amplification of cDNA ends (RACE- PCR)

To obtain cDNA information of *Xenopus laevis* XHNF6 including the 5' and 3' UTR region 5' and 3' RACE PCRs were performed using the *SMARTTMRACE- PCR amplification Kit* (Clontech) according to the manufacturers protocol.

Synthesis of 5' / 3' RACE cDNA

5' / 3' RACE- Ready cDNA, needed for the later PCR amplification step, was reverse transcribed from a total RNA pool.

In the process of reverse transcription in the 5' RACE reaction, the reverse transcriptase adds a poly-G sequence to end of every transcript. This poly-G tail serves as complementary site for a kit- supplied poly-C oligomer (SMART-II Oligo). Docking of this poly C oligo leads to a second transcription initiation side and the transcript will automatically be elongated by an oligo linked sequence. This artificial sequence is binding side for the universal primer used in the following PCR amplification step.

reaction mix:	1 µg	total RNA
	1 µl	5'cDNA synthesis primer
	[1 µl	SMART II oligo (just for 5' RACE)]
	ad 5 µl	dH ₂ O

Reaction mixture was incubated at 70°C for 2 min. in a thermocycler (denaturing) and cooled down for 2 min on ice (primer annealing).

+	2 µl	5× first strand synthesis buffer
	1 µl	20 mM DTT
	1 µl	dNTP Mix (10 mM each)
	1 µl	Power script reverse transcriptase (200 U/µl)

After the addition of first strand synthesis components, cDNA revers transcription was performed at 42°C for 1.5 hr. Product was supplied with 90 µl Tricine- EDTA buffer, incubated for 7 min at 72°C and stored at -20°C.

Amplification of 5' / 3' cDNA ends (RACE- PCR)

For the PCR amplification of 5' / 3' ends a PCR premix was mixed and complemented by 5'-RACE or 3'-RACE specific components

reaction premix:	31 µl	dH ₂ O	
	5 µl	10× PCR buffer	
	1 µl	dNTP mix (each 10mM)	
	1 µl	50× Advantage 2 Polymerase Mix	
<div style="display: flex; justify-content: space-around; margin-top: 10px;"> ↙ ↘ </div>			
+ 5 µl	5'RACE ready cDNA	+ 5 µl	3'RACE ready cDNA
5 µl	10× Universal Primer Mix	5 µl	10× Universal Primer Mix
1 µl	gene specific primer 1 (10 µM)	1 µl	gene specific primer 2 (10 µM)

To amplify gene specific products a „touchdown PCR“ was performed.

thermocycler program:	94°C	5 s	
	72°C	3 min	× 5
	94°C	5 s	
	70°C	10 s	× 5
	72°C	3 min	
	94°C	5 s	
	68°C	10 s	× 35- 40
	72°C	3 min	
	4°C	∞	

PCR product was analysed on a preparative 1.5% agarose gel. Bands of expected size were cut out, gel purified and cloned into pGEMT-E vector.

2.2.4.5 *In vitro* RNA transcription

Transcription of capped sense RNA

Capped sense RNA (capRNA) for microinjection was generated using the SP6 *mMESSAGE mMACHINE™ Kit* according to the manufacturers protocol. Transcripts are synthesised with a 7- methylguanosin „cap“ at the 5' end leading to increase mRNA stability.

reaction mix:	3 µl	linearised plasmid [150 ng]
	1 µl	RNA- polymerase (10 U/µl)
	5 µl	2x rNTP/ CAP Mix
	1 µl	5× Sp6 reaction buffer
	0.2 µl	Pyrophosphatase

The reaction was incubated at 37°C for 2 hr. The template was afterwards digested for 15 min at 37°C using 5 U DNaseI. RNA was purified using *Illustra™ RNAspin Mini Kit* according to the manufacturers protocol. After elution in 25 µl DEPC- H₂O the concentration was measured and the sample aliquoted in 2 µl for storage at -20°C.

Transcription of labeled antisense RNA

Antisense RNA (asRNA) used for *in situ* hybridisation techniques was *in vitro* transcribed from 1µg linearised template using the corresponding polymerase (construct list see 2.1.9) and thereby labeled with digoxigenin (Dig)-11-UTP (Roche) or fluorescein (Flu)-11- UTP (Roche). (Melton et al., 1984)

reaction mix:	5 µl	5× transcription buffer
	4 µl	Dig/ Flu- rNTP Mix
	1 µl	DTT (0.75 mM)
	0.5 µl	RNase OUT
	1 µl	RNA polymerase (Sp6, T7, T3)
	0.5 µl	Pyrophosphatase
	5 µl	template
	ad 25 µl	DEPC- H ₂ O

After 2,5 hr the template was digested for 15 min at 37°C using DNaseI. AsRNA was purified using *Illustra™ RNAspin Mini Kit* according to the manufacturers protocol. After elution in DEPC-H₂O the RNA was analysed on a 2% agarosegel, supplied with 50 µl hybridisation mix and stored until usage at -20°C.

Dig-or Flu- Mix:	2 nM rATP, 2 nM rGTP, 2 nM rCTP, 1.9 nM rUTP, 0.1 nM Dig- or Flu-11-rU TP
------------------	--

2.2.4.6 Whole mount *in situ* hybridisation (WMISH)

Embryos were stained by whole mount *in situ* hybridisation (Harland et al., 1991; modified after Hollemann et al., 1999) using organ or tissue specific markers to visualize effects upon microinjection or chemical treatments.

10× PBS	1.75 M NaCl, 1 M KCl, 65 mM Na ₂ HPO ₄ , 18 mM KH ₂ PO ₄ , pH 7.4
1× PTw	1× PBS, 0.1% (v/v) Tween-20, pH 7.4
100× Denhart's	2% (w/v) BSA, 2% (w/v) PVP, 2% (w/v) Ficoll-400, store -20°C
Heparin	10 mg/ml in DEPC-H ₂ O stock solution, store at -20°C
Torula RNA	50 mg/ml stock solution in DEPC-dH ₂ O, store at -20°C
Proteinase K	20 mg/ml stock (Merck, Darmstadt)
Hybridisation-Mix (Hyb-Mix):	50% (v/v) formamid, 1 mg/ml Torula-RNA, 10 µg/ml Heparin, 1× Denhardt's, 0.1% (v/v) Tween-20 TM , 0.1% (w/v) CHAPS, 10 mM EDTA, 5x SSC in DEPC-H ₂ O
TEA	0.1 M TEA (= 0.675 ml TEA/ 50 ml dH ₂ O), pH 7.5
20× SSC	3 M NaCl, 0.3M NaCitrat, pH 7.4
2× SSC incl. RNases	20 µg/ml RNaseA, 10 U/ml RNaseT1
5× MAB	500 mM maleic acid, 750mM NaCl, pH 7.5 autoclave
10% BMB	10% (w/v) were dissolved slowly at 60°C in 1× MAB, aliquoted in 50ml; stored at -20°C, autoclaved
100% Horse Serum	Horse Serum was heat inactivated for and aliquoted in 50 ml; stored at -20°C
APB	100 mM TrisHCl, 100 mM NaCl, 50 mM MgCl ₂ , 0,1% (v/v) Tween-20 TM , pH 9.0-9.1
BCIP	50 mg/ml in 100% DMSO (Roche Diagnostics)
NBT	100 mg/ml in 70% DMSO (Roche Diagnostics)

Rehydration

MEMFA fixed embryos (30/ glass tube) were rehydrated in reverse ethanol steps on a rotating shaker.

step	EtOH	buffer	time	repeat
1	100%	-	5 min	1 ×
2	75%	H ₂ O 25%	5 min	1 ×
3	50%	H ₂ O 50%	5 min	1 ×
4	25%	PTw 75%	5 min	1 ×
5	-	PTw 100%	5 min	4 ×

Proteinase K treatment

Embryos were treated with 10 µg/ml Proteinase K for optimal penetration of the antisense RNA. Duration of treatment depended on developmental stage of embryos.

stage	time	temp	stage	time	temp
10- 14	10 min	RT	33- 35	25 min	RT
15- 18	12 min	RT	36- 39	28 min	RT
19- 22	15 min	RT	40- 41	30 min	RT
23- 26	20 min	RT	42	32 min	RT
28- 32	22 min	RT	43- 44	35 min	37°C

Table 2: Duration of proteinase K treatment during WMISH for different developmental stages

Acetylation and Refixation

Delicate embryos were transferred to 0.1 M TEA (pH 7.5), acetylated with acetic anhydrid (AA) and refixed in 1× PTw/ 4% (v/v) formaldehyde.

step	buffer	time	repeat
1	TEA	5 min	2 ×
2	TEA + 12.5 µl AA	5 min	1 ×
3	+ 12.5 µl AA	5 min	1 ×
4	1× PTw 100%	5 min	2 ×
5	1× PTw/ 4% FA	20 min	1 ×
6	1× PTw 100%	5 min	5 ×

Hybridisation

The Hybridisation buffer (Hyb-Mix) was preheated in the steam (65°C) of a 68°C water-bath. For hybridisation 1× PTw was removed up to 1 ml and filled with 250 µl Hyb- Mix. The solution was gently mixed. When embryos sink to the bottom liquid was completely removed, refilled with 500 µl Hyb- Mix and then preincubated for 10 min at 65°C in the

shaking waterbath. The solution was replaced by fresh Hyb- Mix in which embryos were prehybridized for 6 hr at 65°C to prevent unspecific RNA binding. The Hyb- Mix, collected and kept for a later washing step at 65°C, was replaced by 500 µl Hyb- Mix including labeled asRNA (1 µg/ml). Hybridization process was performed oN at 65°C in the shaking waterbath.

Washing

The next day the asRNA samples were collected (stored at -20°C for reuse) and the embryos washed with preheated “used” Hyb- Mix for 10 min. The embryos were washed under stringent conditions and treated with 10 µg/ml RNaseA (1 µl/ml) and 10 U/ml RNaseT1 (0,33 µl/ml) to remove unspecific bound and single stranded RNA.

step	buffer	time	temp	repeat
1	Hyb- Mix	10 min	60°C	1×
2	2× SSC	20 min	60°C	3×
3	2× SSC including RNase	60 min	37°C	1×*
4	2× SCC	10 min	RT	1×
5	0.2× SSC	30 min	60°C	2×
6	1× MAB	15 min	RT	1×

*incubation in an 37°C incubator and shaken manually from time to time

Antibody incubation

After the stringent SSC wash the embryos were equilibrated to MAB buffer and incubated in a mixture of 2% Böhriger Mannheim Blocking reagent (BMB) and 20% heat inactivated horse serum (HS) in 1xMAB, to prevent unspecific antibody binding in the later detection step. Hybrids of endogenous RNA and asRNA (Dig- or Flu labeled) were detected by a specific antibody against Digoxigenin or Fluorescein that is coupled to alkaline phosphatase (anti- Dig-AP or anti- Flu-AP).

step	buffer	time	temp	repeat
1	1× MAB	15	RT	3×
2	1× MAB/2%BMB	20	RT	1×
3	1× MAB/2%BMB/ 20% HS	60	RT	1×
4	1× MAB/2%BMB/ 20% HS	240	RT	1×
	α-Dig/ α-Flu 1:5000*			
5	1× MAB	10	RT	1×
6	1× MAB	oN	4°C	

*Sheep-anti-Dig/ Flu; linked with alkaline phosphatase (AP; LaRoche)

Colour detection

Samples were washed multiple times with 1× MAB to reduce background staining upon unspecific antibody binding. To detect labeled RNA- hybrids, embryos were incubated in NBT/ BCIP colour solution. Colour reagents are dephosphorylated by antibody linked alkaline phosphatase, resulting in a coloured precipitate in cells (dark purple for NBT/ BCIP).

step	buffer	time	temp	repeat
1	1× MAB	20 min	RT	3×
2	APB	5 min	RT	2×
3	APB incl. NBT/ BCIP*	3h- 4d	4°C	till staining

* 1.5µl NBT/ ml APB+ 3.5µl BCIP/ ml APB

Colour reaction ending

When embryos showed a clear staining signal, colour reaction was stopped using 100% Methanol. Overstained samples could partially be destained.

step	buffer	time	temp	repeat
1	dH ₂ O	2 min	RT	1×
2	100% MetOH	2-5 min	RT	1×
3	50% MetOH	2 min	RT	1×
4	MEMFA	fixation	4°C	∞

Fast embryo bleaching

After WMISH the colour solution is discarded and embryos washed in 2 ml dH₂O, fixed in 1× MEMFA for 30 min. and 2× 20 min in 5× SSC. Pigments were destained using 5× SSC/ 50% Formamid (v/v) + 1% H₂O₂. After 2× 20 min in 5× SSC embryos were stored in 1× MEMFA.

2.2.5 Vibratome sections

To analyse interembryonic staining embryos were embedded into gelatine/albumine after WMISH (Holleman et al., 1999). On ice, 105 µl 25% glutaraldehyde were stirred into 2 ml gelatine/ albumin and the first layer was poured into a well of an icecube container. Embryos were preincubated for 10 min. in gelatine/ albumine and layed on top of the polymerized layer and remaining liquid removed. A second level of embedding media was poured. After hardening the block was cut to a proper size and the embryo fixed on a cutting board. Using a vibratome 30 µm sections were done in soap containing dH₂O, collected on a glass

slide, airdried and mounted in moviol. Pictures were taken by an phasecontrast microscope (Nomarski-Optik, Axioskop) and digitalized with a camera (DXC-950P Colour Video Camera). Sections were stored at -20°C.

Gelatine/ albumine	Dissolve 4.88 mg/ml gelatine in 1× PBS slowly at 60°C. After cooling down 0.3 g/ ml albumine fraction V and 0.2 mg/ml succrose are added and dissolved oN at 37°C; filtersterilize and store at -20°C.
Moviol 4-88	dissolve 5 g moviol in 20 ml 1x PBS oN, add 10 ml Glycerol and stirr oN. After centrifugation for 30 min at 20000 g the supernatant is aliquoted, pH 6-7; stor at -20°C

2.2.6 Protein work

2.2.6.1 Protein extraction from *Xenopus laevis* embryos

Protein extraction from whole embryos were done to analyse the temporal protein expression pattern of p150/ malectin. 10 Embryos were shock frozen in liquid nitrogen and homogenized on ice in 400 µl homogenisation buffer with a syringe (26 G, Terumo Neolus) and by vortexing. Total protein extracts were separated into membrane and soluble compounds by centrifugating for 10 min at 4°C. The supernatant was transferred into a new tube for FREON lipid extraction. The pellet containing cell debris and membrane compartments was resolved in SDS-sample buffer (20µl/ embryo) by vortexing and heating to 95°C. 1/10 volume was loaded onto a SDS- gel for electrophoretic separation, the remaining sample stored at -20°C.

Homogenisation buffer	50 mM TrisHCL pH 7.5, 150 mM NaCl, 5% Glycerin, 1 mM DTT, 1 tablet/ 10 ml protease inhibitors (Roche) , 50 mM NaF, aliquot store -20°C
-----------------------	---

FREON extraction and TCA Precipitation

Soluble proteins were concentrated after FREON extraction by mixing with 0.1 Vol 1% NaDOC, incubating for 15 min. at RT and supplying 0.22Vol 50% TCA solution. After protein precipitation for 2 hr at 4°C, samples were spin down for 30 min at 4°C with 14.000 rpm. The supernatant was decanted and the pellet washed with 1 ml icecold acetone. After mixing proteins were precipitated for 1h at -80°C, spin for 1 min at max speed, the pellet washed with 70% EtOH, airdried and resuspended in 30 µl dH₂O.

2.2.6.2 SDS- Polyacrylamide gel electrophoresis (PAGE)

SDS- PAGE (Laemmli, 1970) was used to separate proteins according to their molecular weight. Due to SDS, proteins obtain a negative charge that allows them to migrate through polymerized acrylamide in an electric field depending on their molecular weight. Molecular weight of proteins was estimated by comparison to protein standard “Broad Range Marker“ (Biorad). Prior to protein separation in the separation gel, differing in acrylamid concentrations, a the protein extract was focused in a stack gel.

mini gel size (60 × 130 × 0.5 mm)	separation		stack
	<u>12%</u>	<u>15%</u>	<u>12%</u>
30% Acrylamid Mix	4.0 ml	5.0 ml	2.0ml
1.5 M TrisHCl pH 8.8	2.5 ml	2.5 ml	-
0.5 M TrisHCl ph 6.8	-	-	1.3 ml
10% (w/v) APS	0.1 ml	0.1 ml	0.05 ml
10% (w/v) SDS	0.1 ml	0.1 ml	0.05 ml
dH ₂ O	3.3 ml	2.3 ml	1.7 ml

midi gel size (87×77 × 1 mm)	separation		stack
	<u>12%</u>	<u>15%</u>	<u>5%</u>
30% Acrylamid Mix	8.0 ml	10 ml	0.83 ml
1.5 M TrisHCl pH 8.8	5.0 ml	5.0 ml	-
0.5 M TrisHCl ph 6.8	-	-	1.26 ml
10% (w/v) APS	0.2 ml	0.2 ml	0.04 ml
10% (w/v) SDS	0.2 ml	0.2 ml	0.04 ml
dH ₂ O	6.6 ml	4.6 ml	2.77 ml

The stack gel was runned in 1× Laemmli buffer using a selfmade electrophorese chamber with 35 mA for 45 min. Than power was increased to 45 mA for 3 hr. Gels were used for Coomassie blue staining (see 2.2.4.3) or for western blot analysis (see 2.2.4.4).

2× SDS- sample buffer: 120mM TrisHCl pH 6.8, 20% (v/v) Glycerol, 4% (v/v) SDS, 200mM DTT; aliquot and store -20°C
 10× Laemmli buffer: 250 mM Tris, 2.5 M Glycin, 1% SDS, pH 8.3

2.2.6.3 Coomassie staining

After SDS- PAGE, proteins could be visualized by staining the gel for 30 min in coomassie colour solution.

Coomassie colour solution: 40% (v/v) Methanol, 10% (v/v) acetic acid, 50% dH₂O,
0.1% (w/v) Coomassie Blue G-250
Coomassie destaining solution: 40% (v/v) Methanol, 10% (v/v) acetic acid, 50% dH₂O

2.2.6.4 Western blotting

The analysis of one specific protein from whole protein extracts was done by immunodetection assays. Proteins were transferred, blotted, from the SDS gel onto a nitrocellulose membrane (Ø 0.45 µm, BA85; Schleicher & Schuell). Therefore, the gel and nitrocellulose membrane were briefly washed, and 6 gel- size whatman papers were soaked, in 1× protein blotting buffer prior to setting up the „Western Blot sandwich“ (figure 2).

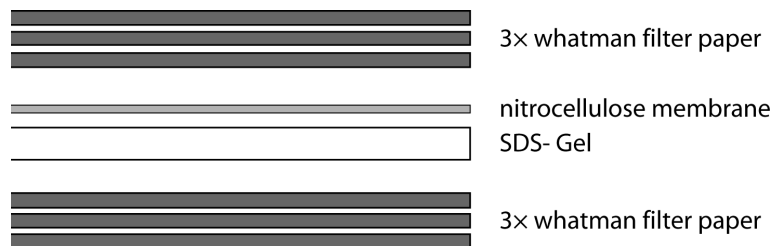


Figure 2: Schematic drawing of a semi-dry western blot sandwich (Khyse-Anderson, 1984)

The proteins were transferred onto the membrane using a blotting cassette (Fastblot B 34, Bi- orad) with 0.8 mA/ cm² for 1 hr. The membrane was washed in 1× PBS /Tween and unspecific binding sites were blocked on at 4°C with 5% (w/v) milc buffer.

The following day the membrane was washed briefly in PBS/Tween. First antibodies were diluted in 5% (w/v) milk buffer and incubated for 1 hr at RT (Mouse- anti- FlagM2 1: 5000; rabbit- anti-p150/ malectin 1:15 000). The blot was washed 3× with PBS/Tween for 10 min. Second antibodies, coupled with horse-radish-peroxidase (HRP), were diluted in PBS/ Tween (goat-anti -rabbit- HRP 1: 5000) and incubated for 1 hr at RT. After an intensive wash with PBS/ Tween protein detection was visualized by chemilumescence using the *ECL+ plus Wetsern Blotting Detection System*. Solution A (50 µl/ cm²) was mixed 40:1 with solution B, poured over the membrane and incubated for 5 min at RT. The membrane was sealed in plastic and exposed to chemilumescence photofilm (GE healthcare) that was afterwards developed (Optimax Type TR).

Protein blotting buffer:	39 mM Glycine, 48 mM Tris Base, 0.037% (v/v) SDS, 20% (v/v) MetOH, pH 9.2, store at 4°C
1× PBS/ Tween:	0.05% (v/v) Tween-20 in 1x PBS

2.2.6.5 Bradford assay

Protein concentration was estimated by Bradford. A standard curve was made using 0- 20 µg BSA (1mg/ml). Dilutions were made in the protein buffer. 1 ml Bradford were added, incubated for 10 min. at RT. Change in Extinction was measured at 595nm. Protein concentration of the sample were estimated using the standard curve. Measurements were done twice.

Bradford solution	100 ml 95% EtOH, 200 ml 88% Phosphoric acid, 350 mg Coomassie G250
Bradford reagent	425ml H ₂ O, 15 ml 95% EtOH, 30 ml 88% Phosphoric acid, 30 ml Bradford solution

2.2.6.6 *In vitro* transcription and translation assay (TnT[®])

The *TnT[®]-coupled reticulocyte lysate system* (Promega) was used to test *in vitro* translation of constructs and to analyse efficiency of morpholino binding. The system is based on a transcription and

Nonradioactive as well as radioactive (hot TNT(hTnT)), using ³⁵S labeled methionine, were performed according to the manufacturers protocol with some modifications.

reaction mix:	6.25 µl	TnT rabbit reticulocyte lysate
	0.5 µl	TnT reaction buffer
	0.25 µl	TnT Sp6 RNA polymerase
	0,25 µl	AA mix (w/o methionin)
	[0.25 µl	(³⁵ S)-methionin (Ci/µmol at 10 µCi/ml)]*
	0.25 µl	RNase Out
	1 µl	DNA template [300 ng/µl]
	[1 µl	morpholino (different concentrations)]*
	ad 12.5 µl	dH ₂ O

* if addition was required

The reaction was incubated at 30°C for 90 min in a thermo block. To analyse products by SDS- PAGE (see 2.2.4.1), samples were mixed with 12.5 µl SDS- sample buffer and heated for 5 min at 95°C before loading 10 µl on a SDS- gel. After electrophoresis, nonradioactive

TnTs were used for western blot analysis. Radioactive SDS- gels were first vacuum dried for 2 hr at 80°C (Geldryer, model 583) and afterwards scanned by a *Variable Mode Image Typhoon 9400* for digital analysis.

2.2.7. Generation of malectin specific antibody

Analysis of intracellular localization, study of embryonic protein expression and conformation of disrupted protein synthesis upon morpholino injection required a malectin specific antibody. The N- terminus of malectin was predicted as signal peptide (aa 1-30), potentially cleaved of during modification processes while the hydrophobic C-terminus was possibly a transmembrane domain (aa 208-276). For the purpose of antigen generation both regions were excluded and just the soluble core domain was overexpressed in bacteria, affinity purified and used for rabbit immunisation.

2.2.7.1 Cloning of malectin core domains

The malectin core domain was PCR amplified out of the pCS2+/p150-ORF plasmid. Four different core fragments were generated to test optimal conditions for overexpression in bacteria. Two different primer sets were used: tg1- 4 (named after collaboration partner Toby Gibson (EMBL, Heidelberg; cloning was done by Günther Stier (EMBL, Heidelberg)).

name	sequence 5'→ 3'
tg1 (for):	GCTGCTCATGAGCGGTCTAGCGGATAAAGTGATCTGG
tg2 (for):	GCTGCTCATGAGCGATAAAGTGATCTGGGCAGTGAATG
tg3 (rev):	GCTGGTACCTTACTCCAGACCTGGGTGAGGCTGC
tg4 (rev):	GCTGGTACCTTAAGGCTGCAGCATTGGGACATC

The resulting four fragments were subcloned into pETZ2-9d vector, in frame to a 6× His-tag (thereby destroying the NcoI (nt 932) cloning site). Correct in frame fusion was confirmed by sequencing. All proteins could be efficiently expressed and purified in bacteria (personal communication with Günther Stier). Due to size advantages the largest construct TG1 was used by Thomas Schallus (EMBL, Heidelberg) for structural analysis by NMR. The smallest fragment TG4 protein was used for antibody generation as subsequently described.

2.2.7.2 Overexpression and purification of antigen

TG4 protein expression and purification was done using the protocol: "E.coli expression-High speed protocols" (Jeanne Perry, UCLA Los Angeles; Günther Stier, EMBL, Heidelberg) with some modifications. **In general, all buffers contained Tris and DTT for protein stabilization, disulfide bond reducing β -mercaptoethanol, proteinase inhibitors as PMSF or PEFAC and nonionic detergents, like NP-40 or Triton-X-100 to remove unbound proteins and nucleic acids from the affinity column. Imidazol competes with proteins for Ni^{2+} -NTA binding sites and prevents at low concentrations ($\geq 20\text{mM}$) unspecific protein binding to Ni^{2+} -beads while at high concentrations ($\leq 100\text{mM}$) it leads to elution of His-tagged proteins.**

The TG4- plasmid was transformed into BL21 (DE3) bacteria by chemical transformation. A 50 ml LB^{Kan} oN- culture was set up at 37°C . The next day oN-culture was diluted to $\text{OD}_{600} = 0.3$ in 37°C prewarmed LB^{Kan} . Protein expression was induced upon 1 mM IPTG and the culture grew for 6 hr to $\text{OD}_{600} = 0.8$ at 25°C to increase protein yield (**highest protein expression occurs during exponential growth phase**). 1 ml samples were taken (0, 2, 4, 6h) to analyse protein synthesis in a time course experiment. **The culture was spin down at $6000 \times g$ for 15 min and resuspended on ice in 10 ml/mg wet weight lysisbuffer using a glass pipet. The suspension was split in 50 ml Falcon tubes, complemented with 100 $\mu\text{g}/\text{ml}$ lysozyme and 1 $\mu\text{g}/\text{ml}$ DNaseI and incubated on ice for 15 min. Cells were completely disrupted by sonification on ice at highest intensity ($2 \times 2\text{ min}$) thereby preventing protein denaturation by spooming. Cell debris were separated by centrifugation for 15 min at $10.000 \times g$ and the clear yellowish supernatant was filtered through 0,45 μm filter (Sartorius).**

For affinity purification, a column (Polyprep, Biorad) was filled with 0.5 ml well mixed Ni^{2+} agarose beads and equilibrated with 5 ml lysisbuffer. The filtered solution was applied to the column that was **drained by gravity. The flow through was collected and reloaded once.** Proteins that bound unspecifically to the beads were washed off under stringent conditions by 5 ml Wash 1 buffer, 5 ml Wash 2 buffer and 5 ml Wash 3 buffer. 100 μl of each flowthrough were kept for an analytic SDS-PAGE analysis. The fusion protein was eluted with 2.5 ml elution buffer. The flowthrough was reloaded twice to elute maximal protein amount. Protein concentration was estimated by Bradford. The column was washed with 1M imidazol and stored with 70% EtOH at 4°C .

To remove the His-tag of the TG4 protein, a TEV protease cleavage was performed oN at 30°C by addition of 40 U/ml enzyme (Invitrogen). Enzymatic cleavage occurred at recognition sequence EBLYFZG located between the $6 \times \text{His}$ - tag and the protein of interest, here TG4. Tag and cleaved off protein were separated by a second Ni^{2+} affinity purification step. Therefore the high imidazol concentration was reduced using a spin column (Vivaspin, 50000 Da). The sample volume was reduced twice to 500 μl in a swing bucket rotor at 4000 rpm and each time refilled with Wash 1 buffer.

For the second affinity purification the Ni²⁺-NTA column was equilibrated with 10 ml Wash 1 buffer. The now „dialysed“ protein sample was applied and collected in the flow through whereas the 6× His-tag carrier remained on the Ni²⁺ column. To increase the protein yield the flow through was reloaded once. After concentration measurement by Bradford, protein was diluted to a 1 mg/ml stock solution aliquoted and stored at -20°C. 5 mg of purified TG4 protein were sent to BioScience, Göttingen (Ritschweg2, 37085 Göttingen, Tel: 0551-25248; e-mail: Bioscience@T-online.de) for rabbit immunization.

Lysisbuffer:	20 mM Tris pH 8.0, 10 mM imidazol pH 8.0, 150 mM NaCl, 0.2% NP-40, 2 mM β-Mercaptoethanol (1:10000) or 5 mM DTT/ DTE, 1 μM PEFAC or 200 μM PMSF
Wash 1 buffer:	= Lysisbuffer without 0,2% NP-40
Wash 2 buffer:	= Washbuffer 1 with 1 M NaCl
Wash 3 buffer:	= Washbuffer 1 with 30 mM imidazol
Elution buffer:	= Washbuffer 1 with 330 mM imidazol, 10% glycerol
Storage buffer:	20 mM Tris pH 8.0, 150 mM NaCl, 2 mM DTT, 10% glycerol
PMSF:	proteinase inhibitor 200 mM stock
PEFAC:	proteinase inhibitor 100 mM stock
1 M IPTG	isopropyl b- D-thiogalactopyranosid
Ni ²⁺ agarose beads:	Quiagen, binding capacity of 5 -10 mg/ ml beads
Polyprep chromatographie column	Biorad

2.2.7.3 Purification of rabbit polyclonal antibody

Crude blood serum was tested after 3 (1st bleeding), 6 (2nd bleeding) and 9 weeks (3rd bleeding) for its antibody content by immuno detection (Western blot, see 2.2.7.4). Protein samples used to test antibody specificity were purified antigen TG4 protein, whole embryo extracts that were further separated into membrane and soluble protein fraction as well as bacterial lysate. The 2nd bleeding was used to extract TG4 antibody by affinity purification using *AminoLink Plus Immobilisation Kit* (Pierce) according to the manufacturers two-step protocol.

Covalent binding of the antigen to agarose beads

The first purification step consisted in covalent binding of the antigen, here 6 × His-tag TG4 protein, to the gel matrix of a supplied column. The matrix is composed of cross-linked 4% agarose beads that were activated to show reactive aldehyde groups reacting with primary amines of the protein. The resulting intermediate, a Schiff Base, is reduced to form a stable secondary amine linkage.

Tris competes as primary amine with amino groups of the linked protein for reactive aldehyde groups thereby reducing binding capacity. To reduce Tris amount in the protein storage buffer, 2 ml TG4 protein (= 10 mg) were diluted 1:3 in coupling buffer pH 10. After equilibrating the column with coupling buffer pH 10, the protein sample was applied and gently mixed in the closed column for 4 hrs. The liquid was drained by gravity and unbound protein was washed off with 5 ml coupling buffer pH 7.2. The covalent linkage between loaded protein and aldehyde groups was induced by the addition of 2 ml coupling buffer pH 7.2 + 40 µl of NaBH₃CN that serves as reducing agent for the reductive alkylation of amines. The reaction was performed by gentle rocking on at 4°C. The alkylation was stopped upon washing the column with 4 ml of quenching buffer containing high Tris concentration. To block free remaining binding sites the column was treated with 2 ml quenching buffer pH 7.2 + 40 µl NaBH₃CN. The blocking was finished by washing uncoupled protein of the beads with 2 × 15 ml Wash solution, followed by a wash of 5 ml Wash solution including NaN₃.

Affinity purification of antibody

In the second step the antibody was affinity purified by specific binding to the linked protein. The column was equilibrated with 6 ml sample buffer. The rabbit serum (15 ml) was filtered (0.45 µm), concentrated using a *VivaSpin* column to 5 ml, diluted 1:1 in sample buffer, incubated batchwise with the agarose matrix at RT for 1 hr, which was then reloaded to a column. The agarose was washed with 12 ml sample buffer prior to elute the antibody in 1 ml fractions with 8 ml elution buffer. The low pH of samples was neutralised by adding 50 µl neutralisation buffer pH 9 to every aliquot.

Protein concentration was measured by Bradford and the fractions of interest were pooled. For antibody storage, elution buffer was exchanged to storage buffer by reducing twice the volume to 100 µl using a *VivaSpin* column. The sample was diluted 1:1 in 100% Glycerol and stored at -20°C.

Coupling buffer pH 10:	0.1 M NaCitrates, 0.05 M NaCO ₃ , store 4°C
Coupling buffer pH 7.2:	0.1 M phosphate, 0.15 M NaCl
Quenching buffer pH 7.4:	1 M TrisHCl pH 8, 0.05% NaN ₃
Wash solution:	1 M NaCl, with and w/o 0.05% NaN ₃ ,
Sodium Cyanoborohydride Solution:	5 M NaBH ₃ CN dissolved in 0.01 M NaOH
Sample buffer:	0.025 M Tris pH 7.2, 0.15 M NaCl,
Elution buffer:	0.1 M glycine•HCl, pH 2.5
Neutralization buffer:	1 M Tris pH 9
Storage buffer pH 7.5:	1×PBS, 1mg/ml BSA, 0.05 NaN ₃ , 50%v/v Glycerol

2.2.8 Eukaryotic cell culture

2.2.8.1 Culturing, media and solutions

To start a new cell culture a cell suspension aliquot was taken from the liquid nitrogen tank, washed in 100% MetOH to prevent *Mycoplasma* contamination, thawed quickly at 37°C and poured in 20 ml prewarmed DMEM+. Cells adhered at 37°C and 5% CO₂ for 4 hr when medium was exchanged to fresh DMEM+ to eliminate toxic DMSO from the freezing media. The here used HeLa and NIH 3T3 cells are adherent cell types that grow as monolayer in a cell culture tissue flask. If cell density becomes too high cell proliferation is inhibited and cells die. To keep optimal growth conditions, cells that covered confluent 80- 90% of the flask (75 cm²) were diluted down in a new culture bottle.

Therefore media was decanted and cell layer washed twice with 1× PBS. Cells were detached from the cultur flask surface by trypsination using 2.5 ml 1× Trypsin- EDTA. Peptidase damage of cells was inhibited by addition of 10 ml DMEM+. An homogenous cell suspension was achieved by carefully pipetting up and down. Cell density was estimated electronically in the “Casy cell counter” by diluting 100 µl cell aliquot in 10 ml Casy solution. For general purpose, 1× 10⁶ cells were transferred to fresh 20 ml DMEM+ and grown at 37°C. For cell transfection experiments 2.5× 10⁵ cells were transferred to 20 ml DMEM+ and grown at 37°C

Eagle’s MEM-media (MEM-)	BioWhittacker, Europe MEM powder 10.4 g/l, 2.38 g/l HEPES, 2.2 g/l NaHCO ₃
Dulbecco's Modified Eagle Medium (DMEM-):	BioWhittacker, Europe DMEM powder 10.4 g/L, 2.2g/l NaHCO ₃ ,
MEM or DMEM+	DMEM, + 10% (v/v) FCS, + 50 µg/ml Gentamycin
100% Fetal Calv Serum (FCS)	Biochrom KG; heat inactivation at 56°C for 45 min. 100 ml aliquotes stored at -20°C.

Gentamycin [10 mg/ml]	Biochrom KG; against Gram negative bacteria, store at 4°C
10× Trypsin-EDTA	BiochromKG; 0.05% (w/v) Trypsin, 0.02% (w/v) EDTA dilute 1:10 in 1× PBS; 50 ml aliquotes stored at -20°C

Media and solutions were sterilized using disposable filter cups (Sarstaedt) under the sterile hood and 5 ml tested at 37°C for 4 days to exclude microorganism contamination. Store at 4°C.

Longterm storage of eukaryotic cells

For longterm storage of cell culture aliquots the trypsinised cell suspension was spin down for 5 min at 2000 g and the pellet was washed with PBS. The cells were resuspended in PBS, cell density estimated as described and $1-3 \times 10^6$ cells/ ml were resuspended in freezing buffer and aliquoted in 1.8 ml cryotubes. To allow a slow but efficient freezing process, tubes were wrapped in paper and frozen at -80°C on prior to store aliquotes in liquid nitrogen.

freezing media	DMEM (NIH 3T3) or MEM (HeLa), 20% (v/v) FCS, 10% (v/v) DMSO
----------------	---

2.2.8.2 Transient cell transfection

Transfection of plasmid DNA into eukaryotic cells was performed using the *lipofectamin 2000* reagent (Invitrogen) according to the manufacturers protocol. One day before transfection, cells were washed with 1× PBS, trypsinized and diluted to 3×10^5 cells/ 2 ml media-/ well (10cm²). The well contained 4 cover slides (Ø 10 mm) for cell adhesion. The transfection mix was prepared and applied to the cells after 24 hr.

Tube 1: 7.5µl lipofectamin/ 250 µl media- , mix and incubate at RT for 5 min

Tube 2: 4µg plasmid DNA/ 250µl media-

Solutions were mixed and incubated at RT for 20 min for micell formation. Meanwhile cells were washed with 1× PBS and supplied with media- . The transfection mix was added to the medium and cells were grown 18, 24, 36, 48 and 72 hr for fixation.

Lipofectamin 2000	Invitrogen; 1 mg/ml, store at -20°C
-------------------	-------------------------------------

2.2.9 Immunofluorescent (IF) protein detection

2.2.9.1 IF in eukaryotic cells

Cover slides with transfected cells were washed with 1× PBS and taken out from the well onto parafilm (cells facing up). Cells were fixed with 3% PFA, permeabilised with 0.5% Triton-X-100, blocked against unspecific antibody binding with 3% BSA and incubated with corresponding first and secondary antibodies that were coupled with fluorescent dyes. Antibody incubation was done in a wet chamber in the dark. Cells nuclei were DAPI stained prior to moviol mounting. Samples were stored at -20°C till confocal microscope analysis.

step	buffer	time	temp	repeat
1	200 µl 1× PBS	wash	RT	3 ×
2	200 µl 3% PFA	40 min	RT	1 ×
3	200 µl 1× PBS	wash	RT	3 ×
4	100 µl 0.5% Triton -X-100	15 min	RT	1 ×
5	200 µl 1× PBS	wash	RT	3 ×
6	100µl 3% (w/v) BSA/1× PBS	15 min	RT	1 ×
7	25 µl 1 st antibody*	1 hr	37°C	1 ×
8	200 µl 1× PBS	wash	RT	3 ×
9	25 µl 2 nd antibody*	1 hr	37°C	1 ×
10	1× PBS	wash	RT	3 ×
11	DAPI nuclei staining	10 min	RT	1x
12	mounting in moviol			

*Dilutions were done in 3% BSA.

3% paraformaldehyde (w/v)	Sigma, dissolve in 1× PBS, store at -20°C
0.5% Triton-X-100 (v/v)	dilute in 1× PBS, store at 4°C
3% BSA (w/v)	Sigma, dissolve in 1× PBS at 37°C, store -20°C
1× PBS	140 mM NaCl, 2.5 mM KCl, 8 mM Na ₂ HPO ₄ , 1.5 mM KH ₂ PO ₄
DAPI	1000× stock in 1x PBS, store at -20°C

2.2.9.2 IF in animal caps

After cutting animal caps stage 9 (0.8×MBS/ 0.8% agarose dishes in 0.8×MBS) let them round up before fixing them in MEMFA.

step	buffer	time	repeat
1	MEMFA	for 1hr at RT (or oN 4°C)	1×
2	1× PtW (5ml Tween /1l PBS)	10 min	3x

Materials and Methods

3	1st antibody	2hr at RT (or oN 4°C)	1×
4	1× PtW	10 min	3x
5	2nd antibody	1hr atRT	1×
	1× PtW	20 min	1×
	1× PBS	10 min	1×
	DAPI in 1× PBS	10min	1×
	PtW to avoid stickiness		

After immunodetection, animal caps were kept in the dark at 4°C in 1× PtW for confocal microscopy.

3 Results

Initiation of organ development in the gastrointestinal tract demands area restricted specification of progenitor cells in the gut epithelium. In mouse, the two transcription factors HNF1 β and HNF6 were reported to play an essential role in context of pancreas specification in the gut tube (Haumaitre et al., 2005). On this background, the first part of this study focused on the characterisation and functional analysis of the transcription factor HNF1 β in context of pancreas development. The transcription factor HNF6 was not previously identified for *Xenopus laevis*, hence the second part concentrated on the isolation and expression of HNF6 and presents first functional data upon its ectopic expression in the endoderm. Concerning the urge for novel pancreas specific genes for descriptive analysis of organogenesis, the third part of this study described the identification and functional characterisation of a novel protein, named malectin, that was identified in a pancreatic cDNA library screen of *Xenopus laevis*.

3.1 Characterisation of HNF1 β during pancreas development

3.1.1 Expression profile of HNF1 β during embryogenesis

In order to characterize HNF1 β function during pancreas development analysis of its spatial distribution was refined, in particular for the developing endoderm (figure 3.1.1).

As previously described by Demartis et al. (1994), endodermal HNF1 β expression was evident at the onset of gastrulation in the involuting vegetal hemisphere (figure 3.1.1, 10 and 10.5) that formed the endodermal germ layer. In accordance with earlier reports, HNF1 β transcripts were clearly detected in the dorsal endoderm slightly expanding into the ventral endoderm. With gastrulation, HNF1 β expression domain was translocated to the ventro-anterior region of the endoderm (figure 3.1.1, 11). At stage 10.5, HNF1 β transcription also started in two broad wedge-shaped domains within the neural ectoderm flanking the midline, where expression rapidly increased (figure 3.1.1, 10.5 to 13). As neurulation proceeded, these HNF1 β positive domains shifted forward to the anterior region of the embryo (figure 3.1.1, 13 to 20) and narrowed into bilateral regions within the neural folds, which

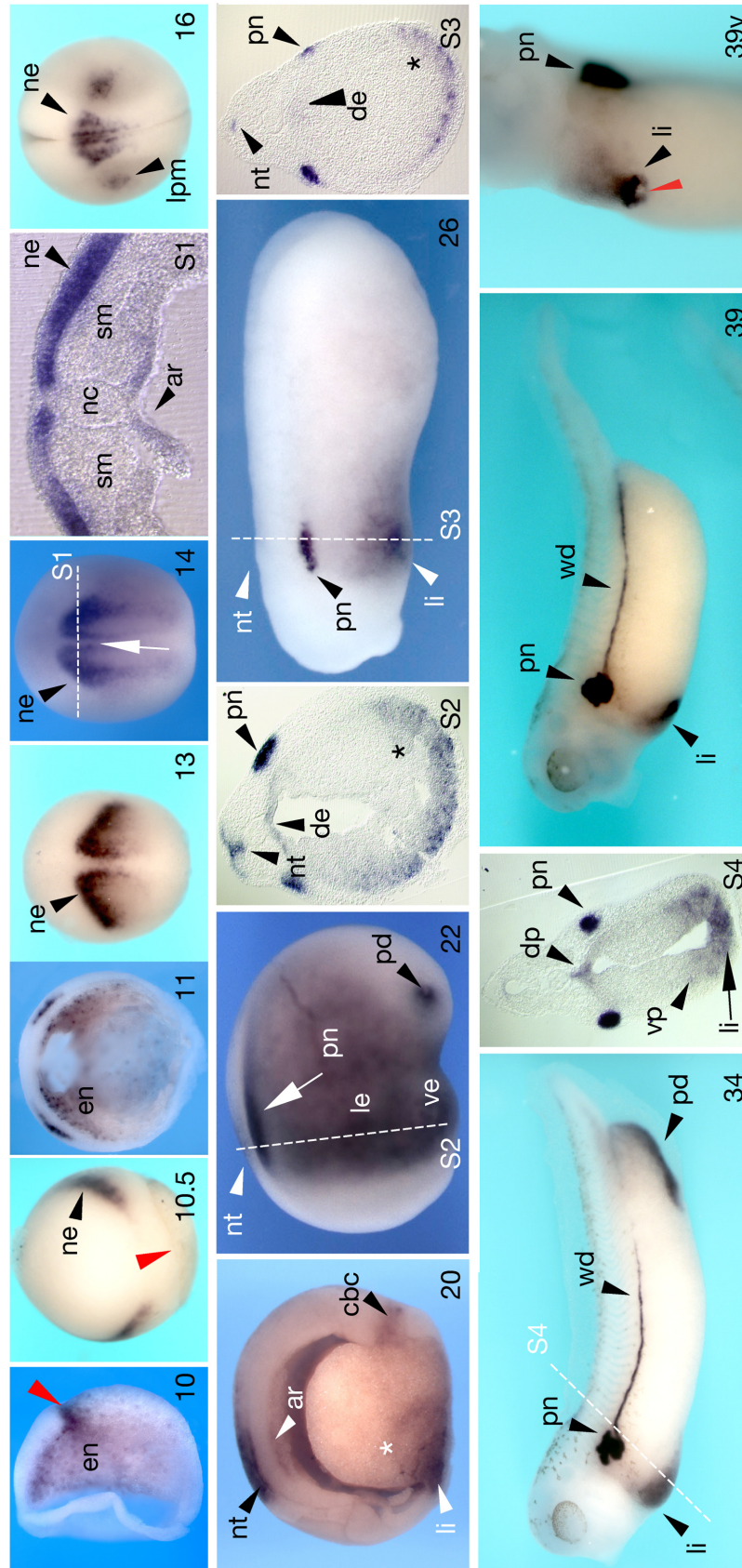


Figure 3.1.1 Expression pattern of HNF1β during *Xenopus laevis* development

Figure 3.1.1 Expression pattern of HNF1 β during *Xenopus laevis* development. HNF1 β expression was analysed by WMISH using embryos of different developmental stages as (indicated in each panel). The plasmid pXLFB3 (Vignali et al., 2000) was used as a template for *in vitro* transcription of digoxigenine labeled asRNA. Early stage 10- 11 embryos were dissected prior WMISH to improve hybridisation. The red arrow head at stage 10 and 10.5 point to the dorsal blastopore lip. Stage 13 to 16 shows dorsal view of early neurula stage embryos, positioned with anterior region to the top. White arrow at stage 14 points to the neural groove. From late neurula stage 20 onwards, embryos are shown in lateral position with the head to the left. Asterisk marks endodermal HNF1 β expression. Embryos were embedded after WMISH in gelatine-albumine for transversal vibratome sectioning (30 μ m, S1- S4). Exact position of the section is indicated as white dashed line in the image of the corresponding embryo. Stage 39v presents a ventral view of stage 39 embryo indicating weak hepatic and stronger gall bladder expression of HNF1 β (black and red arrow head respectively). Abbreviations: (ar) archenteron roof, (cbc) circum blastoporal collar, (de) dorsal endoderm, (dp) dorsal pancreas, (en) endoderm, (le) lateral endoderm, (li) liver, (lpm) lateral plate mesoderm, (nc) notochord, (ne) neural ectoderm, (nt) neural tube, (pd) proctodeum, (pn) pronephros, (sm) somitic mesoderm, (wd) wolfian duct, (ve) ventral endoderm, (vp) ventral pancreas.

converge anteriorly and fuse to the neural tube (figure 3.1.1, 14, S1, 16). In contrast to previous reports (Vignali et al., 2000), mesodermal gene activation of HNF1 β was first detected at stage 16 in the lateral plate mesoderm, giving rise to the presumptive pronephric tissue (figure 3.1.1, 16).

At stage 14, endodermal HNF1 β transcripts were evident in the dorso-anterior archenteron roof (figure 3.1.1, S1), the presumptive dorsal pancreatic domain, as well as in the ventro-anterior endoderm, including cells of the early liver diverticulum and cells that acquire ventral pancreatic cell fate (figure 3.1.1, 14 not shown, see 20). While neural HNF1 β expression decreased at stage 22 (Demartis et al., 1994), its transcription strongly increased in the pronephric anlage and within the endoderm, where transcripts were found in an antero-posterior gradient and in the posteriorly located proctodeum (figure 3.1.1, 22). Transversal sections confirmed that this strong HNF1 β expression was located within the endoderm and was excluded from the surrounding meso- or ectoderm (figure 3.1.1, S2; Demartis et al., 1994).

With proceeding gut tube patterning, HNF1 β expression was confined to the ventral foregut epithelium and to the caudal tip of the endoderm, the proctodeum (figure 3.1.1, 26 and S3). In contrast to previous studies, transversal sections revealed here, with the beginning of pancreatic budding from the foregut epithelium at stage 34, HNF1 β transcription not only occurred in the ventro-anterior gut tube but in particular in the dorsal gut epithelium, “hidden” behind the strong pronephric HNF1 β -expressing domain (figure 3.1.1, 34, S4). Estimating from the position within the endoderm, this dorsal HNF1 β expression domain most likely marked the dorsal pancreatic epithelium while ventral signals were confined to the liver and the ventral pancreatic regions. As in general, staining of the yolky endoderm represented a technical challenge; it cannot be excluded that HNF1 β expression also occurred in the foregut domain in between the pancreatic anlagen, representing the prospective duodenal epithelium. Broad HNF1 β expression in the foregut resembled the

gastrointestinal transcript distribution that was reported for zebrafish and mouse and indicated a conserved expression profile in vertebrates (Haumaitre et al., 2005; Sun and Hopkins, 2001). After neurulation, neural HNF1 β expression dramatically regressed whereas, mesodermal transcription was detected in the proximal and distal tubules of the differentiating renal anlage. In late tadpole stages, HNF1 β transcription is predominantly seen in the excretory system, namely the developing proximal nephrostomes and the caudal extending wolffian duct as well as in the liver and gall bladder. Transcription in the pancreas remarkably decreased (figure 3.1.1, 39 and 39v).

The refined expression pattern of HNF1 β clearly demonstrated early dorsal endodermal expression that was spatially retracted during subsequent development to the ventral foregut endoderm, including the liver. In addition, on transversal sections it was demonstrated for the first time, that HNF1 β was also expressed in the ventral as well as the dorsal pre-pancreatic endoderm by the onset of pancreas formation at stage 34. Therefore it was of further interest to elucidate the necessity of HNF1 β in respect to pancreas development in *Xenopus laevis*.

3.1.2 Functional characterisation of HNF1 β during pancreas development

To investigate the role of the transcription factor HNF1 β during pancreas development in *Xenopus laevis* loss- and gain- of- function experiments were performed. In the loss-of- function approach, HNF1 β protein synthesis was inhibited by injection of antisense morpholino oligonucleotides that were targeted to the prospective endoderm. In the endoderm, their specific binding to HNF1 β mRNAs repressed protein translation. Effects on endodermal organogenesis, in particular the pancreas, that were caused by HNF1 β protein knockdown were investigated by analyzing changes in RNA levels of pancreas specific proteins. Changes in transcript levels were monitored by whole mount in situ hybridisation (WMISH) or semiquantitative RT-PCR.

For the gain of function approach, increase in HNF1 β activity was achieved by artificially overexpressing the transcription factor in the endoderm. This was achieved by microinjection of *in vitro* transcribed HNF1 β sense „capRNA“. Analogous to the loss- of- function approach, HNF1 β capRNA was targeted to the prospective endoderm and effects on endodermal organogenesis were determined by changes in RNA levels of pancreatic marker genes, using WMISH and semiquantitative RT-PCR.

3.1.2.1 Knockdown of HNF1 β leads to pancreatic hypoplasia

Verification of efficient translational inhibition by morpholino oligonucleotides

Depletion of HNF1 β was achieved by injection of antisense morpholino oligonucleotides directed against two different sites of the HNF1 β mRNA. HNF1 β -Mo1 was designed to target the conserved 5' end of the HNF1 β -ORF beginning with the translation initiation site ATG. In order to prove specificity for morpholino induced phenotypes, a second morpholino was designed. This HNF1 β -Mo2 was directed against the 5'UTR region of HNF1 β coding sequence (figure 3.1.2). Due to its pseudo-tetraploid genome, some proteins are coded by a second gene copy, so called pseudoallele. As consequence *Xenopus laevis* expresses in addition to regular proteins their functionally redundant pseudo allelic partner. Pseudoallel-transcripts differ in their nucleic acid sequence, in particular in the 5' untranslated regions (5'UTR).

Also for HNF1 β , EST sequences for pseudoalleles were identified by EST database search, demonstrating a three nucleic acid difference compared to the wild type HNF1 β -mRNA sequence. Theoretically, these mismatches could impair proper binding of the HNF1 β -Mo2 to pseudoallelic RNA targets thereby allowing protein translation of the redundant HNF1 β variant and consequently increase the probability of an incomplete HNF1 β protein knockdown. However, according to information from the manufacturer, it is rather unlikely that three mismatches prevent morpholino binding (<http://www.gene-tools.com>). Efficient inhibition of protein translation by recognising an HNF1 β mRNA target was determined in

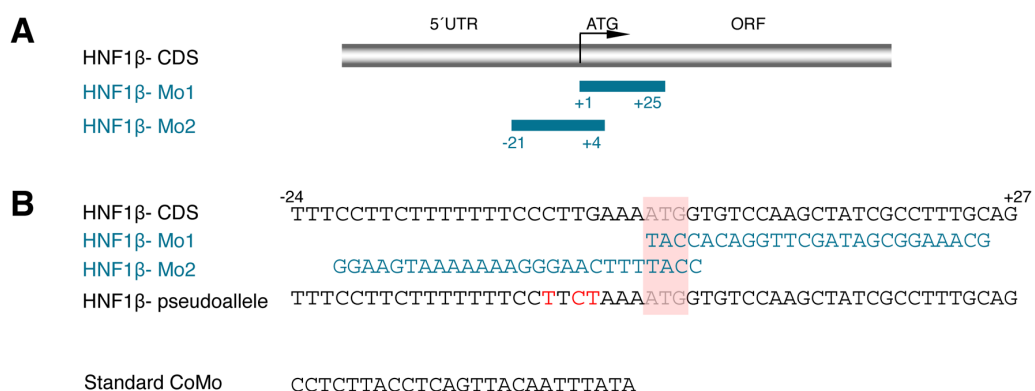


Figure 3.1.2 Position and sequence of HNF1 β - specific morpholinos. (A) The scheme indicates the position of the two HNF1 β specific morpholinos (HNF1 β -Mo1 and HNF1 β -Mo2, blue bars) relative to the coding sequence (CDS) of HNF1 β (NCBI: NM_001087216; grey bar). Numbers state the nucleic acid position with +1 beginning at the translation initiation site ATG. (B) Sequences of HNF1 β -Mo1 and -Mo2 (blue) are stated below the scheme. HNF1 β -Mo1 targets the beginning of the ORF at the translation initiation site ATG (grey, underlined in red). HNF1 β -Mo2 targets the 5'UTR region overlapping the ATG. EST database search identified a pseudoallele (NCBI: BU903744) that showed three mismatches compared to the HNF1 β -CDS. Last, the sequence of the unspecific standard control morpholino is stated (CoMo; GeneTools).

in vitro and *in vivo* approaches (figure 3.1.3). For this purpose, the 5' end sequence of the HNF1 β coding sequence (CDS) complementary to the HNF1 β -Mo1 and HNF1 β -Mo2 sequence, was fused upstream and in frame to the coding sequence of the green fluorescent protein (GFP; HNF1 β -5'end-GFP; Collart et al., 2005).

In vitro, translational inhibition upon morpholino binding was tested in a radioactive combined transcription and translation assay („hot“TNT (hTNT), figure 3.1.3, A). The HNF1 β -5'end-GFP plasmids served as template for *in vitro* transcription of capRNA that was directly used as template for *in vitro* translation. In the translation process ³⁵S-methionine was incorporated into the synthesised protein which allowed autoradiographic detection of the translation product (figure 3.1.3., A). As seen in the autoradiogram of the

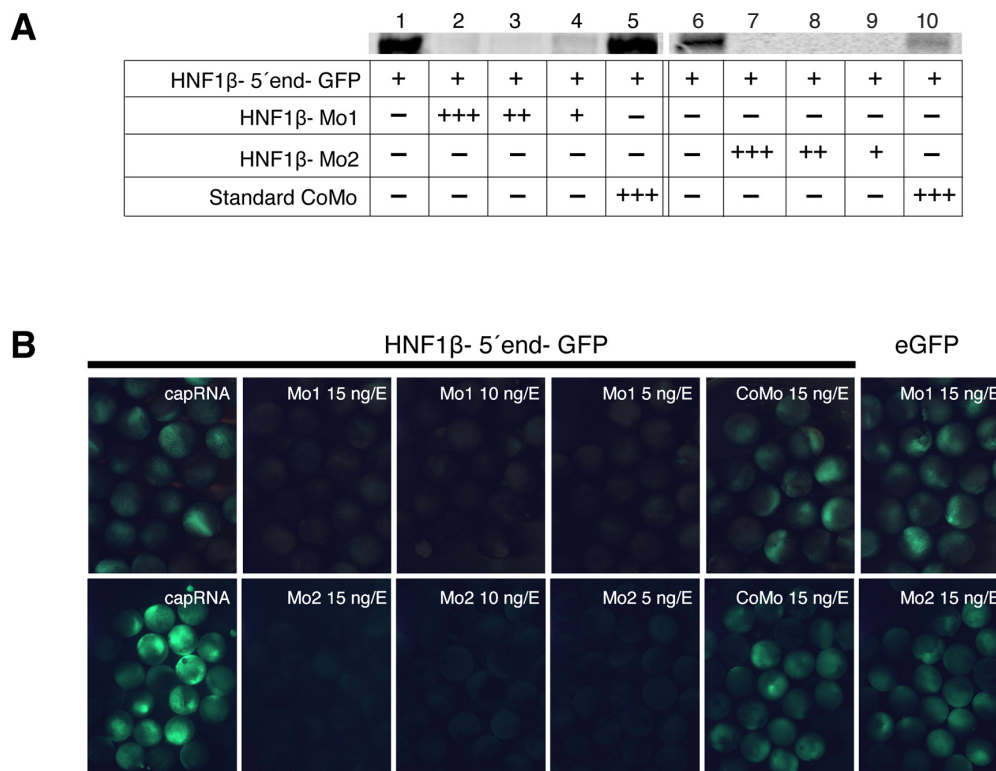


Figure 3.1.3 Determination of knockdown efficiency of HNF1 β - specific morpholinos. (A) *In vitro*: combined transcription and translation assay (hTNT) was performed to reveal recognition of target sequence by HNF1 β -Mo1 (lane1- 4) and HNF1 β -Mo2 (lane 6-10). Autoradiogram shows translation product of the reaction. Table below states the composition of each reaction for each lane. 300 ng of HNF1 β -5'end-GFP construct were used in each reaction alone, or in combination with different amounts of HNF1 β -Mo1 or HNF1 β -Mo2 or unspecific control morpholino (CoMo; +++= 0.5 pmol; ++ = 0.2 pmol; + = 0.1 pmol). Weaker band in the second CoMo reaction is due to a loading mistake (B) *In vivo*: HNF1 β -5'end-GFP capRNA was *in vitro* transcribed and injected into the animal pole of a two cell stage embryo (black bar) alone (capRNA, 100 pg/ E) or in combination with different amounts of HNF1 β - Mo1, HNF1 β - Mo2 or CoMo (15 pg/E, 10pg/E and 5pg/E as stated in each panel). After 24 hr binding efficiency was scored according to GFP fluorescence. The presence of either morpholino efficiently blocks HNF1 β -5'end-GFP translation, whereas injection of CoMo does not impair protein synthesis. Specificity of HNF1 β - Mo1 and HNF1 β - Mo2 to its target sequence was also confirmed by wild type GFP fluorescence (eGFP), by coinjecting eGFP capRNA (100 pg/E).

hTNT, *in vitro* translation of the HNF1 β -5'end-GFP fusion protein remained unaffected in the absence of morpholinos. Addition of the first morpholino, HNF1 β - Mo1, efficiently repressed protein translation in a concentration dependent manner, as addition of low amounts (here, 0.5 pmol/ reaction) did not completely impair HNF1 β -5'end-GFP synthesis (figure 3.1.3, A, lane 4). The second morpholino, HNF1 β -Mo2, blocked HNF1 β protein translation in all concentrations tested. Addition of an unspecific standard control morpholino (CoMo), directed against human β -globin- pre- mRNA, did not abolish HNF1 β protein synthesis in the *in vitro* assay.

In order to determine knockdown efficiency *in vivo*, the HNF1 β - 5'end-GFP encoding capRNA was *in vitro* transcribed and 100 pg coinjected with either HNF1 β -Mo1 or HNF1 β -Mo2 into two-cell stage embryos (figure 3.1.3, B). After 24 hr, effective inhibition of protein synthesis in presence or absence of morpholinos was monitored by loss of GFP fluorescence in the embryo. In contrast to the *in vitro* assay, the lowest amount of 5 ng of HNF1 β -Mo1 or HNF1 β -Mo2 inhibited protein translation of the HNF1 β -5'end-GFP protein. Conversely, a three fold higher dose of the unspecific CoMo (15 ng/E) did not prevent HNF1 β -5'end-GFP protein translation. Target specificity of HNF1 β -Mo1 and HNF1 β -Mo2 were further confirmed by coinjecting wildtype GFP capRNA (eGFP, 100pg/E) with 15 ng of HNF1 β - Mo1 or HNF1 β - Mo2. As expected GFP fluorescence was not abolished in this experiment, proving selectivity of HNF1 β -Mo1 and HNF1 β -Mo2 for HNF1 β mRNA target. Although both experiments cannot exclude off target effects or predict the extent to which expression of the endogenous HNF1 β protein is inhibited, they prove recognition of the morpholino target sequence and provide strong evidence that translational inhibition occurs in the embryo. In order to achieve high knockdown efficiency of HNF1 β protein translation HNF1 β -Mo1 and HNF1 β -Mo2 were coinjected into the embryo and effects on pancreas development were investigated by analysis of pancreatic marker genes.

Inhibition of HNF1 β reduced expression of pancreatic marker genes

After confirming specificity of HNF1 β -Mo1 and HNF1 β -Mo2 to the target sequence both morpholinos were coinjected (0.5 pmol each) to knockdown HNF1 β protein translation within the embryo. To target the prospective endoderm, morpholinos were injected radially into the vegetal pole of a four-cell stage embryo. In order to reveal the role of HNF1 β during pancreas organogenesis, embryos were cultured till early tadpole stage and effects on pancreas development were analysed by investigating changes in pancreas specific marker gene expression. In order to exploit the role for HNF1 β in pancreas specification, expression of the pancreatic progenitor markers XlHbox8 and Xp48 were tested. To reveal effects on endocrine or exocrine cell fate specification, transcription levels of the earliest endocrine specific gene insulin and of the exocrine specific gene XPDip were determined (figure 3.1.4).

Expression of the first pancreatic progenitor marker *XIHbox8* is initiated at stage 28 in the foregut. *XIHbox8* is one of the earliest genes that is specifically expressed in the prospective ventral and dorsal pancreatic epithelium while it additionally marks the duodenal progenitor cells (Wright et al., 1989). At stage 32, *XIHbox8* expression was still confined to the ventral and dorsal pancreatic anlage as well as the intermediate duodenal region of all uninjected control embryos (figure 3.1.4, A, white arrow head, black bracket and black arrow respectively). At this stage the dorsal pancreatic anlage begins to evaginate from the gut epithelium into the surrounding mesenchyme. The majority of embryos that were injected with 0.5 pmol of unspecific control morpholino (88%) demonstrated no alteration of *XIHbox8* expression (figure 3.1.4 B, E). Only 12% (2/16) showed a size reduction of the *XIHbox8* expressing domain in the anterior endoderm. In *HNF1 β -Mo1+2* injection, pancreatic *XIHbox8* expression was not detectable in 98% of the embryos at stage 32,

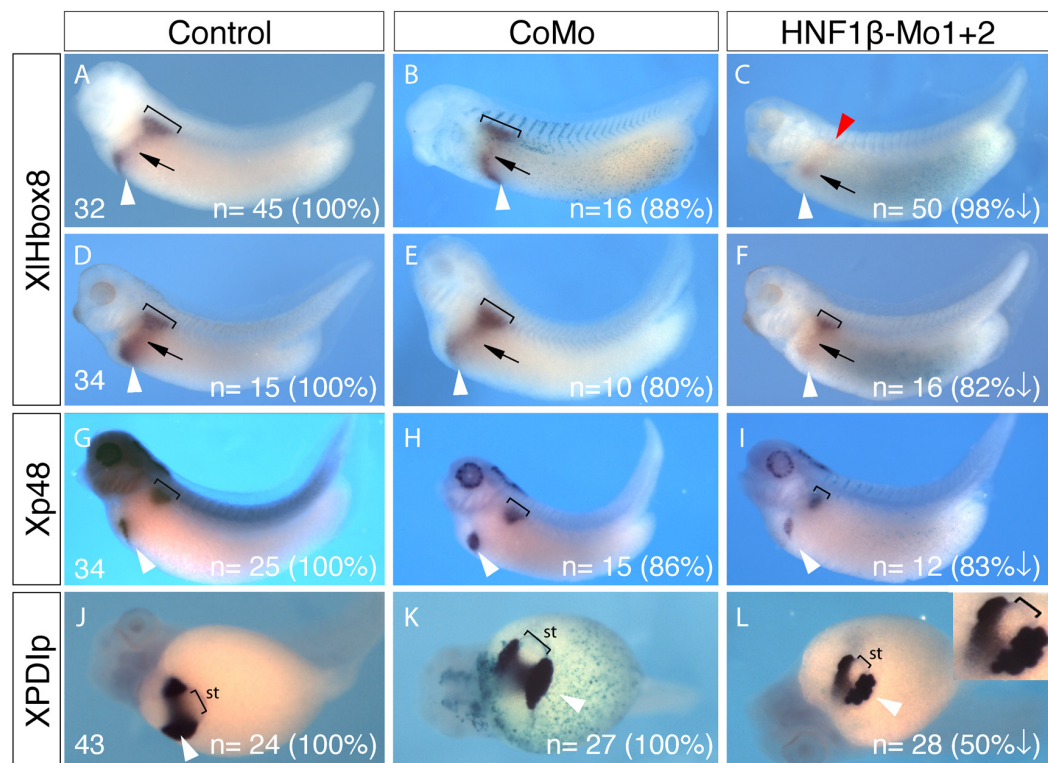


Figure 3.1.4 Knockdown of *HNF1 β* reduces expression of pancreatic marker genes. *HNF1 β* protein translation was inhibited upon combined injection of *HNF1 β* specific antisense morpholinos *HNF1 β -Mo1+2* (each 0.5 pmol/E). Correct microinjection was traced by coinjection of β -galactosidase capRNA (50pg/ E). Embryos were cultured till control siblings reached desired developmental stage and analysed for pancreatic marker gene expression by WMISH. Embryos are shown with in a lateral view with the head to the left (A- I) and from a ventral view (J- L). Analysed marker genes are stated to the left. Stages are stated as small numbers to the bottom left in A, D, G, J. Effects on marker gene expression were compared to effects in embryos injected with unspecific control morpholino (CoMo, 1pmol/E; B, E,H, K). White arrow heads point to the ventral pancreatic anlage (A-I), brackets size the dorsal pancreatic rudiment (A-I), red arrow head points to the presumptive dorsal pancreatic domain (C). In panel J-L, the white arrow head points to the fused pancreatic organ that shows altered morphology by protrusion formation in its exocrine compartment; objective enlargement 60 \times ; (st) stomach. n= states the total number of embryos analysed for each marker. Percent values in brackets indicate the amount of embryos showing the presented phenotype. Inset in L shows morphological affected pancreatic lobe.

most of them still maintaining weak duodenal expression XIHbox8 expression between the presumptive pancreatic domains (figure 3.1.4, compare B and C). By the time of pancreatic budding at stage 34, control embryos and CoMo injected embryos (8/ 10= 80%) showed regular XIHbox8 transcription in the pancreatic and duodenal territories (figure 3.1.4 , D). The remaining 20% of CoMo injected embryos revealed a slight size reduction in the ventral pancreatic expression domain. In contrast, 98% of HNF1 β - Mo1+2 injected embryos presented weak increase in XIHbox8 expression in the dorsal pancreatic endoderm as compared to HNF1 β -Mo1+2 injected embryos at stage 32, though it was spatially restricted to a smaller territory (figure 3.1.4, compare D,E and F). Increased transcription level was also represented by stronger duodenal XIHbox8 expression although it did not exhibit the level of regular XIHbox8 expression seen in control embryos. Only 18% (2/16) presented regular XIHbox8 expression while the ventral pancreatic XIHbox8 expression was still undetectable in 82%. This result indicated that HNF1 β was required within the endoderm to activate XIHbox8 expression in the pancreatic and duodenal epithelium.

The second pancreatic progenitor marker that was analysed in HNF1 β depleted embryos was Xp48. As known from its expression profile, Xp48 expression was evident in the gut epithelium at stage 28 (Afelik et al., 2006). In contrast to XIHbox8, Xp48 is exclusively expressed in the ventral and dorsal pancreatic epithelium where its expression peaked with pancreatic budding at stage 34. As seen in control embryos the ventral Xp48 positive epithelium extends ventro-posterior along the liver diverticulum (figure 3.1.4, G; white arrow and bracket respectively). Despite a minimal reduction of the ventral Xp48 expressing region in 86% of injected embryos, the CoMo did not alter Xp48 expression (figure 3.1.4, H). Caudal extension of Xp48 expression in the ventral as well as in the dorsal pancreatic region was remarkably reduced in 83% of HNF1 β -Mo1+2 injected embryos (figure 3.1.4, I; bracket). This result demonstrated that HNF1 β was also required for Xp48 expression in the pancreatic region and only 17% (2/12) remained unaffected. Hence, HNF1 β activity in the endoderm seems to influence Xp48 expression. In contrast to XIHbox8 expression, HNF1 β knockdown did not completely impair Xp48 gene activation in the pancreatic epithelium providing evidence for a distinct regulatory mechanism for Xp48 gene induction in the endoderm.

As reported from a previous study (Afelik et al., 2006), both pancreatic progenitor markers are required to induce pancreas formation in the gut endoderm. The majority of the pancreas is composed of the exocrine tissue. In *Xenopus laevis* the first exocrine differentiation marker is the enzyme XPDIp whose transcripts demarcate the territory of the pancreatic lobes from stage 39 onwards. At stage 43, the pancreatic lobes are fused to one organ and

the branching epithelium exhibits strong proliferative activity that promotes size increase and organ morphogenesis. To investigate whether reduced expression of pancreatic precursor genes as *XIHbox8* and *Xp48* in *HNF1 β* depleted embryos was a transient effect or whether lack of their activity affects subsequent pancreatic growth, the organ size was estimated in *HNF1 β -Mo1+2* injected embryos by the size of *XPDIp* expressing territory at stage 43. In 100% of uninjected embryos or *CoMo-* injected embryos organ size was unaffected (figure 3.1.4, J and K), whereas 50% of *HNF1 β Mo1+2* injected siblings showed an obvious size reduction of the fused pancreatic organ at stage 43. Size reduced organ showed morphological divergence forming small protrusions rather than a condensed exocrine tissue structure (figure 3.1.4, L, inset). Decrease in *XPDIp* positive territory together with the observed impaired expression of pancreatic progenitor markers *XIHbox8* and *Xp48* suggested that *HNF1 β* was required in the gut endoderm for pancreas specification as well as for organ outgrowth and differentiation. On this background it was of further interest to investigate effects of *HNF1 β* on endocrine cell differentiation.

At stage 32, few cells that lay scattered in the dorsal pancreatic epithelium initiate insulin expression. Gene expression of insulin is detectable in the dorsal endoderm from stage 32 onwards (Kelly and Melton, 2000). The endocrine hormone insulin is therefore the first marker gene for endocrine cell differentiation in the pancreas. These early insulin-expressing cells migrate along within the pancreatic epithelium and accumulate anteriorly in the dorsal pancreatic rudiment at stage 36 (Kelly and Melton, 2000). So far, it remained obscure how or when these first endocrine cells are specified in the dorsal gut region.

Interestingly, embryos that were injected with *HNF1 β - Mo1+2* demonstrated a reduced size of insulin-expressing region (figure 3.1.5, A). Determination of the cell number of insulin-positive cells per embryo revealed that *HNF1 β -Mo1+2* injected embryos had less insulin-positive cells than uninjected control or *CoMo-* injected embryos. At stage 34, scattered insulin-positive cells that are located in a caudal extending area of the dorsal gut endoderm move anterior along with the evaginating bud clustering in the dorsal rudiment. Reduction in insulin cell number and the size of insulin-expressing region could arise from slight differences in developmental staging or a naturally occurring variation in cell position.

In order to specify effects on insulin expression, the exact number of insulin-positive cells in the dorsal gut epithelium was determined and compared between uninjected control embryos, control morpholino injected embryos and embryos injected with *HNF1 β Mo1+2* (figure 3.1.5; B). As presented in the graph, injection of *HNF1 β* specific morpholinos significantly reduced the average number of insulin-expressing cells to 15 cells per embryo, compared to 23 cells in uninjected control embryos or to the average number of 20 cells

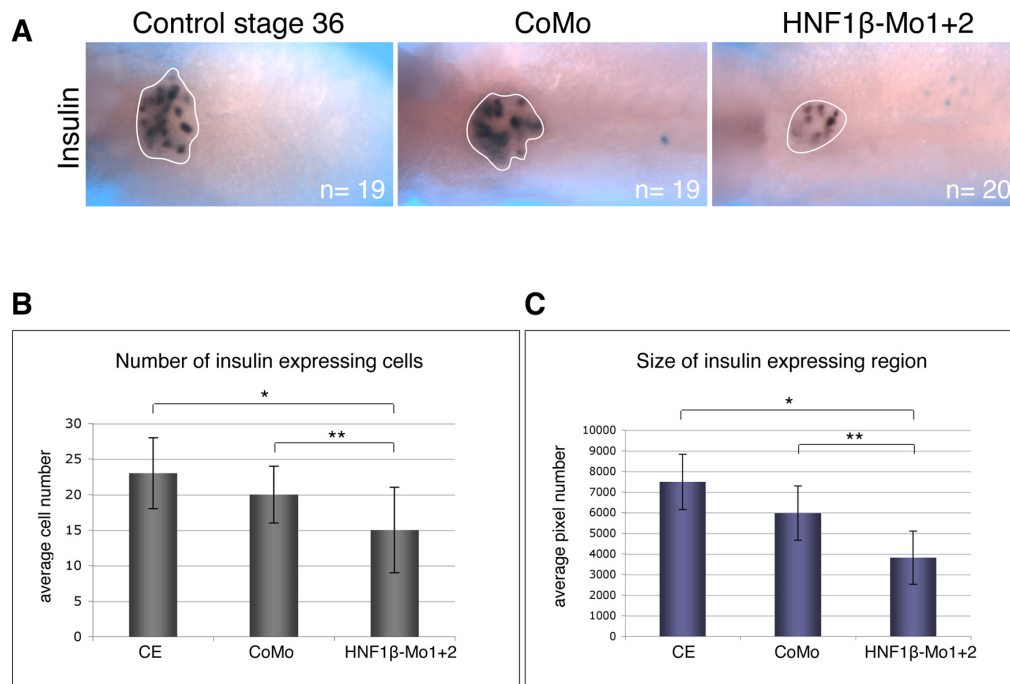


Figure 3.1.5 Knockdown of HNF1 β leads to reduced insulin expression. (A) After WMISH, insulin expression was analysed in stage 36 embryos after removing the overlying notochord and surrounding tissues. White line marks the insulin expressing region whose size was determined by morphogenetic measurements. Two independent experiments were performed and the total number of embryos (n) was used for quantification. (B) Columns indicate the average number of insulin positive cells counted in the dorsal gut epithelium of a stage 36 embryo. Error bars indicate the standard deviation. control embryos (CE)= 23 \pm 5; control morpholino injected embryos (CoMo)= 20 \pm 4; HNF1 β -Mo1+2 injected embryos (HNF1 β -Mo1+2)= 15 \pm 6. *: p-value < 0.0001; **: p-value = 0.0046 (p-value from unpaired two-tailed students t-test calculated using free available online software *graphpad*). (C) Columns indicate the average number of pixels per insulin-expressing region. Pixel number was quantified for each region using the software ImageJ. Values are given as mean \pm standard deviation of the mean CE= 7481 \pm 1340; CoMo= 5 968 \pm 1319; HNF1 β -Mo1+2= 3811 \pm 1289). *: p-value < 0.0001; **: p-value < 0.0001 (p-value from unpaired two-tailed students t-test calculated using free available online software *graphpad*).

in CoMo- injected embryos. 90% (18/ 20) of HNF1 β -Mo1+2 injected embryos contained less insulin positive cells than the average value of uninjected controls and 75% (15/ 20) of HNF1 β -Mo1+2 injected embryos presented less insulin positive cell than the average value of CoMo injected embryos. CoMo injected embryos also appeared to be slightly impaired in activation of insulin expression compared to uninjected control embryos (57% , 11/19) however to less extend than HNF1 β - Mo1+2 injected embryos.

The decreased number of insulin positive cells was also evident in the smaller range of insulin positive territory within the dorsal gut epithelium, comparing HNF1 β -depleted embryos with CoMo-injected or uninjected controls (figure 3.1.5, C). 80% of HNF1 β -Mo1+2 injected embryos showed a size reduction in comparison to CoMo- injected siblings. Although the downregulation of insulin expression was so far not quantified by real-time RT-PCR, the decreased cell number in association with a decrease in expression domain argued for significance of effect of HNF1 β depletion on insulin expression in the dorsal en-

doderm. Using the same batch of embryos for injections, these results also argued against a natural occurring variance in insulin positive cells or a variance due to developmental stage difference. In an attempt to confirm morpholino induced repression of pancreas formation, HNF1 β -WT capRNA was coinjected with HNF1 β -Mo1+2 (Vignali et al., 2000). However, the rescue experiments failed due to 100% lethality of injected embryos.

In summary, depletion of HNF1 β caused reduction of XIHbox8 and Xp48 expression, a reduced amount of insulin positive cells as well as pancreatic hypoplasia evident in a smaller expression domain of XPDip.

Obviously, HNF1 β activity was not only crucial for activation pancreatic progenitor genes XIHbox8 and Xp48 but also for activation of differentiation markers as insulin. These data suggested that HNF1 β is required in the endoderm for pancreas specification and endocrine differentiation.

3.1.2.2 Induction of HNF1 β expands expression of pancreatic marker genes

To further investigate the requirement of HNF1 β for pancreas development, the transcription factor activity was upregulated in the endoderm by microinjection of HNF1 β encoding capRNA. For this purpose, the HNF1 β -ORF (1683 bp) was isolated by RT-PCR from total RNA extracts of stage 39 embryos and cloned into the pCS2+ expression vector (figure 3.1.6, A; Vignali et al., 2000). This construct coding for the wildtype HNF1 β protein (HNF1 β -WT) served as a template for *in vitro* transcription of sense „capRNA“ that was injected into embryos in a different amounts, ranging from 500 to 10 pg/ embryo. To target increased HNF1 β expression within the endoderm, HNF1 β -WT capRNA was coinjected with β -galactosidase capRNA radially into the vegetal pole of four-cell stage embryos. Embryos were grown to tailbud stage 33 in order to investigate changes on RNA expression levels of pancreatic marker genes as the pancreatic progenitor markers XIHbox8 and Xp48, the exocrine marker XPDip and the endocrine marker insulin.

From previous studies, focusing on the mesoderm inducing activity of HNF1 β , it was expected that ectopic endodermal expression of HNF1 β (1 ng- 500pg/ E) in *Xenopus laevis* would not affect embryonic development (Vignali et al., 2000). Surprisingly, in this study, vegetally injected embryos (500 pg/ E) revealed severe gastrulation defects resulting in high embryonic lethality (data not shown) and serious embryonic malformations in surviving embryos at stage 34 (figure 3.1.6, B).

The most striking difference observed between the HNF1 β overexpression analysis and the overexpression performed in the earlier study, is that overactivation of HNF1 β upon capRNA injection did not result in any obvious phenotype. Sequence comparison of the

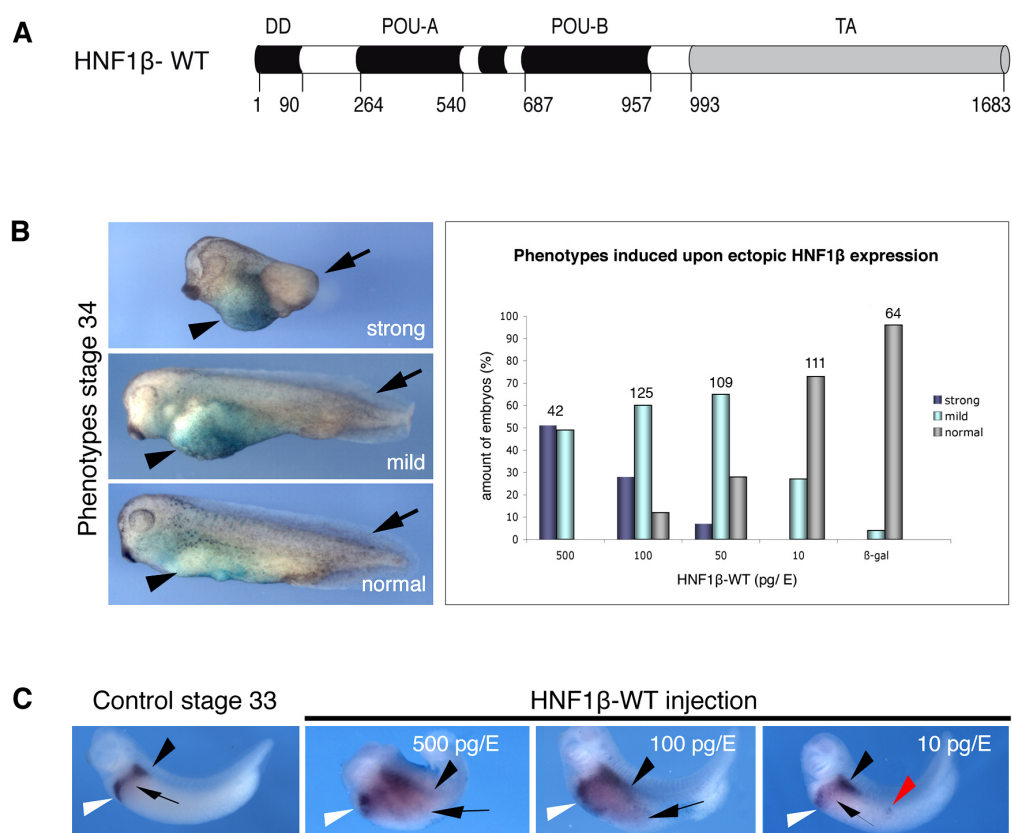


Figure 3.1.6 Phenotypes induced upon ectopic expression of HNF1β in the endoderm. (A) Schematic drawing of the HNF1β-WT construct, including the HNF1β-ORF (1686 bp). The transcription factor HNF1β consists of an N-terminal DNA binding domain (black bar) that is composed of a dimerisation domain (DD) and two DNA binding motifs (POU-A and POU-B) and a C-terminal transactivation domain (TA, grey bar; Wu et al., 2004). Numbers below the bar indicate the nucleotide position in the HNF1β coding sequence. (B) HNF1βWT capRNA was *in vitro* transcribed and injected radially into the vegetal pole of four cell stage embryos in an amount ranging (500- 10 pg/E). Correct localisation of injected capRNA was traced by β-galactosidase staining. Embryonic malformations, induced upon HNF1β-WT injection, were classified into three groups: the strong phenotype (reduced head structures: small eyes and forehead, short trunk (black arrow), ventro-anterior endoderm expansion (black arrow head), the mild phenotype (less axis shortening, anterior endoderm enlargement) and normal phenotype that was indistinguishable from control embryos at stage 34 (not indicated in the panel). The graph represents the percentage of embryos that showed strong, mild or normal phenotype depending on the injected amount of HNF1β-WT capRNA (pg/E). Numbers on top of the columns state total number of embryos from two independent experiments (table 3.1) The legend shows the colour code of the three phenotype groups. (C) Effect on pancreas development upon ectopic activation of HNF1β in the endoderm was investigated by analysis of gene expression of the pancreatic progenitor marker XIHbox8 at stage 33. Injected amounts of HNF1β-WT capRNA are indicated in each panel. Total number of embryos n for each sample: control, 500 pg/E= 32; 100 pg/E= 39, 50 pg/E= 32, 10 pg/E= 42. Embryos injected with 500pg/E HNF1β-WT capRNA showed a broad homogenous expansion of XIHbox8 expression towards the caudal tip of the embryo. Ventral and dorsal pancreatic expression domains are marker with white and black arrow head respectively. The posterior boundary of XIHbox8 expression in the duodenum is pointed out by black arrow. Note that XIHbox8 expansion is concentration dependent (100- 10pg/E), showing ectopic territories in distinct loci of the posterior gut tube at low concentrations (red arrow head).

obtained construct from R.Vignali that was efficiently used for WMISH analysis, with the here isolated HNF1 β ORF identified insertion of a thymidine nucleotide at position 1414. This point mutation results in an HNF1 β mutant containing a DNA binding region but lacking a functional transactivation domain. This was most probably the reason for the absence of an embryonic phenotype.

Embryonic malformations were classified into three phenotype-groups: strong, mild and normal. The strong phenotype was predominantly obtained upon injection of high amounts of HNF1 β -WT capRNA (500 pg/ E). It was characterised by **reduced head and trunk structure** as well as anterior endoderm expansion. **The milder phenotype still showed enlargement** of the anterior endoderm however less trunk deformations and defects in head formation. The normal phenotype was undistinguishable from control embryos at stage 34. These deformation were concentration dependent as they became less severe with decreasing amount of injected HNF1 β -WT capRNA (figure 3.1.6; graph, table 3.1).

To specify the apparent endodermal malformations for pancreas development, injected embryos were analysed for changes in RNA levels of the pancreatic marker gene *XIHbox8* by WMISH (figure 3.1.6, C). Its expression was strongly upregulated in the pancreas as well as in the duodenal region and its expression expanded posteriorly upon HNF1 β overexpression. This effect decreased in a concentration dependent manner as seen by injection of lower capRNA concentration (100 and 50 pg/ E). **Injection of 500 pg HNF1 β -WT capRNA** caused not only a strong malformation phenotype but it also increased lethality of injected embryos up to 100% (data not shown). Injection of 100 pg HNF1 β -WT capRNA lead predominantly to a mild phenotype and lethality decreased to 50%.

Contradictory to the previous report (Vignali et al., 2000), injections performed in this study demonstrated that ectopic expression of HNF1 β in the whole endoderm, including regions where endogenous HNF1 β expression is low, affected embryogenesis of *Xenopus laevis*. Enlargement of the anterior endoderm was associated with caudal expansion of the endogenous *XIHbox8* expression domains, namely the pancreas and the duodenum. Interestingly the homogenous expansion of *XIHbox8* towards the posterior end was dependent

HNF1 β -WT	n	strong	mild	normal
500 pg/E	42	51% (22/42)	49% (20/42)	0%
100 pg/E	125	28% (35/125)	60% (76/125)	12% (14/125)
50 pg/E	109	7% (8/109)	65% (71/109)	28% (29/109)
10 pg/E	111	0%	27% (30/111)	73% (81/111)
β -gal 500 pg/E	64	0%	4% (2/64)	96% (61/64)

Table 3.1 Phenotypes induced upon ectopic expression of HNF1 β in the endoderm Table states total number of embryos (n) obtained from from two different experiments and the percentage of embryos showing strong, mild or normal phenotype. 500pg/E β -galactosidase encoding RNA were injected to exclude unspecific effect by micromanipulation of the embryo.

on the level of ectopic HNF1 β expression. High HNF1 β capRNA concentration lead to homogenous extension of the XIHbox8 expressing region, implying an HNF1 β induced expansion of the endogenous expression domain. Low concentration revealed additional XIHbox8 positive cells in additional distinct territories of the posterior intestine. Combining the reduction of XIHbox8 gene expression in the HNF1 β loss of function experiment with the reverse complement result in the HNF1 β gain of function approach, it was postulated that HNF1 β is an upstream regulator of the pancreatic progenitor gene XIHbox8 within the endoderm. Although, it remained unclear whether it was a direct or indirect regulatory mechanism.

The transcription factor HNF1 β is expressed already at gastrula stage in the involuting endoderm. High levels of HNF1 β activity in the early embryo was lethal and caused severe embryonic malformations implying an early function during embryogenesis. Therefore it was of further interest to determine the exact time point for HNF1 β requirement in the endoderm, in particular regarding later pancreas formation from the gut tube.

To address this question, a time point inducible HNF1 β protein was generated by fusing the HNF1 β -ORF to the ligand binding domain of the human glucocorticoid receptor (GR-LBD, figure 3.1.7; Gammill and Sive, 1997). In the cell, heat shock proteins (Hsp) bind to the GR domain keeping the fusion-protein in an inactive state in the cytosol. After addition of the steroid hormone dexamethason (Dex), Hsps dissociate, thereby releasing the transcription factor that can translocate to the nucleus.

To confirm obtained data of HNF1 β loss- and gain of function, the HNF1 β coding sequence was also fused to the repressor domain of the *Engrailed* transcription factor from *Drosophila* (EngRP) in combination with the GR-LBD. This HNF1 β - EngGR fusion protein maintained a dominant repressor activity and was inducible upon Dex application. Since the transcription factor HNF1 β is known to function as positive regulator, its transforma-

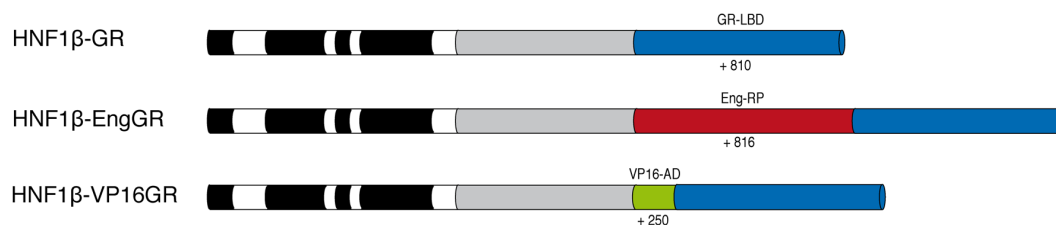


Figure 3.1.7 HNF1 β constructs used for gain- and loss of function approaches. The HNF1 β -ORF was PCR amplified out of the pCS2+ HNF1 β -WT construct and fused to the ligand binding domain of the glucocorticoid receptor (GR-LBD). Activity of the HNF1 β -GR fusion protein was activated by application of 1x dexamethason (+Dex). In addition, activity of HNF1 β function was repressed or enhanced by fusing the HNF1 β -ORF to the repressor domain of the engrailed transcription factor (Eng-RD, 810bp, red) as well as to the activation domain of the viral transcription factor VP16 (VP16-AD, 250bp, green) including the GR-LBD. HNF1 β -EngGR maintains a dominant negative activity whereas HNF1 β -VP16GR maintained a strong activator activity.

tion into a dominant negative repressor by EngGR fusion depleted its endogenous function. As consequence, injection of HNF1 β -EngGR capRNA was expected to cause a similar reduction of pancreatic marker expression as observed upon HNF1 β - Mo1+2 injection. A similar approach was performed in the previous study by the group of Vignali (Vignali et al., 2000). Although in their study, the HNF1 β transactivation domain was not fused to the EngRP domain but replaced it, and it was not fused to the GR-LBD.

To confirm effects upon ectopic activation of HNF1 β in the endoderm, transcription factor activity was also increased upon injection of HNF1 β -VP16GR capRNA. Here, HNF1 β activity was **additional enhanced by fusion to the dominant activator domain of the viral transcription factor VP16 (VP16-AD)**.

Ectopic expression of the pancreatic progenitor marker XlHbox8 provided evidence for an activating role of HNF1 β during pancreas development. To determine the time window for HNF1 β necessity, the hormone-inducible HNF1 β -GR protein was overexpressed in the endoderm. Therefore HNF1 β -GR capRNA (75 pg/E) was **radial injected into the vegetal pole** of four-cell stage embryos. HNF1 β function was activated upon Dex-treatment by the end of gastrulation stage 13 and at the onset of gut tube patterning stage 20. Analogous to HNF1 β -Mo1+2 injection, effects on pancreas specification were determined by analyzing changes in transcription of the pancreatic markers XlHbox8 and Xp48, XPDip and insulin.

In control embryos XlHbox8 was detected in the ventral and dorsal pancreatic territory as well as in the intermediate duodenal region (figure 3.1.8, A). 50% of HNF1 β -GR injected embryos that were not activated by Dex-treatment (-Dex) showed regular XlHbox8 transcription in the endogenous expression domains. 44% revealed a slightly caudal expansion of the endogenous XlHbox8 positive regional and a weak ectopic expression in the ventro-posterior region of the endoderm (figure 3.1.8, B) that was clearly seen in the remaining 2% (appendix; figure 8.1).

Upon early Dex mediated activation of HNF1 β in the endoderm, embryos showed enlargement of the anterior endoderm that was similar to the mild phenotype in HNF1 β -WT injections. In 15% (4/26) this posterior expansion was homogenous throughout the endoderm and endogenous expression domains were not clearly distinguishable. In addition, these embryos showed within the homogenous transcript distribution few smaller territories that were positioned to the ventroposterior region of the embryo, similar as in embryos without Dex treatment. In 70% the origin of the posterior expanding XlHbox8 expressing region was defined to the ventral and in particular to the dorsal pancreatic expression domains. After removing the overlaying notochord, it was observed that this dorsal pancreatic Xl-

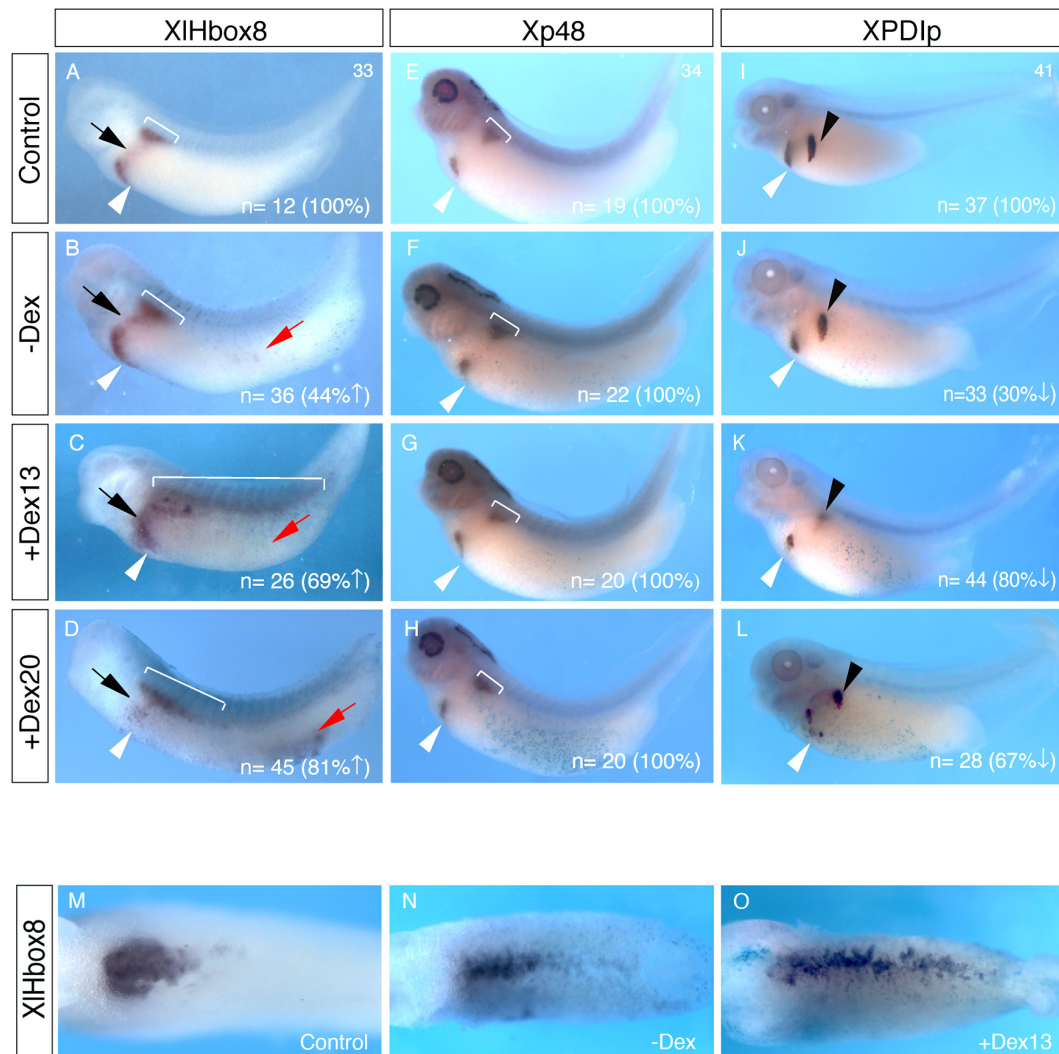


Figure 3.1.8 Changes in pancreatic marker gene expression upon ectopic activation of HNF1 β . HNF1 β was ectopically activated in the endoderm by injecting HNF1 β -GR capRNA (75pg/E) radially into the vegetal pole of a four-cell stage embryo. HNF1 β activity was induced at late gastrula stage 13 and prior organ formation at stage 20 by application of dexamethason (+Dex 13, +Dex20). Uninjected control embryos were also treated with Dex. Correct microinjection was traced by coinjecting β -galactosidase capRNA. Embryos were cultured till control siblings reached desired stage and analysed by WMISH for changes in pancreatic marker gene expression (indicated to the left). n= total number of embryos. Numbers in brackets indicated percentage of embryos showing the most frequent phenotype as indicated in the panel. \uparrow = increased expression; \downarrow = decreased expression. White arrow head: ventral pancreatic expression domain, bracket: sizes the early dorsal pancreatic expression domain; black arrow: duodenal XIHbox8 expression; red arrow: extopic territories of XIHbox8 expression; black arrow head: dorsal pancreatic lobe. M: dorsal expression domains of XIHbox8 in uninjected control embryo. N: -Dex embryos; O: expanded dorsal XIHbox8 expression along the midline of +Dex13 embryo.

Hbox8 expansion did not occur in a broad territory of the epithelium but it was rather spatially restricted to the central and most dorsal region, expanding caudally along the midline (figure 3.1.8, M-O). Later induction at stage 20 did not activate XIHbox8 expression to such an extent, however 72% of examined embryos revealed an ectopic XIHbox8 positive territories in a distinct ventro-posterior region comparable to embryos without

Dex (figure 3.1.8, D). Embryos treated at stage 26 did not show posterior induced *XIHbox8* transcription and resembled untreated embryos (not shown). The vast distribution of *XIHbox8* transcription in the endoderm in early HNF1 β activated embryos resembled the induction obtained in embryos that were injected with HNF1 β -WT capRNA.

Expression of the second pancreatic precursor marker Xp48, that was restricted to the ventral and dorsal pancreatic rudiments, was not affected to the same extent than it was seen for *XIHbox8* expression although some early treated embryos (figure 3.1.8; G, E) showed a slight increase in the ventral pancreatic expression domain. As the difference was remarkably small, this increase in Xp48 transcription could derive from naturally occurring differences during bud formation rather than a specific effect upon ectopic HNF1 β expression.

In order to investigate the role of HNF1 β for later pancreas development, injected embryos were examined for alteration in XPDIP expression, representing the first exocrine differentiation marker in *Xenopus laevis*. Against the expectation, ectopic endodermal activation of HNF1 β resulted in 80% of the embryos in a decreased ventral and dorsal pancreatic rudiment, compared to uninduced embryos as well as control embryos. Reduced pancreatic size was also obtained upon later HNF1 β induction at stage 20. Together with the loss of function data it was concluded that HNF1 β was required but not sufficient to drive pancreatic outgrowth and differentiation.

As for the loss of function approach it was of further interest to analyse changes in expression of the first endocrine marker insulin. In comparison to embryos without Dex, HNF1 β -GR injected embryos that were early activated at stage 13, revealed an increase in insulin positive cells that were located more posteriorly in a larger insulin expressing domain (figure 3.1.9 A; +Dex13). Interestingly, in few embryos insulin positive cells were found in more distal regions of the dorso-lateral endoderm. On the background of previous studies in *Xenopus laevis*, this was the first time observed, that early insulin expression was ectopically induced in the dorsal endoderm upon misexpression of a transcription factor, thereby providing evidence, that HNF1 β plays a crucial role in endocrine cell fate determination within the dorsal pancreatic anlage. Specificity of the effect for the early increase of HNF1 β function in the endoderm, was confirmed since activation at stage 20 did not augment the amount insulin-positive cells to such an extent. It was noteworthy that the number of insulin expressing cells in +Dex13 embryos did not only increase but also mislocated more posteriorly so that insulin positive cells were found in a larger territory expanding posteriorly within the dorsal endoderm. Later HNF1 β activation did not result in an increase of insulin-positive cells nor in obvious mislocation of insulin positive cells (figure 3.1.9, A; +Dex20). Induction of HNF1 β activity at stage 26, prior to pancreas speci-

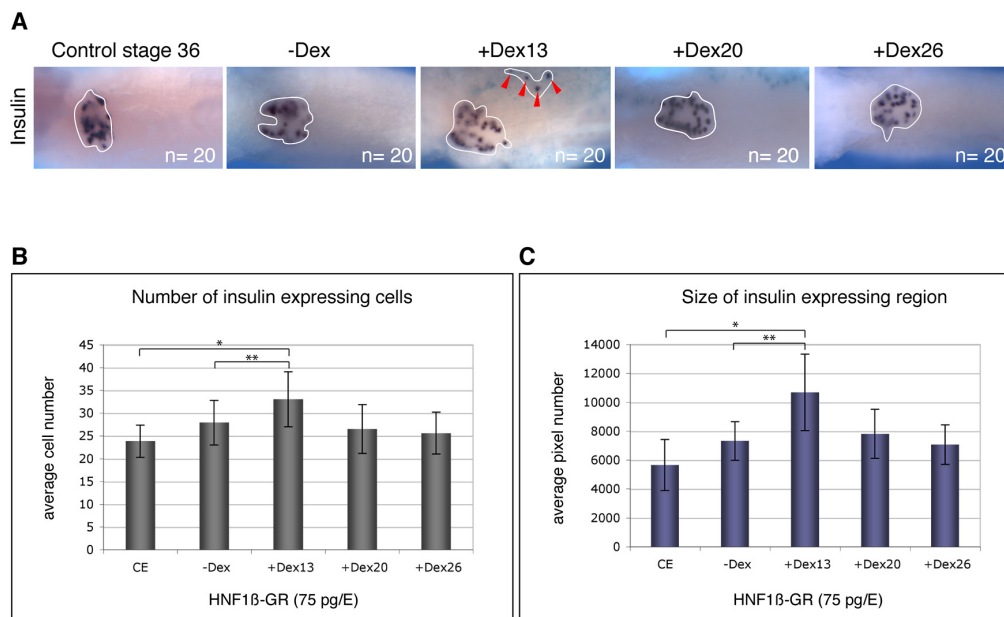


Figure 3.1.9 Ectopic activation of HNF1 β leads to induced insulin expression.

(A) Embryos injected with HNF1 β -GR capRNA (75pg/E) were analysed for changes in insulin expression by WMISH. HNF1 β activity was induced upon Dex-treatment at stage 13, stage 20 and stage 26 (+Dex13, +Dex20, +Dex26). Insulin expression was analysed in stage 36 embryos after removing the overlying notochord and surrounding tissues. White line marks the insulin expressing region whose size was determined by morphogenetic measurements. Two independent experiments were performed and the total number of embryos (n) was used for quantification. Early activation of HNF1 β at stage 13 promoted endocrine cell fate in the dorsal endoderm and induced ectopic insulin expression in the dorso-lateral regions (red arrow heads). 85% (17/20) of +Dex13 embryos obtained more or the same amount of insulin positive cells that the average number of -Dex embryos. Out of these 80%, 23% (4/17) revealed ectopic insulin expression in more distal loci of the dorso-lateral endoderm. (B) Columns indicate the average number of insulin positive cells counted in the dorsal gut epithelium of a stage 36 embryo. In total 20 embryos were analysed for changes in insulin expression. Error bars indicate the standard deviation. control embryos (CE)= 24 \pm 4; -Dex= 28 \pm 5; +Dex13= 33 \pm 6, +Dex20= 27 \pm 5, +Dex16= 26 \pm 5; Error bars indicate standard deviation. *p-value < 0.0001; **p-value=0.0068 (p-values from unpaired two-tailed student's t-test was calculated using online available software *graphpad*). (C) Overactivation of HNF1 β increases the size of insulin expressing domain. Morphogenetic quantification was done on images taken of WMISH-embryos. Quantification was done using ImageJ software. Early activation of HNF1 β lead to enlargement of insulin expressing region compared to CE and untreated embryos (-Dex). Average pixel numbers: CE= 5656 \pm 1768; -Dex= 7318 \pm 1325; +Dex13= 103681 \pm 2645; +Dex 20= 7811 \pm 1698; +Dex26= 7067 \pm 1374. Error bars indicate standard deviation *p-value < 0.0001; **p-value < 0.0001 (p-values from unpaired two-tailed student's t-test was calculated using online available software *graphpad*).

fication by XlHbox8 and Xp48 expression did not alter insulin activation in comparison to untreated embryos. Analogous to HNF1 β - Mo1+2 injection, the effect on cell number and region size was quantified.

The observed increase of insulin-positive cells in WMISH, was reflected in the quantification of cell number and morphogenetic quantification of insulin expressing domain in injected embryos after early and late ectopic HNF1 β activation as well as in untreated controls without Dex, (figure 3.1.9, B and C). To reduce the possibility of natural occurring variances in insulin expression or differences according to embryonic staging, insulin positive

cells were counted in a total of 20 embryos deriving from two independent experiments. Despite the slight increase of insulin positive cells that was already detected in HNF1 β -GR injected but untreated embryos, cell number increased significantly upon early activation of HNF1 β function (figure 3.1.9, B; +Dex13). 85% (17/20) of these embryos showed the same or higher number of insulin positive cells than the average value of 28, obtained in uninduced embryos. Interestingly, in 23% (4/17) few of these insulin positive cells escaped their posterior expanded expression domain and were mislocated in more posterior regions of the endoderm. Cell number increase upon later activation was less evident and comparable to injected but untreated embryos (figure 3.1.9, B).

Not only cell number but also the size of insulin expressing region was measured and compared with uninduced and induced HNF1 β function. As expected from the increase in insulin cell number, early HNF1 β activation (figure 3.1.9, +Dex13) resulted in an expanded insulin-expressing region while expansion upon later HNF1 β activation was not apparently enlarged as compared to uninduced embryos (figure 3.1.9, C). In addition few embryos showed ectopic insulin positive cells in the dorso-lateral region. Data obtained upon ectopic expression of HNF1 β in the endoderm argued that HNF1 β not only regulated XlHbox8 activation but it was also involved in endocrine cell specification.

As HNF1 β injected embryos exhibit a smaller pancreatic bud, based on XPDlp expression, it was concluded that HNF1 β regulates formation of the pancreatic organ but not organ outgrowth. HNF1 β function in the endoderm was required in the dorsal pancreatic epithelium to induced XlHbox8 expression which promotes endocrine at the expense of exocrine cell differentiation. Since overexpression caused a reduction of XlHbox8 in the ventral foregut, it was speculated that HNF1 β plays a different role in the ventral pre-pancreatic endoderm, maybe by influencing development of the adjacent liver.

Together, overexpression data demonstrated that HNF1 β positively regulated XlHbox8 and insulin expression whereas it did not affect Xp48 gene expression. These findings imply a function in pancreas specification as well as in cell differentiation. Data from ectopic overexpression are in accordance with data from HNF1 β depletion. In addition time point specification provided evidence that HNF1 β function plays a role already during gastrulation.

In an attempt to confirm the data obtained in loss and gain of function studies of HNF1 β , the dominant repressor protein HNF1 β - EngGR and the activator protein HNF1 β - VP-16GR were injected into embryos and resulting effects on pancreas development monitored by WMISH analysis of XlHbox8 (figure 3.1.10, appendix figure 7.1).

The fusion protein HNF1 β - EngGR has a strong repressor activity, antagonising endogenous activity of HNF1 β - WT. Injection into embryos, caused a similar reduction of dor-

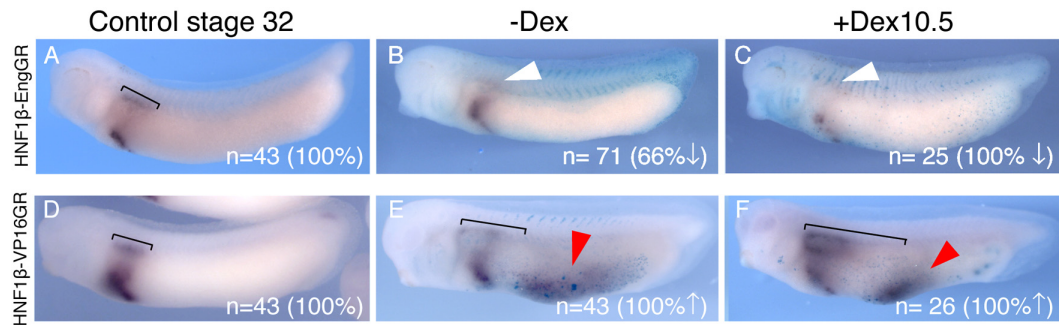


Figure 3.1.10 HNF1 β positively regulates XIHbox8 expression. HNF1 β coding sequence was fused to the dominant repressor domain of the transcription factor engrailed (HNF1 β -EngGR) or the dominant activation domain of VP16 transcription factor (HNF1 β -VP16GR). Both proteins were additionally fused to GR-LBD to allow induction of transcription factor activity by Dex at stage 13 (+Dex10.5). n= states total number of embryos of one experiment. Number in brackets indicate amount of embryos in percent showing presented phenotype. Injection of HNF1 β -EngGR capRNA caused a decrease in XIHbox8 expression of injected embryos (100pg/E) that were treated with dexamethason, in particular in the dorsal pancreatic region (C; white arrow). 47/71 (66%) of injected but untreated embryos (-Dex) showed regular expression of XIHbox8. In the remaining 24/71 (33%) XIHbox8 transcripts were depleted. Activation of HNF1 β function by injecting 100pg/E HNF1 β -VP16GR capRNA (100pg/E) caused an increase in XIHbox8 expression (F; +Dex13). Note that also the uninduced fusion protein caused XIHbox8 expansion compared to control (E).

sal pancreatic XIHbox8 expression at stage 30 as observed for translational inhibition of HNF1 β (figure 3.1.10, A-C). The ventral pancreatic XIHbox8 transcription was not impaired. This results supported the idea, that HNF1 β played a different role in dorsal versus ventral pancreas specification. Enhancing HNF1 β function in the endoderm upon injection of capRNA, encoding the transcriptional activator HNF1 β -VP16GR, phenocopied XIHbox8 induction of ectopic expressing of HNF1 β -WT or HNF1 β -GR at early activation upon Dex treatment. Apart from the ectopic ventro-posterior expression, the dorsal XIHbox8 positive domain was also slightly expanded towards the anterior domain of the embryo. This change in XIHbox8 expression phenocopied the effect caused upon RA treatment (Chen et al., 2004).

In summary, the data obtained in the loss- and gain of function approaches argued that the transcription factor HNF1 β played a multifunctional role in the endoderm: (1) it is necessary but not sufficient to promote pancreas formation in the endoderm (2) it is necessary and sufficient to promote early endocrine cell differentiation in the dorsal pancreas (3) it played a role in specifying the position of the pancreatic anlage along the anterior-posterior axis of the gut tube.

Interestingly a similar induction of XIHbox8 and insulin gene expression was reported in a previous study Dissecting the role of retinoic acid (RA) in organogenesis (Chen et al., 2004). Embryos treated with RA showed a posterior expansion of the dorsal XIHbox8 expression domain whereas ventral and duodenal regions remained unaffected. Also the

insulin expressing domain was posteriorly shifted. The number of insulin positive cells increased at stage 36. In contrast, treatment with the synthetic chemical compound BMS453, RA receptor (RAR) antagonist, induced the reverse phenotype, a decreased *XIHbox8* RNA expression as well as a reduction of insulin positive cells. In this context it was tempting to investigate the relationship between HNF1 β and RA signalling.

3.1.3 Requirement of RA- signalling for HNF1 β expression

3.1.3.1 HNF1 β expression is responsive to RA- signalling

A previous study reported that RA signalling is required already during gastrula stage to determine a pancreatic precursor cell population in the forming endoderm. RA is synthesised by the enzyme RALDH2 that is expressed at gastrula stage in the mesoderm. RA induces directly and indirectly expression of its downstream target genes in the neighbouring tissues. At gastrula stage, the transcription factor HNF1 β is expressed adjacent to RALDH2 in the involuting mesendoderm (compare figure 1.3 with figure 3.1.1) making it a suitable candidate to be activated by RA signalling. To investigate the influence of RA on HNF1 β expression in the endoderm, embryos were treated at blastula stage 9 for 1 hr with 5 μ M RA or 1 μ M BMS453. BMS453 is a synthetic retinoid, classified as arotonoid (Schulze et al., 2001) that antagonises RA on RAR. Embryos were fixed at stage 10.5, 25, 33 and 36 and analysed for changes in HNF1 β RNA levels using WMISH and semiquantitative RT-PCR.

Expression in control embryos was consistent with the expression pattern as previously described in this study, although in this experiment staining of targeted HNF1 β RNA was in general weaker (figure 3.1.11). HNF1 β expression is detectable in the neural ectoderm and endoderm where it persisted till tailbud stage 33. HNF1 β was also detected in the developing nephric system from stage 16 onwards (figure 3.1.11, B). Due to technical limitations, it was difficult to stain for targeted HNF1 β transcripts in the yolky endoderm (figure 3.1.11, S1- S6).

At stage 33, the onset of pancreatic budding from the gut epithelium, the broad endodermal transcript distribution gets restricted to the prospective liver and pancreatic region (figure 3.1.11, C, S2). In contrast to its strong meso- and endodermal expression, neuronal HNF1 β expression is decreased (figure 3.1.11, S2). As the pancreatic organ differentiation proceeds, expression of HNF1 β is clearly detectable in the liver, the developing kidney as well as the proctodeum (figure 3.1.11, D).

Compared to control embryos, RA treated siblings showed a strong HNF1 β activation in the neural ectoderm as well as the involuting endoderm, evident as stained rim edging the yolk plug (figure 3.1.11, E). Strong increase in HNF1 β expression in ecto- and endoderm as

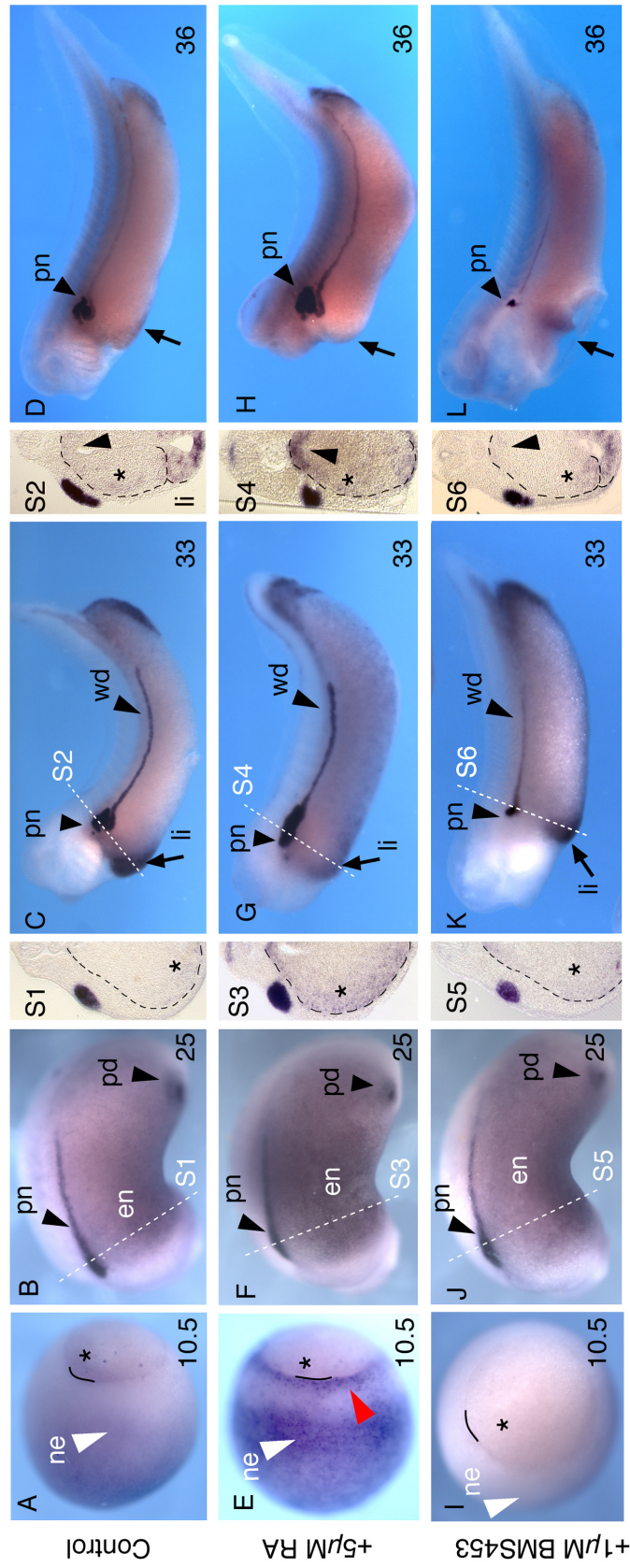


Figure 3.1.11 HNF1β expression is responsive to RA- signalling

Figure 3.1.11 HNF1 β expression is responsive to RA- signalling. Embryos were treated at late blastula stage 9 for 1 hr with 5 μ M RA or 1 μ M BMS453 and cultured till developmental stages indicated to the right of each panel. Embryos were fixed and stained for HNF1 β expression by WMISH. pGEMT-LFB3 was used as template for digoxigenin labeled asRNA. Note, that staining is in general weaker than shown in HNF1 β expression pattern figure 3.1.1. At stage 10.5 the dorsal blastopore lip is represented as black line. Asterisk marks the endoderm. From tailbud stages on embryos are shown in a lateral view with head to the left. Tailbud stage embryos were embedded in gelatine albumine for transversal sectioning (30 μ m, S1-S6). Position of the section in the embryo is indicated by a white dashed line. In sections, a black dashed line surrounds the endoderm (S1-S6). In S2 and S6 the black line also marks the border between liver and ventral pancreas. If compared to control embryos (A-D), RA treatment leads to broad expansion of HNF1 β expression to in the neural ectoderm as well as meso- and endoderm (E- H) in particular in the dorsal endoderm as pointed out with black arrow head in S2, 4, 6. In contrast, inhibition of RA signalling by BMS453 leads to a reduction of HNF1 β expression (I-L). Efficiency of chemical treatment is confirmed by morphological defects as seen in the absence of head structures upon RA treatment and edema formation upon BMS453 treatment. Abbreviations: (de) dorsal endoderm, (en) endoderm, (li) liver, (ne) neural ectoderm, (nt) neural tube, (pd) proctodeum, (pn) pronephros, (ve) ventral endoderm, (vp) ventral pancreas, (wd) wolfian duct.

well as in the forming nephric system was evident during subsequent development (figure 3.1.11, stage 25, F). The pronephric capsule as well as the developing Wolfian duct were increased in size and expanded posteriorly. Also, induced HNF1 β RNA levels upon RA treatment allowed transcript detection throughout the endoderm, also in transversal sections (figure 3.1.11, S3, S4). At stage 33, HNF1 β transcripts were reduced in the ventro- anterior endoderm. Transversal section revealed that in particular, the previously undetectable HNF1 β transcription became evident in the dorsal gut epithelium. This result indicated that HNF1 β activation especially in the dorsal region was responsive to RA signalling (figure 3.1.11; S4). In the latest stage analysed, HNF1 β expression in the ventro- anterior region was too weak to estimate an RA induced effect on endodermal HNF1 β transcription (figure 3.1.11; H). In accordance with a previous study (Cartry et al., 2006) persistent activation of RA signalling at stage 36 was evident in the increase in pronephric size, that was marked by HNF1 β expression in comparison to control embryos (figure 3.1.11; H).

A complement approach to investigate the requirement of RA for HNF1 β expression in the endoderm was performed treating embryos with the RAR antagonist BMS453. Treatment with BMS453 caused reduction of HNF1 β expression from gastrula stage onwards in the ectoderm. Due to weak endodermal staining it was not possible to estimate whether endodermal HNF1 β expression was also affected in comparison to control (figure 3.1.11 I- L; S5, S6). Effective BMS453 treatment was however confirmed regarding the disrupted formation of the mesoderm derived kidney (figure 3.1.11, K, L, black arrow; Cartry et al., 2006). At later stages (figure 3.1.11; L) BMS treated embryos developed large edema in the ventro-anterior endoderm. In reverse complement to RA treatment the diminished renal anlage was detected by the dramatically reduced HNF1 β expression that was restricted to the most anterior region of the excretory system.

Altogether, these findings indicated that HNF1 β expression was responsive to RA signal-

ling in the endoderm, already at gastrula stage and that its expression was especially induced in the presumptive dorsal pancreatic epithelium. Therefore, HNF1 β might be RA downstream target, activated at gastrula stage and possibly mediating early RA signalling that is required for pancreas development. It was therefore of further interest to investigate how HNF1 β expression was activated by RA- signalling in the forming endoderm.

3.1.3.2 HNF1 β responds to RA- signalling in the endoderm

According to the previous study by Chen et al. (2004) pancreatic precursor cells were determined by RA in the dorsal region of the involuting vegetal hemisphere. A more recent study by the same group showed that RA acts directly and indirectly on the endoderm where activation of differentially expressed RAR receptors regulate later pancreas specific gene expression in the dorsal versus the ventral endoderm.

With the onset of gastrulation, HNF1 β transcription was evident in the forming endoderm, adjacent to the expression domain of the RA synthesizing enzyme RALDH2 (compare figure 1.1.4 and figure 3.1.1). This observation aroused the interest to investigate whether RA was required for endodermal gene expression of HNF1 β . In order to investigate the necessity for RA on isolated endoderm, changes in HNF1 β transcription were analysed in vegetal explants upon activation and inhibition of RA signalling. RA signalling was activated by culturing explants in RA while reduced RA signalling activity was achieved by treating explants with BMS453.

Whole vegetal explants were dissected by the with of gastrulation by removing the surrounding ecto- and mesodermal germ layers (figure 3.1.12). After dissection, explants were treated RA or BMS453 and cultured till approximately stage 17. Total RNA was extracted and analysed for changes in marker gene expression by semiquantitative RT-PCR (figure 3.1.12, B). HNF1 β transcripts were detected in untreated control embryos and untreated whole vegetal explants. As expected from the result of WMISH, upon activation of RA signalling HNF1 β expression was increased in whole embryos as well as in isolated explants (figure 3.1.12). As HNF1 β was detectable in the absence of exogenous RA, the onset HNF1 β expression did not appear to depend on RA signalling. In addition it was reported that HNF1 β expression was initiated right after MBT, meaning before RA synthesis. Nevertheless, this experiment indicated that HNF1 β transcription in the endoderm was promoted by RA- signalling during gastrulation. The pan- mesodermal marker brachury (Xbra) was analysed to assure mesoderm free explant preparations that would exclude instructive mesoderm derived signals that promote HNF1 β activation within the endoderm. In comparison to control embryos, Xbra expression in the isolated explants is remarkably low approving proper tissue isolation. The still detectable Xbra expression is in accordance

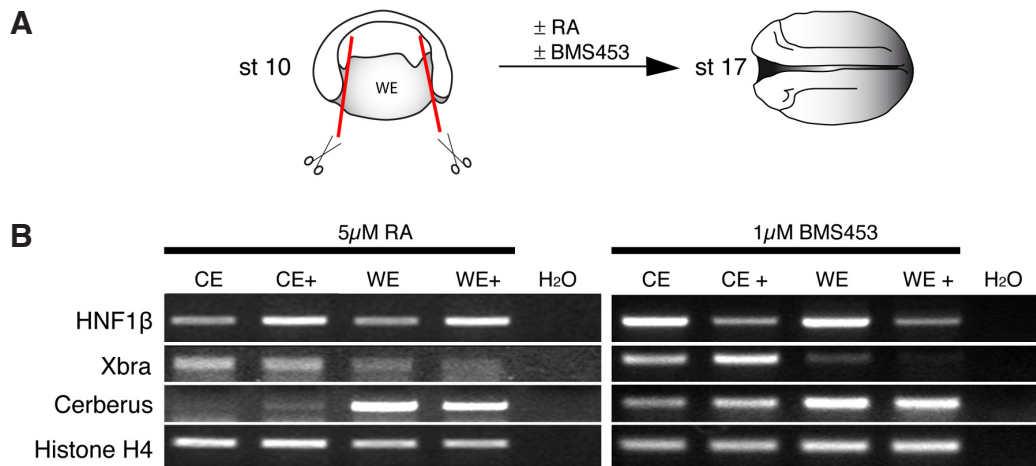


Figure 3.1.12 HNF1β expression in the endoderm is responsive to RA signalling. (A) Requirement of RA signalling for HNF1β expression in the endoderm was analysed by semiquantitative RT-PCR. Vegetal explants were dissected at the onset of gastrulation stage 10 (st 10, dorsal blastopore lip is located to the right, red lines with scissors indicate sectioned area). After dissection, explants were treated for 1 hr with 5 μM RA or 1 μM BMS453, retransferred to 1× MBS and cultured for 24 hr at 16°C. (B) Total RNA was extracted of treated and untreated embryos (control embryos CE; CE+ RA; CE +BMS) and whole explants (WE, WE+ RA, WE + BMS) and used for analysis of gene expression by semiquantitative RT-PCR. Analysed genes are listed to the left. Oligonucleotides used were: HNF1β-RT for/rev (56°C, 30 ×), the mesodermal marker Xbra (Xbra-for/rev; 56°C, 33 ×), dorsal endodermal marker Cerberus (Cerberus-for/rev; 57°C, 28 ×) and the house-keeping gene Histone H4 to equalize RNA amounts (Histone H4 for/rev)

with previous studies revealing autonomous mesoderm gene activation in early endoderm explants (Gamer and Wright, 1995).

Vegetal explants differentially express certain genes along the anterior-posterior axis of the forming endoderm such as Cerberus (Bouwmeester et al., 1996; Zorn et al., 1999) that is expressed in the early dorsal endoderm at gastrula stage, that translocates towards the anterior region during subsequent embryo elongation. Transcripts of the anterior endodermal marker Cerberus were present in low amounts in total embryonic extracts whereas they were enriched in the endoderm thereby confirming effective endoderm preparation. Cerberus expression was unaffected upon RA treatment. Conversely, inhibition of RA signalling by BMS453 treatment caused a strong downregulation of HNF1β transcription in treated embryos as well as in isolated explants (figure 3.1.12). Mesoderm contamination was excluded according to vanished Xbra detection. Cerberus transcripts were enriched in endoderm explants again confirming proper explant preparation. These data confirm the idea that HNF1β expression within the endoderm was regulated by RA signalling. However, the fact that HNF1β transcription was not completely abolished by inhibition of RA signalling indicates that additional signals within the endoderm, as for instance GATA transcription factors (Afouda et al., 2005) are responsible to maintain minimal HNF1β expression.

3.1.3.3 HNF1 β expression responds to RA- signalling in the dorsal and ventral endoderm

At early gastrula stage HNF1 β expression was predominantly confined to the dorsal territory of the involuting endoderm. Pan et al. (2007) revealed that RA is sufficient to induce pancreatic gene expression in the dorsal but not the ventral endoderm. Concerning HNF β as RA downstream target to mediate RA signalling for later pancreas organogenesis. It was of further interest to exploit whether RA differentially activated HNF1 β expression in the dorsal versus the ventral endoderm. To address this question, changes of HNF1 β expression were specified in early endodermal explants that were dissected into dorsal and ventral halves, that were afterwards treated with 5 μ M RA or 1 μ M BMS453.

HNF1 β RNA levels did not remarkably differ between untreated control embryos, untreated dorsal or untreated ventral endoderm explants (figure 3.1.13, stage 10). Upon RA treatment HNF1 β expression was increased in control embryos and dorsal endoderm explants while HNF1 β expression in the ventral endoderm only slightly differed from untreated ventral explants. Analysis of Xbra RNA levels confirmed mesoderm free tissue explants. The anterior endodermal marker gene Cerberus was expected to be enriched in the dorsal endoderm, compared to whole embryos and ventral endoderm explants indicating that enrichment of endodermal transcripts was less efficient as in the previous WE explant preparation and in the preparation of the BMS453 treatment. The pancreatic precursor gene XlHbox8 is autonomously expressed in the anterior endoderm at mid-neurula stages (Gamer and Wright, 1995) and was shown to be activated upon RA treatment (Chen et al., 2004). In accordance to previous studies (Pan et al., 2007) the pancreatic precursor marker XlHbox8 was not detected in isolated dorsal endodermal explants and was only expressed upon exogenous RA treatment, indicating that these explants adopted pancreatic fate. XlHbox8 was also detectable in ventral endodermal explants, that gives rise to the more posterior gut endoderm, contradictory to earlier reports (Pan et al., 2007), indicating that segregation of dorso-ventral endoderm was difficult by the onset of gastrulation. However, also in ventral endodermal tissue, XlHbox8 expression was elevated upon RA treatment indicating that chemical treatment was efficient and specific for gene activation.

Vice versa, inhibition of RA signalling using the RAR antagonist BMS453 repressed HNF1 β transcription in whole embryos and remarkable in the dorsal and ventral endoderm. Coacting mesoderm derived signals were excluded according to weak Xbra expression. Cerberus was weakly detected in whole embryonic RNA extracts while in endodermal RNA extracts, in particular the dorsal endoderm, Cerberus transcripts were enriched. According to XlHbox8 gene induction upon RA treatment, inhibition of RA signalling in BMS treated explants repressed XlHbox8 transcription confirming efficient chemical treatment

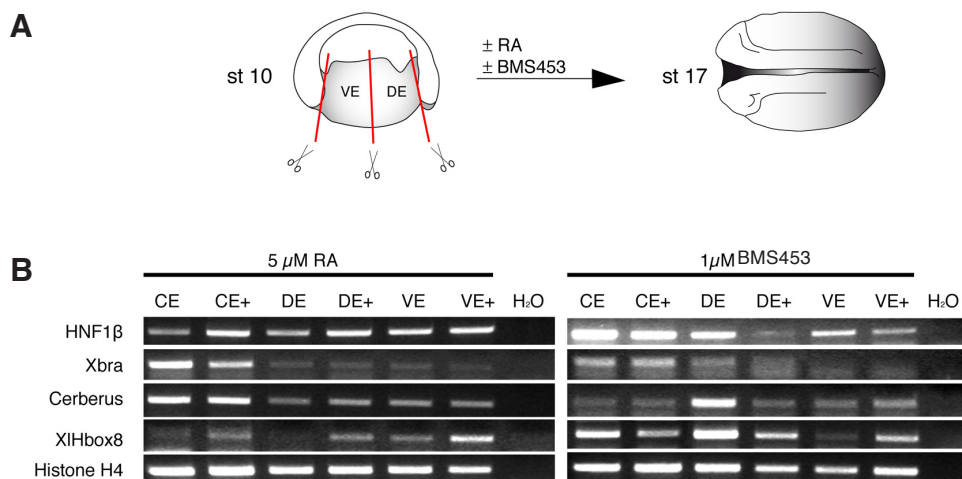


Figure 3.1.13 HNF1 β expression in the dorsal and ventral endoderm is responsive to RA- signalling.

(A) Schematic drawing of explant preparation. Explants were dissected at stage 10-10.5 and separated into ventral (VE) and dorsal halves (DE) according to the position of the dorsal blastopore lip (red lines). After dissecting, explants were treated with 5 μ M RA or 1 μ M BMS453 for 1hr and then transferred to 1x MBS. After 24 hr, total RNA extracts were isolated and used for gene expression analysis by semiquantitative RT-PCR. CE: whole control embryos stage 17. (B) Left panel shows changes in marker gene expression in whole embryos (CE), dorsal explants (DE) and ventral explants (VE) upon activation of RA signalling by RA treatment (+). RA induces HNF1 β to the same extent in the dorsal as well as the ventral endoderm. HNF1 β using oligonucleotides XHNF1 β -RT-for/rev; the pan-mesodermal marker Xbra (Xbra-for/rev); the anterior endodermal marker Cerberus (Cerberus-for/rev) and the pancreatic progenitor marker XIHbox8 (XIHbox8-for/rev). The right panel shows changes in marker gene expression upon inhibition of RA signalling by BMS453 treatment (+). Differences of Cerberus and XIHbox8 transcript level between both experiments are due to differing quality of RNA preparations.

and specific effects on gene activation. Although these findings remain to be quantified by realtime RT-PCR these results clearly demonstrated that endodermal HNF1 β expression was under control of RA- signalling.

In summary, the data obtained in the first part of this study clearly demonstrated that HNF1 β was expressed in the early endoderm where it was coexpressed with the pancreatic progenitor markers XIHbox8 and Xp48 within the dorsal and ventral prepancreatic epithelium by the onset of organogenesis.

It was further shown, that HNF1 β expression in the endoderm was under control of RA signalling as HNF1 β transcription levels were elevated upon RA treatment and decreased upon BMS453 treatment. In tailbud stages 25 to 33, this increase in HNF1 β expression occurred in particular in the dorsal gut epithelium. At this stage the dorsal gut epithelium including pancreatic progenitor cells marked by the first pancreas specific genes XIHbox8 and Xp48. These XIHbox8- Xp48 positive cells give rise to all exocrine and endocrine cell types of the mature pancreas.

Loss and gain of function experiments indicated that HNF1 β was necessary and sufficient to induce XIHbox8 expression in the pancreatic region and to promote differentiation of insulin positive cells in the dorsal gut endoderm. In contrast the expression of Xp48 was

only weakly affected upon HNF1 β depletion, supporting the idea that Xp48 and XIHbox8 are differentially regulated in the gut epithelium. In this regard, the second part of the study focused on isolation and characterisation of the *Xenopus laevis* homologue of the transcription factor HNF6, that was reported as upstream regulator of Ptf1a/p48 in mouse.

3.2 Isolation and characterisation of HNF6/ onecut-1 in *Xenopus laevis*

Studies in mouse indicated that in addition to HNF1 β , the transcription factor onecut-1, also called HNF6, functions as activator for gene expression of the first pancreatic progenitor genes XIHbox8 and Xp48 in the gut epithelium (Jaquemin et al., 2003a). In contrast to HNF1 β , HNF6 has not been identified in *Xenopus laevis*. In order to study its function in pancreas organogenesis, in particular as upstream regulator of XIHbox8 and Xp48, *Xenopus laevis* HNF6 homologue was isolated and its detailed expression profile was generated. Finally, first functional studies were initiated by ectopic protein expression in the endoderm and the resulting effects on pancreas development were monitored by changes in marker gene expression of Xp48 and Trypsin.

3.2.1 Isolation of an onecut transcription factor

To isolate the HNF6 homologue from *Xenopus laevis*, three nucleotide databases (NCBI, <http://www.ncbi.nlm.nih.gov/blast/Blast.cgi>, Altschul et al., 1997; Ensemble, <http://www.ensembl.org/index.html>; JGI, <http://genome.jgi-psf.org/Xentr4/Xentr4.home.html>) were screened for available sequence information of *Xenopus* using the mouse HNF6 DNA sequence (NCBI: NM008262). Several EST-sequences (for instance NCBI: CX397211) and a full length HNF6 coding sequence were annotated for *Xenopus tropicalis* (NCBI: BC135775) but no sequence information was available for *Xenopus laevis*. Since the sequence identity between *Xenopus tropicalis* and *Xenopus laevis* is generally high, this full length sequence served as template to design specific oligonucleotides that were used to isolate the entire *Xenopus laevis* HNF6 coding sequence using 3'RACE- and 5'RACE-PCR methods.

Regarding the time point of induction of XIHbox8 and Xp48 gene expression in the pre-pancreatic endoderm, total RNA was extracted from a mix of stage 28 to stage 34 embryos and used for 3'RACE and 5'RACE cDNA synthesis. For the following PCR step, *Xenopus* specific primers were used to isolate a 3'end and 5'end fragments including sequence information of the coding region. These amplified PCR fragments were subcloned into pGEMT-E vector, analysed by sequencing and compared to the *Xenopus tropicalis* sequen-

ces subsequently. While the 3' end, including the translational stop codon TGA, was isolated in a 3'RACE-PCR using the XHNF6 3'RACE primer, the 5' end could not be isolated by 5'RACE-PCR although different combinations of oligonucleotides (XHNF6-5'RACE 1- 3) were used.

In a second attempt to isolate a 5' end sequence of *Xenopus laevis* HNF6, a *Xenopus laevis* λ - Zap Express cDNA head library (Hollemann et al., 1996) was screened using the vector specific primer CMV_for and the *Xenopus* specific oligonucleotide CX397211_rev. Obtained PCR fragments were subcloned into pGEMT-E. Subsequent sequence analysis resulted in one sequence of 573 bp with high sequence homology to the *Xenopus tropicalis* oncut-1 sequence. This isolated *Xenopus laevis* sequence included the translation initiation site ATG. The missing intermediate domain of the coding sequence (between ATG and TGA) was isolated using *Xenopus laevis* specific oligonucleotides matching the ATG and TGA sides (X1_HNF6-5'ClaI; X1_HNF6-3'XhoI). Finally, all three obtained fragments were used to compose the entire *Xenopus laevis* coding sequence including 265 bp of 5'-untranslated region (5'UTR), an ORF of 1482 bp and a 3'UTR of 220 bp (figure 3.2.1). The coding sequence was translated into corresponding amino acids that resulted in a protein of 492 aa with a calculated weight of 54 kD (MacMolly software, figure 3.2.2). This protein was aligned to sequences of known HNF6 homologues from other species in order to confirm its HNF6 identity.

3.2.2 The *Xenopus laevis* oncut protein corresponds to HNF6/ oncut-1

The name of the oncut transcription factor family is based on the first identified cut protein from *Drosophila melanogaster* (Blochlinger et al., 1988). All oncut family members contain a characteristic C-terminal DNA binding domain, composed of one CUT motif

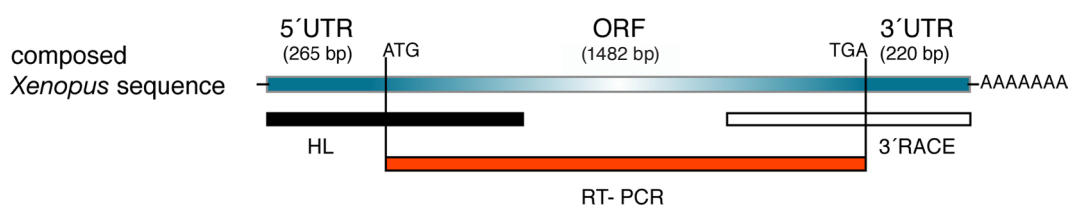


Figure 3.2.1 Isolation of an oncut transcription factor from *Xenopus laevis*. Schematic drawing of the the isolation of the coding sequence (blue) of the *Xenopus laevis* oncut protein that was composed of three isolated sequences: the 5' end of the coding sequence, including the translation initiation site ATG and 265 bp of the 5'UTR was isolated from a *Xenopus laevis* λ - Zap Express cDNA head library (HL, black). A 3' end fragment, including the translational stop codin TGA and containing 220 bp of the 3'UTR, was isolated by 3'RACE-PCR out of stage 28-34 total RNA extract (3' RACE, white, oligonucleotide: HNF6-3' RACE). The ORF of 1482 bp was amplified by RT-PCR out of stage 28-34 total RNA extract using the oligonucleotides matching the translation start (ATG) and stop (TGA) sides (red, X1_HNF6-5'ClaI; X1_HNF6-3'XhoI).

and one downstream HOMEBOX motif. In contrast, the N-terminus differs between onecut family members classifying them into three subgroups: onecut-1, 2 and 3 (OC-1, 2 and 3).

To assign the here identified *Xenopus laevis* protein to one of these subgroups, the amino acid sequence was compared to onecut family members of other organism (alignment software: CLC Free Workbench, appendix figure 7.4). Sequence comparison with eukaryotic homologues revealed that the isolated *Xenopus laevis* protein was closely related to onecut-1/ HNF6. 96% of the *Xenopus laevis* HNF6 (XHNF6) protein residues were identical to *Xenopus tropicalis* and 79% were identical to the mouse and human onecut-1. The zebrafish homologue showed 75% identical amino acids. **While the N-terminus differed strongly** between different organism, the C-terminal DNA binding site showed remarkable high conservation of amino acid sequence in the CUT and HOMEBOX domain (table 3.2).

As reported from studies in mouse, HNF1 β and HNF6 were both responsible for activation of the pro-pancreatic transcription factors Pdx1 and p48 in the developing murine gut tube. In general, regulation of gene expression by transcription factors occurs directly by binding to specific promotor sites of the target gene. Therefore regulator and downstream target must be expressed at the same time and in the same tissue.

In order to investigate the differential role of XHNF6 and HNF1 β to direct pancreatic development in *Xenopus* in particular regarding the onset of pancreatic pregenerator marker Xp48, a detailed expression profile of HNF6 was generated and compared to the expression of the co-regulator HNF1 β and their postulated downstream targets XHbox8 and Xp48.

3.2.3 Comparative expression analysis of XHNF6 within the endoderm

3.2.3.1 XHNF6 expression precedes the onset of pancreatic marker genes

In order to be an upstream regulator of Xp48, XHNF6 should be coexpressed with its downstream target. To elucidate the role of XHNF6 during pancreas development in *Xenopus laevis* it was therefore necessary to determine its temporal and spatial expression pattern.

Using semiquantitative RT-PCR on RNA that was extracted from different developmental stages, first HNF6 transcription was detected at stage 15 (figure 3.2.3). From there onwards HNF6 expression level remained constant till end of neurulation. From there on, Transcript levels slightly increased during tadpole stage 26 until stage 42. In contrast, HNF1 β transcription was already detectable during gastrulation stage 10.5 showing increasing transcription levels by stage 12 (see also figure 3.1.1; Vignali et al., 2000; Demartis et al., 1994).

organism	identical/ total amino acids	total % identity	% identity CUT (aa 282- 362)	% identity Homeobox (aa 414- 468)
<i>X. tropicalis</i> (AAI35776)	473/ 493	96	100	100
<i>M. musculus</i> (NP_032288)	396/ 465	79	100	100
<i>H. sapiens</i> (NP_004489)	396/ 465	79	100	100
<i>Z. onecut</i> (NP_956867)	372/ 461	75	99	98
<i>M. onecut 2</i> (NP_919244)	270/ 505	54	99	92
<i>M. onecut 3</i> (NP_6131972)	205/ 490	41	98	83
<i>H. onecut 2</i> (NP_004843)	264/ 485	52	99	91
<i>H. onecut 3</i> (XP_944823)	211/ 494	42	98	83
<i>D. melanogaster</i> (NP_524842)	167/ 1081	32	90	82

Table 3.2 Sequence homology between isolated XHNF6 and onecut proteins. Name of organism and sequence accession number is stated to the left. The amount of identical amino acids to total residue number of the homologue is compared (second column). Amount of identical residues compared to XHNF6 is calculated as percentage (third column). The onecut DNA binding domain is composed of the CUT and HOMEBOX motif that is highly conserved between all onecut family members. Percentage calculated (fourth and fifth column) indicate motif identity compared to the CUT (aa 282- 362) and HOMEBOX (aa 414- 468) domain of XHNF6 (fourth and fifth column). Strikingly, the DNA binding sites of all onecut-1 homologues are 100 % identical to *Xenopus laevis*.

In respect to HNF1 β , a splice variant HNF1 β -B, lacking 26 amino acids in the DNA binding domain, was previously identified in humans (Wu et al., 2004). It was speculated that also in *Xenopus laevis* such an HNF1 β variant exists and that it might play a redundant role during organogenesis (HNF1 β - Δ 26; Wu et al., 2004). Sequence information from humans indicated that splicing occurred in the region of intron II. To find out whether *Xenopus laevis* also expressed an HNF1 β - Δ 26 splice variant, the second intron was amplified from genomic DNA of *Xenopus laevis*. Based on this intron II sequence, oligonucleotides were designed that would detect both HNF1 β variants. Amplification during RT-PCR would result in two fragments: one fragment corresponding to the wildtype HNF1 β fragment (317 bp) and the alternatively spliced fragment (239 bp). However only the large fragment was amplified by RT-PCR indicating that only one HNF1 β variant exists in *Xenopus laevis*.

Further, XHNF6 expression levels during development were also compared to gene transcription of its potential downstream targets XIHbox8 and Xp48. XIHbox8 is known to be weakly transcribed in the anterior endoderm from stage 12 onwards (Gamer and Wright, 1995), here seen as a faint band at stage 15 (figure 3.2.3). Its expression strongly increases by the time of regionalisation of the primitive gut, where XIHbox8 becomes predominant in the pre-pancreatic and duodenal epithelium at stage 28. This expression profile was very similar to the temporal gene induction observed for XHNF6 that also revealed higher transcript levels what matches with the increase in expression level of XIHbox8 during gut tube

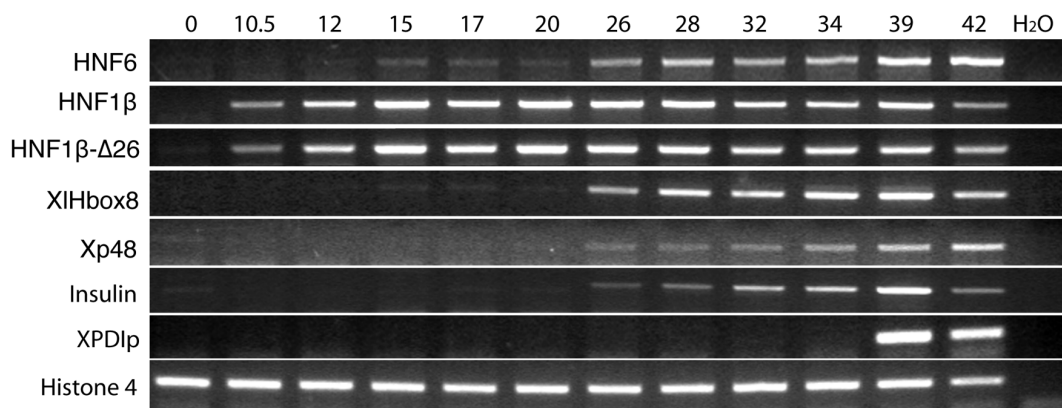


Figure 3.2.3 XHNF6 preceds expression of pancreatic marker genes. Induction of XHNF6 expression was compared to the onset of expression of liver and pancreatic marker genes by semiquantitative RT-PCR. Total RNA was extracted from embryos of different developmental stages as stated on top of each lane. Oligonucleotides used for RT-PCR reaction were: XHNF6: CX397211-for/ rev; HNF1 β -RT for/ rev; HNF1 β - Δ 26 for/ rev; XIHbox8-RT-for/ rev; Xp48-RT-for/ rev; Insulin RT-for/ rev; XPD1p-RT-for/ rev. Histone H4 amplification was used to equalize RNA amounts. H₂O was used as negativ control.

patterning (figure 3.2.3, stage 26). As known from previous studies, the second pancreatic progenitor marker Xp48 is detectable by the end of neurulation (stage 20) with increasing amounts at stage 26 (figure 3.2.3). Shortly after first detection of XHNF6 transcripts. Also Xp48 expression levels increased, like XHNF6 and XIHbox8, by stage 26 representing the time point of pancreas specification in the foregut endoderm (Afelik et al., 2006). XHNF6 transcription was persistent by the time of endocrine and exocrine cell differentiation as seen in comparison to the expression of the earliest endocrine gene insulin and the earliest exocrine differentiation marker XPD1p (Afelik et al., 2004; Kelly and Melton 2000).

Despite the marginal transcript level of XIHbox8 at stage 15, these data demonstrated that XHNF6 expression preceded the onset of pancreatic marker gene expression. As already mentioned, synchronized expression of the activator and downstream target in time and tissue is required for direct gene activation. The RT-PCR experiment determined the time but not the place of XHNF6 transcription. In order to specify the spatial transcript distribution, a detailed spatial expression pattern was generated for XHNF6 during *Xenopus laevis* embryogenesis, and its transcript distribution was compared to expression domains of XIHbox8 and Xp48 by the onset of pancreatic budding at stage 34.

3.2.3.2 XHNF6 is expressed in the neural tissue and anterior endoderm

Spatial distribution of XHNF6 was analysed by WMISH using a digoxigenin labeled asRNA targeting the entire coding sequence of XHNF6. As shown in (figure 3.2.4 A) XHNF6 expression is first evident at stage 16 in two small elongated territories orthogonal to the

midline of the anterior embryonic region. Dissection of the embryo revealed that the staining was in the ectodermal layer. Two faint lines of expression expanded to the posterior end. Position and shape of the anterior expression domains resembled the site of Krox20 transcription that marks prospective hindbrain regions rhomdomere 3 and 5 and the migrating neural crests that become the third branchial arch (Bradley et al., 1993). The two caudal expression lines represent the presumptive closing neural tube. It was noteworthy that initial Xp48 transcription was activated in similar neural territories by the end of neurulation.

At stage 20, XHNF6 expression is found in the forming mid- and hindbrain region, the closing neural tube and the lateral migrating neural crest cells which give rise to the lateral line placodes (Schlosser and Northcutt, 2000; figure 3.2.4, B). **First endodermal expression** became weakly detectable at stage 24 in the ventro-anterior endoderm (figure 3.2.4, C, D, asterisk). At this stage, XHNF6 was also found in the optic anlage and the migrating neural crest cell where it was segregated into the distinct lateral placodes (figure 3.2.4 C). By stage 34, the two rhomdomeres patterned the hindbrain region that was passing over into the mid- and forebrain territory. However, its expression was strictly end persistent excluded from intermediate structures as the midbrain-hindbrain boundary (figure 3.2.4 G, J, M, Q). Transversal sections located XHNF6 expression in the eye to the presumptive retinal pigment epithelium and retina resembling expression of the retinal marker Otx2 (figure 3.2.4, S1; Viszian et al., 2000). Neural expression was confined to differentiating neurons located in the intermedial and marginal zone of the spinal cord. The endodermal XHNF6 transcription was elevated in the ventro anterior endoderm marking the liver diverticulum. Ventro-anterior expression was extending towards the dorso-anterior region marking the presumptive ventral and dorsal pancreatic domain. Here, XHNF6 transcription was restricted to the prospective liver and ventral pancreas (figure 3.2.4, E, H; transversal section S1 and S2), living up to its name as „liver enriched hepatic nuclear factor 6“.

During subsequent development the neural crest placodes further differentiated into distinct anlagen. The neural XHNF6 transcription persisted ubiquitously in differentiating cells of the ventral spinal cord. At this stage HNF6 expression was excluded from the lens tissue, but its retinal staining was not defined to any restricted retinal zone or layer (figure 3.2.4, S3, S4; Viszian et al., 2000). **Although it was not evident from transversal sections**, in whole embryos endodermal XHNF6 transcription was clearly seen in the forming liver and the ventral pancreatic domain expanding to the dorsal gut endoderm. From the position within the embryo it was estimated that XHNF6 and Xp48 are coexpressed in same territories during embryogenesis in the neural as well as endodermal territories (Dullin et

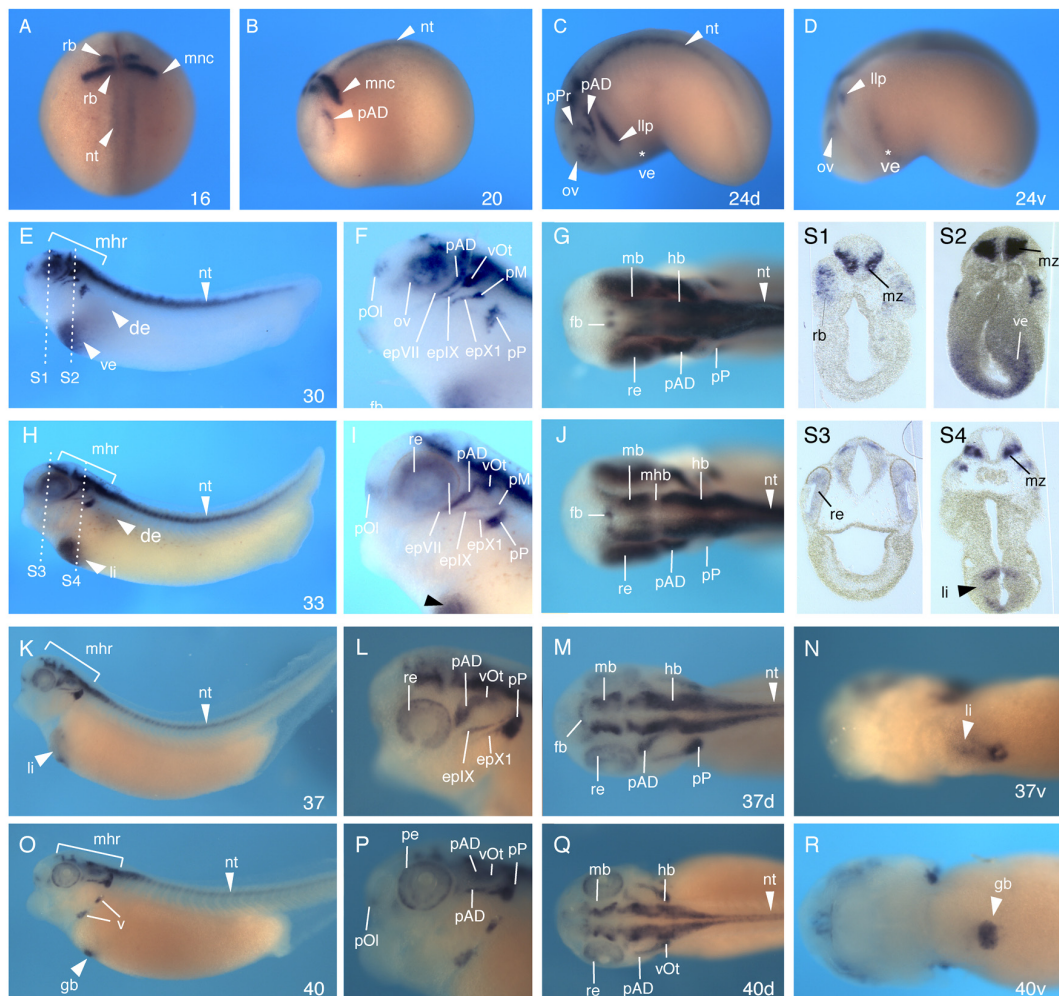


Figure 3.2.4 Expression pattern of HNF6 during *Xenopus laevis* development. Spatial distribution of HNF6 transcripts during development was analysed by WMISH using embryos of different developmental stages. The XHNF6-pGEMT construct encoding the entire ORF, served as template to transcribe digoxigenine labeled asRNA. XHNF6 transcripts were detected from stage 16 onwards in the neural ectoderm, the presumptive robdomeres, the migrating neural crest cells and the closing neural tube. From stage 24, XHNF6 transcription is first visible in the ventro-anterior endoderm (asterisk), where it gets spatially restricted to the liver, ventral pancreas and to the gall bladder at later tadpole stage 41. Stage 16 embryo is positioned anterior to the top (A). Late neurula and tailbud stage embryos are positioned laterally with anterior to the left (B-R). D: ventral view of embryo stage 25 in C (asterisk indicates the anterior endoderm). F, I, L, P: show enlarged head regions of the embryo to the left - E, H, K, O respectively. G, J, M, Q: enlarged dorsal view of the mid-brain-hindbrain region (bracket) of embryos to the left - E, H, K, O respectively. S1-S4 transversal gelatine albumine sections of the embryo to the left. Position of the section is indicated in the embryo as white dashed line. N,R: ventral view of the embryo to the left K,O respectively. Abbreviations: (de) dorsal endoderm, (epIX) glossopharyngeal epibranchial placodes, (epX1) first vagal epibranchial placodes, (epVII) facial epibranchial placodes, (fb) forebrain, (gb) gall bladder, (hb) hindbrain, (llp) lateral line placode, (li) liver, (mb) midbrain, (mhr) midbrain hindbrain region, (mhb) midbrain hindbrain boundary, (li) liver, (mz) marginal zone, (mz) marginal zone, (nt) neural tube, (pAD) antero-dorsal lateral line, (pM) middle lateral line placodes, (pOI) olfactory bulb, (pOt) otic placode, (pP) posterior lateral line placodes, (ov) optic vesicle, (rb) robdomeres, (re) retina, (v) migratory primordia of the ventral trunk lines, (vOt) otic vesicle, (ve) ventral endoderm.

al., 2007; Afelik et al., 2006). With differentiation of head structures, XHNF6 expression is found in the outer region of the retina the presumptive pigment epithelium, although transversal sections are required to confirm the exact region within the pigment epithelium. **Endodermal expression in the liver is maintained whereas pancreatic expression faints** and is not detectable by stage 37. At this stage XHNF6 transcription in the liver marginally decreases in the anterior liver diverticulum and gets spatially confined to the most dorsal edge of the liver diverticulum that segregates to the form the gall bladder (figure 3.2.4 K, N, O,R) which was clearly distinct in the ventroanterior endoderm by stage 41.

Analysis of transcript distribution in whole embryos revealed that HNF6 was expressed in the neural tissue, the neural crest and in the endoderm. This expression was coincident with the expression profile observed in mouse (Rausa et al., 1997). The similar expression pattern favored the idea that XHNF6 played a conserved role during pancreas development. In context of this study, it was very interesting to observe that XHNF6 expression in the anterior endoderm was evident at stage 24, before the onset of Xp48 in the pancreatic epithelium. This anterior endoderm included the bipotential cell population that eventually gives rise to liver and ventral pancreas. This was in agreement with expression profiles in mice increasing expression during subsequent development in this domain, in particular by the onset of pancreatic budding by stage 33, provided evidence for a functional role of HNF6 in liver and pancreas development.

3.2.3.3 XHNF6 is expressed in the ventral and dorsal pancreas

The spatial expression pattern of XHNF6 demonstrated that by the onset of pancreatic budding (stage 33/34), it was transcribed in the anterior ventral endoderm. If HNF6 was indeed the postulated upstream activator of Xp48 in the regulatory cascade, both transcription factors should be coexpressed in the ventral pancreas. **At this stage the liver primordium is located adjacent to the ventral pancreatic anlage in the gut epithelium.** Before delamination from the gut tube, both primordia are marked by differential expression of organ specific genes as the hepatic transcription factor Hex (XHex) and the pancreatic transcription factor Xp48 (figure 3.2.5).

In order to specify the region of XHNF6 expression in both organ primordia, its transcript distribution was compared to the spatial distribution of XHex and Xp48 RNA as well as the transcript localisation of pancreatic marker gene XIHbox8 and the anterior foregut marker gene HNF1 β . Control embryos were stained by WMISH targeting the expression of the hepatic marker XHex (figure 3.2.5, A, S1), **the anterior foregut marker HNF1 β** (figure 3.2.5, B, S2), **the identified XHNF6** (figure 3.2.5, C, S3), **the pancreatic progenitor markers**

XIHbox8 and Xp48 (figure 3.2.5 D, S4 and E, S5 respectively).

XHex expression domains included the thyroid and proctodeum as well as the most ventral region of the anterior foregut, the liver diverticulum. In comparison, XHNF6 transcription was also detected more dorsally in the budding ventral pancreatic rudiments. The two XHNF6 positive regions adjacent to the dorsal side of the liver correlated with the location for Xp48 and XIHbox8 staining in the ventral pancreas (compare figure 3.2.5 C with D,E and S3 with S4, S5). However it remained unclear, whether XHNF6 was also expressed in the dorsal prepancreatic endoderm.

In the dorsal pancreatic rudiment HNF1 β expression was still detectable as faint staining whereas the dorsal endoderm seemed devoid of any XHNF6 transcripts (figure 3.2.5, compare B and C, S2 and S3). Studies in mouse reported of XHNF6 transcripts in both organ primordia, therefore rising the question whether absence of XHNF6 transcription in the dorsal gut epithelium was real or whether it was due to technical limitations of the staining procedure as seen for the detection of low HNF1 β RNA levels in the yolky endoderm. In order to overcome this technical constraint, XHNF6 gene expression within the endoderm was analysed by semiquantitative RT-PCR.

3.2.3.4 XHNF6 and HNF1 β are expressed in the dorsal endoderm

To focus on the XHNF6 transcript distribution in the endoderm, it was crucial to isolate the endoderm from other XHNF6 expressing tissues. As known from the generated spatial expression pattern (figure 3.2.5), the XHNF6 gene was activated in the head region and the neural tube. To determine exclusively endodermal XHNF6 transcript levels, other HNF6 positive tissues were removed as depicted in the scheme (figure 3.2.6). Further, the isolated whole embryonic endoderm was dissected into its dorsal and ventral endodermal part. Total RNA of each fraction was extracted and used for semiquantitative RT-PCR analysis. XHNF6 gene activation was compared with transcript levels the anterior foregut marker HNF1 β and insulin, that is exclusively expressed in the dorsal pancreatic rudiment. To assure that endoderm was devoid of neural tissue, cross- contamination was excluded by analysis of the neuronal differentiation marker n- tubulin.

As expected, the anterior foregut marker HNF1 β is expressed in the dorsal and ventral foregut whereas transcripts of the endocrine gene insulin were only detectable in the dorsal fraction thereby confirming proper isolation of dorsal endoderm. As just mentioned, detected XHNF6 expression could also originate from neuronal tissues, although this possibility was eliminated by the absence of the neuronal differentiation marker n- tubulin.

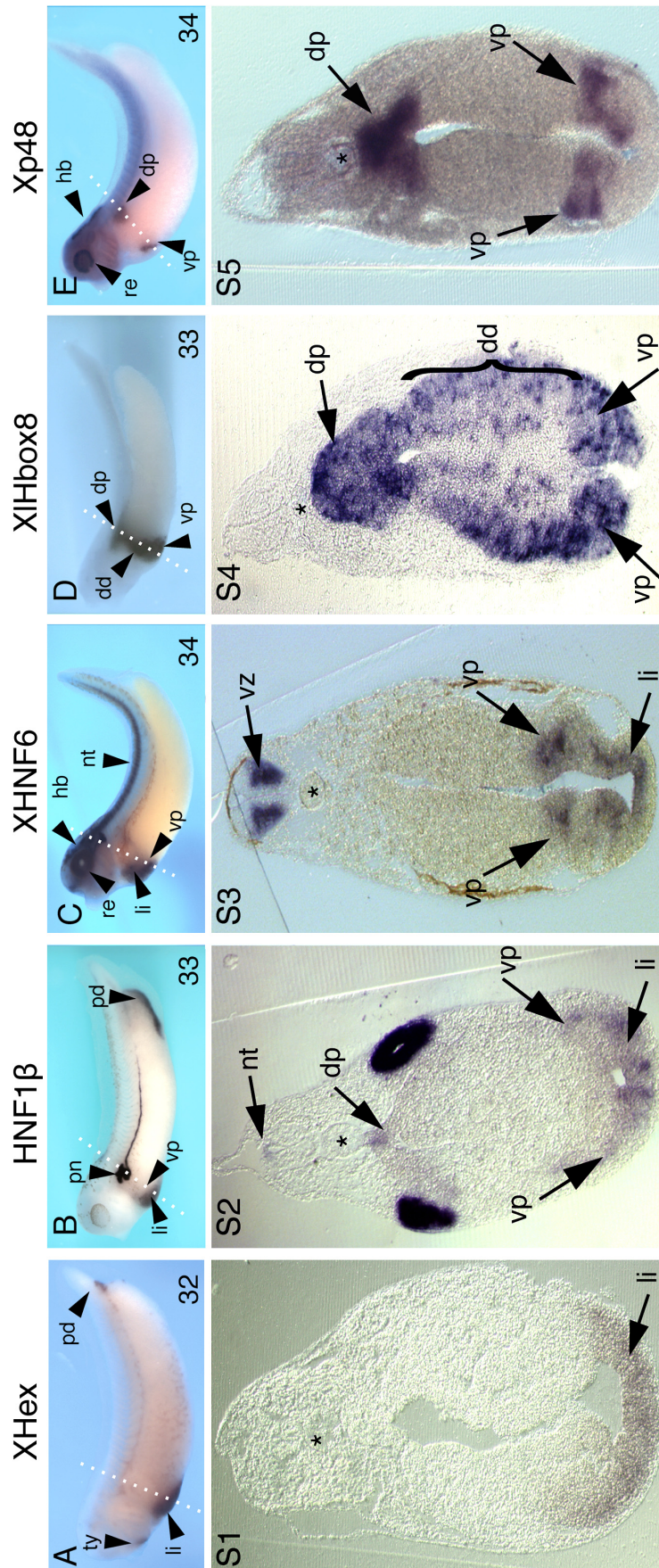


Figure 3.2.5 XHNF6 is expressed in the ventral pancreas. Expression of XHNF6 was compared by WMISH to expression of the liver precursor marker XHex, the anterior endoderm marker HNF1 β as well as to its potential pancreatic downstream targets XIHbox8 and Xp48. Transversal sections were performed to reveal transcript distribution in the endoderm at the onset of pancreatic budding stage 34. Whole embryos are positioned lateral with the head to the right. Developmental stage is indicated as number to the right. White line indicated position of the section shown underneath the whole embryo. Abbreviations: (dd) duodenum, (dp) dorsal pancreas, (li) liver, (ty) thyroid, (pn) pronephros, (vp) ventral pancreas, (pd) proctodeum, (hb) hindbrain, (nt) neural tube, (re) retina, (vz) ventricular zone. Asterisk marks the endoderm.

These data confirmed, that similar to mouse (Rausa et al., 1997), XHNF6 expression occurred in the ventral and dorsal endoderm.

3.2.3.5 Tissue distribution of XHNF6 in adult *Xenopus laevis*

Finally, to complete the detailed expression profile of XHNF6, its expression was examined in tissues of the adult frog by RT-PCR. In the adult, tissue distribution correlates with observed expression domains during development, namely the liver, the pancreas and the brain (figure 3.2.7).

Altogether, the data obtained by the detailed expression study of XHNF6 revealed that it is activated early in the anterior endoderm, prior to the onset of XIHbox8 and Xp48. These findings support the idea that also in *Xenopus laevis* XHNF6 is involved in pancre-



Figure 3.2.6 XHNF6 is expressed in the dorsal and ventral endoderm by the onset of pancreatic budding. XHNF6 expression was analysed by semiquantitative RT-PCR on total RNA extracts of stage 34 embryos (CE). To specify its endodermal expression the embryo was dissected into whole embryonic endoderm (WEE), whole dorsal embryonic endoderm (WDE) and whole ventral embryonic endoderm (WVE). H₂O was used as negative control. XHNF6 is expressed similar to HNF1 β in the WDE as well as in the WVE. In contrast insulin is just detectable in the area of the dorsal pancreas. To exclude neuronal origine for HNF6 transcripts the neuronal differentiation marker N-tubulin was tested. Histone H4 served to equalize RNA amount. Primers used: XHNF6: CX397211-for/ rev; HNF1 β -RT-for/ rev; Insulin RT-for/ rev; N-tubulin for/rev; Histone H4-for/ rev.

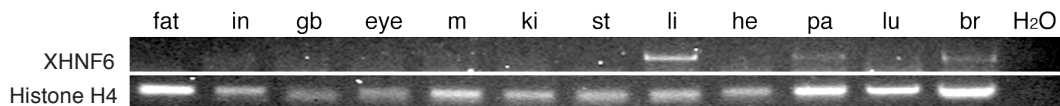


Figure 3.2.7 XHNF6 is expressed in liver, pancreas and brain of the adult *Xenopus laevis*. Distribution of XHNF6 in the mature frog was analysed by RT-PCR using oligonucleotides CX397211_for/rev on total RNA extracts from adult organs. Histone H4 was analysed to equalize RNA amounts. Abbreviations: (in) intestine, (gb) gall bladder, (m) muscle, (ki) kidney, (st) stomach, (li) liver, (he) heart, (pa) pancreas, (lu) lung, (br) brain.

atic organogenesis and underlines its potential role as upstream regulator of the pancreatic marker gene Xp48.

3.2.4 Functional characterisation of XHNF6 during pancreas development

In order to study the role of XHNF6 during pancreas development, the coding sequence was cloned into the pCS2+ expression vector (XHNF6_ClaI/ XHNF6_XhoI). The pCS2+/XHNF6 construct, containing the entire ORF (1482 bp), was used for *in vitro* transcription of XHNF6 capRNA. In the previous study that underlined the requirement for Xp48 expression to direct pancreatic cell fate in the foregut 800 pg capRNA were injected per embryo. Here, 750 pg HNF6 capRNA were directed to the endoderm by radial injection into the vegetal pole of a four-cell stage embryo. Embryos were cultured till late tadpole stages to analyse changes in pancreatic marker gene expression as Xp48 and the exocrine marker trypsin used to illustrate organ size.

Upon ectopic expression of XHNF6 in the endoderm, 90% showed an increase of the Xp48 positive territory indicating an enlargement of the pancreatic lobes. The dorsal lobe ranged from its dorsal position nearly to the most ventral domain. Size expansion was in particular seen from the ventral side of the embryos (figure 3.2.8 B; B and C). The ventral pancreas evaginated from the gut epithelium as two distinct buds that are separated by the caudal tip of the liver diverticulum. Due to gut rotation movements, these two ventral buds come in apposition and fuse to give rise to the ventral pancreatic lobe at stage 41. Upon XHNF6 overexpression, the two ventral buds showed an increased staining intensity, enlarged territory and they were connected to each other by a thin Xp48 positive stripe that was located posterior to the posterior liver tip. Increased Xp48 expression would consequently promote exocrine pancreas specification leading to an enlarged organ size (Afelik et al., 2006).

To order to analyse XHNF6 function during development, embryos were injected with XHNF6 capRNA and cultured until stage 43 and analysed for expansion of exocrine tissue using the exocrine enzyme trypsin (figure 3.2.8 A; C). At this stage, the pancreatic lobes

have already fused to one organ that is positioned underneath the stomach and duodenum due to gut rotation movements (figure 3.2.8 A; D). Since the exocrine compartment represents the majority of the pancreatic tissue, it was possible to judge pancreatic size according to the trypsin expressing region. 100% of the injected embryos developed an enlarged pancreatic organ. In addition, 20% of these embryos not only showed enlarged pancreas

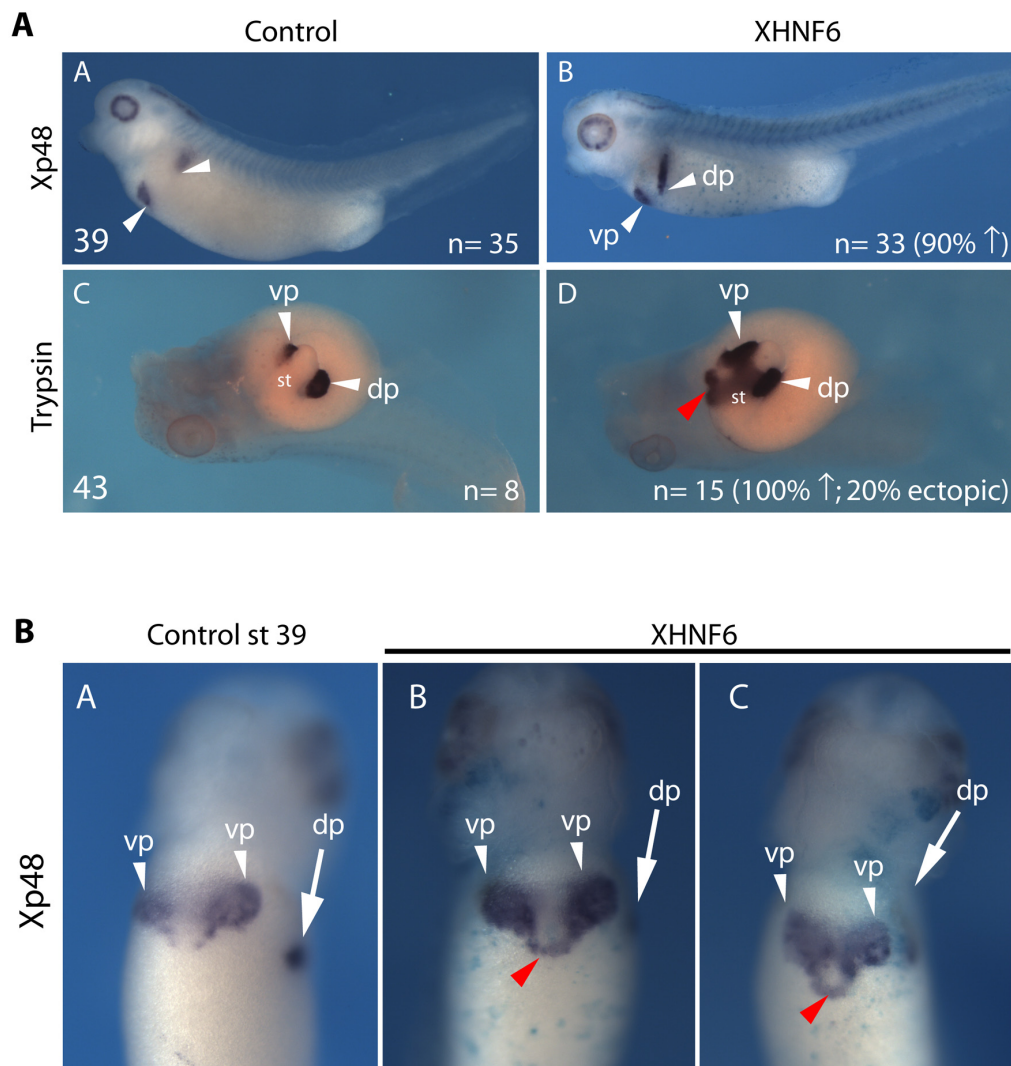


Figure 3.2.8 Ectopic expression of XHNF6 promotes pancreas development. (A) Embryos were injected with XHNF6 capRNA, cultured till stage 39 and analysed for changes in expression of its potential downstream target Xp48 (750 pg/E; A, B) as well as for changes in organ size according to the exocrine compartment that was marked by the exocrine enzyme trypsin. Compared to control, overexpression of XHNF6 led to expanded Xp48 expression domain in the ventral as well as in the dorsal pancreatic anlage (B, D; white arrow and black arrow respectively). Small numbers to the left indicate developmental stage. n = total number of embryos; percentage in brackets states number of embryos showing the presented phenotype. In panel D, all 15 embryos presented enlarged exocrine compartment of the pancreas compared to control embryos (C). 3 embryos (20%) showed ectopic trypsin expressing cells in the anterior foregut. (B) As seen in the ventral close up view of two XHNF6 injected embryos (B; C), the Xp48 positive region was not only enlarged in the ventral pancreatic epithelium (vp) but also ventro-posteriorly expanded (red arrow head). (dp) dorsal pancreas (vp) ventral pancreas. (st) stomach

but also ectopic trypsin- positive regions in the anterior foregut. Since the pancreatic lobes fused it cannot be judged whether this additional trypsin positive tissue originated from the ventral or dorsal pancreatic rudiment. It was noteworthy that the trypsin positive regions were positioned in the neighbouring intestinal tissue of the endogenous Xp48 expression domain.

A recent study in *Xenopus laevis* revealed that the transcription factor Xp48 was also crucial for endocrine cell differentiation (Afelik et al., 2006). Hence, it would be of interest to analyse effects on insulin gene activation upon ectopic HNF6 expression.

In summary, the second part of this study focused on the isolation of the *Xenopus laevis* homologue XHNF6 that was suggested to function as a direct upstream activator of Xp48 during pancreas development. On this background, both transcription factors have to be coexpressed in the endoderm at the same time and in the same location. A detailed expression pattern analysis revealed that XHNF6 transcription was initiated prior to the onset of Xp48 in the anterior foregut endoderm. XHNF6 positive region included the ventral and dorsal prepancreatic epithelium, indicating that XHNF6 could function as upstream regulator of Xp48. Preliminary gain of function data obtained from ectopic XHNF6 expression in the endoderm resulted in an increased Xp48 positive region in the foregut endoderm as well as in an enlargement of the organ. It is a matter of course that loss of function approaches by XHNF6 depletion are necessary to confirm and further specify the function of XHNF6 on Xp48. Nevertheless, these preliminary data strongly support the idea that similar to mouse, XHNF6 also plays a crucial role in pancreas development of *Xenopus laevis*.

3.3 Malectin, a novel ER resident protein in *Xenopus laevis*

As seen from the functional analysis of the transcription factors HNF1 β and HNF6, these tissue specific genes are useful tools to study organogenesis, since they mark specifically the pancreatic organ and illustrate any developmental alterations. For this purpose, the identification of novel genes uniquely expressed in the pancreatic tissue would be a great advancement to improve the descriptive analysis of pancreas development. Based on this idea, the third aspect in this study focused on the characterisation of a putative pancreas specific marker gene in *Xenopus laevis*.

In an attempt to identify new pancreas specific markers, a hybridization screen on tadpole stage embryos was performed using asRNAs generated from clones of an adult pancreas

cDNA library (Afelik et al., 2004). Among others, clone p150 (pancreas clone 150) showed expression in the pancreas at stage 41. **Sequence analysis of the cDNA library clone pBK-CMV- p150 (3.6 kb, table 3.3) revealed an ORF of 828 bp coding for a protein of 276 aa.** To obtain further informations on homologous genes, BLAST searches were performed with the full length nucleotide, ORF as well as protein sequence using the NCBI, Ensemble and JGI databases. Sequence comparisons revealed homologues in lower and higher eukaryotes. Comparison of the protein sequences revealed a strikingly high amino acid similarity in vertebrates (figure 3.3.1).

Pancreatic staining observed in late *Xenopus laevis* tadpoles and the high conservation of up to 89% among vertebrates, prompted us to investigate the role of p150 during organogenesis. Since the p150 protein was functionally not yet described, its characterisation was approached in two different ways: (1) by characterising its biochemical properties, including its protein structure and interaction partners, and (2) by analysing its role during embryogenesis of *Xenopus laevis*, in particular during pancreas development.

The first aspect was intensively investigated by the group of Claudia Muhle-Goll (EMBL, Heidelberg) that collaborated by solving the p150 protein structure by NMR and performing biochemical interaction studies. According to their findings of specific interaction with the disaccharide maltose, the protein “p150” was renamed **malectin** as it will be further referred to in context of this study (Schallus et al., 2008).

The second aspect concerned the functional relevance of malectin during pancreas development. In this context, the late pancreatic expression pattern of malectin was determined in greater detail by acquisition of an expression profile during *Xenopus laevis* embryogenesis. This included the temporal characterisation of gene induction and spatial localisation

organism	nucleotide ID	protein ID	% identity
<i>Xenopus laevis I</i>	NM_001091743/BC072149	AAH72149	-
<i>Xenopus laevis II</i>	NM_001087063/ BC042341	AAH42341	96% (205/212)
<i>Xenopus tropicalis</i>	CT030323	n.a.	n.a.
<i>Homo sapiens</i>	NM_014730	NP_055545.1/ KIAA0152	89% (221/247)
<i>Dario rerio</i>	NM_001113618	NP_001107090	71% (199/279)
<i>Mus musculus</i>	AK129066.1	BAC97876	86% (224/259)
<i>Rattus norvegicus</i>	NM_001013983	NP_001014005	88% (219/247)
<i>Canis familiaris</i>	XM_846298	XP_851391	87% (227/259)
<i>Drosophila melanogaster</i>	NM_136243.2	NP_610087	40% (123/307)
<i>Caenorhabditis elegans</i>	NM_066550.1	NP_498951	35% (98/276)
<i>Onithorhynchus anatinus</i>	XM_001511731	XP_001511781.1*	88% (189/214)

Table 3.3: Sequence comparison of malectin with eukaryotic homologues. ID: NCBI accession numbers; n.a.: not annotated. %identity: indicates the number of identical residues in percent between *Xenopus laevis* malectin and eukaryotic homologues, also presented in total numbers in brackets. *Similar to platelet-derived growth factor receptor alpha polypeptide

of transcripts and endogenous protein.

In order to reveal its role during pancreas organogenesis, loss- and gain of function approaches were also performed for malectin by injection of antisense morpholinos and of *in vitro* transcribed malectin capRNA.

3.3.1 Malectin is an ubiquitously expressed protein

Malectin expression was analysed on the RNA level by WMISH and semiquantitative RT-PCR as well as on the protein level by immunodetection. By WMISH, stage 1 to stage 13 embryos showed a weak and diffuse staining that did not remarkably differ from unspecific background staining (not shown). Region specific expression of malectin transcripts was first observed at neurula stage 1 (stage 18 to 20) in the anterior neural ectoderm, the neural folds and the neural crest (figure 3.3.2 A; stage 18 and 20). At tadpole stage 32, malectin was broadly expressed including the neural crest placodes, otic vesicle, pronephros, the tail tip, the neural tube but also in the retina. Interestingly, at this stage malectin expression was upregulated in a distinct structure in the mid-dorsal head region, namely the hatching



Figure 3.3.1 Sequence comparison of *Xenopus laevis* malectin with eukaryotic homologues. Aligned eukaryotic protein sequences and corresponding accession number are stated to the left. Small numbers to the right indicate the amino acid position. Residues differing from a consensus sequence are highlighted in red. Protein fragment of *Xenopus laevis* malectin which was used for structural analysis by NMR is marked by a blue bar (Schallus et al., 2008). Sequence analysis using SMART-tool predicted putative protein domains: an N-terminal signal peptide (aa 1- 25; red bar), an intermediate predicted globular domain (aa 26- 256, blue bar), and an hydrophobic C-terminal transmembran domain (aa 256- 276, yellow bar). Note, that malectin sequence contains a negative charged serial sequence of glutamic acid (E) at aa 230- 242.

gland (figure 3.3.2; A 32, inset). **Malectin remained expressed in neural crest derivatives** during subsequent development, while additional transcripts appeared in the differentiating pancreas at stage 41.

To determine the exact time point of malectin transcription, the original clone obtained from the cDNA library screen (pBK-CMV-p150) was used to design malectin specific oligonucleotides to analyse temporal malectin gene expression by semiquantitative RT-PCR (figure 3.3.2, B). In contrast to the WMISH, semiquantitative RT-PCR on total RNA extracts from stage V oocytes and different embryonic stages embryos (stages V, 0- 42) revealed a presence of malectin transcripts already in oogenesis that persisted in at constant expression level throughout development.

In order to detect the time course of protein synthesis, a malectin specific antibody was generated and used for immunodetection analysis of the malectin protein in different embryonic stages (figure 3.3.2, B). According to the detailed sequence information obtained by the collaborating group of Claudia Muhle-Goll (SMART protein domain prediction tool), it was suggested that malectin was a type I transmembrane protein (Schallus et al., 2008). For this reason, membrane protein fractions of embryos with different stages were analysed for the presence of malectin protein. Embryos of different developmental stages were homogenised, and membrane debris pelleted. The malectin protein was specifically detected using a newly generated *Xenopus laevis* specific malectin antibody that was directed against the intermediate lectin like domain of the protein (aa 30-254, see 2.2.10). This antibody detected very specifically one single protein band with an estimated size of 30kD that matched the predicted size of malectin protein (30kD). This protein band was evident in all stages tested. Hence, it was demonstrated that also malectin protein was present from early embryogenesis onwards indicating a constant translational activity.

Expression analysis of malectin in adult tissues of *Xenopus laevis* revealed an ubiquitous expression in all analysed tissues albeit with varying transcription levels (figure 3.3.2; C). Weak expression was detected in eye, kidney and the heart whereas muscle, gall bladder, stomach, liver and lung. Also the pancreas demonstrated high transcript levels. According to the specific expression of XPDIP that was detected in the pancreas and stomach tissue preparations (Afelik et al., 2004) it was excluded that the broad expression derived from cross contamination during the RNA purification procedure.

Altogether, malectin expression was shown to be present throughout development in a rather ubiquitously manner than in a germlayer specific way or in a spatially restricted territory.

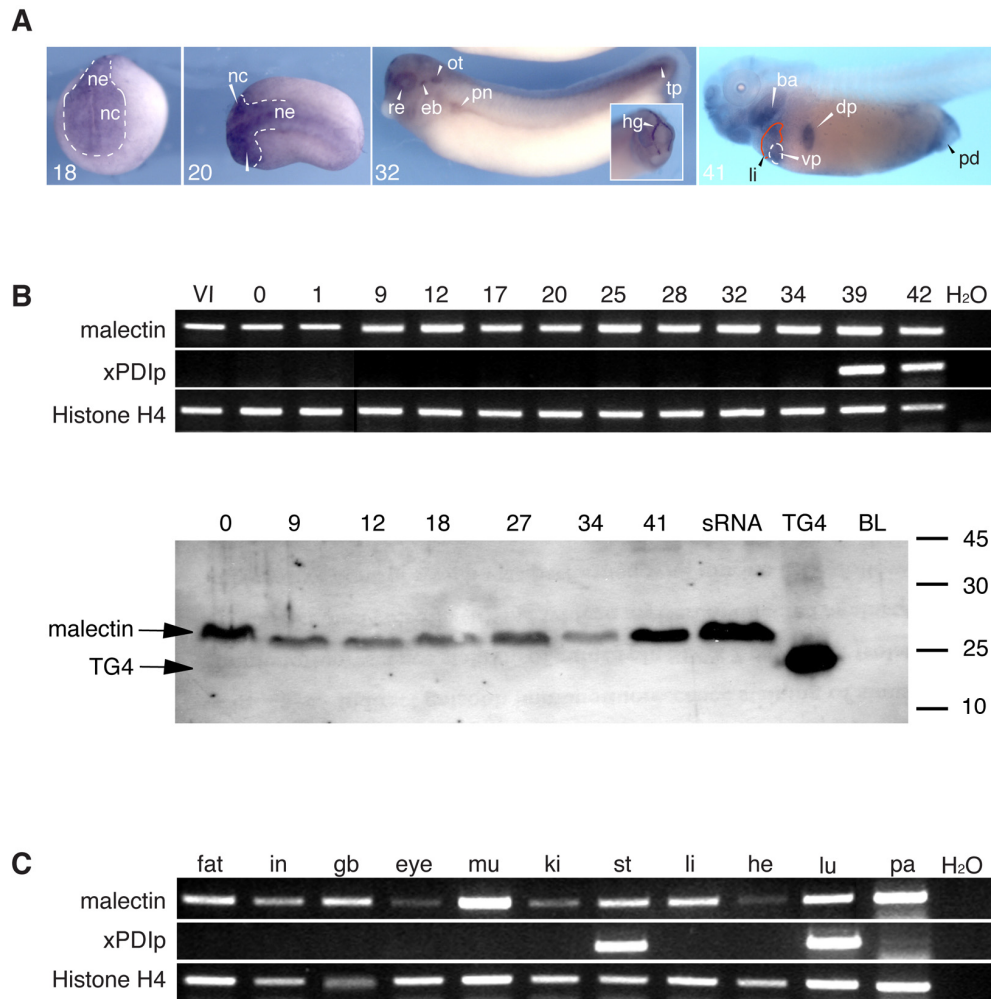


Figure 3.3.2: Spatial and temporal expression profile of malectin in *Xenopus laevis* embryos and adult.

(A) Spatial distribution of malectin was analysed by WMISH. pBK-CMV-p150 full length clone was linearised with BamHI and Dig-labeled antisense RNA was transcribed with T7-RNA-polymerase. From stage 18 onwards, malectin is expressed in the anterior neuroectoderm (ne) and neural crest (nc, white arrow heads). At stage 32, it is restricted to the retina (re), otic vesicle (ot), epibranchial placodes (eb), pronephros (pn) and the tail tip (tp) as well as to the hatching gland (hg, front view of the head, inset). At stage 41, transcripts are detected in the liver (li, framed in red), the adjacent ventral pancreas (vp, framed in white) and dorsal pancreas (dp) as well as in branchial arches (ba), oesophagus (oe) and proctodeum (pd). (B) Activation of malectin gene expression was determined by semiquantitative RT-PCR on total RNA extracts and by Westernbot on embryonic protein extracts. Total RNA amount was equalised to 100 ng/ μ l for 10 μ l reaction for cDNA synthesis. dH₂O was used as negative control. Histone H4 was used equalise RNA amounts. Oligonucleotides used were p150/malectin-RT_for/ p150/malectin-RT_rev, Histone H4-for/ Histone H4 rev; XPD1p-for/rev. Malectin transcription is persistent throughout development as compared to pancreas specific protein disulfide isomerase (XPD1p) that is initiated at stage 39. Developmental stages (Nieuwkoop and Faber, 1967) are indicated as numbers on top of each lane. VI=stage VI oocyte. For immunodetection analysis, membrane protein fractions were generated of different developmental stages. 10 embryos were homogenised using a syringe. The suspension was centrifuged to obtain membraneous compartments which were resolved in 20 μ l sample buffer /embryo. 10 μ l sample (0.5 embryo equivalents) were loaded per lane of a 12.5% SDS-Gel. After SDS-PAGE, proteins were transferred onto a nitrocellulose membrane. Endogenous malectin protein was detected using a polyclonal malectin specific antibody (rabbit-anti-malectin; 1:15000) and the secondary antibody goat-anti-rabbit-HRP (Santa Cruz, 1:5000). Numbers on top of the lanes indicated developmental stages; BL = bacteria lysate was used as negative control, TG4= purified malectin protein (aa 30-208) which was used as antigen for rabbit immunisation. The band shift in stage 0 results from a gel artefact (C) Malectin expression in adult tissues was analysed by RT-PCR. It shows ubiquitous distribution in comparison to XPD1p which is detected only in pancreas and stomach. Abbreviations are not defined in A: gall bladder (gb); heart (he); intestine (in); kidney (ki); lung (lu); muscle

The presence of malectin from the beginning of embryogenesis on to the mature amphibian, together with its dispersed transcript localisation and late onset of expression in the pancreatic tissue, favored the idea that malectin rather maintained a general function during embryogenesis than a restricted role during pancreas organogenesis.

3.3.2 Malectin resides in the endoplasmic reticulum (ER)

The detailed analysis of the embryonic expression pattern of malectin was completed by studies on its intracellular localization. For this purpose, malectin was ectopically expressed in the embryos as well as in eukaryotic cell lines, where its intracellular localisation was investigated by immunofluorescent detection of overexpressed malectin protein.

For this purpose, malectin constructs were generated, which included a „flag- tag“ positioned internally between the presumptive N- terminal signal peptide and the protein core (N- flag-malectin; figure 3.3.3; A), since N- terminal tags might be cleaved off with the N- terminal predicted signal peptide, and tags to the hydrophobic C- terminus could stay attached in a membrane compartment. In general, signal peptide serve to target a protein to and intracellular compartment or to drive its sorting and extracellular secretion. As the signal peptide of malectin was only a predicted protein domain, it was of interest to determine the significance of the signal peptide for intracellular localisation of malectin. To adress this question a deletion construct was generated where the tagged malectin was lacking the first 26 amino acids, the potential signal peptide (Δ N- flag- malectin). Correct protein synthesis of the wild type malectin, N- flag-malectin and Δ N- flag- malectin were confirmed by immunodetection of *in vitro* synthesised proteins (nonradioactive TNT; not shown) as well as by detecting the *in vivo* synthesised proteins. For the later ones, capRNA that coded for N- flag- malectin or Δ N- flag- malectin was injected into the animal pole of *Xenopus laevis* embryos. At stage 10, embryos were homogenised and membrane protein fractions prepared which were analysed for N- flag- malectin or Δ N- flag-malectin by immunodetection using the malectin specific antibody as well as a flag-epitop specific antibody.

In uninjected control embryos, the malectin specific antibody recognised a single protein band (figure 3.3.3 B, lane 1). Estimating its size and detecting a protein band of similar size in the injected embryos, it was assumed that this lower band represented the endogenous malectin protein. Embryos injected with capRNA encoding either N- flag-malectin or Δ N- flag- malectin showed a additional overlying bands that were missing in the uninjected control embryo (figure 3.3.3 B, lane 2 and 3). This experiment indicated that N-flag-malectin and Δ N- flag- malectin were both translated in the embryo. While N- flag- malectin,

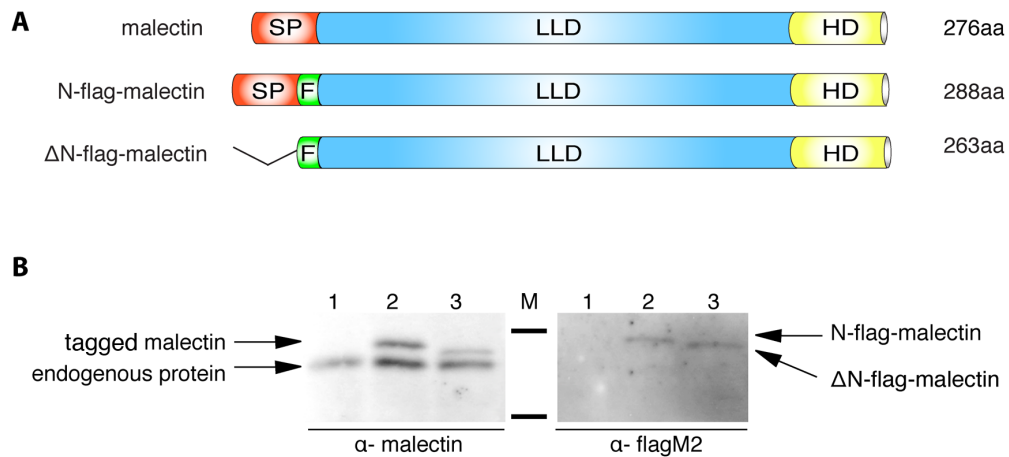


Figure 3.3.3 Malectin constructs generated for protein overexpression. (A) Schematic drawing of the flag-tagged malectin constructs used malectin overexpression. Detailed sequence analysis (Schallus et al., 2008) predicted that the wildtype (WT) malectin contains an N-terminal signal peptide (SP, aa 1-26, red), a conserved lectin-like domain (LLD, aa 27-255, blue) and a hydrophobic C-terminal domain (HD, aa 255-276, yellow). N-flag-malectin includes an additional flag-tag (F; epitope DYKDDDDK, green) between the SP and LLD. The Δ N-flag-malectin construct lacks the SP. (B) Correct protein translation of malectin constructs was confirmed by immunodetection *in vitro* (data not shown) and *in vivo* using antibodies directed either against malectin (rabbit-anti-malectin 1:15000) or mouse-anti-flagM2 (1:10000). lane 1: uninjected control embryos, endogenous malectin after SP cleavage (27.5 kD); lane 2: N-flag-malectin (32 kD); lane 3: Δ N-flag-malectin (29 kD). Marker (M) bands indicated show 37kD and 25 kD (*precision plus protein standard*, Biorad).

with a calculated molecular weight of 32 kD, was detected above the endogenous malectin, the Δ N-flag-malectin, with a calculated molecular weight of 29 kD, was also detected above the endogenous protein with a calculated weight of 30 kD. Detection of N-flag-malectin or Δ N-flag-malectin using a flag-epitope specific antibody, confirmed their identity as the protein extracts of control embryos did not reveal any detectable protein. Hence the size difference between the tagged and endogenous malectin proteins could only result from protein modification. It could not be excluded, that the endogenous protein undergoes posttranslational processing, e.g cleavage of the signal peptide (figure 3.3.1; aa 1-25). This would result in a product with a calculated weight of 27.5 kD. However further experimental evidence as by injection of Δ N-malectin was not acquired. Nevertheless, this experiment confirmed correct *in vivo* protein translation of N-flag-malectin or Δ N-flag-malectin and the constructs were used for subsequent analysis of the intracellular localisation of malectin.

The analysis of intracellular localisation of malectin was approached in two different ways. The first approach was performed by bilateral microinjection of 100 pg capRNA that coded for N-flag-malectin or Δ N-flag-malectin into the animal pole of two-cell stage *Xenopus laevis* embryos. Animal cap explants were dissected at stage 8-9. *In vivo* translated proteins were detected by immunofluorescent labeling in dissected animal caps (figure 3.3.4.; A). N-

flag- malectin or Δ N- flag- malectin proteins were detected using an flag-epitope specific antibody followed by immunodetection using fluorescent dye-labeled secondary antibody. Images that were taken with a confocal microscope that was suitable for liquid incubation. Fluorescent protein detection revealed, that N-flag-malectin was not dispersed throughout the cytoplasm but clustered in small granular perinuclear structures. In contrast, Δ N- flag-malectin protein, that was devoid of the signal peptide, showed a rather diffuse cytoplasmic distribution, partially aggregating and partially translocated into the nuclear space (figure 3.3.4; A, asterisk). This finding favored the idea that malectin protein was translocated to a cellular compartment with its signal peptide where it was integrated into the membrane by its hydrophobic C-terminus. However, a more detailed specification of the organelle was not achieved due to the technical limitations in the use of animal cap explants.

Therefore, the second approach to identify the intracellular localisation of malectin made use of transient eukaryotic cell transfections. Plasmids coding for N-flag-malectin or Δ N-flag- malectin were transfected in 3T3 mouse fibroblasts. Similar to the animal cap system, N- flag- malectin was concentrated in small territories in the cytoplasm as if it was accumulated in subcellular compartments. Co-detection of the ER-resident heat shock protein Hsp47, revealed partially overlapping localisation of N- flag- malectin and Hsp47 (figure 3.3.4 B; A- C). This finding provided evidence for the localisation of malectin in the endoplasmic reticulum (ER), although it did not exclude the possibility that the observed ER localisation was an overexpression artefact caused by artificial accumulation of the N- flag-malectin protein in the cell. Attempts to detect the endogenous protein using anti- malectin antibody failed to technical difficulties. Deletion of the N- terminus of malectin did result in an unequal cytoplasmic distribution and partially forming cytosolic aggregates (figure 3.3.4 B, D- E). As Δ N- flag- malectin (29 kD) did not exceed the exclusion size of the nuclear pore (30 kD) it was partially diffusing into the nucleus (Schallus et al., 2008).

To further support the idea of an ER residence for malectin, a time course experiment was performed (figure 3.3.3; B). N- flag- malectin overexpressing cells were fixed after 12, 24 and 48 hr and the overexpressed N- flag- malectin was detected by immunofluorescence labeling. After 18 hr, fluorescent detection of N- flag- malectin was weakly observed in small perinuclear tubular structures that resembled the extensive membrane network of the ER. Over time, extended translated N- flag- malectin accumulated in the ER (24, 48 hr) where it was arrested and partially aggregated in larger areas in the perinuclear rim and distinct loci of the cytoplasm (figure 3.3.3; B). Even after 48 hr, malectin protein was not translocated to the plasma membrane or showed cytoplasmic distribution. Instead, it remained confined to the ER. These results supported the idea, that malectin was an ER resident protein that was not translocated to the cell surface or secreted into the extracel-

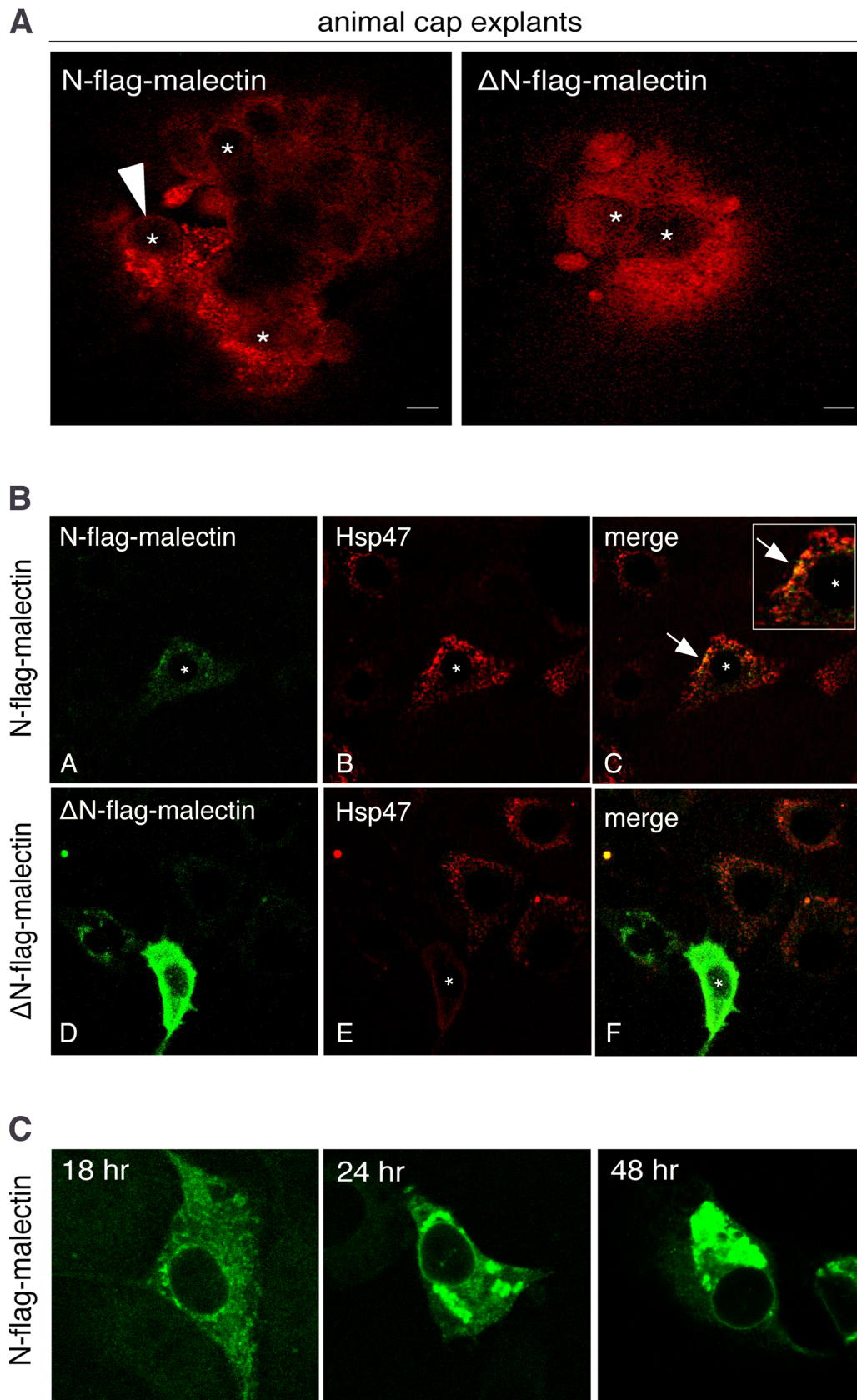


Figure 3.3.4 Malectin resides in the endoplasmic reticulum

Figure 3.3.4 Malectin resides in the endoplasmic reticulum. The intracellular localisation of malectin was analysed in cell transfection experiments. **(A)** N-flag-malectin and Δ N- flag-malectin capRNA (100 pg/E) were injected into the animal pole of a two cell stage embryo. At blastula stage animal cap explants were dissected and left to roll up for 30 min. Caps, were fixed in MEMFA, washed in PBS/Tween, blocked in 3% BSA/ PBS and used for antibody staining (1st antibody: mouse-anti-FlagM2; 2nd antibody: rabbit-anti-mouse-Alexa595). Images were taken using a confocal microscope (Zeiss LSM 510 META, 63x; Carl Zeiss, Oberkochen). Asterisk indicates the nuclei. White arrow head points to staining in the nuclear rim. White bar indicates size of 20 μ m. **(B)** NIH-3T3 mouse fibroblasts were transfected with 4 μ g plasmid of flag-tagged malectin using lipofectamin 2000 (Invitrogen). After a 24h- incubation, cells were washed with PBS, fixed with 3% PFA, permeabilized using 0.5% Triton-x-100 and blocked with 3% BSA/PBS. Antibodies used were diluted 1:200 in 3% BSA/ PBS: mouse- anti- ratHsp47 (MoBiTec), goat- anti- mouse- Alexa 595 (Invitrogen), rabbit- anti- Flag- FITC (Sigma). Images were taken using a confocal microscope Zeiss LSM 510 META, 63x (Carl Zeiss, Oberkochen; A- E) and a Leica DRM IRE2 TCS SP2, 63x (Leica, Bensheim; G- I) and processed for presentation with Adobe Photoshop CS2. N-flag-malectin (green) is found in a membraneous compartment around the nucleus (A- I, asterisk). Counterstaining using an antibody against the ER resident chaperone Hsp47 (red), reveals that malectin is colocalised in with the chaperone in the ER (merge, enlarged inset). Deletion of the N-terminal signal peptide results in a broad cytoplasmic distribution of malectin. Note that Δ N- flag- malectin still aggregates in membraneous compartments due to its C-terminal transmembrane domain. **(C)** A time course experiment shows that N-flag-malectin protein accumulates in perinuclear membrane or clustures in distinct territories within the cell (white arrow heads). Note that it is not translocated to the plasma membrane. Hours after cell transfection are indicated in each panel.

lular space. However, it did not exclude the possibility that malectin was synthesised in the ER but later translocated to a different membraneous compartment.

Altogether, the permanent and ubiquitous expression of malectin during development and in the adult organism in combination with its presumed ER localisation implied a regulating cell-autonomous role for malectin. As malectin was expressed in the pancreatic lobes at late tadpole stages (figure 3.3.2), and in context of the topic of this study, it was interesting to determine the effect on pancreas development resulting from depletion of malectin protein in *Xenopus laevis* embryos.

3.3.3 Functional analysis of malectin in *Xenopus laevis* organogenesis

Determination of knockdown efficiency of malectin specific morpholinos

In order to study functional relevance of malectin during embryogenesis in *Xenopus laevis*, loss- and gain of function approaches were performed.

Loss of malectin function was achieved by translational inhibition of malectin upon morpholino injection. Two malectin specific antisense morpholinos (malectin- Mo1 and malectin- Mo2) were designed, targeting the region of translational initiation (figure 3.3.5). Efficiency of translational inhibition was tested *in vitro* and *in vivo*.

In vitro, the morpholino binding efficiency was examined in a combined radioactive transcription and translation assay. Addition of malectin-Mo1 to the *in vitro* reaction in different concentrations (50, 20 and 10 μM) efficiently repressed malectin translation in a concentration dependent manner, whereas addition of unspecific control morpholino did not inhibit protein translation. In contrast, addition of same amounts of malectin-Mo2 (50, 20 and 10 μM) did not inhibit protein translation as efficiently as malectin-Mo1 as seen by a clear detectable band in the autoradiogram (figure 3.3.6; A).

To analyse morpholino efficiency *in vivo*, the N- terminal coding sequence of malectin was fused in frame to the coding sequence of GFP that were subsequently used for capRNA transcription (N-p150-GFP, 5'UTR-p150-GFP, figure 3.3.6; B). 100 pg of capRNA were coinjected with different morpholino amounts (100, 50 and 10 μM) into the animal pole blastomeres of a four-cell stage embryo. GFP fluorescence was analysed at stage 10. The presence of malectin-Mo 1 or malectin-Mo 2 inhibited translation of the GFP-fusion protein in all amounts tested, whereas expression of a wild type GFP was not affected (eGFP, figure 3.3.6; B). In contrast, injection of an unspecific control morpholino (CoMo) did not abolish translation of the GFP-fusion protein. These results showed specific morpholino binding to its target sequence and efficient inhibition of protein translation for malectin-Mo1 and malectin-Mo2.

Misexpression of malectin in the embryo disrupts proper tissue formation

As the major focus of this study was devoted to understanding of regulatory processes in the endoderm that eventually lead to pancreas formation, effects on malectin misexpres-

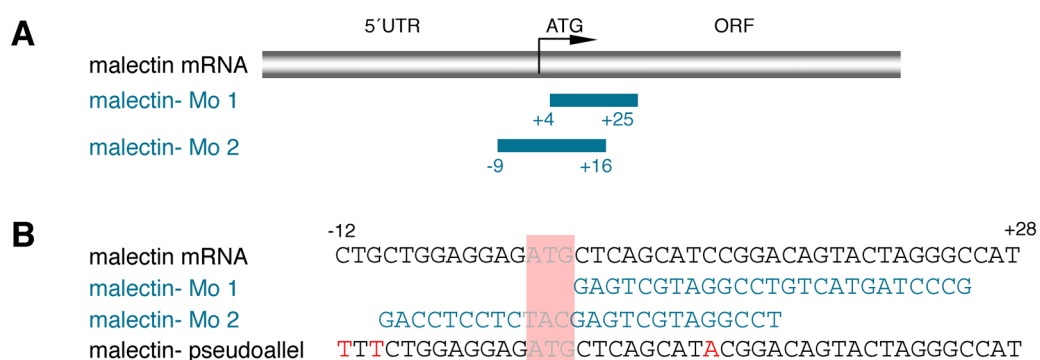


Figure 3.3.5 Position and sequences of malectin- specific morpholinos. (A) The scheme indicates the position of the two of malectin specific morpholinos (malectin-Mo1 and malectin-Mo2, blue bars) relative to the malectin coding sequence (CDS, NCBI: NM_001091743; grey bar). Numbers state the nucleic acid position with +1 beginning at the translation initiation site ATG. (B) Sequences of malectin- Mo1 and malectin- Mo2 (blue) are stated below the scheme. Malectin- Mo1 targets the beginning of the ORF, one codon downstream of the translation initiation site ATG (grey, underlined in red). Malectin- Mo2 targets the 5'UTR region overlapping the ATG. EST database search indentified a pseudoallele (NCBI: BJ062208) that showed one mismatch compared to the malectin mRNA. According to GeneTool information, one mismatch should not impair morpholino binding.

sion were primarily examined in the prospective endoderm. For this purpose, 100 μM of malectin-Mo1 was radially injected into the vegetal pole of a four-cell stage embryo and traced by coinjection of β -galactosidase encoding capRNA. Embryos were cultured till stage 41, when endodermal expression of malectin was evident in the hepatic and pancreatic tissue. Effects on liver and pancreas formation were monitored by expression analysis

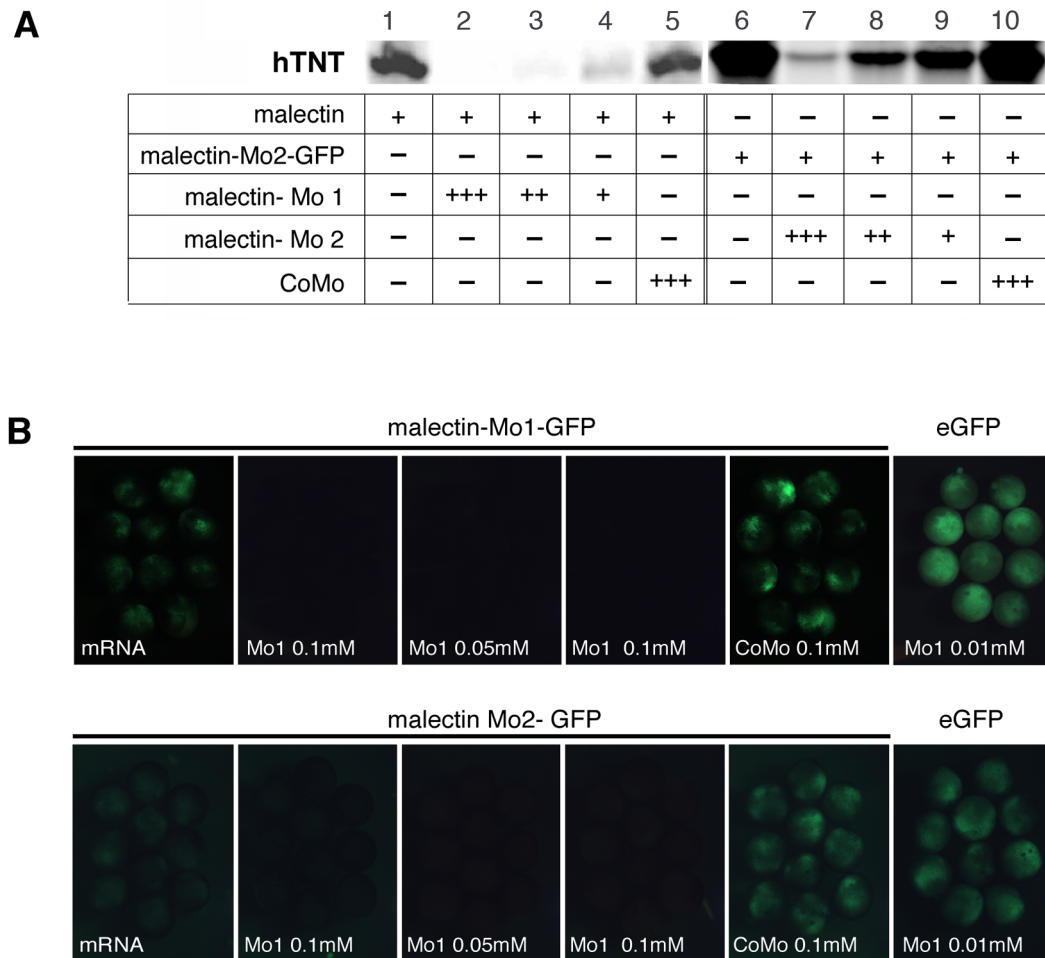


Figure 3.3.6 Determination of knockdown efficiency of malectin- specific morpholinos. (A) Morpholino binding specificity was analysed prior to injection by an *in vitro* radioactive transcription and translation assay (hTNT, Promega). 300ng pCS2±malectin plasmid served as template for *in vitro* transcription of malectin mRNA, followed by translation of malectin protein with incorporation of ^{35}S -methionine. Addition of malectin Mo-1 depleted malectin translational in a concentration dependent manner (+++= 0.05mM; ++ = 0.03mM, + = 0.01mM). To test Mo2, the 5'UTR of malectin was fused to the ORF of myc-GFP (malectin- Mo2-GFP). 300ng plasmid were used in the hTNT reaction. Upon addition of malectin-Mo2, protein translation was less efficiently blocked in amounts tested. In contrast application of an unspecific control morpholino (CoMo) has no effect on protein synthesis. (B) Inhibition of protein translation was further tested *in vivo*. The N-terminal SP was fused to GFP, malectin- Mo1-GFP. CapRNA of malectin- Mo1-GFP and malectin-Mo2-GFP were *in vitro* transcribed and injected into animal pole of *Xenopus* embryos (100 pg/E) alone or with Mo in different amounts (0.1- 0.01mM). Binding efficiency was scored the next day according to GFP fluorescence. In both cases coinjection of Mo inhibits protein synthesis. Note that in contrast to hTNT, efficient inhibition is also evident for Mo2. Oligonucleotide specificity against malectin is further confirmed by GFP fluorescence in embryos that were coinjection with Mo and eGFP capRNA (100 μg / E). In contrast coinjection of CoMo does not interfere with malectin-Mo1-GFP or malectin-Mo2-GFP protein synthesis.

of organ specific marker genes as the pancreas specific XPDip (Afelik et al., 2004) and the hepatic transcription factor XHex (figure 3.3.7; Newman et al., 1997).

Malectin-Mo1 injected embryos showed an bulky enlargement of the anterior endoderm, gut coiling defects and dramatically reduced pancreatic (91%) and hepatic lobes (63%, figure 3.3.7; A-C) as it was demarked by expression domain of XPDip and Hex. As small organ rudiments were still detectable, it was excluded that the loss of pancreatic and hepatic structures was due to default marker gene detection. This finding indicated that inhibition of malectin function in the endoderm affected liver and pancreas formation by the time of its endogenous expression. General unspecific side effects caused by microinjection were controlled by injecting a standard control morpholino (CoMo, 1.6 pmol). In contrast, in 57% of control morpholino injected embryos showed no reduction in organ size, either for pancreas not for the liver. The remaining 43% were only slightly reduced and not rudimentary as seen in malectin-Mo1 injected embryos. In order to ectopically express malectin in embryos 100pg/E of malectin capRNA was injected into control siblings and cultured till late tadpole stage 40 and organogenesis analysed with organ specific markers.

Ectopic expression of malectin in the endoderm lead to similar pleiotropic morphological defects in the anterior endoderm associated with loss of hepatic and pancreatic domains. In addition, mesoderm derivatives as trunk and anterior head structures were severely affected.

Altogether, inhibition or ectopic activation of malectin in the endoderm revealed a rather heterogenic effect that did not only disturbed formation of one particular organ but rather the general formation of the entire endoderm. Since malectin was detected throughout

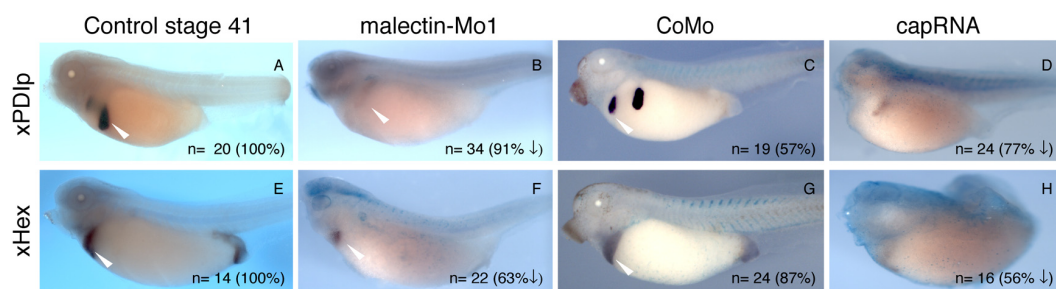


Figure 3.3.7 Misexpression of malectin affects endoderm development. Inhibition of malectin by malectin-Mo1 injection (1.6 pmol/E) as well as ectopic expression by capRNA injection (100pg/ E) leads embryonic malformations in the anterior endoderm. WMISH was performed using organ specific marker genes as XPDip marking the pancreas and XHex marking the liver lobe. xPDip positive domain was severely affected upon malectin-Mo1 injection (A- C, white arrow head). Also the hepatic XHex positive region was reduced (E- G, white arrow head). n= total number of embryos. Numbers in brackets state the number of embryos in percent, presenting the shown phenotype. Arrow down indicated reduction of marker gene expression. (data not shown). (p) pancreas, (li) liver, (pd) proctodeum.

development and was only at later stages evident in the endoderm, it is obscure when and how malectin plays a role in endoderm formation.

The third part of this study focused on the characterisation of a putative pancreas specific marker gene that showed later pancreatic expression and a high amino acid conservation between vertebrate homologues. Unlike expectations a detailed expression profile revealed a constant and rather ubiquitous gene activation during development. Intracellular localisation assays revealed an ER residence of malectin. Together with the pleiotrophic developmental effects upon malectin misexpression it was suggested that malectin played more of a general role during embryogenesis than specifically for pancreas development.

In summary, this study has shown that **HNF1 β is expressed in the ventral and dorsal pancreatic anlagen. HNF1 β is required but not sufficient to induce pancreas development in *Xenopus laevis*.** This result is similar to data obtained from mouse and zebrafish. Conversely to mouse and zebrafish, knockdown of HNF1 β in *Xenopus laevis* did not result in either a depletion of Xp48 expression nor in a complete loss of pancreas.

It was also shown, that HNF1 β is required and sufficient to induce early endocrine cell differentiation. This is the first time, that a transcription factor regulates the early onset of insulin gene expression within the dorsal pancreatic rudiment. It remains obscure whether late endocrine cell differentiation is affected and if HNF1 β promotes directly or indirectly endocrine cell differentiation.

HNF1 β is responsive to RA in the early endoderm. Herewith it was shown for the first time, that **early HNF1 β expression was responsive to RA in the endoderm and not only in the ecto- or mesoderm.** Regarding the possibility of HNF1 β linking early RA- signalling and late pancreas formation, it still remains unclear whether HNF1 β mediates **directly or indirectly the RA induced signal.**

The isolated XHNF6 is expressed in the dorsal and ventral endoderm. HNF6 is therefore coexpressed with its potential downstream targets Pdx1/XIHbox8 and Ptf1a/p48. Upon overexpression, XHNF6 promotes pancreas development. It remains to be investigated when and how XHNF6 is required for pancreas specification and cell differentiation in *Xenopus laevis*.

Malectin is an ubiquitously expressed ER resident protein that maintains a rather general role than a specific function during organogenesis. Considering its role in the N-glycosylation pathway, it would be intriguing to reveal its putative function in regulation of signalling pathways, as BMP and Wnt, involved in embryogenesis.

4 Discussion

Defects in pancreas organogenesis are the cause of severe clinical conditions including diabetes type I, which is characterised by absence or dysfunction of insulin producing β -cells. It is therefore of high interest to determine regulatory factors that are involved in pancreas development and the differentiation of β -cells. Pancreas specification in the anterior foregut epithelium is controlled by a complex cross-talk of transcription factors. From studies in the mouse, it was suggested that the homeobox transcription factor HNF1 β and the onecut protein HNF6 participate in this specification process by activating the pancreatic progenitor genes Pdx1/XIHbox8 and Ptf1a/Xp48 in the pre-pancreatic gut epithelium (Haumaitre et al., 2005).

In addition to these transcription factors, it was also shown that instructive signals from the surrounding tissues, such as RA- signalling, are required to direct pancreatic cell fate (Martin et al., 2005; Molotkov et al., 2005). Continuative studies in *Xenopus laevis* revealed that in amphibians, RA plays a crucial role in controlling dorsal pancreas prepatterning already during gastrulation when the germ layers are formed (Chen et al., 2004). It was revealed that early RA- signalling is crucial for endocrine at the expense of exocrine cell differentiation. But how these early RA induced prepatterning events are linked to the actual onset of pancreatic precursor gene expression or early induction of endocrine differentiation markers as insulin remain obscure.

In this regard, this study focused on the analysis of regulatory mechanisms that occur between gastrulation in the early embryo and the induction of XIHbox8 and Xp48 expression in the pancreatic endoderm. In general, gene activation is regulated by transcription factors that function in a hierarchical cascade of upstream regulators and downstream targets. Knockout studies in the mouse have identified two upstream candidates for regulation of Pdx1/XIHbox8 and Ptf1a/p48 expression, namely HNF1 β and HNF6 (Haumaitre et al., 2005; Jaquemain et al., 2003a).

This study focused on the functional characterisation of HNF1 β and HNF6 during pancreas development of *Xenopus laevis*. As in *Xenopus*, the HNF6 was not yet identified, the HNF6 homologue was isolated, analysed for its expression during embryogenesis and tested for its potential to activate pancreatic gene transcription. In order to investigate the

functional roles of HNF1 β and HNF6 on pancreas development, gain-and loss of function approaches were performed. HNF1 β function was investigated by protein knockdown as well as by ectopic protein expression in the context of pancreas development. Resulting effects on organogenesis were monitored by expression analysis of pancreas specific marker genes.

The fact that HNF1 β was reported as RA target gene in the neural tissue (Pouilhe et al., 2007, Hernandez et al., 2004) rised the interest to study the requirement of RA for HNF1 β expression within the endoderm (Demartis et al., 1994).

Intensive research on pancreatic specification and cell differentiation demands the identification of new pancreas specific marker genes as tool to mark segregating cell types. Hence, as a minor aspect, this study focused on the characterisation of a novel pancreas expressed protein, named malectin.

4.1 The requirement of HNF1 β for pancreas development

In *Xenopus laevis*, HNF1 β was extensively discussed regarding mesodermal kidney development (Bohn et al., 2003) and it was reported to contribute as GATA4-5-6 downstream target to early endoderm formation in *Xenopus laevis* (Afouda et al., 2005). However, its function in respect to endoderm organogenesis, as it was investigated in mouse or zebrafish (Haumaitre et al., 2005; Lokmane et al., 2008; Sun and Hopkins, 2001), was rather neglected for the *Xenopus* system.

To adress the question of HNF1 β function during endoderm organogenesis, here in respect to pancreas formation, it was necessary to refine the previous reported spatial and temporal expression patterns in the endoderm. Detailed expression analysis was achieved by WMISH on embryos of different developmental stages (figure 3.1.1). Transversal sections clearly traced HNF1 β expression to the early endoderm including the the dorsal region, where it became progressively restricted to the anterior foregut, including liver and prospective pancreas. This observation was in accordance with previously published expression patterns (Demartis et al., 1994; Vignali et al., 2000; Afouda et al., 2005). But for the first time, it was clearly shown, that HNF1 β was not only expressed within the anterior endoderm, but in particular in the ventral and the dorsal pre-pancreatic regions. This detail in the HNF1 β expression profile was remarkable in order to explore the importance of HNF1 β during pancreas development in *Xenopus laevis*.

Pancreas development in *Xenopus laevis* begins with the region-specific expression of the pancreatic progenitor markers XlHbox8 and Xp48 in the foregut. Studies from mouse described HNF1 β as upstream regulator for Pdx1/XlHbox8 and Ptf1a/48 (Haumaitre et al., 2005). HNF1 β expression was activated in the foregut from developmental stage E8.5, preceding the onset of Pdx1/XlHbox8 and Ptf1a/Xp48 expression. At stage E9.5 the three transcription factors were coexpressed within the pre-pancreatic epithelium (Haumaitre et al., 2005).

In this study, it was also demonstrated for *Xenopus laevis*, that endodermal HNF1 β expression preceded the onset of its suggested downstream targets XlHbox8 and Xp48. HNF1 β not only preceded but it also overlapped with XlHbox8 and Xp48 expression domains by the onset of pancreatic budding (figure 3.1.1; figure 3.2.4). This match in temporal and spatial gene activation of HNF1 β and XlHbox8 and Xp48 in the territory of the prospective pancreas argued for a regulatory link between these transcription factors in specification and differentiation of the pancreas, as it was hypothesised from studies in mouse.

4.1.1 HNF1 β is necessary for pancreas specification

To define the necessity for HNF1 β in pancreas development in *Xenopus laevis*, downregulation of protein function was performed by HNF1 β specific antisense morpholino injection. Morpholinos were targeted to the whole endoderm by radial injection into the vegetal pole. Downregulation of HNF1 β protein in *Xenopus laevis* embryos leads to pancreatic hypoplasia, based on XPDip expression (figure 3.1.4). The smaller pancreatic organ showed morphological abnormalities as protrusions of the exocrine compartment. The pancreatic progenitor marker XlHbox8 that is normally expressed strongly in the duodenal and pancreatic epithelium from stage 28 onwards, was severely reduced in its pancreatic expression upon HNF1 β depletion. First, pancreatic XlHbox8 expression was detectable in the dorsal pancreatic rudiment by stage 34 while the ventral rudiment was still devoid of HNF1 β transcripts.

Expression of the second pancreatic marker gene Xp48 was also downregulated upon HNF1 β depletion by stage 34, in particular in the ventral pancreas. Although it was not repressed to the same extent than XlHbox8 (figure 3.1.4). Reduction of both pancreatic progenitor genes suggested that HNF1 β was necessary for pancreas specification in the gut epithelium. Unlike the complete pancreatic agenesis seen in HNF1 β -deficient mice (Haumaitre et al., 2005), HNF1 β -depleted *Xenopus laevis* embryos still generated a small pancreatic organ that seemed to derive from dorsal and ventral lobes (figure 3.1.4). Under the constraint of the technical limitations in protein knockdown upon morpholino injections

(Eisen and Smith, 2008), generation of a hypoplastic complete pancreas could also derive from an partial knockdown of HNF1 β within the endoderm (figure 3.1.3). As known from recent overexpression studies a combined activation of XIHbox8 and Xp48 is required to specify pancreatic cell fate in the foregut region (Afelik et al., 2006). The occurrence that ventral XIHbox8 expression was inhibited by morpholino injection by stage 34 made it rather unlikely that Xp48 expression was evident due to an incomplete HNF1 β knockdown in the endoderm of *Xenopus laevis* (reviewed in Eisen and Smith, 2008). It was concluded that Xp48 might be regulated by an additional factor within the pancreatic epithelium. Ergo, the remnant XIHbox8 protein induced in the dorsal pancreatic region in combination with the remaining Xp48 protein might be sufficient to make the anterior foregut competent to adopt pancreatic cell fate and to generate a small organ. A recent study by Stanger et al. (2007) revealed that the number of pancreatic progenitor cells determines organ size affecting exocrine and endocrine tissue in mouse.

These results are in agreement with studies in HNF1 β -deficient mice, reporting that lack of HNF1 β leads to pancreatic hypoplasia (Haumaitre et al., 2005). The ventral prospective pancreatic region was devoid of Pdx1 and Ptf1 expression resulting in total absence of the ventral pancreatic bud. In the dorsal pancreas, Pdx1 was initiated and budding occurred, however, outgrowth and morphogenesis were impaired. Consequently, the dorsal pancreatic remnant regressed and disappeared by E13.5 and the epithelium was devoid of any endocrine cells. The delayed onset of dorsal Pdx1 and p48 expression indicated a maintaining rather than inducing activity of HNF1 β for Pdx1 and p48 transcription within the pancreatic epithelium and thereby promoting outgrowth and morphogenesis. In accordance it was proven, that size reduction upon HNF1 β depletion was based on impaired proliferation (Haumaitre et al., 2005).

To exclude incomplete protein knockdown, a second approach to inhibit HNF1 β function was performed by repressing endogenous HNF1 β activity by its fusion to the engrailed repressor domain (Vignali et al., 2000). This repressor construct has a similar reducing effect on XIHbox8 repression in the foregut domain as morpholino injections, in particular the dorsal endoderm. In contrast to previous studies (Vignali et al., 2000), it was not possible to rescue the repression of XIHbox8 expression by ectopic expression of HNF1 β within the endoderm. Coinjection of HNF1 β and HNF1 β - Mo1+2 resulted in high lethality instead. This data confirmed that HNF1 β was necessary to activate XIHbox8 in the pancreatic endoderm but it still remained unclear whether HNF1 β directly or indirectly promoted XIHbox8 activation. As no binding studies were done for HNF1 β binding to the XIHbox8 promoter, data from the mouse system argue for a direct activation of XIHbox8 by HNF1 β (Gerrish et al., 2001).

4.1.2 HNF1 β is not sufficient for pancreas formation

To analyse if HNF1 β is sufficient for pancreas formation, the reverse complement experiment was performed to characterise its regulatory capacity during pancreas development. Ectopic HNF1 β activation within the endoderm was achieved by overexpression of HNF β encoding capRNA, as wild type, constitutive active HNF1 β -VP16 fusion or time point inducible GR fusion. Injection was done radially into the vegetal pole of *Xenopus laevis* embryos targeting the HNF1 β protein to the whole endoderm.

In all cases, pan-endodermal induction of HNF1 β activity resulted in an posterior extension of XIHbox8 in the endoderm (figure 3.1.8; appendix 7.1). This XIHbox8 expansion was either seen as homogenous expansion with decreased transcript levels in the endogenous XIHbox8 expression domains or XIHbox8 positive regions were still evident in the dorsal and ventral pre-pancreatic endoderm. In this case, expression extended towards the caudal tip in the dorsal rudiment and the ventral expression was ectopically detected in ventro-posterior regions. This increased XIHbox8 expression was most evident upon early activation of HNF1 β protein after gastrulation. Later time-points of hormone treatment resulted in less, and rather region specific XIHbox8 expression. The dorsal expression domain was still expanded however approaching its regular size in the dorso-anterior foregut. The ventral pancreatic expression domain was rather reduced and XIHbox8 expression was detected in discrete loci of the ventro-posterior gut endoderm (figure 3.1.8, appendix 7.1. A). If HNF1 β is required for XIHbox8 activation, ectopic HNF1 β activation in more posterior regions could be the cause for ectopic XIHbox8 expression in these posterior domains.

This result clearly demonstrated that HNF1 β was sufficient to initiate XIHbox8 expression within the endoderm and argued for a direct activating role of HNF1 β for XIHbox8 expression. Furthermore, the discrete XIHbox8 positive loci in the posterior endoderm that were induced upon late-stage treatment provided evidence for a cell fate conversion of posterior intestinal cells into ventral pancreatic or duodenal tissue. It remained to be examined whether detected expansion of XIHbox8 expression in the posterior intestine is indeed pre-pancreatic endoderm or whether XIHbox8 positive cells in the intestine undergo cell-fate conversion into other XIHbox8 expressing endodermal tissues as stomach or duodenum.

The later idea was supported by the fact, that posterior regions obtained upon HNF1 β activation, did not result in additional pancreatic territories based on the exocrine tissue marker XPDIp (figure 3.1.8).

Otherwise, lack of extra pancreatic lobes in XIHbox8 overexpressing embryos was reasonable according to reports in chicken, showing that ectopic activation of Pdx1 in chicken endodermal explants. PDX1 induced multiple pancreatic protrusions in the posterior gut endoderm however Pdx1 was not sufficient to drive pancreatic organ growth and differentiation of pancreatic cell lineages (Grapin-Botton et al., 2001). Absence of pancreatic tissue

would be in agreement with a recent study in *Xenopus laevis*, showing a combined expression of XIHbox8 and Xp48 was necessary to direct pancreatic cell fate in the endoderm (Afelik et al., 2006). In addition, two reasons argued additionally for a pancreas specific XIHbox8 expansion in the dorsal and ventral endoderm: (1) dorsal XIHbox8 expansion occurred in a small remarkable rim along the dorsal midline (figure 3.1.8), and (2) the XIHbox8 expansion in the ventral region was spatially restricted to the most ventro-posterior domain resembling an **interrupted extension from the endogenous ventral domain**.

As induction of ventro- posterior ectopic XIHbox8 expression was associated with a reduction of ventro- anterior XIHbox8 expression, it was suggested that HNF1 β might have an additional function in A-P patterning of the gut tube (figure 3.1.8). **Interestingly, a similar ventro- posterior expansion of XIHbox8 was observed in a recent study elucidating the role of Wnt- signaling in anterior endoderm patterning (McLin et al., 2007).** In this study, inhibition of Wnt-signaling was required to permit posterior cell fate conversion of posterior intestine into XIHbox8 positive pancreatic endoderm, providing evidence for a regulatory mechanism between HNF1 β and Wnt- signalling.

While ectopic expression of HNF1 β in the endoderm caused an expansion of pancreatic progenitor gene XIHbox8 it did not obviously affect expression of the second pancreatic progenitor marker Xp48 (figure 3.1.8). The occurrence that Xp48 expression domain was only slightly reduced upon HNF1 β depletion and not remarkably affected upon ectopic HNF1 β expression favors the idea of a differential regulation of Xp48 by another upstream regulator within the pre-pancreatic epithelium.

First promoter analysis in mouse revealed a contradictive HNF1 β binding site in the Xp48 promoter (Haumaitre et al., 2005) supporting the idea that HNF1 β directly regulated Xp48 activation in mouse. So far, preliminary promoter analysis of the *Xenopus tropicalis* Xp48 promoter though did not reveal HNF1 β target sequences (Lennart Opitz, personal communication) favoring the idea of an alternate transcriptional activator, for instance HNF6.

Interestingly, ectopic activation of HNF1 β within the endoderm perturbed pancreas development. This effect was evident in the diminished ventral and dorsal pancreatic lobes (figure 3.1.8). In general, size reduction can occur due to apoptosis, impaired specification, inhibited proliferation, induced differentiation or cell fate conversion.

Although no experimental proof was obtained, size reduction due to apoptosis was rather unlikely based on observations in HNF1 β -deficient mice, which did not reveal an increase in apoptotic cells within the foregut domain (Haumaitre et al., 2005). Decrease in pancreatic size could result in perturbed differentiation into pancreatic progenitor cells by a delayed cell cycle exit of proliferating foregut. Ongoing epithelial cell proliferation would reason the increase in endodermal cell mass and would explain impaired differentiation

processes and would explain the enlargement of the ventro-anterior endoderm that was observed in the mild phenotype of HNF1 β overexpressing embryos (figure 3.1.6). Inhibited cell cycle exit and perturbed pancreas organogenesis were observed for ectopic activation of Notch-signalling in the proliferating pancreatic epithelium in mouse (Hald et al., 2003; Murtaugh et al., 2003). By overactivation of Notch- signaling, it was shown that pancreatic precursor cells maintained their proliferative stage and repressed differentiation leads to size reduced pancreas formation. In agreement, depletion of HNF1 β , which showed a confined expression to the foregut epithelium, revealed impaired endoderm outgrowth and expansion that was evident by a decrease in proliferating cells (Lokmane et al., 2008). In this study, impaired specification of pancreatic precursor cells was excluded as XIHbox8 expression was strongly increased.

In addition, Pdx1/XIHbox8 was shown to act antiproliferative in gastric cancers and was reported as a negative regulator of the expression of the mitotic gene C-Myc (Ma et al., 2008; Chen et al., 2007). Therefore, it is rather possible that high levels of Pdx1/XIHbox8 in the gut, as obtained in this study upon HNF1 β activation, promote cell-cycle exit and impaired proper proliferation and outgrowth of the branching pancreatic epithelium. This hypothesis is supported by observations that loss of C-Myc expression in the pancreatic epithelium leads to reduced proliferation of epithelial and acinar precursor cells. Advanced cell-cycle exit comes along with an increase in endocrine cell differentiation (Nakhai et al., 2008; Zhou et al., 2007). Similar, endocrine differentiation was observed upon inhibition of Notch signaling (Jensen et al., 2000).

In *Xenopus laevis* endocrine cells are exclusively specified in the dorsal pancreatic anlage at stage 32. Size reduction of the dorsal pancreatic rudiment could therefore result from extensive endocrine cell differentiation. This idea was supported by an increase in XIHbox8 expression that came along with an increased number of insulin positive cells expressed in the dorsal gut epithelium which were posteriorly mislocalised and appeared in distant caudal regions of the gut endoderm. However, it was contradictive to previous results that never described an obvious alteration in this early endocrine gene expression upon ectopic expression of Xp48 or XIHbox8 (Afelik et al., 2006).

As HNF1 β is known to be involved in anterior-posterior patterning in the ecto- and mesoderm it could also be that it played a similar role in A- P axis formation in the endoderm. By the time of gut tube patterning at stage 20-22, HNF1 β is expressed in an anterior-posterior gradient and was later also confined to the liver diverticulum. Studies in mouse revealed that HNF1 β was required for liver and bile duct specification (Lokmane et al., 2008; Coffinier et al., 2002). In *Xenopus laevis*, the liver diverticulum lays anterior and adjacent

to the ventral pancreas. Therefore, it could be that induced activation of HNF1 β caused cell fate conversion of ventral pancreatic cells into hepatocytes in the foregut endoderm or shifting the position of the ventral pancreas towards the posterior gut endoderm.

Differences in XlHbox8 gene activation in the ventral and dorsal gut epithelium also supported the idea of a differing regulatory system that might be responsible for segregation of ventral pancreas and the adjacent liver (Deutsch et al., 2001). However, this aspect demands further analysis using hepatic and posterior endodermal marker genes. In summary it was concluded that HNF1 β is required but not sufficient onto induce pancreatic formation within the endoderm.

4.2 The requirement of HNF1 β for endocrine cell differentiation

In mouse, the majority of endocrine cells derive from the branching pancreatic epithelium at E13 in a process of massive endocrine cell differentiation named secondary transition. This step in pancreatic development is defined by the onset of expression of the pro-endocrine gene Ngn3. Ngn3 positive cells subsequently differentiate into all endocrine cell types of the mature pancreas. However, few glucagon and insulin positive cells are spotted in the early intestinal gut epithelium during primary transition and appeared in the pancreatic epithelium prior the onset of the endocrine precursor gene Ngn3 (Gradwohl et al., 2000). Their real origin remained obscure.

In *Xenopus laevis* the pro-endocrine gene Ngn3 has not been described so far. Hence, the insulin is the earliest endocrine differentiation marker that is expressed exclusively within the dorsal pancreatic anlage from stage 32 onwards (Kelly and Melton, 2000). It was suggested that these early endocrine cells correspond to the endocrine cells of the primary transition in mouse. It remains obscure how differentiation of these early endocrine cells is regulated. In a later differentiation wave at stage 45 a second group of insulin producing endocrine cells differentiates in the pancreatic epithelium. These cell were demonstrated to depend on XlHbox8 and Xp48 expression in the organ specification process (Afelik et al., 2006). As reported, ectopic activation of either XlHbox8 or Xp48 alone, or in combination, did not result in any obvious increase of early insulin expressing cells. Inhibition of both keyregulators by antisense morpholino knockdown did not affect cell number of early insulin positive cells. But they remained clustered in the dorso- anterior endoderm due to gut coiling defects. However, late endocrine cell differentiation was perturbed (Afelik et al., 2006). As late endocrine differentiation was impaired it was postulated that early and later endocrine cell specification is differentially regulated, with the early differentiation being independent of both pancreatic progenitor markers. Similar observations in mouse and

zebrafish indicated that early endocrine gene activation was independent from Pdx1/XlHbox8 and Ptf1a/p48 whereas late endocrine differentiation was perturbed (Burlison et al., 2008, Lin et al., 2004).

Is HNF1 β necessary and sufficient for endocrine cell differentiation?

In this study, Hnf1 β depletion caused a significant reduction of early insulin positive cells (figure 3.1.5) that was associated with a decrease in Xhlbox8 and Xp48 expression in the dorsal pancreas. It was not analysed whether late hypoplastic pancreas of HNF1 β depleted embryos was also devoid of late endocrine cells.

Recent studies from mouse and *Xenopus laevis* support the idea that early endocrine cell differentiation is independent of Pdx1/XlHbox8 and Xp48 (Afelki et al., 2006; Burlison et al., 2008). In *Xenopus laevis*, XlHbox8 and Xp48 depleted embryos revealed impaired gut coiling and in addition cluster formation of insulin positive cells in the anterior foregut but apparently revealed no alteration in the number of insulin positive cells (Afelik et al., 2006). Here, HNF1 β depletion upon morpholino injection also induced gut coiling defects (not shown) that could explain the reduced range of insulin positive region in the gut epithelium. However, quantification of insulin positive cells not only demonstrated a reduced size of expansion but a significant reduction in cell number. The reverse complement phenotype obtained upon ectopic activation of HNF1 β argues for a real decrease in insulin transcription.

In an attempt to further quantify putative changes in insulin expression between control and HNF1 β morpholino injected embryos, insulin transcription levels were determined using semiquantitative RT-PCR on RNA from whole embryo endoderm (not shown). In this one time experiment though levels of insulin transcription were not apparently altered as expected from the finding by WMISH. Hence, further quantification of insulin repression using realtime PCR is strongly recommended to confirm the idea of HNF1 β inducing insulin gene activation and to determine to which extend the level of insulin transcription is affected upon HNF1 β downregulation.

In the reverse complement study, ectopic activation of HNF1 β within the endoderm caused a strong increase in insulin positive cells suggesting that HNF1 β was sufficient to activate insulin expression within the dorsal endoderm (figure 3.1.9). One possibility would be that HNF1 β activates insulin directly on the promotor. But HNF1 β was only weakly expressed in the dorsal endoderm at the time point of early endocrine differentiation peaks. Thereby rising the question of an intermediate regulator. Ectopic HNF1 β function in the posterior region caused an posterior induction of XlHbox8. Interestingly, the XlHbox8 positive territory was confined along the midline. This extending dorsal pancreatic XlHbox8 positive epithelium overlapped with the region of insulin positive cells that were also mislocated to

more posterior regions of the endoderm. As mentioned, Pdx1 originally reported as Insulin promoting factor 1 (Ipf1) in mouse, directly activates insulin expression and is required for β -cell generation (Jonsson et al., 1995; Watada et al., 1996; Gannon et al., 2008). Hence, posterior increase in XlHbox8 and insulin expression suggests that also in *Xenopus laevis* insulin expression is regulated by the transcription factor XlHbox8.

In HNF1 β $-/-$ mice, reduced Pdx1/XlHbox8 expression inhibited pancreatic branching and outgrowth and also impaired endocrine cell differentiation (Haumaitre et al., 2005). Also studies in zebrafish report that Pdx1/XlHbox8 repression perturbed pancreas specification and endocrine differentiation (Song et al., 2006) that was also seen in human MODY5 patients (Wang et al., 2004). Hence, the other possibility for induction of early insulin transcription in *Xenopus laevis* proposes that it is not HNF1 β that directly activated insulin gene expression but rather XlHbox8 as HNF1 β downstream mediator.

Contradicting previous reports of unaffected early insulin expression upon XlHbox8 morpholino injection (Afelik et al., 2006), first data obtained in this study upon XlHbox8 morpholino injection (data not shown) favor the idea that XlHbox8 is required for this early insulin expression in the dorsal epithelium. As dorsal XlHbox8 expression was driven by HNF1 β , this transcription factor cross talk could provide a regulatory mechanisms explaining early induction of insulin expression exclusively in the dorsal gut epithelium. It would also represent a conserved regulatory way for endocrine cell differentiation in vertebrates. However, it still remains obscure which regulatory mechanism promotes insulin expression in selected cells scattered in the XlHbox8 positive epithelium. Further experiments are required to finally determine the origin of early insulin positive cells in *Xenopus*.

In summary the results obtained describe two distinct functions for the transcription factor HNF1 β in context of pancreas development: (1) an early role in pancreas specification within the gut epithelium by controlling XlHbox8 gene expression and (2) a later role in endocrine cell differentiation by promoting insulin gene expression in the dorsal gut endoderm. The fact that HNF1 β is only weakly expressed in the dorsal pancreas at stage 34 and gets reduced by the time where insulin differentiation peaks (stage 36), favors the idea that it acts indirectly on insulin gene induction. One candidate that could mediate HNF1 β activity in the dorsal pancreatic epithelium is XlHbox8. Following suggestions from zebrafish (Song et al., 2006), it can be speculated that HNF1 β activates XlHbox8 expression in the dorsal pancreatic endoderm which- maybe via Ngn3-, directs endocrine cell differentiation. In addition HNF1 β appears to play a role in localising the ventral pancreas along the anterior-posterior axis of the gut tube.

4.3 HNF1 β is a mediator for RA-signalling in the endoderm

The posterior expansion of XlHbox8 in the dorsal endoderm and the increase of insulin positive cells that was induced upon pan-endodermal activation of HNF1 β resembled the result observed upon activation of RA- signaling (Chen et al., 2004). It was demonstrated that RA caused a caudal extension of the XlHbox8 positive expression domain and promoted insulin expression on the expense of exocrine tissue in the dorsal endoderm (Chen et al., 2004). In addition early RA promoted ventral exocrine tissue and also HNF1 β promoted ventro-posterior expansion of the XlHbox8 domain.

Nevertheless, some discrepancies between ectopic HNF1 β activity and increased RA signalling were observed. Head structures in RA treated embryos were nearly abolished, while they were only reduced in HNF1 β depleted embryos. In contrast to posterior XlHbox8 extension upon HNF1 β overexpression, exogenous RA treatment also lead to an anterior reposition of insulin positive cells. This indicated that not only HNF1 β is required but other signalling mechanism control correct A-P position of differentiating cells along the gut tube (table 4).

HNF1 β expression was initiated after MBT in the vegetal hemisphere of the blastula stage embryo that gives rise to the endodermal germlayer (Vignali et al., 2000). By the onset of gastrulation the RA synthesizing enzyme RALDH2 is expressed in the involuting mesoderm, adjacent to the endogenous HNF1 β expression domain (figure 1.5). Earlier studies in *Xenopus laevis* (Demartis et al., 1994) and zebrafish (Song et al., 2006) indicated that HNF1 β was a RA responsive gene within the endoderm. Hence it was hypothesised that HNF1 β could link early RA induced prepatterning steps in the dorsal endoderm in order to promote pancreas development, in particular endocrine cell differentiation (Stafford et al., 2004; Chen et al., 2004). However it remained unclear when HNF1 β expression was activated by RA and how it could mediate induction of pancreas development. So it was intriguing to investigate the role of RA to promote HNF1 β gene activation. Therefore RA-signalling was activated in blastula stage embryos upon RA treatment and inhibited using the RAR antagonist BMS453 (Chen et al., 2004).

Expression analysis of HNF1 β in RA treated embryos revealed slight induction within the endoderm at early stages while BMS453 treatment revealed no effect compared to control. During subsequent development it was evident that endodermal expression level of HNF1 β was elevated whereas BMS453 treatment rather repressed HNF1 β transcription (figure 3.1.11). In particular, expression by the stage of pancreatic budding (stage 34), HNF1 β expression was strongly increased in the dorsal pancreatic region. It was an established idea that RA is required for specification of the dorsal but not the ventral pancreas. This was conserved between vertebrates (Stafford and Prince 2002, Chen et al., 2004, Martin

treatment	dorsal XIHbox8	insulin	exocrine	ventral XIHbox8	gut coiling defect	p48
RA	+	+	-	+	+	+
HNF1 β	+	+	-	++	+	uc
BMS453	-	-	-	uc	+	-
HNF1 β -Mo1+2	-	-	-	-	+	-

Table 4 Comparison of RA and HNF1 β induced effects on pancreas development. First column indicated manipulation of the embryos. The next columns indicate expression levels of XIHbox8 in the dorsal or ventral endoderm, level of endocrine cell differentiation (endo), size of dorsal exocrine compartment (exo), and gut coiling effect. (+) elevated, (-) reduced, (++) ectopic, (uc) unchanged.

et al., 2005). The increased HNF1 β expression at stage 34 showed that the RA effect was persistent through time and not a transient event. This result favored the idea of a putative role of HNF1 β as RA mediator for dorsal pancreas specification.

In order to analyze direct activation of endodermal HNF1 β expression, RA and BMS453 treatments were done on whole endodermal explants and analysed by semiquantitative RT-PCR. HNF1 β gene activation was altered upon exogenous application of RA and downregulated upon BMS453 treatment. This data provided evidence that endodermal HNF1 β expression was responsive to **direct RA- signalling**.

A recent study reported that dorsal and ventral endoderm was differentially responsive to RA- signalling (Pan et al., 2007). As early HNF1 β expression was in particular seen in the dorsal involuting endoderm, representing the prospective pancreatic tissue, it was of further interest to reveal whether HNF1 β expression in the dorsal versus the ventral endoderm differed in responsivity to RA (figure 3.1.12). Therefore whole endoderm explants were dissected and treated with RA or BMS453. HNF1 β was slightly elevated in dorsal and ventral endoderm explants and its expression was remarkably reduced in dorsal and ventral explants upon BMS453 treatment. These findings indicate that HNF1 β expression is regulated by RA within the endoderm. But HNF1 β was not obviously differentially responsive to RA signalling in the dorsal versus the ventral endoderm. However, this data remained to be confirm by **quantitative RT-PCR**.

The morphogen RA is synthesised by RALDH2 in the adjacent dorsal involuting mesoderm and secreted into the neighbouring endoderm. Assuming the formation of a dorso-ventral morphogen gradient, it can be speculated that under physiological conditions, dorsal HNF1 β expression is stronger influenced by RA than ventral HNF1 β expression and that this expression difference determines the role of HNF1 β during organ specification. Exog-

enous RA or BMS453 treatment lacked this differential gradient formation and therefore might activate or inhibit ventral HNF1 β expression to the same extent than in the dorsal explant tissue. As consequence, this resulted in a comparable HNF1 β gene activation or inhibition in dorsal and ventral explants.

Taken together, the results of this study support the idea that HNF1 β is responsive to early RA signalling within the endoderm to direct dorsal pancreas development and endocrine cell differentiation, whereas it plays a distinct role in ventral pancreas specification. Hence, it would be of interest to investigate the effect on dorsal or ventral HNF1 β expression upon region specific manipulation of RA- signalling.

A previous study in zebrafish was investigating the role of RA in directly acting on the endoderm to induce β -cell fate (Stafford et al., 2006) and it was shown that RA was not able to rescue insulin expression in the absence of vHNF1, the zebrafish homologue, whereas vHNF1 overexpression restored insulin expression when RA- signalling was inhibited (Song et al., 2006). A recent study suggested a role of RALDH1 within the pancreas to promote endocrine cell differentiation (Öström et al., 2008). Data obtained in this study, as the RA-induced dorsal expression of HNF1 β at stage 34, the HNF1 β induced posterior expansion of XlHbox8 and the increase in insulin positive cells, together with previous findings, provided strong evidence that HNF1 β acts as RA downstream target mediating instructive signals for dorsal pancreas formation and endocrine cell differentiation.

Apart from RA, many other signalling pathways were related to pancreas formation as the secreted factors SHH, BMPs and FGF (Hebrok et al., 1998; Kim et al., 2001; Hart et al., 2000). In the study by Chen et al., it was reported that RA induced expansion of XlHbox8 expression within the dorsal endoderm was associated with a decreased expression of SHH. As shown in chick repression of SHH was crucial to permit Pdx1/ XlHbox8 expression in the pancreatic epithelium (Hebrok et al., 1998). Otherwise inhibition of RA caused an expansion of the SHH expression domain in the endoderm. Antagonising action of SHH and RA was also demonstrated in chicken limb bud and zebrafish fin formation (Helm et al., 1994; Niswanderer et al., 1994). In zebrafish, endoderm formation and patterning relied on BMP signalling (Tiso et al., 2002). In the same study it was demonstrated that vHNF1 was dependent on early active BMP signaling and it was responsible to mediate BMP dependent endocrine cell differentiation in zebrafish.

Conversely, in *Xenopus laevis* it was shown that BMP- and also Wnt- signalling must be repressed in the early dorsal endoderm in order to make the future anterior endoderm competent to acquire pancreatic cell fate (Pan et al., 2007; McLin et al., 2007; Spagnoli et al.,

2008). In addition, it was shown that RA- and BMP- signalling interacted with each other. Therefore it would be intriguing to analyse changes in early HNF1 β expression within the dorsal endoderm in response to modulated BMP- and Wnt- signalling.

4.4 Ectopic activation of XHNF6 promotes pancreas development

In HNF1 β loss and gain of function experiments it appeared that the expression of the second pancreatic key regulator Xp48 was less severely affected than XIHbox8 (figure 3.2.4, figure 3.2.8). Therefore it was postulated that Xp48 might be differentially regulated in the gut endoderm. From knockout studies in mouse it was postulated that the onecut transcription factor HNF6 might function as upstream regulator for Pdx1/ XIHbox8 and Ptf1/ Xp48. In this context we isolated the *Xenopus laevis* homologue XHNF6 and characterised its expression pattern by WMISH and semiquantitative RT-PCR and compared it to its potential downstream targets Xp48 and XIHbox8. In order to be an upstream regulator spatial and temporal overlapping expression patterns were required. Regarding endoderm patterning and pancreas development, it was very interesting to detect XHNF6 transcription by the onset of gut tube patterning stage 22 in a small territory of the ventral foregut (figure 3.2.1). Expression increased and was spatially restricted to the liver and presumptive ventral and dorsal pancreatic anlage by stage 34. Hence, HNF6 was expressed in the anterior endoderm before the initiation of Xp48 and XIHbox8. Spatial restriction of XHNF6 to the liver diverticulum was very similar to the anterior endodermal expression domain of HNF1 β , living up for their names as liver enriched transcription factors. With the beginning of pancreatic budding at stage 34, XHNF6 was clearly detectable in the ventral pancreatic region, whereas the dorsal pancreatic expression was only detectable by RT-PCR. HNF6 expression in mouse (Landry et al., 1997) as well as in zebrafish (Hong et al., 2002) demonstrated early onset of expression in the developing nervous system and in the endoderm derivatives as liver and pancreas. In the pancreas it was described in early progenitor cells, later becoming restricted to the pancreatic acinar and ductal cells (Pierreux et al., 2006). In the adult *Xenopus* tissue, XHNF6 transcripts were identified in the liver, brain and pancreas while in mouse transcripts were in addition found in the testis and spleen (Lemaigre et al., 1996). In accordance with its early endodermal expression, gene knockout studies in mice have shown that HNF6 played an important role in liver and biliary duct formation (Clotman et al., 2005), as well as in pancreas organogenesis (Poll et al., 2006). During pancreas formation it was in particular described as direct regulator of Pdx1 and Ngn3 expression (Maestro et al., 2003).

In an attempt to characterise the function of XHNF6 during pancreas development the protein was panendodermal expressed by HNF6 capRNA injection. HNF6 overexpression caused an enlargement of the pancreatic territory as it was depicted upon Xp48 expression. In addition, at later stage 43 the pancreatic lobe was not only increase but additionally expanded into an anterior region. Extended trypsin positive domain resembled the enlargement of the pancreatic domain that was observed upon ectopic activation of Xp48 (Afelik et al., 2006). As clearly evident in that study, p48 induced enlargement of the pancreas was restricted to the endogenous XIHbox8 positive region within stomach and duodenum, proving that a combined activation of XIHbox8 and p48 is required for pancreas specification in the gut tube. Assuming that HNF6 is an upstream regulator of Xp48, its ectopic activation would cause a comparable cell fate conversion of stomach into pancreas. As seen in the Xp48 expression of an HNF6 induced stage 39 embryo, it appeared that in particular the ventral Xp48 expression domain was extended. As the pancreatic lobes are fused at stage 43, it is difficult to judge about the origin of the ectopic tissue, although from the position of the extending tissue it also appeared to derive from the ventral pancreatic lobe. So far HNF6 would be the first identified transcription factor that is required selectively for the specification of the ventral pancreas. In addition it would be the first upstream regulator of Xp48 described in *Xenopus*. However, these overexpression data are still very preliminary and further gain- and loss of function experiments have to be performed to confirm and specify HNF6 function during pancreas development in *Xenopus laevis*.

4.5 Malectin, a novel ER resident protein in *Xenopus laevis*

The descriptive analysis of developmental defects during embryogenesis depends on a suitable set of genetic markers. One criteria for a suitable marker is a spatial and temporal defined expression in order to distinguish specific cell subgroups from the surrounding tissue.

Many tissue specific markers were already identified in context of pancreas organogenesis (Chen et al., 2003; Afelik et al., 2004; Zorn and Mason, 2001) but the increase in detailed knowledge about cell specification and differentiation processes demands for new and more specific genetic markers.

In an attempt to identify new pancreas specific marker genes a cDNA library screen was performed of an adult pancreas cDNA library from *Xenopus laevis* using the WMISH technique (Afelik et al., 2004). Among others, the clone named “p150” showed pancreatic ex-

pression and in addition a highly conserved amino acid sequence in vertebrates. Together these findings rised the interest to further exploit embryonic expression of p150 and to determine its potential function during pancreas organogenesis. By the time of first experimental investigation p150 was an unknown gene product- a white spot on the protein map. Hence p150 characterisation was approached in two ways: (1) by characterisation of its biochemical properties and (2) by analysing its expression and function during pancreas development. **The first aspect was intensively investigated by the group of Claudia Muhle- Goll (EMBL, Heidelberg) that collaborated by solving p150 protein structure and renaming it “malectin”, according to its strong binding to the dissacharide maltose (Schallus et al., 2008).** The second aspect concerned the functional relevance of malectin during pancreas development. In this context, pancreatic expression of malectin was completed by generation of a detailed expression profile during *Xenopus laevis* organogenesis (figure 3.3.2). Against expectations of an pancreas specific gene activation, the detailed expression analysis revealed a constant and ubiquitous presence of malectin in the embryo. Although it was expressed in different germ layer derivatives, it was still noteworthy that malectin was expressed especially in secreting tissues as the hatching gland, liver and pancreas. As described in Medaka (Yamamoto T, 1975) the hatching gland is a endodermal derived organ that synthesises an enzyme called chorionase. Chorionase is required to digest the vitellin membrane during hatching phase, releasing the embryo into the medium. Also the pancreas is an endodermal derived organ that is highly active in secretion by synthesising digestive enzymes and educing them into the gastrointestinal tract.

Broad malectin expression was persistent in adult tissues (figure 3.3.2; tissue nothern blot: <http://www.kazusa.or.jp/huge/gfimage/northern/html/KIAA0152.html>). This broad expression pattern implied an early general role during embryogenesis rather than a later specific function during pancreas organogenesis. On the background, that the major signalling pathways during embryogenesis often play different roles depending on time and location of their activation, and concerning that most of these signalling pathways are remarkably conserved troughout animal kingdom, it was still intriguing to exploit malectins role during *Xenopus laevis* embryogenesis. In this respect, malectin also showed a remarkable high conservation among vertebrate, as also seen for the major signalling molecules. Two systems were used in order to specify the intracellular localisation of malectin: detection of a flag- tagged malectin protein in animal cap explants and detection of overexpressed flag-tagged malectin protein in transient transfected eukaryotic cells (figure 3.3.4). Here, malectin protein was detected in small, partially elongated aggregates where it accumulated upon time. After 48 hr, malectin positive region was encompassing a large territory. This could be due to membrane clustering that might be induced by the high protein content in transfected cells that does not represent regular physiological conditions. The

time course experiment spanning 48 hr did not show malectin translocation to the cell surface but it rather stayed in a perinuclear region, resembling the position of the trans-golgi network (Simpson et al., 2006). Although a detailed analysis by codetection of different organ specific proteins was not performed, the shape of the tubular system and partial malectin colocalisation with the ER resident protein Hsp47 (Tasab et al., 2000) provided strong evidence for a ER localisation of malectin (Schallus et al., 2008).

The expression profile of malectin indicated an early and broad distribution of malectin protein during embryogenesis. It was therefore suggested that malectin played a more general rather than a specific regulatory role during embryogenesis that would concern in context of this study the formation of the pancreas. At late tadpole stages malectin transcription was spatially restricted to the pancreatic lobes (figure 3.4.2) and the adjacent liver whereas surrounding tissues as stomach and duodenum as well as intestine were devoid of malectin transcripts. In respect to the underlying idea of this study, it was still interesting to know whether malectin might affect organ formation.

Functional characterisation of malectin protein was approached by loss and gain of function assays targeting the endoderm. For loss of function, malectin protein translation was downregulated in the whole embryo by morpholino injection. For the gain of function approach malectin protein was ectopically expressed in the whole endoderm. To target the later prospective endoderm morpholino was injected into the vegetal pole of the embryo thereby causing protein depletion by the onset of expression in the pancreas and liver. From the temporal expression profile that determined on RNA and protein level, it was known that malectin was already present in the embryo by the timepoint of injection. Together with its ubiquitous transcript distribution it was suggested that malectin exerts a general role during embryonic development. In both cases misexpression of malectin induced strong endodermal malformation associated with embryonic malformations and reduction in organ specific marker gene expression (figure 3.3.7). Although it appeared that malectin interfered with organ formation, these experiments did not further clarify how or when malectin was responsible to induce pleiotropic phenotype. As malectin was ubiquitously expressed in space and time it was most likely that malectin played a secondary role and interfered with late organogenesis by inhibitory events in proliferation or by inducing apoptosis or necrosis of the malectin expressing tissue.

This hypothesis additionally supported by the fact, that structural and biochemical analysis of malectin proposed that the ER resident protein was involved in the N-glycosylation pathway (Schallus et al., 2008). NMR analysis revealed a novel lectin-like domain that specifically interacted with glucose-polymers. In the cell, the only glucose polymers exist

in the ER, namely nigerose and kojibiose. These two di-glucose residues are the substrate of the two ER resident enzymes glucosidase I and glucosidase II which are responsible for the synthesis of the glucose-precursor molecule (Essentials in Glycobiology, 1999).

A role in regulation of N-glycosylation of secreted proteins links malectin to signalling molecules (BMP-1; Garrigue-Antar et al., 2002) and cell surface receptors. Signalling molecules are essential for germ layer formation, among them BMP4 that regulates endoderm and induces mesoderm and is as consequence essential for axis formation (anterior-posterior axis (AP) and dorso-ventral axis (DV)). BMP4, a member of the transforming growth factor β (TGF β) -superfamily, is synthesised as large precursor protein that undergoes proteolytic maturation and N-glycosylation along the secretory pathway.

Assuming that malectin indeed maintains a regulative role in the N-glycosylation pathway and it is expressed from early stage onwards, its misexpression in the early embryo, either by overexpression or inhibition, should affect early embryogenesis already during germ-layer formation. However, inhibition of protein translation by antisense morpholino injection might be silenced as the protein is already present in the unfertilized embryo. During later organogenesis, malectin morpholino might be effective as it targets regions of high transcription.

Recently a similar function for glycosylation mechanism that regulate TGF- β signalling during embryogenesis was identified in the regulation for the O-glycosylation pathway (Herr et al., 2008). This study revealed an important role of a N-acetylgalactosaminyl-transferase in the regulation of TGF-beta signalling. This novel regulatory mechanism is evolutionarily conserved and, thus, might provide a new paradigm for the regulation of TGF-beta signalling in vertebrates. In this regard, future investigations are intriguing to elucidate the role of malectin for signalling pathway regulation.

5 Abbreviations

(v/v)	percent per volume	HEPES	4-(2-Hydroxyethyl)-1-piperazin
(w/v)	percent per weight	kb	kilobasepair
μL	mikroliter	kD	Kilodaltona
α	anti	IPTG	Isopropylthiogalactosid
amp	ampicillin	incl.	including
AP	alkali phosphatase	l	litre
APB	alkaline phosphate buffer	LB	Luria broth base Medium
APS	ammoniumpersulfate	LOF	loss of function
dH ₂ O	bidestilled water	lacZ	β-galactosidase gene
aa	amino acid	M	Molar
bp	basepair	mA	Milliampere
BCIP	5-bromo-4-chloro-3-indolyl-phosphate	MAB	maleic acid buffer
BMB	Boehringer Mannheim Block	max.	maximal
BMS453	bristol meyers squib	MEM	MOPS-EGTA-MgSO ₄ buffer
BSA	bovine serum albumine	MEMFA	+ 1% formaldehyde
°C	degree celcius	MetOH	methanol
cDNA	complementary DNA	mg	milligramm
CHAPS	3-[(3-Cholamidopropyl) dime-thylammonio-]1-propansulphate	min	minute
DBD	DNA binding domain	ml	milliliter
DEPC	diethylpyrocarbonate	mM	millimolar
DIG-UTP	digoxigenin 11-2'-deoxyuridin-5'-triphosphate	μg	micro gram
DMSO	Dimethylsulfoxid	μl	microliter
DNA	desoxiribonucleicacid	MODY	maturity onset diabetes of the young
DTT	1,4-Dithiotreitoll	MOPS	4- Morpholinopropansulfonic acid
dNTP	desoxyribonucleotides	mRNA	messenger ribonucleic acidsäure
<i>E. coli</i>	<i>Escherichia Coli</i>	MuLV	murine leukemia Virus
EDTA	Ethylen-diamin-tetra acetat	nm	nanometer
EGTA	Ethylen-glycol-bis-tetra acetat	OD	optical density
est	expressed sequence tag	oN	over night
ER	Endoplasmic reticulum	ORF	open reading frame
et al.,	et alter	PAGE	polyacrylamid gelectrophoreses
EtBr	ethidium bromid	PBS	phosphate buffered saline
EtOH	ethanol	PCR	polymerase chain reaction
FCS	fetal calv serum	pH	prepondirance of hydrogen ions
g	gramm	PMSF	phenylmethylsulfonylfluorid
Gal	galactosidase	PP	pancreatic polypeptide
GOF	gain of function	PTU	N-phenylthiourea
bHLH	basic helix-loop-helix	RA	retinoic acid
hr	hour	rpm	rounds per minute

Abbreviations

RT-PCR	reverse transcription polymerase chain reaction	UV	ultraviolet light
RT	room temperature	V	Volt
s	second	W	Watt
SDS	sodiumdodecylsulfat	× g	
SSC	sodiumchlorid/ sodiumcitrate	X- gal	5-Bromo-4-chloro-3-indolyl-D-galactopyranosid
Taq	<i>Thermus aquaticus</i>	∞	forever
TAE	Tris acetat EDTA		

6 Bibliography

Afelik S., Chen Y., Pieler T. (2006)

Combined ectopic expression of Pdx1 and Ptf1a/p48 results in the stable conversion of posterior endoderm into endocrine and exocrine pancreatic tissue., *Genes Dev.* 1;20(11):1441-6.

Afelik S., Chen Y., Pieler T. (2004)

Pancreatic protein disulfide isomerase (XPDIp) is an early marker for the exocrine lineage of the developing pancreas in *Xenopus laevis* embryos., *Gene Expr Patterns.* 4(1):71-6.

Afouda B.A., Ciau-Uitz A., Patient R. (2005)

GATA4, 5 and 6 mediate TGFbeta maintenance of endodermal gene expression in *Xenopus* embryos., *Development.* 132(4):763-74.

Altschul, S.F., Madden, T.L., Schaffer, A.A., Zhang, J., Zhang, Z., Miller, W., and Lipman, D.J. (1997) Gapped BLAST and PSI-BLAST: A new generation of protein database search programs., *Nucleic Acids Res.* 25: 3389-3402.

Apelqvist A., Li H., Sommer L., Beatus P., Anderson D.J., Honjo T., Hrabe de Angelis M., Lendahl U., Edlund H. (1999)

Notch signalling controls pancreatic cell differentiation., *Nature.* 26;400(6747):877-81.

Bach I., Mattei M.G., Cereghini S., Yaniv M. (1991)

Two members of an HNF1 homeoprotein family are expressed in human liver., *Nucleic Acids Res.* 11;19(13):3553-9.

Bach I., Yaniv M. (1993)

More potent transcriptional activators or a transdominant inhibitor of the HNF1 homeoprotein family are generated by alternative RNA processing., *EMBO J.* 12(11):4229-42.

- Barbacci E., Reber M., Ott M.O., Breillat C., Huetz F., Cereghini S. (1999)
Variant hepatocyte nuclear factor 1 is required for visceral endoderm specification., *Development*. 126(21):4795-805.
- Bier E., Vaessin H., Shepherd S., Lee K., McCall K., Barbel S., Ackerman L., Carretto R., Uemura T., Grell E., (1989)
Searching for pattern and mutation in the *Drosophila* genome with a P-lacZ vector. *Genes Dev*; 3(9):1273-87.
- Blitz I.L., Andelfinger G., Horb M.E. (2006)
Germ layers to organs: using *Xenopus* to study “later” development., *Semin Cell Dev Biol*. 17(1):133-45. Epub 6. Review.
- Blochlinger K., Bodmer R., Jack J., Jan L.Y. and Jan Y.N. (1988)
Primary structure and expression of a product from cut, a locus involved in specifying sensory organ identity in *Drosophila*. *Nature* 333: 629–635.
- Bohn S., Thomas H., Turan G., Ellard S., Bingham C., Hattersley A.T., Ryffel G.U. (2003)
Distinct molecular and morphogenetic properties of mutations in the human HNF1beta gene that lead to defective kidney development., *J Am Soc Nephrol*. 14(8):2033-41.
- Bort R., Martinez-Barbera J.P., Beddington R.S., Zaret K.S. (2004)
Hex homeobox gene-dependent tissue positioning is required for organogenesis of the ventral pancreas., *Development*. 131(4):797-806.
- Bouwmeester T., Kim S., Sasai Y., Lu B., De Robertis E.M. (1996)
Cerberus is a head-inducing secreted factor expressed in the anterior endoderm of Spemann’s organizer., *Nature*. 15;382(6592):595-601.
- Bradley L.C., Snape A., Bhatt S., Wilkinson D.G. (1993)
The structure and expression of the *Xenopus* Krox-20 gene: conserved and divergent patterns of expression in rhombomeres and neural crest. *Mech Dev*. 40(1-2):73-84.
- Bullock W.O., Fernandez J.M., Stuart J.M. (1987)
XL1-Blue: a high efficiency plasmid transforming *Escherichia coli* strain with beta-galactosidase selection. *Biotechniques* 5: 376-379.

- Burlison J.S., Long Q., Fujitani Y., Wright C.V., Magnuson M.A. (2008)
Pdx-1 and Ptf1a concurrently determine fate specification of pancreatic multipotent progenitor cells., *Dev Biol.* 1;316(1):74-86.
- Cartry J., Nichane M., Ribes V., Colas A., Riou J.F., Pieler T., Dollé P., Bellefroid E.J., Umbhauer M. (2006)
Retinoic acid signalling is required for specification of pronephric cell fate., *Dev Biol.* 1;299(1): 35-51.
- Cereghini S, Blumenfeld M, Yaniv M. (1988)
A liver-specific factor essential for albumin transcription differs between differentiated and dedifferentiated rat hepatoma cells. *Genes Dev.*; 2(8):957-74.
- Cereghini S. (1996)
Liver-enriched transcription factors and hepatocyte differentiation., *FASEB J.* 10(2):267-82.
- Chalmers A.D., Slack J.M. (2000)
The *Xenopus* tadpole gut: fate maps and morphogenetic movements., *Development.* 127(2):381-92.
- Chen L., Yan H.X., Chen J., Yang W., Liu Q., Zhai B., Cao H.F., Liu S.Q., Wu M.C., Wang H.Y. (2007)
Negative regulation of c-Myc transcription by pancreas duodenum homeobox-1., *Endocrinology.* 148(5):2168-80.
- Chen Y., Pan F.C., Brandes N., Afelik S., Sölter M., Pieler T. (2004)
Retinoic acid signaling is essential for pancreas development and promotes endocrine at the expense of exocrine cell differentiation in *Xenopus*., *Dev Biol.* 1;271(1):144-60.
- Chen Y., Pollet N., Niehrs C., Pieler T. (2001)
Increased XRALDH2 activity has a posteriorizing effect on the central nervous system of *Xenopus* embryos., *Mech Dev.* 101(1-2):91-103.
- Chomczynski P., Sacchi N. (1987)
Single-step method of RNA isolation by acid guanidinium thiocyanate-phenol-chloroform extraction. *Analyt Biochem.* 162, 156–159.
- Clotman F., Jacquemin P., Plumb-Rudewicz N., Pierreux C.E., Van der Smissen P., Dietz H.C., Courtoy P.J., Rousseau G.G., Lemaigre F.P. (2005)
Control of liver cell fate decision by a gradient of TGF beta signaling modulated by Onecut transcription factors; *Genes Dev.* 15;19 (16):1849-54.

Clotman F., Lannoy V.J., Reber M., Cereghini S., Cassiman D., Jacquemin P., Roskams T., Rousseau G.G., Lemaigre F.P. (2002)

The onecut transcription factor HNF6 is required for normal development of the biliary tract., *Development*. 129(8):1819-28.

Coffinier C., Gresh L., Fiette L., Tronche F., Schütz G., Babinet C., Pontoglio M., Yaniv M. and Barra J. (2002)

Bile system morphogenesis defects and liver dysfunction upon targeted deletion of hnf1beta., *Development* 129: 1829–1838.

Collart C., Verschuere K., Rana A., Smith J.C., Huylebroeck D. (2005)

The novel Smad-interacting protein Smic1 regulates Chordin expression in the *Xenopus* embryo., *Development*. 132(20):4575-86.

Copeman J.B., Cucca F., Hearne C.M., Cornall R.J., Reed P.W., Rønningen K.S. (1995)

Linkage, disequilibrium mapping of a type 1 susceptibility gene (IDDM7) to chromosome 2q31-q33. *Nature Genet*. 9: 80–85.

D'Amour K.A., Bang A.G., Eliazar S., Kelly O.G., Agulnick A.D., Smart N.G., Moorman M.A., Kroon E., Carpenter M.K., Baetge E.E. (2006)

Production of pancreatic hormone-expressing endocrine cells from human embryonic stem cells., *Nat Biotechnol*. 24(11):1392-401.

De Simone V., De Magistris L., Lazzaro D., Gerstner J., Monaci P., Nicosia A. and Cortese R. (1991)

LFB3, a heterodimer-forming homeoprotein of the LFB1 family, is expressed in specialized epithelia. *EMBO J*. 10: 1435–1443.

Demartis A., Maffei M., Vignali R., Barsacchi G., De Simone V. (1994)

Cloning and developmental expression of LFB3/HNF1 beta transcription factor in *Xenopus laevis*., *Mech Dev*. 47(1):19-28.

Deutsch G., Jung J., Zheng M., Lóra J., Zaret K.S. (2001)

A bipotential precursor population for pancreas and liver within the embryonic endoderm., *Development*. 128(6):871-81.

Dullin J.P., Locker M., Robach M., Henningfeld K.A., Parain K., Afelik S., Pieler T., Perron M. (2007)

Ptf1a triggers GABAergic neuronal cell fates in the retina., *BMC Dev Biol.* 2;7:110.

Edlund H. (2002)

Pancreatic organogenesis--developmental mechanisms and implications for therapy., *Nat Rev Genet.* 3(7):524-32.

Eisen J.S., Smith J.C. (2008)

Controlling morpholino experiments: don't stop making antisense., *Development.* 135(10):1735-43.

Fajans S.S., Bell G.I., Polonsky K.S. (2001)

Molecular mechanisms and clinical pathophysiology of maturity-onset diabetes of the young., *N Engl J Med.* 27;345(13):971-80.

Finney M. (1990)

The homeodomain of the transcription factor LF-B1 has a 21 amino acid loop between helix 2 and helix 3., *Cell.* 12;60(1):5-6.

Frayling T.M., Evans J.C., Bulman M.P., Pearson E., Allen L., Owen K., Bingham C., Hannemann M., Shepherd M., Ellard S., Hattersley A.T. (2001)

beta-cell genes and diabetes: molecular and clinical characterization of mutations in transcription factors. *Diabetes.* 50 Suppl 1:S94-100.

Fukuda A., Kawaguchi Y., Furuyama K., Kodama S., Horiguchi M., Kuhara T., Koizumi M., Boyer D.F., Fujimoto K., Doi R., Kageyama R., Wright C.V., Chiba T. (2006)

Ectopic pancreas formation in Hes1 -knockout mice reveals plasticity of endodermal progenitors of the gut, bile duct, and pancreas. *J Clin Invest.* 116(6):1484-93.

Gamer L.W., Wright C.V. (1995)

Autonomous endodermal determination in *Xenopus*: regulation of expression of the pancreatic gene *XIHbox 8*. *Dev Biol.* 171(1):240-51.

Gammill L.S., Sive H. (1997)

Identification of *otx2* target genes and restrictions in ectodermal competence during *Xenopus* cement gland formation., *Development.* 124(2):471-81.

Gannon M., Ables E.T., Crawford L., Lowe D., Offield M.F., Magnuson M.A., Wright C.V. (2008)
pdx-1 function is specifically required in embryonic beta cells to generate appropriate numbers of endocrine cell types and maintain glucose homeostasis., *Dev Biol.* 15;314(2):406-17.

Garrigue-Antar L., Hartigan N., Kadler K.E. (2002)
Post-translational modification of bone morphogenetic protein-1 is required for secretion and stability of the protein. *J Biol Chem.* 8;277(45):43327-34.

Gerrish K., Cissell M.A., Stein R. (2001)
The role of hepatic nuclear factor 1 alpha and PDX-1 in transcriptional regulation of the pdx-1 gene., *J Biol Chem.* 21;276(51):47775-84.

Ghosh B., Leach S.D. (2006)
Interactions between hairy/enhancer of split-related proteins and the pancreatic transcription factor Ptf1-p48 modulate function of the PTF1 transcriptional complex., *Biochem J.* 1;393(Pt 3):679-85.

Gradwohl G., Dierich A., LeMeur M., Guillemot F. (2000)
neurogenin3 is required for the development of the four endocrine cell lineages of the pancreas., *Proc Natl Acad Sci U S A.* 15;97(4):1607-11.

Grapin-Botton A., Majithia A.R., Melton D.A. (2001)
Key events of pancreas formation are triggered in gut endoderm by ectopic expression of pancreatic regulatory genes., *Genes Dev.* 15;15(4):444-54.

Gu G., Dubauskaite J., Melton D.A. (2002)
Direct evidence for the pancreatic lineage: NGN3+ cells are islet progenitors and are distinct from duct progenitors., *Development* 129(10):2447-57.

Hald J., Hjorth J.P., German M.S., Madsen O.D., Serup P., Jensen J. (2003)
Activated Notch1 prevents differentiation of pancreatic acinar cells and attenuate endocrine development., *Dev Biol.* 15;260(2):426-37.

Hale M.A., Kagami H., Shi L., Holland A.M., Elsasser H.P., Hammer R.E., MacDonald R.J. (2005)
The homeodomain protein PDX1 is required at mid-pancreatic development for the formation of the exocrine pancreas. *Dev. Biol.* 286: 225–237.

- Hanahan D., Jessee J. and Bloom F.R. (1991)
Plasmid transformation of *Escherichia coli* and other bacteria. In: J. H. Miller, Editor, *Methods in Enzymology*, Academic Press, San Diego: 63–113.
- Harland R. M. (1991)
In situ hybridization: an improved whole-mount method for *Xenopus* embryos. *Methods Cell Biol* 36, 685-95.
- Hart A., Papadopoulou S., Edlund H. (2003)
Fgf10 maintains notch activation, stimulates proliferation, and blocks differentiation of pancreatic epithelial cells. *Dev Dyn*. 228(2):185-93.
- Hart A.W., Baeza N., Apelqvist A., Edlund H. (2000)
Attenuation of FGF signalling in mouse beta-cells leads to diabetes., *Nature*. 14;408(6814):864-8.
- Hattersley A.T., Turner R.C., Permutt M.A., Patel P., Tanizawa Y., Chiu K.C., O’Rahilly S., Watkins P.J., Wainscoat J.S. (1992)
Linkage of type 2 diabetes to the glucokinase gene., *Lancet*. 30;339(8805):1307-10.
- Haumaitre C., Barbacci E., Jenny M., Ott M.O., Gradwohl G., Cereghini S. (2005)
Lack of TCF2/vHNF1 in mice leads to pancreas agenesis., *Proc Natl Acad Sci USA*. 1;102(5):1490-5.
- Hebrok M., Kim S.K., Melton D.A. (1998)
Notochord repression of endodermal Sonic hedgehog permits pancreas development., *Genes Dev*. 1;12(11):1705-13.
- Henry G.L., Melton D.A. (1998)
Mixer, a homeobox gene required for endoderm development., *Science*. 3;281(5373):91-6.
- Henry G. L., Brivanlou I. H., Kessler D. S., Hemmati-Brivanlou A. and Melton D. A (1996).
TGF-signals and a prepattern in *Xenopus laevis* endodermal development. *Development* 122, 1007-1015.
- Hernandez R.E., Rikhof H.A., Bachmann R., Moens C.B. (2004)
vhnf1 integrates global RA patterning and local FGF signals to direct posterior hindbrain development in zebrafish. *Development*. 131(18):4511-20.

- Herr P., Korniychuk G., Yamamoto Y., Grubisic K., Oelgeschläger M. (2008)
Regulation of TGF-(beta) signalling by N-acetylgalactosaminyltransferase-like 1. *Development*. 135(10):1813-22.
- Holland A.M., Góñez L.J., Naselli G., Macdonald R.J., Harrison L.C. (2005)
Conditional expression demonstrates the role of the homeodomain transcription factor Pdx1 in maintenance and regeneration of beta-cells in the adult pancreas. *Diabetes*. 54(9):2586-95.
- Hollemann T., Chen Y., Grunz H., Pieler T. (1998)
Regionalized metabolic activity establishes boundaries of retinoic acid signalling., *EMBO J*. 15;17(24):7361-72.
- Hollemann T., Schuh R., Pieler T., Stick R. (1996)
Xenopus Xsal-1, a vertebrate homolog of the region specific homeotic gene spalt of Drosophila. *Mech Dev*. 55(1):19-32.
- Hollemann, T., Panitz, F., Pieler, T. (1999)
In situ hybridisation techniques with Xenopus laevis embryos. In: Richter, J.D. (Ed.), *A Comparative Methods Approach to the Study of Oocytes and Embryos*. Oxford Univ. Press, New York, 279-290.
- Hong S.K., Kim C.H., Yoo K.W., Kim H.S., Kudoh T., Dawid I.B., Huh T.L. (2002)
Isolation and expression of a novel neuron-specific onecut homeobox gene in zebrafish. *Mech Dev*. 112 (1-2):199-202.
- Horb M.E., Shen C.N., Tosh D., Slack J.M. (2003)
Experimental conversion of liver to pancreas. *Curr Biol*. 21;13(2):105-15.
- Horb M.E., Slack J.M. (2001)
Endoderm specification and differentiation in Xenopus embryos. *Dev Biol*. 15;236(2):330-43.
- Horb M.E., Slack J.M. (2002)
Expression of amylase and other pancreatic genes in Xenopus. *Mech Dev*. 113(2):153-7.
- Horikawa Y., Iwasaki N., Hara M., Furuta H., Hinokio Y., Cockburn B.N., Lindner T., Yamagata K., Ogata M., Tomonaga O., Kuroki H., Kasahara T., Iwamoto Y., Bell G.I. (1997)
Mutation in hepatocyte nuclear factor-1 beta gene (TCF2) associated with MODY. *Nat Genet*. 17(4):384-5.

Jacquemin P., Durviaux S.M., Jensen J., Godfraind C., Gradwohl G., Guillemot F., Madsen O.D., Carmeliet P., Dewerchin M., Collen D., Rousseau G.G., Lemaigre F.P. (2000)

Transcription factor hepatocyte nuclear factor 6 regulates pancreatic endocrine cell differentiation and controls expression of the proendocrine gene *ngn3*, *Mol Cell Biol.* 20 (12):4445-54.

Jacquemin P., Lannoy V.J., Rousseau G.G., Lemaigre F.P. (1999)

OC-2, a novel mammalian member of the ONECUT class of homeodomain transcription factors whose function in liver partially overlaps with that of hepatocyte nuclear factor-6., *J Biol Chem.* 274(5):2665-71.

Jacquemin P., Lemaigre F.P., Rousseau G.G. (2003)

The Onecut transcription factor HNF-6 (OC-1) is required for timely specification of the pancreas and acts upstream of Pdx-1 in the specification cascade., *Dev Biol.* 1;258(1):105-16.

Jacquemin P., Yoshitomi H., Kashima Y., Rousseau G.G., Lemaigre F.P., Zaret K.S. (2006)

An endothelial-mesenchymal relay pathway regulates early phases of pancreas development., *Dev Biol.* 1;290(1):189-99.

Jarikji Z.H., Vanamala S., Beck C.W., Wright C.V., Leach S.D., Horb M.E. (2007)

Differential ability of Ptf1a and Ptf1a-VP16 to convert stomach, duodenum and liver to pancreas., *Dev Biol.* 15;304(2):786-99.

Jensen J., Pedersen E.E., Galante P., Hald J., Heller R.S., Ishibashi M., Kageyama R., Guillemot F., Serup P., Madsen O.D. (2000)

Control of endodermal endocrine development by *Hes-1*, *Nat Genet.* 24(1):36-44.

Jones C.M., Kuehn M.R., Hogan B.L., Smith J.C., Wright C.V. (1995)

Nodal-related signals induce axial mesoderm and dorsalize mesoderm during gastrulation., *Development.* 121(11):3651-62.

Jonsson J., Ahlgren U., Edlund T., Edlund H. (1995)

IPF1, a homeodomain protein with a dual function in pancreas development., *Int J Dev Biol.* 39(5):789-98.

Jonsson J., Carlsson L., Edlund T., Edlund H. (1994)

Insulin-promoter-factor 1 is required for pancreas development in mice., *Nature.* 13;371(6498):606-9.

- Kawaguchi Y., Cooper B., Gannon M., Ray M., MacDonald R.J., Wright C.V. (2002)
The role of the transcriptional regulator Ptf1a in converting intestinal to pancreatic progenitors.,
Nat Genet. 32(1):128-34.
- Kelly O.G., Melton D.A. (2000)
Development of the pancreas in *Xenopus laevis*., *Dev Dyn.* 218(4):615-27.
- Kim S.K., Hebrok M., Melton D.A. (1997)
Notochord to endoderm signaling is required for pancreas development., *Development.*
124(21):4243-52.
- Kissinger C.R., Liu B.S. Martin-Blanco E., Kornberg T.B. and Pabo C.O. (1990)
Crystal structure of an engrailed homeodomain-DNA complex at 2.8 Å resolution: a framework for
understanding homeodomain-DNA interactions. *Cell* 63: 579–590.
- Krapp A., Knöfler M., Ledermann B., Bürki K., Berney C., Zoerkler N., Hagenbüchle O., Wellauer
P.K. (1998)
The bHLH protein PTF1-p48 is essential for the formation of the exocrine and the correct spatial
organization of the endocrine pancreas., *Genes Dev.* 1;12(23):3752-63.
- Kroon E., Martinson L.A., Kadoya K., Bang A.G., Kelly O.G., Eliazar S., Young H., Richardson M.,
Smart N.G., Cunningham J., Agulnick A.D., D'Amour K.A., Carpenter M.K., Baetge E.E. (2008)
Pancreatic endoderm derived from human embryonic stem cells generates glucose-responsive in-
sulin-secreting cells in vivo., *Nat Biotechnol.* 26(4):443-52.
- Kyhse-Andersen J. (1984)
Electroblotting of multiple gels: a simple apparatus without buffer tank for rapid transfer of proteins
from polyacrylamide to nitrocellulose., *J Biochem Biophys Methods.* 10(3-4):203-9.
- Laemmli UK. (1970)
Cleavage of structural proteins during the assembly of the head of bacteriophage T4. *Nature.* Aug
15;227(5259):680-5.
- Lammert E., Cleaver O., Melton D. (2001)
Induction of pancreatic differentiation by signals from blood vessels., *Science.* 19;294(5542):564-7.

- Landry C., Clotman F., Hioki T., Oda H., Picard J.J., Lemaigre F.P., Rousseau G.G. (1997)
HNF-6 is expressed in endoderm derivatives and nervous system of the mouse embryo and participates to the cross-regulatory network of liver-enriched transcription factors; *Dev Biol.* 15;192 (2):247-57.
- Lemaigre F.P., Durviaux S.M., Truong O., Lannoy V.J., Hsuan J.J., Rousseau G.G. (1999)
Hepatocyte nuclear factor 6, a transcription factor that contains a novel type of homeodomain and a single cut domain; *Proc Natl Acad Sci USA.* 3;93(18):9460-4.
- Lin J.W., Biankin A.V., Horb M.E., Ghosh B., Prasad N.B., Yee N.S., Pack M.A., Leach S.D. (2004)
Differential requirement for *ptf1a* in endocrine and exocrine lineages of developing zebrafish pancreas.; *Dev Biol.* 15;274(2):491-503.
- Lokmane L., Haumaitre C., Garcia-Villalba P., Anselme I., Schneider-Maunoury S., Cereghini S. (2008)
Crucial role of vHNF1 in vertebrate hepatic specification.; *Development.* 135(16):2777-86.
- Ma J., Chen M., Wang J., Xia H.H., Zhu S., Liang Y., Gu Q., Qiao L., Dai Y., Zou B., Li Z., Zhang Y., Lan H. Wong B.C. (2008)
Pancreatic duodenal homeobox-1 (PDX1) functions as a tumor suppressor in gastric cancer, *Carcinogenesis.* 29(7):1327-33.
- Maden M. (2001)
Role and distribution of retinoic acid during CNS development.; *Int Rev Cytol.* 209:1-77.
- Maestro M.A., Boj S.F., Luco R.F., Pierreux C.E., Cabedo J., Servitja J.M., German M.S., Rousseau G.G., Lemaigre F.P., Ferrer J. (2003)
Hnf6 and Tcf2 (MODY5) are linked in a gene network operating in a precursor cell domain of the embryonic pancreas.; *Hum Mol Genet.* 15;12(24):3307-14.
- Marlétaz F., Holland L.Z., Laudet V., Schubert M. (2006)
Retinoic acid signaling and the evolution of chordates. *Int J Biol Sci.* 2(2):38-47.
- Martín M., Gallego-Llamas J., Ribes V., Kedinger M., Niederreither K., Chambon P., Dollé P., Gradwohl G. (2005)
Dorsal pancreas agenesis in retinoic acid-deficient *Raldh2* mutant mice.; *Dev Biol.* 15;284(2):399-411.

- Masui T., Long Q., Beres T.M., Magnuson M.A., MacDonald R.J. (2007)
Early pancreatic development requires the vertebrate Suppressor of Hairless (RBPJ) in the PTF1 bHLH complex., *Genes Dev.* 15;21(20):2629-43.
- Matt N., Ghyselinck N.B., Wendling O., Chambon P., Mark M. (2003)
Retinoic acid-induced developmental defects are mediated by RAR β /RXR heterodimers in the pharyngeal endoderm., *Development.* 130:2083-2093
- McLin V.A., Rankin S.A., Zorn A.M. (2007)
Repression of Wnt/beta-catenin signaling in the anterior endoderm is essential for liver and pancreas development., *Development.* 134(12):2207-17.
- Melton D.A., Krieg P.A., Rebagliati M.R., Maniatis T., Zinn K., Green, M.R. (1984)
Efficient in vitro synthesis of biologically active RNA and RNA hybridization probes from plasmids containing a bacteriophage SP6 promoter. *Nucl Acids Res*, 12, 7035–7056.
- Molotkov A., Molotkova N., Duyster G. (2005)
Retinoic acid generated by Raldh2 in mesoderm is required for mouse dorsal endodermal pancreas development., *Dev Dyn.* 232(4):950-7.
- Mullis K.B. and Faloona F.A. (1987)
Specific Synthesis of DNA in vitro via a Polymerase-Catalyzed Chain Reaction. *Methods in Enzymology* vol. 155(F): 335-50.
- Murtaugh L.C., Law A.C., Dor Y., Melton D.A. (2005)
Beta-catenin is essential for pancreatic acinar but not islet development., *Development.* 132(21):4663-74.
- Murtaugh L.C., Stanger B.Z., Kwan K.M., Melton D.A. (2003)
Notch signaling controls multiple steps of pancreatic differentiation., *Proc Natl Acad Sci U S A.* 9;100(25):14920-5.
- Murtaugh L.C. (2007)
Pancreas and beta-cell development: from the actual to the possible., *Development.* 134(3):427-38.
- Nakhai H., Siveke J.T., Mendoza-Torres L., Schmid R.M. (2008)
Conditional inactivation of Myc impairs development of the exocrine pancreas., *Development.* 135(19):3191-6.

Nekrep N., Wang J., Miyatsuka T., German M.S. (2008)

Signals from the neural crest regulate beta-cell mass in the pancreas., *Development*. 135(12):2151-60.

Neve B., Fernandez-Zapico M.E., Ashkenazi-Katalan V., Dina C., Hamid Y.H., Joly E., Vaillant E., Benmezroua Y., Durand E., Bakaher N., Delannoy V., Vaxillaire M., Cook T., Dallinga-Thie G.M., Jansen H., Charles M.A., Clément K., Galan P., Hercberg S., Helbecque N., Charpentier G., Prentki M., Hansen T., Pedersen O., Urrutia R., Melloul D., Froguel P. (2005)

Role of transcription factor KLF11 and its diabetes-associated gene variants in pancreatic beta cell function., *Proc Natl Acad Sci USA*. 29;102(13):4807-12.

Newman C.S., Chia F., Krieg P.A. (1997)

The XHex homeobox gene is expressed during development of the vascular endothelium: overexpression leads to an increase in vascular endothelial cell number., *Mech Dev*. 66(1-2):83-93.

Nicosia A., Monaci P., Tomei L., De Francesco R., Nuzzo M., Stunnenberg H., Cortese R. (1990)

A myosin-like dimerization helix and an extra-large homeodomain are essential elements of the tripartite DNA binding structure of LFB1., *Cell*. 29;61(7):1225-36.

Nieuwkoop P.D. and Faber J. (1967)

Normal Table of *Xenopus laevis* (Daudin), North Holland, Amsterdam.

Nikolova G., Jabs N., Konstantinova I., Domogatskaya A., Tryggvason K., Sorokin L., Fässler R., Gu G., Gerber H.P., Ferrara N., Melton D.A., Lammert E. (2006)

The vascular basement membrane: a niche for insulin gene expression and Beta cell proliferation., *Dev Cell*. 10(3):397-405.

Niswander L., Jeffrey S., Martin GR, Tickle C. (1994)

A positive feedback loop coordinates growth and patterning in the vertebrate limb. *Nature*. Oct 13;371(6498):609-12.

Noy N. (2000)

Retinoid-binding proteins: mediators of retinoid action., *Biochem J*. 15;348 Pt 3:481-95.

Offield M.F., Jetton T.L., Labosky P.A., Ray M., Stein R.W., Magnuson M.A., Hogan B.L., Wright C.V. (1996)

PDX-1 is required for pancreatic outgrowth and differentiation of the rostral duodenum., *Development* 122:983-995

- Ohlsson H., Karlsson K., Edlund T. (1993)
IPF1, a homeodomain-containing transactivator of the insulin gene. *EMBO J* 12:4251–4259
- Oliver-Krasinski J.M., Stoffers D.A. (2008)
On the origin of the β - cell., *Genes Dev.* 1;22(15):1998-2021.
- Öström M., Loffler K.A., Edfalk S., Selander L., Dahl U., Ricordi C., Jeon J., Correa-Medina M., Diez J., Edlund H. (2008)
Retinoic acid promotes the generation of pancreatic endocrine progenitor cells and their further differentiation into beta-cells., *PLoS ONE.* 30;3(7):e2841.
- Pan F.C., Chen Y., Bayha E., Pieler T. (2007)
Retinoic acid-mediated patterning of the pre-pancreatic endoderm in *Xenopus* operates via direct and indirect mechanisms., *Mech Dev.* 124(7-8):518-31.
- Pieler T., Chen Y. (2006)
Forgotten and novel aspects in pancreas development., *Biol Cell.* 98(2):79-88. Review.
- Pierreux C.E., Poll A.V., Kemp C.R., Clotman F., Maestro M.A., Cordi S., Ferrer J., Leyns L., Rousseau G.G., Lemaigre F.P. (2006)
The transcription factor hepatocyte nuclear factor-6 controls the development of pancreatic ducts in the mouse; *Gastroenterology.* 130 (2):532-41.
- Poll A.V., Pierreux C.E., Lokmane L., Haumaitre C., Achouri Y., Jacquemin P., Rousseau G.G., Ceregghini S., Lemaigre F.P. (2006)
A vHNF1/TCF2-HNF6 cascade regulates the transcription factor network that controls generation of pancreatic precursor cells; *Diabetes.* 55(1):61-9.
- Pouilhe M., Gilardi-Hebenstreit P., Desmarquet-Trin Dinh C., Charnay P. (2007)
Direct regulation of vHnf1 by retinoic acid signaling and MAF-related factors in the neural tube. *Dev Biol.* 15;309(2):344-57.
- Raeder H., Johansson S., Holm P.I., Haldorsen I.S., Mas E., Sbarra V., Nermoen I., Eide S.A., Grevle L., Bjørkhaug L., Sagen J.V., Aksnes L., Søvik O., Lombardo D., Molven A., Njølstad P.R. (2006)
Mutations in the CEL VNTR cause a syndrome of diabetes and pancreatic exocrine dysfunction., *Nat Genet.* 38(1):54-62.

Rausa F., Samadani U., Ye H., Lim L., Fletcher C.F., Jenkins N.A., Copeland N.G., Costa R.H. 1997
The cut-homeodomain transcriptional activator HNF-6 is coexpressed with its target gene HNF-3
beta in the developing murine liver and pancreas., *Dev Biol.* 15;192(2):228-46.

Reber M., Cereghini S. (2001)

Variant hepatocyte nuclear factor 1 expression in the mouse genital tract., *Mech Dev.* 100(1):75-8.

Rey-Campos J., Chouard T., Yaniv M., Cereghini S. (1991)

vHNF1 is a homeoprotein that activates transcription and forms heterodimers with HNF1., *EMBO
J.* 10(6):1445-57.

Rupp R.A., Snider L., Weintraub H. (1994)

Xenopus embryos regulate the nuclear localization of XMyoD., *Genes Dev.* 1;8(11):1311-23.

Saiki (1988)

Primer-directed enzymatic amplification of DNA with a thermostable DNA polymerase. *Science*
vol. 239:. 487-91.

Sambrook, J., Fritsch, E.F., Maniatis, T. (1989).

Molecular Cloning- A Laboratory Manual. Second Edition, Text Book, ISBN 0-87969-309-6

Sanger F., Nicklen S., and Coulson A. R. (1977)

DNA sequencing with chain-terminating inhibitors. *Proc Natl Acad Sci U S A.*; 74(12):5463-5467

Sasai Y., Lu B., Piccolo S., De Robertis E.M. (1996)

Endoderm induction by the organizer-secreted factors chordin and noggin in Xenopus animal
caps., *EMBO J.*; 2;15(17):4547-55.

Schallus T., Jaekch C., Fehér K., Palma A.S., Liu Y., Simpson J.C., Mackeen M., Stier G., Gibson T.J.,
Feizi T., Pieler T., Muhle-Goll C. (2008)

Malectin: A Novel Carbohydrate-binding Protein of the Endoplasmic Reticulum and a Candidate
Player in the Early Steps of Protein N-Glycosylation. *Mol Biol Cell.*;19(8):3404-3414.

Schlosser G., Northcutt R.G. (2000)

Development of neurogenic placodes in *Xenopus laevis*. *J Comp Neurol.*; 6;418(2):121-46.

Schulze G.E., Clay R.J., Mezza L.E., Bregman C.L., Buroker R.A., Frantz J.D. (2001)

BMS-189453, a novel retinoid receptor antagonist, is a potent testicular toxin.

Toxicol Sci.; 59(2):297-308.

Schwitzgebel V.M., Scheel D.W., Conners J.R., Kalamaras J., Lee J.E., Anderson D.J., Sussel L., Johnson J.D., German M.S. (2000)

Expression of neurogenin3 reveals an islet cell precursor population in the pancreas., *Development*. 127(16):3533-42.

Sellick G.S., Barker K.T., Stolte-Dijkstra I., Fleischmann C., Coleman R.J., Garrett C., Gloyn A.L., Edghill E.L., Hattersley A.T., Wellauer P.K., Goodwin G., Houlston R.S. (2004)

Mutations in PTF1A cause pancreatic and cerebellar agenesis., *Nat Genet*. 36(12):1301-5.

Simpson J.C., Nilsson T., Pepperkok R. (2006)

Biogenesis of tubular ER-to-Golgi transport intermediates., *Mol Biol Cell*. 17(2):723-37.

Song J., Kim H.J., Gong Z., Liu N.A., Lin S. (2007)

Vhnf1 acts downstream of Bmp, Fgf, and RA signals to regulate endocrine beta cell development in zebrafish., *Dev Biol*. 15;303(2):561-75.

Spagnoli F.M., Brivanlou A.H. (2008)

The Gata5 target, TGIF2, defines the pancreatic region by modulating BMP signals within the endoderm., *Development*. 135(3):451-61.

Stafford D., Hornbruch A., Mueller P.R., Prince V.E. (2004)

A conserved role for retinoid signaling in vertebrate pancreas development., *Dev Genes Evol*. 214(9):432-41.

Stafford D., Prince V.E. (2002)

Retinoic acid signaling is required for a critical early step in zebrafish pancreatic development., *Curr Biol*. 23;12(14):1215-20.

Stafford D., White R.J., Kinkel M.D., Linville A., Schilling T.F., Prince V.E. (2006)

Retinoids signal directly to zebrafish endoderm to specify insulin-expressing beta-cells., *Development*. 133(5):949-56.

Stanger B.Z., Tanaka A.J., Melton D.A. (2007)

Organ size is limited by the number of embryonic progenitor cells in the pancreas but not the liver., *Nature*. 22;445(7130):886-91.

- Stoffers D.A., Ferrer J., Clarke W.L., Habener J.F. (1997)
Early-onset type-II diabetes mellitus (MODY4) linked to IPF1., *Nat Genet.* 17(2):138-9.
- Sun Z. and Hopkins N. (2001)
vhnf1, the MODY5 and familial GCKD-associated gene, regulates regional specification of the zebrafish gut, pronephros, and hindbrain, *Genes Dev.* 15: 3217–3229.
- Tasab M., Batten M.R., Bulleid N.J. (2000)
Hsp47: a molecular chaperone that interacts with and stabilizes correctly-folded procollagen., *EMBO J.* 15;19(10):2204-11.
- Tiso N., Filippi A., Pauls S., Bortolussi M., Argenton F. (2002)
BMP signalling regulates anteroposterior endoderm patterning in zebrafish., *Mech Dev.* 118(1-2):29-37.
- Tronche F., Yaniv M. (1992)
HNF1, a homeoprotein member of the hepatic transcription regulatory network., *Bioessays.* 14(9):579-87. Review.
- Tulachan S.S., Doi R., Kawaguchi Y., Tsuji S., Nakajima S., Masui T., Koizumi M., Toyoda E., Mori T., Ito D., Kami K., Fujimoto K., Imamura M (2003)
All-trans retinoic acid induces differentiation of ducts and endocrine cells by mesenchymal/epithelial interactions in embryonic pancreas., *Diabetes.* 52(1):76-84.
- Turner D.L., Weintraub H. (1994)
Expression of achaete-scute homolog 3 in *Xenopus* embryos converts ectodermal cells to a neural fate., *Genes Dev.* 15;8(12):1434-47.
- Vanhorenbeeck V., Jenny M., Cornut J.F., Gradwohl G., Lemaigre F.P., Rousseau G.G., Jacquemin P. (2007)
Role of the Onecut transcription factors in pancreas morphogenesis and in pancreatic and enteric endocrine differentiation., *Dev Biol.* 15;305(2):685-94.
- Varki A., Cummings R., Esko J., Freeze H., Hart G., Marth J. (editors) (1999)
Essentials of Glycobiology, Plainview (NY): Cold Spring Harbor Laboratory Press

- Viczian A.S., Vignali R., Zuber M.E., Barsacchi G., Harris W.A. (2003)
XOtx5b and XOtx2 regulate photoreceptor and bipolar fates in the *Xenopus* retina., *Development*. 130(7):1281-94.
- Vignali R, Poggi L, Madeddu F, Barsacchi G. (2000)
HNF1(beta) is required for mesoderm induction in the *Xenopus* embryo. *Development*;127(7):1455-65.
- Vize P.D., Melton D.A., Hemmati-Brivanlou A., Harland R.M. (1991)
Assays for gene function in developing *Xenopus* embryos., *Methods Cell Biol.* 36:367-87.
- Wang L., Coffinier C., Thomas M.K., Gresh L., Eddu G., Manor T., Levitsky L.L., Yaniv M., Rhoads D.B. (2004)
Selective deletion of the Hnf1beta (MODY5) gene in beta-cells leads to altered gene expression and defective insulin release., *Endocrinology*. 145(8):3941-9.
- Watada H., Kajimoto Y., Miyagawa J., Hanafusa T., Hamaguchi K., Matsuoka T., Yamamoto K., Matsuzawa Y., Kawamori R., Yamasaki Y. (1996)
PDX-1 induces insulin and glucokinase gene expressions in alphaTC1 clone 6 cells in the presence of betacellulin., *Diabetes*. 45(12):1826-31.
- Wiebe P.O., Kormish J.D., Roper V.T., Fujitani Y., Alston N.I., Zaret K.S., Wright C.V., Stein R.W., Gannon M. (2007)
Ptf1a binds to and activates area III, a highly conserved region of the Pdx1 promoter that mediates early pancreas-wide Pdx1 expression., *Mol Cell Biol*. 27(11):4093-104.
- Wright C.V., Schnegelsberg P., De Robertis E.M. (1989)
XIHbox 8: a novel *Xenopus* homeo protein restricted to a narrow band of endoderm. *Development*. 105(4):787-94.
- Wu G, Bohn S, Ryffel GU. (2004)
The HNF1beta transcription factor has several domains involved in nephrogenesis and partially rescues Pax8/lim1-induced kidney malformations. *Eur J Biochem.*;271(18):3715-28.
- Xanthos J.B., Kofron M., Wylie C., Heasman J. (2001)
Maternal VegT is the initiator of a molecular network specifying endoderm in *Xenopus laevis*. *Development*. 128(2):167-80.

Yamagata K., Furuta H., Oda N., Kaisaki P.J., Menzel S., Cox N.J., Fajans S.S., Signorini S., Stoffel M., Bell G.I. (1996)

Mutations in the hepatocyte nuclear factor-4 α gene in maturity-onset diabetes of the young (MODY1). *Nature*. 5;384(6608):458-60.

Yamamoto T. (1975)

Hatching gland and hatching enzyme. *Medaka (killifish): Biology and strains.*, Yamamoto, Tokio (ed.), Keigaku Pub.Co., Tokyo: 73-79.

Yasuo H., Lemaire P. (1999)

A two-step model for the fate determination of presumptive endodermal blastomeres in *Xenopus* embryos. *Curr Biol*. 26;9(16):869-79.

Yee N.S., Yusuff S., Pack M., (2001)

Zebrafish *pdx1* morphant displays defects in pancreas development and digestive organ chirality, and potentially identifies a multipotent pancreas progenitor cell., *Genesis*, 30(3):137-40.

Yoshitomi H., Zaret K.S. (2004)

Endothelial cell interactions initiate dorsal pancreas development by selectively inducing the transcription factor *Ptf1a*., *Development*. 131(4):807-17.

Zaret K.S. (2008)

Genetic programming of liver and pancreas progenitors: lessons for stem-cell differentiation., *Nat Rev Genet*. 9(5):329-40.

Zeynali B., Dixon K.E. (1998)

Effects of retinoic acid on the endoderm in *Xenopus* embryos. *Dev Genes Evol* 208:318–326

Zhang J., Houston D.W., King M.L., Payne C., Wylie C., Heasman J. (1998)

The role of maternal *VegT* in establishing the primary germ layers in *Xenopus* embryos., *Cell*. 21;94(4):515-24.

Zhou Q, Brown J, Kanarek A, Rajagopal J, Melton DA.(2008)

In vivo reprogramming of adult pancreatic exocrine cells to beta-cells. *Nature*. 27. Epub ahead of print

Zorn A.M., Butler K., Gurdon J.B. (1999)

Anterior endomesoderm specification in *Xenopus* by Wnt/beta-catenin and TGF-beta signalling pathways. *Dev Biol.* 15;209(2):282-97.

Zorn A.M., Mason J. (2001)

Gene expression in the embryonic *Xenopus* liver. *Mech Dev.* 103(1-2):153-7.

7 Appendix

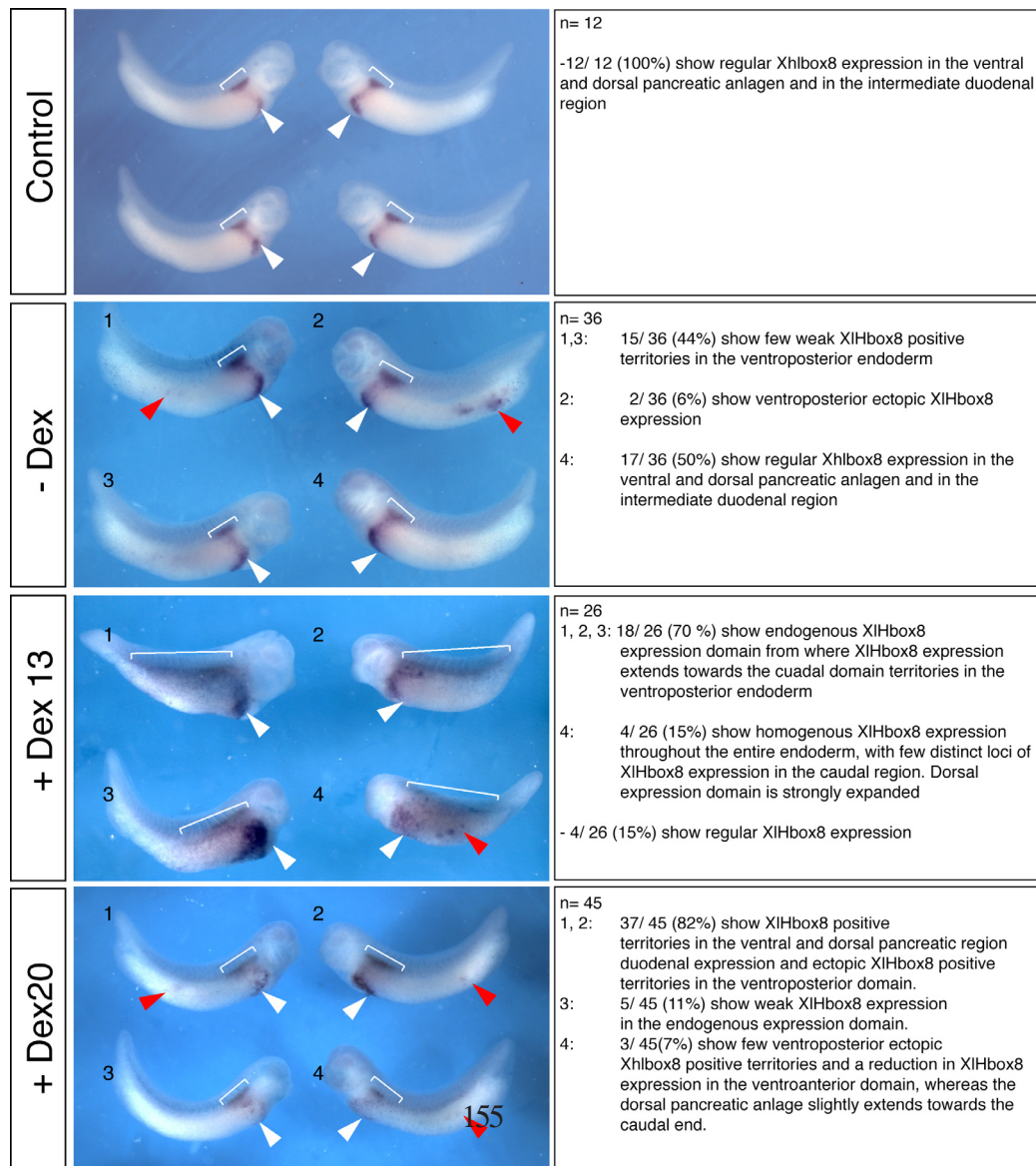
7.1 Effect on XlHbox8 expression upon ectopic activation of HNF1 β 

Figure 7.1 Effect on XlHbox8 expression upon ectopic activation of HNF1 β . Embryos were injected with 100 pg/E HNF1 β - GR capRNA and cultured till stage 32. HNF1 β -GR was activated by Dex treatment at stage 13 and 20 (+Dex13 and +Dex20). White arrow head points to the ventral pancreas. Red arrow head points to the posterior ectopic XlHbox8 positive territories. Bracket sizes the dorsal XlHbox8 positive expression domain that is expanded in injected embryos upon early Dex treatment.

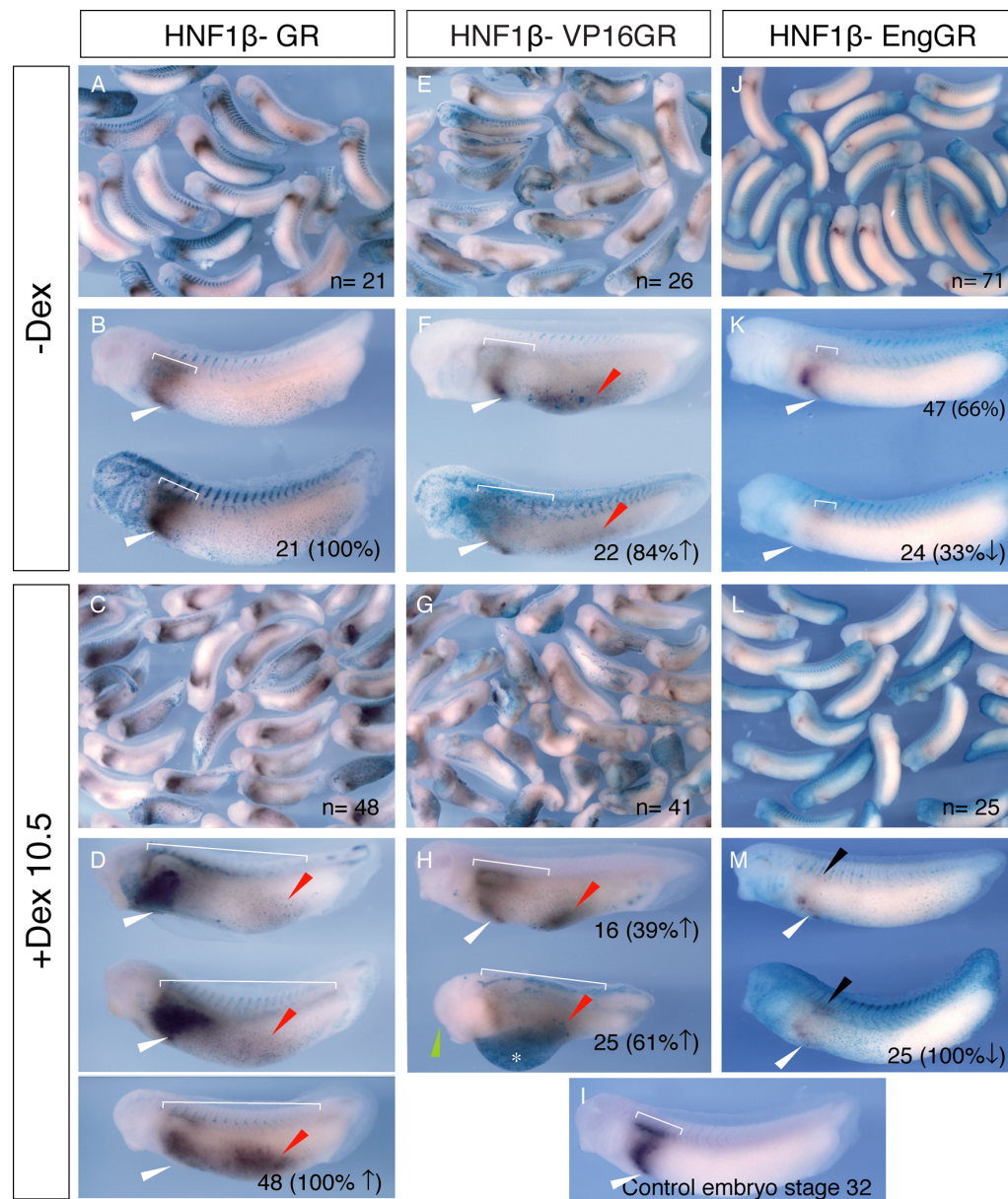
7.2 Phenotypes induced upon misexpression of HNF1 β 

Figure 7.2 Phenotypes induced upon misexpression of HNF1 β . Embryos were injected with 100 pg/E HNF1 β - GR, HNF1 β -VP16GR and HNF1 β - EngGR. HNF1 β was activated by Dex treatment at stage 10.5. Embryos were grown till stage 32 and analysed for changes in expression of XIHbox8. Embryos are shown in lateral view with head to the left. n= indicates the total number of embryos. Numbers in brackets show the percentage that is increased or decreased, compared to control. White arrow points to the location of the ventral pancreas, red arrow points to the ventro- posterior ectopic expression of XIHbox8. White bracket indicates the size of the dorsal pancreatic rudiment (A- I). Black arrow point to the presumptive dorsal pancreatic region (J- M). Green arrow head indicated reduction of anterior head structures. \uparrow = increase; \downarrow = decrease. asterisk indicates edema formation.

The expression of XIHbox8 is strongly influenced upon HNF1 β misexpression. Early ectopic HNF1 β activation either upon HNF1 β - GR injection or HNF1 β - VP16GR injection caused a broad caudal expansion of the dorsal and ventral XIHbox8 expression domain. In addition, XIHbox8 expression appeared ectopically in ventroposterior territories of the embryos. Strong activation of HNF1 β is evident in the untreated control embryos (-Dex) that already show XIHbox8 expansion. Upon HNF1 β -VP16 activation, embryos not only show increase in XIHbox8 expression but also show edema formation in the foregut, similar to RA treated embryos at that stage (Chen et al., 2004). 100% of HNF1 β -EngGR injected embryos show decreased XIHbox8 expression. 66% untreated HNF1 β -EngGR injected embryos already show reduced pancreatic but regular duodenal staining.

7.3 Statistical values of affected insulin expression upon HNF1 β misexpression

A

Number of insulin positive cells per embryo

embryo	CE	CoMo	HNF1 β mo1+2
1	29	21	19
2	23	26	18
3	14	25	10
4	16	20	16
5	23	15	21
6	24	28	23
7	22	15	28
8	12	23	14
9	22	23	21
10	27	23	22
11	21	22	10
12	25	16	16
13	24	18	10
14	28	13	11
15	22	15	12
16	25	23	16
17	27	23	18
18	29	20	7
19	27	20	8
20			8
AV	23	20	15
SD	5	4	6

Size of insulin expressing region per embryo

embryo	CE	CoMo	HNF1 β -Mo1+2
1	8249	6491	3618
2	10876	4488	4396
3	7147	7154	2329
4	6111	3502	3773
5	7774	7866	4388
6	8020	5853	5092
7	7314	6645	5657
8	9081	4348	5798
9	7077	3698	2742
10	7670	7616	5183
11	7837	5862	1316
12	5314	6313	3030
13	6285	5858	3600
14	5766	4984	3307
15	8158	8222	3399
16	7090	5767	3127
17	7709	6471	5899
18	8929	6475	3274
19	5725	5774	4434
20			1848
AV	7481	5968	3811
SD	1340	1319	1289

B

Number of insulin positive cells per embryo

embryo	CE	-Dex	+Dex13	+Dex20	+Dex26
1	22	34	39	31	22
2	25	28	42	19	19
3	18	25	29	20	22
4	20	37	45	22	23
5	16	25	35	26	23
6	25	20	40	25	26
7	28	23	30	27	23
8	25	30	25	16	28
9	20	28	23	25	35
10	23	30	30	25	24
11	27	36	35	35	32
12	21	26	30	29	21
13	25	27	26	28	35
14	24	23	35	22	25
15	28	30	29	36	21
16	22	26	39	35	24
17	25	33	28	28	30
18	27	19	38	31	25
19	29	32	30	25	24
20	27	26	33	25	30
AV	24	28	33	27	26
SD	4	5	6	5	5

Size of insulin expressing region per embryo

embryo	CE	-Dex	+Dex13	+Dex20	+Dex26
1	5380	6618	14073	6864	7360
2	4068	8042	13773	4194	5297
3	4201	9336	11069	8270	5539
4	4371	8073	13120	6739	6463
5	4311	8504	9544	8203	9541
6	3531	8359	15380	8421	4701
7	2340	5349	8934	7872	8656
8	5274	7083	16328	5426	5884
9	5136	7004	9339	10991	5755
10	4015	8099	10748	9366	7456
11	7670	6993	10055	9465	7761
12	7837	6838	10483	7186	6474
13	5314	9322	7040	7008	8979
14	6285	7521	8398	4636	6917
15	5766	6887	9297	9602	7205
16	8158	4359	8190	8195	5425
17	7090	5049	12068	9233	7983
18	7709	8726	7811	9015	6947
19	8929	7046	10147	7682	8165
20	5725	7150	7819	7859	8837
AV	5656	7318	10681	7811	7067
SD	1768	1325	2645	1698	1374

Table 5: Statistical values of affected insulin expression upon HNF1 β misexpression(A) Effect on insulin expression in HNF1 β loss of function **(B)** Effect on insulin expression on HNF1 β gain of function. First column indicates amount of embryos evaluated. CE= uninjected control embryos. -Dex = untreated control embryos. +Dex 13-26: Dexamethason treated embryos. CoMo= controlmorpholino injected embryos. HNF1 β -Mo1+2= embryos injected with HNF1 β specific morpholinos. AV= average value. SD= standard deviation.

7.4 Sequence alignment of XHNF6 and eukaryotic oncut proteins

			20		40		60		80	
Xl oncut-1	MNAQLTMDVI	GDLHGVSHE	MPSTADMMS	SPHHRGSVTH	RSNHLS-AHP	RSMGMASILD	GGDYHHHHHH	H-RPPDHALT	78	
Xt oncut-1	MNAQLTMDAI	GDLHGVSHE	VPGTADLMGS	SPHHRGSVTH	RSNHLS-AHP	RSMGMASILD	GGDYHHHHHH	HHRPPDHALT	79	
h.oncut-1	MNAQLTMEAI	GELHGVSHEP	VPAPADLLGG	SPHARSVAH	RGSHLPPAHP	RSMGMASLLD	GGSGGGDYHH	HHRAPHEHSLA	80	
m.oncut-1	MNAQLTMEAI	GELHGVSHEP	VPAPADLLGG	SPHARSVAH	RGSHLPPAHP	RSMGMASLLD	GGSGGGDYHH	HHRAPHEHSLA	80	
z.oncut-1	MNAQLSMENI	GDLHGVSHEP	VHSAADLMTG	DSAHHRSHRS	SLS----	AHA	RSMGMASILD	SGD-----YHH	HRPPEHPGLA	72
h.oncut-2	-----	-----	NPELTMSLG	TLHGARGGGS	GGGGGGGGGG	GGGGPGHEQE	LLASPSPHHA	RRGPRCSLRG	61	
m.oncut-2	MKAAYTAYRC	LTKDLEGGAM	NPELTMSLG	TLHGVPVGGG	GGGGGGGGGG	GGGGPGHEQE	LLASPSPHHA	GRGAAGCSLRG	80	
h.oncut-3	MELSLLESLGG	LHSVAHAQAG	ELLSPGHARS	AAAQHRGLVA	PGRPGLVAGM	ASLLDGGGGG	GGGGAGGAGG	AGSAGGGADF	80	
m.oncut-3	MELSLLESLGG	LHGVTQAQAG	ELLSPGHARS	AAAQHRSLVA	SRPGLVAGM	ASLLDGGGAG	GGG-AGGAGA	AGAAGGGPDF	79	
DrosoHNF6	MDSLNDI IDH	QTFSQELVED	ASEF I TVGHH	SERPSQSSQQ	PNSGQDLTMS	MQD I I SCPVK	HRTCASAGSG	SASGSDSVVM	80	
		100		120		140		160		
Xl oncut-1	-----	-----	-----	-----	-----	-----	-----	-----	78	
Xt oncut-1	-----	-----	-----	-----	-----	-----	-----	-----	79	
h.oncut-1	-----	-----	-----	-----	-----	-----	-----	-----	80	
m.oncut-1	-----	-----	-----	-----	-----	-----	-----	-----	80	
z.oncut-1	-----	-----	-----	-----	-----	-----	-----	-----	72	
h.oncut-2	-----	-----	-----	-----	-----	-----	-----	-----	61	
m.oncut-2	-----	-----	-----	-----	-----	-----	-----	-----	80	
h.oncut-3	-----	-----	-----	-----	-----	-----	-----	-----	80	
m.oncut-3	-----	-----	-----	-----	-----	-----	-----	-----	79	
DrosoHNF6	V I DALGQGNR	QSAYQ I VPQQ	LQRNMPLPF	G LL ERDRQH M	QHGREVNTS P	VDFVSSD I NL	DGLTVDADVS	QTDHSQETA V	160	
		180		200		220		240		
Xl oncut-1	-----	-----	-----	-----	-----	-----	-----	-----	78	
Xt oncut-1	-----	-----	-----	-----	-----	-----	-----	-----	79	
h.oncut-1	-----	-----	-----	-----	-----	-----	-----	-----	80	
m.oncut-1	-----	-----	-----	-----	-----	-----	-----	-----	80	
z.oncut-1	-----	-----	-----	-----	-----	-----	-----	-----	72	
h.oncut-2	-----	-----	-----	-----	-----	-----	-----	-----	61	
m.oncut-2	-----	-----	-----	-----	-----	-----	-----	-----	80	
h.oncut-3	-----	-----	-----	-----	-----	-----	-----	-----	80	
m.oncut-3	-----	-----	-----	-----	-----	-----	-----	-----	79	
DrosoHNF6	KQEQLL I VQ	SKSQDQSHRR	I RMLVDVSV	NSGLGVHVDD	MDE I SSDGVG	CDDEGVTL SH	QHLL EQEEQF	GLTSHHPHLQ	240	
		260		280		300		320		
Xl oncut-1	-----	-----	-----	GP LHPTMTACD	T-----	-----	-----	-----	91	
Xt oncut-1	-----	-----	-----	GP LHPTMTACD	T-----	-----	-----	-----	92	
h.oncut-1	-----	-----	-----	GP LHPTMTACE	T-----	-----	-----	-----	93	
m.oncut-1	-----	-----	-----	GP LHPTMTACE	T-----	-----	-----	-----	93	
z.oncut-1	-----	-----	-----	TH LHPAMSMACE	A-----	-----	-----	-----	85	
h.oncut-2	-----	-----	-----	PP PPTAHQELG	TAAAAAAAAA	RSAMVTSMAS	I LDGGDYRPE	LS I PLHHAMS	113	
m.oncut-2	-----	-----	-----	PP PP-TAHQELG	TAAAAAAAAA	RSAMVTSMAS	I LDGSDYRPE	LS I PLHHAMS	131	
h.oncut-3	-----	-----	-----	RG ELAG	-----	-----	-----	PLH	89	
m.oncut-3	-----	-----	-----	RG ELAG	-----	-----	-----	PLH	88	
DrosoHNF6	PHTQ I IHGLH	QRSTHSEMGL	DNGHGEVLSV	I VHSQDS DKE	DCE ENDDGDA	EGDLENE DDD	ERDSRSRQL	LSHSSYQTLT	320	
		340		360		380		400		
Xl oncut-1	-----	PPGM SMSSTY TLLT	PLQL LPP I ST	VSDKFP	-----	-----	-----	-----	121	
Xt oncut-1	-----	PPGM SMSSTY TLLT	PLQL LPP I ST	VSDKFP	-----	-----	-----	-----	122	
h.oncut-1	-----	PPGM SMPTTY TLLT	PLQL LPP I ST	VSDKFP	-----	-----	-----	-----	123	
m.oncut-1	-----	PPGM SMPTTY TLLT	PLQL LPP I ST	VSDKFP	-----	-----	-----	-----	123	
z.oncut-1	-----	PPGM SMSSTY TLLT	PLQL LPP I ST	VSDKFP	-----	-----	-----	-----	115	
h.oncut-2	-----	MSCDS SPPGM	GMSNTY TLLT	PLQL LPP I ST	VSDKFP	-----	-----	-----	149	
m.oncut-2	-----	MSCDS SPPGM	GMSNTY TLLT	PLQL LPP I ST	VSDKFP	-----	-----	-----	167	
h.oncut-3	-----	PAMGMACEAP	GLGGTY TLLT	PLQH LPP LAA	VADK FQHAAA	AAAVAGAHGG	-----	-----	139	
m.oncut-3	-----	PAMGMACEAP	GLGGTY TLLT	PLQH LPP LAA	VADK FQHAAA	---VAGAHGG	-----	-----	134	
DrosoHNF6	SVNDRLS SPG	FSQTSYATLT	PIQL LPP I ST	MSEKFAYSGH	I SGGSDGDT	VNGDGAGGGV	VEVGEVTNQS	SEATGTVSI	400	
		420		440		460		480		
Xl oncut-1	-----	-----	-----	-----	-----	-----	-----	-----	121	
Xt oncut-1	-----	-----	-----	-----	-----	-----	-----	-----	122	
h.oncut-1	-----	-----	-----	-----	-----	-----	-----	-----	123	
m.oncut-1	-----	-----	-----	-----	-----	-----	-----	-----	123	
z.oncut-1	-----	-----	-----	-----	-----	-----	-----	-----	115	
h.oncut-2	-----	-----	-----	-----	-----	-----	-----	-----	149	
m.oncut-2	-----	-----	-----	-----	-----	-----	-----	-----	167	
h.oncut-3	-----	-----	-----	-----	-----	-----	-----	-----	139	
m.oncut-3	-----	-----	-----	-----	-----	-----	-----	-----	134	
DrosoHNF6	SGNATSSVCS	NNDCSSFSAL	SMP I GSHGLG	LGVLSGVQSP	FSSYEKLSM	I SPPPNYL V	SCDLHSVSG	RVINS SHLQL	480	
		500		520		540		560		
Xl oncut-1	-----	-----	-----	-----	-----	-----	-----	-----	121	
Xt oncut-1	-----	-----	-----	-----	-----	-----	-----	-----	122	
h.oncut-1	-----	-----	-----	-----	-----	-----	-----	-----	123	
m.oncut-1	-----	-----	-----	-----	-----	-----	-----	-----	123	
z.oncut-1	-----	-----	-----	-----	-----	-----	-----	-----	115	
h.oncut-2	-----	-----	-----	-----	-----	-----	-----	-----	149	
m.oncut-2	-----	-----	-----	-----	-----	-----	-----	-----	167	
h.oncut-3	-----	-----	-----	-----	-----	-----	-----	-----	139	
m.oncut-3	-----	-----	-----	-----	-----	-----	-----	-----	134	
DrosoHNF6	SHNGNKEEG	THEHTRPAD	VNGGKFSYTG	H I SRGDSVD	DVNGEKFSFS	DH I SGGSDG	EDANREKFI Y	SDH I SEGENG	560	
		580		600		620		640		
Xl oncut-1	-----	H---HHHH	HH-----PH	QRI AANVSGS	FTLMRDERG-	LATMNNLYS P	YHKEVTGMGQ	SLSPLSGSGL	179	
Xt oncut-1	-----	H---HHHH	HH-----PH	QRI PGNVSGS	FTLMRDRRG-	LASMNNLYS P	YHKEVTGMGQ	SLSPLSGSGL	180	
h.oncut-1	-----	H---HHHH	HHHHHHPHHH	QRLAGNVSGS	FTLMRDERG-	LASMNNLYT P	YHKDVAGMGQ	SLSPLSSSGL	187	
m.oncut-1	-----	H---HHHH	HHHHHHPHHH	QRLAGNVSGS	FTLMRDERG-	LASMNNLYT P	YHKDVAGMGQ	SLSPLSGSGL	187	
z.oncut-1	-----	H---HHHH	HHHHHH-HPH	QRI PGNVSGS	FTLMRDRRG-	LAPMNNLYS P	YHKDVASMGQ	SLSPLSGSGL	178	
h.oncut-2	-----	HPPHHHP	HHHHHHHH--	QRLSGNVSGS	FTLMRDERG-	LAPMNNLYS P	YKEMPMSQS	LSP LAATPLG	214	
m.oncut-2	-----	HPPHHHP	HHHHHHHHHH	QRLSGNVSGS	FTLMRDERG-	LPSMNNLYS P	YKEMPMSQS	LSP LAATPLG	234	
h.oncut-3	-----	HPHAHP	AAAPPPPPP	QRLAASVSGS	FTLMRDERAA	LASVGHLYG P	YGKELPAMGS	PLSPLPALP	207	
m.oncut-3	-----	HPHAHP	ATAPPPPPP	QRLAASVSGS	FTLMRDERAA	LASVGHLYG P	YGKELPAMGS	PLSPLPALP	201	
DrosoHNF6	PDVNSGTNWL	QHHSEREVRL	HMPVPAELEA	RFIHSERRT	RLNVPPARGS	LSRHLAPNA P	ICPADWKADD	WKHSNAGVVS	640	
		660		680		700		720		
Xl oncut-1	GS I HSAQQGL	PHYAHPSAAM	PTDKMLTPNG	FEAHPAMLP	RHGEQLTPQ	SAGMVP INGI	ARHPHAHLNA	QSHGQI LAST	259	
Xt oncut-1	GS I HGAQQGP	PHYAHPSAAM	PTEKMLTPNG	FEAHPAMLT	RHGEQLTTP	SAGMVP INGI	PHHPHAHLNA	QSHGQI LAST	260	
h.oncut-1	GS I HNSQQGL	PHYAHPGAAM	PTDKMLTPNG	FEAHPAMLG	RHGEQLTPT	SAGMVP INGL	PHHPHAHLN	AQHGQLLGT	267	
m.oncut-1	GS I HNSQQGL	PHYAHPGAAM	PTDKMLTPNG	FEAHPAMLG	RHGEQLTPT	SAGMVP INGL	PHHPHAHLN	AQHGQLLGT	267	
z.oncut-1	SG I HNSQQGL	PHYAHPGATM	PAEKMLTPNG	FEAHPAMLA	RHGEQHMSA	SASMVP INVI	HHHPHAHLNA	QGHQVLGST	258	
h.oncut-2	NGLGGLHNA-	-QQLPNYGP	PGHDKMLSPN	FDAAHTAML	RGEQLSRGL	GTPPAAMMSH	LNGLHPGHT	QSHGVLAPS	292	
m.oncut-2	NGLGGLHNA-	-QQLPNYGP	PGHDKMLSPN	FDAAHTAML	RGEQLSRGL	GTPPAAMMSH	LNGLHPGHT	QSHGVLAPS	312	
h.oncut-3	PALHGAPQPP	PPPPPLTAA	YGPPGLAGD	KLLPPAAFEP	HAALLGRAED	ALARGLPGGG	GGTSGGAGS	GSAAGLLAPL	287	
m.oncut-3	PALHSAQPP	PPPP---LAA	YGAPGLAGD	KLLPPAAFEP	HAALLGRAED	ALARGLPGGG	GGAGGGGAG	GAAAGLLAPL	278	
DrosoHNF6	LTADMPVVVS	LTPTPPPLRD	DSVSGIKQNE	RSSPGHREFY	FLDKSQEPS	VVADQCSPGI	NGTPQSVCVI	HQQSPSALGN	720	



Figure 7.3 Sequence alignment of XHNF6 and eukaryotic oncut proteins. Compared sequences correspond to organisms stated to the left. Sequence accession numbers are listed in table 3.1. Identical residues are underlined in red. Numbers on top of each lane indicates number of residues. Numbers to the right state position of amino acid. Lines indicate residue gaps between sequences. Residues underlined in rose are identical between vertebrates but differ from Drosophila. The CUT domain is framed in green and the HOMEBOX domain is framed in red.

List of publications

Schallus T., **Jaech C.**, Fehér K., Palma A.S., Liu Y., Simpson J.C., Mackeen M., Stier G., Gibson T.J., Feizi T., Pieler T., Muhle-Goll C. (2008)

Malectin: A Novel Carbohydrate-binding Protein of the Endoplasmic Reticulum and a Candidate Player in the Early Steps of Protein N-Glycosylation.

Mol Biol Cell.;19(8):3404-3414.

Acknowledgements

I am very thankful to Prof. Dr. Tomas Pieler for giving me the opportunity to work on these interesting projects in his laboratory and for scientific guidance.

I also want to thank Prof. Dr. Ernst Wimmer for accepting the correference.

My special thanks go to our collaborators Claudia Muhle- Goll, Toby Gibson and Thomas Schallus for their great interest and support in the malectin project.

In addition, I am very grateful to Katja Köbernick and Stephan Seiler for scientific discussions, proof reading and advice.

My profound thanks go to Marion Dornwell, not only for the enormous technical support but also for her daily encouragement in accomplishing the challenge of climbing the “PhD” summit.

In this respect, I really appreciated the help of my labmates, former and present ones, in particular Yonglong, Fong Cheng, Andreas, Ilona, Patrick, Johanna and Marie for creating a pleasent working atmosphere by joyful chats, relaxing “tea times” and coffee breaks.

I am deeply grateful to my friend Karin, my family and especially to Ingo- Felix for his patience and encouragement during all these years.

Curriculum Vitae

Name: Jäckh, Maria Pilar Christine
Date of birth: 18.09.1978
Place of birth: Heidelberg, Germany
Nationality: German

Education

since 2004 PhD, Georg- August- University Göttingen
Göttinger Center for Molecular Bioscience (GZMB),
Dept. Developmental Biochemistry

2004 Diploma, Ruprecht-Karls University Heidelberg

1999— 2000 University of Windsor (Ont), Canada

1997— 2004 Ruprecht-Karls University Heidelberg, Biology

1997 Abitur, Bunsengymnasium Heidelberg

Herewith I declare, that I prepared the PhD thesis „Transcription factor networks directing pancreas development in *Xenopus laevis*” on my own and with no other sources and aids than quoted.

15. 09. 2008

.....
submission date

.....
Christine Jäckh

